Delft University of Technology
Faculty of Electrical Engineering, Mathematics and Computer Science
Delft Institute of Applied Mathematics

On the Cheyette short rate model with stochastic volatility

A thesis submitted to the
Delft Institute of Applied Mathematics
in partial fulfillment of the requirements

for the degree

MASTER OF SCIENCE
in
APPLIED MATHEMATICS

by

Bart Hoorens

Delft, the Netherlands
June 2011

TU Delft

MSc THESIS APPLIED MATHEMATICS

"On the Cheyette short rate model with stochastic volatility"

Bart Hoorens

Delft University of Technology

Prof. dr. ir. C.W. Oosterlee	**Responsible professor**
Prof. dr. ir. G. Jongbloed	Dr. ir. F.J. Vermolen
Dr. D. Kandhai	Msc. C. González Sterling

June 2011 Delft, the Netherlands

Acknowledgements

This master thesis is done at the CMRM Trading department of ING Bank Amsterdam. I did this project in the Quantitative Analytics team, under supervision of Drona Kandhai, Carlos González Sterling and Veronica Malafaia. My supervisor from the TU Delft was Kees Oosterlee, professor at the Numerical Analysis group of DIAM. I would like to thank my supervisors Kees Oosterlee, Drona Kandhai, Carlos González Sterling and Veronica Malafaia for all their guidance throughout this project. The same thanks should also go to all my colleagues at ING Bank, who gave me support to make this project succesful. Without the help of these persons, this thesis would not be a success.

Abstract

The purpose of this thesis is to compare the Hull-White short rate model to the Cheyette short rate model. The Cheyette short rate model is a stochastic volatility model, that is introduced to improve the fit of the implied volatility skew to the market skew. Both models are implemented with piecewise constant parameters to match the term structure. We calibrate the Cheyette model to the EURO, USD and KRW swaption markets and compare the calibration results to the Hull-White model. We propose an efficient implementation method to speed up the calibration process. In general we see that the Cheyette model gives indeed a better fit, in particular for the EURO and KRW markets. The models with calibrated parameters are used to price exotic interest rate derivatives by Monte Carlo simulation. Comparing the results of the Cheyette model to the results of the Hull-White model, can give insight in the skew and curvature impact on exotic interest rate derivatives. We consider digital caplets, digital caps, range accrual swaps, callable range acrruals and a callable remaining maturity swap. The price impact on digital caplets and digital caps are in line with static replication. By this we mean that the prices computed with static replication are better matched by the Cheyette model than by the Hull-White model. For the callable range accrual on LIBOR we have to be more careful, since a one-factor model cannot be calibrated to two market skews per option maturity. This implies that the price of the underlying range accrual is not in line with static replication, since we calibrate to co-terminal swaptions, while the underlying depends on the cap market. For the callable remaining maturity swap we do not encounter this issue, since the underlying depends on the same co-terminal swaption skews. For a callable RMS we observe that the Hull and White model underestimates the option price, compared to the Cheyette model.

Glossary

bp	Basis point, a unit equal to 1/100th of 1%.
$L(S,T)$	Spot LIBOR rate for a time interval $[S,T]$, see (2.1).
$P(t,T)$	The zero-coupon bond price, contracted at time t with maturity T. This is the fundamental quantity in interest rate derivatives pricing. See (2.7).
$r(t)$	The short rate at time t, see (2.5). Short rate models are modelling this mathematical variable.
$\tau(T,S)$	The year fraction between time T and time S.
Pay IRS, Recv IRS	Payer interest rate swap respectively receiver interest rate swap. See Sections 2.2.3 and 2.2.4.
Swap rate	That rate on the fixed leg such that, both the Pay IRS and Recv IRS, are worth zero. See section 2.2.5.
Swaption	An option where the holder has the right but not the obligation to enter into a plain vanilla interest rate swap. See Section 2.2.6.
ATM swaption	A swaption where the fixed rate K of the fixed leg is equal to the swap rate of the underlying swap.
Annuity	Numeraire corresponding to the swap measure. See Formula (2.18).
$\mathbb{Q}^0$	The risk neutral measure corresponding to the money market account as a numeraire.
$\mathbb{Q}^T$	The T forward measure with the zero-coupon bond $P(t,T)$ as a numeraire.
$\mathbb{Q}^{1,m}$	The swap measure, with the annuity as a numeraire.
Black's model	A model to value european style options. See Section 2.1
$\mathcal{N}(x)$	The standard normal distribution function evaluated in x.
Fundamental transform	This is the Fourier inversion method described in Section 5.3.1.
Riccati ODEs	This is a class of non linear ODEs. In this thesis we refer to the system given by Equation (5.27).
Implied volatility	The value of σ such that Black's price matches the reference price.
DD	The displaced diffusion formulation of the Cheyette model. This model is discussed in Chapter 4.
DDSV	The displaced diffusion with stochastic volatility formulation of the Cheyette model. This model is discussed in Chapter 5.
QE-scheme	The Quadratic Exponential scheme to simulate the CIR variance process, described in Section 5.6.
Co-terminal	A series of swaptions whose expiry plus tenor is equal.
KRW	Korean Won market.
RAC	Range accrual where the observation index is the LIBOR rate, see Section 7.1.2.
CRAC	Callable range accrual on LIBOR, see Section 7.1.3.
RMS	Remaining maturity swap, see Section 7.1.3.
LS	Longstaff and Schwartz method, see [23].
SR	Static replication, the decomposition of a digital into two caplets or floorlets, see Section 7.1.1.

Contents

Chapter 1

Introduction and research objectives

This thesis is about the Cheyette stochastic volatility model, belonging to the class of short rate models. The short rate $r(t)$ is a mathematical quantity representing the interest rate valid for an infinitsimally short period of time from time t. Short rate models are frequently used to price interest rate derivatives. The interest rate derivatives market is the largest derivatives market in the world and a wide range of products are traded. Roughly speaking we have three levels, the plain vanilla instruments like swaps, caps and swaptions. The intermediate level is the class of convexity derivatives, examples are range accruals, in-arrears swaps and constant maturity swaps. The third level are the exotic derivatives like, target redemption notes, callable range accruals and snowballs.

For the plain vanilla instruments we do not need advanced models to price them. A plain vanilla interest rate swap is priced on the yield curve. To price swaptions we can use Black's model, this model is equivalent to the Black and Scholes model that is well-known from equity world. For the convexity derivatives and exotic interest rate derivatives, we cannot apply Black's model, since this model only applies to European-style options. In interest rate modelling there are two important classes of models to value those derivatives, first of all the short rate models and secondly the LIBOR market models. We can use these models for the valuation of exotic interest rate derivatives. In this thesis we restrict ourselves to the class of short rate models.

In interest rate modelling we are interested in modelling the short rate, since there is a relationship between the short rate and the zero-coupon bond price. The zero-coupon bond price is a fundamental quantity in interest rate derivatives pricing. In Chapter 2 we give some background information on interest rate modelling. We introduce the definitions of the short rate, zero-coupon bond and several plain vanilla interest rate products. We use these definitions throughout this thesis. We recommend this chapter for people who are not familiar with interest rate derivatives.

One popular short rate model is the Hull-White model. This model has the following properties. There exists an analytic formula for the zero-coupon bond price, it is a mean reverting process, which is a desired property in interest rate modelling and moreover the state variables are Gaussian distributed. Due to the last property there are analytic formulas to price plain vanilla interest rate products like bond options, caps and swaptions. In general, pricing models are calibrated to plain vanilla market instruments. Due to the analytic formulas, there is a fast calibration to these instruments. A drawback of the Hull-White model is that in general we have a poor fit to the market skew. In Chapter 3 of this thesis we will go more into detail on this.

The first research objective is to improve on this shortcoming of the Hull-White model. Therefore we investigate a different class of short rate models, the Cheyette models. In this thesis we consider the displaced diffusion formulation of the Cheyette model. We subdivide the theoretical discussion into two parts. In Chapter 4 we discuss the displaced diffusion formulation without stochastic volatility and in Chapter 5 we discuss the displaced diffusion model with stochastic volatility. We show that the stochastic volatility model has control of the level, skewness and curvature of the implied volatility skew. We expect that this is sufficient to improve the fit to the market skew. In these chapters we focus on a detailed derivation of the closed-form swaption price, since the Cheyette model is not analytically tractable this swaption price will be an approximation of the true model implied swaption price. Moreover we contribute an efficient implementation method, which allows us for an efficient calibration. After we have provided the theoretical discussion of the Cheyette stochastic volatility model, we compare numerical results from the Cheyette model to the results from the Hull-White model.

In Chapter 6 we discuss the calibration of the Cheyette stochastic volatility model to the swaption market. We show calibration results for three different currencies and three historical sets of market data.

The second research objective is to investigate the price impact of the Cheyette stochastic volatility model on (exotic) interest rate derivatives, this will be the main topic of Chapter 7. We consider a digital cap, a range accrual swap, a callable range accrual and a callable remaining maturity swap. We investigate the price impact between the Hull-White model and the Cheyette stochastic volatility model, which is the skew and curvature impact of the Cheyette model. We expect that the market price of a digital, obtained with static replication, is better matched by the DDSV model than by the Hull-White model. Hence we expect that the Cheyette model gives a more consistent price of a series of digitals, a range accrual. This is important for the valuation of a callable range accrual, since this contract has a Bermudan-style option to enter into a range accrual where the legs are reversed relative to the underlying range accrual of the contract.

Chapter 2

Plain vanilla interest rate derivatives

This chapter is for readers who are not familiar with interest rate products, different types of interest rates and some well known pricing formulas such as the risk neutral pricing formula and Black's formula. This chapter discusses the following topics:

- Interest rates and pricing formulas, see Section 2.1.
- Interest rate derivatives, see Section 2.2.
- Pricing swaptions under different measures, see Section 2.3.

It is important to have clear in mind what we mean with time. Unless otherwise stated we assume all times to be year fractions. If we write $\tau(S,T)$ for the year fraction between two year fractions S and T, it is clear that $\tau(S,T) = T - S$. In case we have two dates, $D_1 = (d_s, m_s, y_s)$ and $D_2 = (d_t, m_t, y_t)$, $\tau(D_1, D_2)$ depends on the choice of market conventions. One example is the Actual/360 convention. In this case a year is assumed to be 360 days long. The year fraction between two dates D_1 and D_2 is

$$\frac{D_2 - D_1}{360}.$$

Therefore, the year fraction between January 4, 2000 and July 4, 2000 is 182/360, since there are 182 days between these dates (leap year). We refer to [1] for more information about day count conventions.

2.1 Interest rates and pricing formulas

Definition 2.1. We denote by $P(t,T)$ the value of a zero-coupon bond at time t, which pays 1 at maturity T i.e. $P(T,T) = 1$. Remember that we assume all times to be in year fractions. For $t \leq T$;

1. The **spot LIBOR-rate** for a time interval $[S,T]$ is given by:

$$L(S,T) = \frac{1}{T-S}\left(\frac{1}{P(S,T)} - 1\right). \tag{2.1}$$

2. The **simply compounded forward LIBOR rate** contracted at time t for the interval $[S,T]$ is defined by:

$$F_{lib}(t;S,T) = \frac{1}{(T-S)}\left(\frac{P(t,S)}{P(t,T)} - 1\right) \quad \text{for } 0 \leq t \leq S. \tag{2.2}$$

Notice that for $t = S$

$$F_{lib}(S;S,T) = \frac{1}{(T-S)}\left(\frac{P(S,S)}{P(S,T)} - 1\right) = \frac{1}{(T-S)}\left(\frac{1}{P(S,T)} - 1\right) = L(S,T),$$

i.e. the simply compounded forward rate equals the spot LIBOR-rate.

3. The **continuously compounded spot rate** for the period $[S,T]$ is defined by:

$$R(S,T) = -\frac{\log(P(S,T))}{T-S}. \tag{2.3}$$

4. The **instantaneous forward rate with maturity T, contracted at time t** is defined by:

$$f(t,T) = -\frac{\partial \log(P(t,T))}{\partial T}. \tag{2.4}$$

5. The instantaneous **short rate** at time t is given by:

$$r(t) = f(t,t). \tag{2.5}$$

Theorem 2.2. From the Fundamental Theorem of Asset Pricing it is well-known that the price at time t of any contingent claim with payoff $V(T)$ at time T is given by:

$$V(t) = \mathbb{E}^{\mathbb{Q}^0}\left[e^{-\int_t^T r(s)ds} V(T) \middle| \mathcal{F}_t\right], \tag{2.6}$$

where the expectation is taken under the risk neutral measure $\mathbb{Q}^0$.

Proof. For a proof of this theorem we refer to [2]. □

Corollary. The price of a zero-coupon bond at time t with maturity T is given by:

$$P(t,T) = \mathbb{E}^{\mathbb{Q}^0}\left[e^{-\int_t^T r(s)ds} \middle| \mathcal{F}_t\right], \tag{2.7}$$

since $V(T) = P(T,T) = 1$.

Theorem 2.3. Given a European call option, with maturity T, on an underlying with value $V(t)$. Define:

- $0 \leq t \leq T$.
- $\mu(t)$ the forward price of V at time t of a contract with maturity T, i.e., $\mu(t) = \mathbb{E}^{\mathbb{Q}^T}[V(T)|\mathcal{F}_t]$, where the expectation is taken under the T-forward measure.
- K the strike of the option.
- σ the volatility of the forward price.

Assuming that conditioned on the information available at time t, $V(T)$ is distributed log-normal with mean $\mu(t)$ and standard deviation $\sigma\sqrt{T-t}$, then the price of a European call option with strike K is given by:

$$\begin{aligned} C(t) &= V(t)\mathcal{N}(d_1) - KP(t,T)\mathcal{N}(d_2) = P(t,T)\left\{\frac{V(t)}{P(t,T)}\mathcal{N}(d_1) - K\mathcal{N}(d_2)\right\} \\ &= P(t,T)\left\{\mathbb{E}^T\left[\frac{V(T)}{P(T,T)}\right]\mathcal{N}(d_1) - K\mathcal{N}(d_2)\right\} = P(t,T)\left\{\mu(t)\mathcal{N}(d_1) - K\mathcal{N}(d_2)\right\}, \end{aligned} \tag{2.8}$$

with

$$\begin{aligned} d_1 &= \frac{\log(\mu(t)/K) + \sigma^2(T-t)/2}{\sigma\sqrt{T-t}}, \\ d_2 &= d_1 - \sigma\sqrt{T-t}, \\ \mathcal{N}(x) &= \int_{-\infty}^{x} \frac{1}{\sqrt{2\pi}} e^{-\frac{1}{2}s^2} ds. \end{aligned}$$

This theorem is known as Black's Pricing Theorem. When we use Black's formula in this text we mean the formula given by this theorem.

Proof. The proof of

$$C(t) = V(t)\mathcal{N}(d_1) - KP(t,T)\mathcal{N}(d_2),$$

is based on the general pricing theorem of Geman-El Karoui-Rochet , we refer to [3] p.361 for a proof. The other equalities in (2.8) are straight forward.

□

2.2 Interest rate derivatives

In this section the definitions of some interest rate derivatives are given.

Define $\mathcal{T}_m := \{T_0, T_1, \ldots, T_m\}$ in year fractions and $\tau^{(m)} := \{\tau_1, \ldots, \tau_m\}$ where

$$\tau_i := \tau(T_{i-1}, T_i) = T_i - T_{i-1}.$$

2.2.1 Fixed rate bond

Given a fixed rate K, a notional amount N and a set of payment dates $\mathcal{T}_m \backslash \{T_0\}$, a fixed interest rate bond is an instrument whose coupon payments are given by:

$$V_i^{fix}(T_i) = \begin{cases} N\tau_i K & i \in \{1, 2, \ldots, m-1\} \\ N\tau_m K + N & i = m \end{cases}$$

Using the zero-coupon bond $P(t, T_i)$ as a numeraire, the value at time $t \leq T_0$ of a payment at time T_i is given by:

$$\frac{V_i^{fix}(t)}{P(t,T_i)} = \mathbb{E}^{\mathbb{Q}_i^T}\left[\left.\frac{V_i^{fix}(T_i)}{P(T_i,T_i)}\right| \mathcal{F}_t\right] \Leftrightarrow V_i^{fix}(t) = P(t,T_i)V_i^{fix}(T_i),$$

where the expectation is taken under the T_i-forward measure. Note that we take the expectation of a constant. The value at time t of the fixed rate bond is the sum of these time t values.

$$V_{\mathrm{B}_{fix}}(t) = \sum_{i=1}^{m} P(t,T_i)V_i^{fix}(T_i). \tag{2.9}$$

2.2.2 A floating rate bond

Given a floating interest rate, in general the $L(T_{i-1},T_i)$ LIBOR rate, a notional amount N and a set of payment dates $\mathcal{T}_m\backslash\{T_0\}$, a floating interest rate bond is an instrument whose coupon payments are given by:

$$V_i^{fl}(T_i) = \begin{cases} N\tau_i L(T_{i-1},T_i) & i \in \{1,2,\ldots,m-1\} \\ N\tau_m L(T_{m-1},T_m) + N & i = m \end{cases}$$

Using the zero-coupon bond $P(t,T_i)$ as a numeraire, the value at time $t \leq T_0$ of a payoff at time T_i is given by:

$$V_i^{fl}(t) = P(t,T_i)\mathbb{E}^{\mathbb{Q}_i^T}\left[V_i^{fl}(T_i) \middle| \mathcal{F}_t \right],$$

where the expectation is taken under the T_i-forward measure. A simple calculation, using the fact that $\mathbb{E}^{\mathbb{Q}_i^T}\left[L(T_{i-1},T_i) | \mathcal{F}_t \right] = F_{lib}(t;T_{i-1},T_i)$, Equation (2.2) and assuming that the year fraction corresponding to the spot LIBOR-rate equals the year fraction with respect to our day count convention[1], shows that

$$V_i^{fl}(t) = \begin{cases} N(P(t,T_{i-1}) - P(t,T_i)) & i \in \{1,2,\ldots,m-1\} \\ NP(t,T_m) + N(P(t,T_{m-1}) - P(t,T_m)) & i = m \end{cases}$$

Hence the value at time t of the floating rate bond is given by:

$$V_{\mathrm{B}_{floating}}(t) = \sum_{i=1}^{m} V_i^{fl}(t) = NP(t,T_0). \tag{2.10}$$

2.2.3 Plain Vanilla Payer Interest Rate Swap (Pay IRS)

Given a notional amount N, a fixed rate K, and a set of payment dates $\mathcal{T}_m\backslash\{T_0\}$, a Pay IRS is a contract where the holder pays at T_i the amount $N\tau_i K$ and receiver the amount $N\tau_i L(T_{i-1},T_i)$. In the plain vanilla case the payments are made in the same currency. In general the notionals are not exchanged between both parties. This is a safe assumption, since at time T_m, the exchange of the same notional between both parties has no financial effect. To derive the value of a Pay IRS we can assume that at time T_m both parties exchange the notional. We can then see this as a contract where the holder pays a fixed rate bond and receives a floating rate bond in exchange. Hence the value of the Pay IRS is given by:

$$V_{\text{P-IRS}}(t) = NP(t,T_0) - NP(t,T_m) - \sum_{i=1}^{m} P(t,T_i)N\tau_i K. \tag{2.11}$$

The swap tenor is defined as the distance between T_0 and T_m.

[1] This is the case when we assume the Actual 360 day count conventions.

2.2.4 Plain Vanilla Receiver Interest Rate Swap (Recv IRS)

This is the same contract as a Pay IRS, but in this case the holder receives the fixed leg and pays the floating leg. The value of the floating Recv IRS is the value of the Pay IRS with a negative sign.

$$V_{\text{R-IRS}}(t) = NP(t, T_m) - NP(t, T_0) + \sum_{i=1}^{m} P(t, T_i) N \tau_i K. \tag{2.12}$$

2.2.5 Swap Rate

Given a Pay IRS or a Recv IRS, the corresponding swap rate is the rate K of the fixed leg such that the Pay IRS (or Recv IRS) is worth zero at time t. Equating Equation (2.11) or (2.12) to zero yields:

$$S_{0,m}(t) = \frac{P(t, T_0) - P(t, T_m)}{\sum_{i=1}^{m} P(t, T_i)\tau_i}. \tag{2.13}$$

2.2.6 Plain Vanilla Swaptions

A swaption is a contract where the holder has the right, but not the obligation, to enter into a plain vanilla (receiver or payer) swap at some future time T_0, the option maturity. We start with a discussion of a payer swaption. Let N and K be the notional amount and fixed rate respectively, of this underlying payer swap. At time T_0 a party will exercise the option if the underlying swap has positive value. I.e. the following inequality holds

$$N - NP(T_0, T_m) - \sum_{i=1}^{m} P(T_0, T_i) N \tau_i K \geq 0.$$

Or equivalent $S_{0,m}(T_0) > K$, with $S_{0,m}(T_0)$ corresponding to an identical swap as that of the underlying swaption, since $S_{0,m}(T_0)$ is the fixed rate that makes the underlying swap worth zero at time T_0. At all payment dates $T_i \in \mathcal{T}_m$, with $1 \leq i \leq m$ there is a cashflow equal to

$$N\tau_i \max(S_{0,m}(T_0) - K, 0), \quad i \in \{1, \ldots, m\}.$$

When we assume Black's model, we can calculate the value of this payer swaption at time $t \leq T_0$. Looking at the individual cashflows it is obvious that this can be expressed as a European call contract on the swap rate with strike K. We assume that $S_{0,m}(T_0)$ is log-normal conditional on the information at time t with mean $S_{0,m}(t)$, and standard deviation $\sigma\sqrt{T_0 - t}$. Using Black's Formula, the value at time t of the payer swap is given by (see [1])

$$\begin{aligned} V_{\text{P-swaption}}(t) &= N\left(\sum_{i=1}^{m} \tau_i P(t, T_i)\right)\left[S_{0,m}(t)\mathcal{N}(d_1) - K\mathcal{N}(d_2)\right], \\ d_1 &= \frac{\log\left(\frac{S_{0,m}(t)}{K}\right) + \frac{1}{2}\sigma^2(T_0 - t)}{\sigma\sqrt{(T_0 - t)}}, \\ d_2 &= d_1 - \sigma\sqrt{T_0 - t}, \end{aligned} \tag{2.14}$$

where σ is the volatility of the forward swap rate. This quantity is retrieved from market data.

With similar reasoning we can discuss the receiver swaption. One can derive that this is a European put option on the swap rate. Assuming Black's model, the value at time $t \leq T_0$ of a receiver swaption is given by (see [1]):

$$V_{\text{R-swaption}}(t) = N\left(\sum_{i=1}^{m} \tau_i P(t,T_i)\right)\left[K\mathcal{N}(-d_2) - S_{0,m}(t)\mathcal{N}(-d_1)\right], \tag{2.15}$$

where d_1 and d_2 are the same as in Equation (2.14).

If $K = S_{0,m}(t)$, then we call this an at the money (ATM) swaption.

2.2.7 Caps and floors

An interest rate cap is designed to provide insurance, for the holder which has a loan on a floating rate, against the floating rate rising above a certain level. This level is called the cap-rate K. A cap is the sum of a number of basic contracts, known as caplets, which are defined as follows:

Definition 2.4. Given two times $T_i > T_{i-1}$, with $\tau_i = T_i - T_{i-1}$, we define the T_{i-1}-caplet with rate K_i and nominal amount N_i as a contract that pays at time T_i:

$$N_i\tau_i \max(L(T_{i-1},T_i) - K_i, 0), \quad i = 1,2,\ldots,m.$$

At time T_{i-1} we observe $L(T_{i-1},T_i)$ in the market, but the payoff takes place at time T_i. A cap can be seen as m caplets with the same strike $K_i = K$ and notional $N_i = N$. The value of a cap at time $t < T_0$ is the sum of the values of the individual caplets at time t.

It is easy to see that a caplet is a European call contract. If we assume Black's model to value this option then the value of caplet i is given by:

$$\begin{aligned} \mathbf{Caplet}_i(t) &= N_i\tau_i P(t,T_i)\left[F_{lib}(t;T_{i-1},T_i)N(d_1) - K_iN(d_2)\right], \\ d_1 &= \frac{\log\left(\frac{F_{lib}(t;T_{i-1},T_i)}{K}\right) + \frac{1}{2}\sigma_i^2(T_0-t)}{\sigma_i\sqrt{(T_0-t)}}, \\ d_2 &= d_1 - \sigma_i\sqrt{T-t}. \end{aligned} \tag{2.16}$$

Here we assume the simply compounded LIBOR rate $L(T_{i-1},T_i)$, conditional on the information at time t, log-normal distributed with mean $F_{lib}(t,T_{i-1},T_i)$. The volatility parameter σ_i is retrieved from market data. Hence the value of a cap at time $t < T_0$ with Black's Formula is

given by:

$$V_{\text{cap}}(t) = \sum_{i=1}^{m} \mathbf{Caplet}_i(t),$$

with $\mathbf{Caplet}_i(t)$ from Equation (2.16).

An interest rate floor is designed to provide insurance, for the holder which has a loan on a floating rate, against the floating rate rising below a certain level. This level is called the floor-rate K. A floor is the sum of a number of basic contracts, known as floorlets. A floorlet differs from a caplet in the sense that it pays at time T_i:

$$N_i\tau_i \max(K_i - L(T_{i-1}, T_i), 0), \quad i = 1, 2, \ldots, m.$$

At time T_{i-1} we observe $L(T_{i-1}, T_i)$ in the market, but the payoff takes place at time T_i. A floor can be seen as m floorlets with the same strike $K_i = K$ and notional $N_i = N$. The value of a floor at time $t < T_0$ is the sum of the values of the individual floorlets at time t.

It is easy to see that a floorlet is a European put contract. If we assume Black's model to value this option then the value of floorlet i is given by:

$$\begin{aligned} \mathbf{Floorlet}_i(t) &= N_i\tau_i P(t, T_i)\left[K_i N(-d_2) - F_{lib}(t; T_{i-1}, T_i)N(-d_1)\right], \\ d_1 &= \frac{\log\left(\frac{F_{lib}(t;T_{i-1},T_i)}{K}\right) + \frac{1}{2}\sigma_i^2(T_0 - t)}{\sigma_i\sqrt{(T_0 - t)}}, \\ d_2 &= d_1 - \sigma_i\sqrt{T - t}. \end{aligned} \tag{2.17}$$

Hence the value of a floor at time $t < T_0$ with Black's Formula is given by:

$$V_{\text{floor}}(t) = \sum_{i=1}^{m} \mathbf{Floorlet}_i(t),$$

with $\mathbf{Floorlet}_i(t)$ from Equation (2.17).

2.3 Pricing swaptions under different measures

Let $\mathcal{T}_m = \{T_0, T_1, \ldots, T_m\}$ be a set of dates in year fractions, with T_0 being the swaption maturity and $T_1, \ldots, T_m$ the payment dates. We recall that the value of Pay IRS is given by Formula (2.11). Setting this equation to zero and solving for the fixed interest rate yields the swap rate at time t, see Equation (2.13).

$$S_{0,m}(t) = \frac{P(t, T_0) - P(t, T_m)}{\sum_{i=1}^{m} P(t, T_i)\tau_i} = \frac{P(t, T_0) - P(t, T_m)}{P_{1,m}(t)},$$

where we defined

$$P_{1,m}(t) := \sum_{i=1}^{m} P(t, T_i)\tau_i. \tag{2.18}$$

$P_{1,m}(t)$ is called the annuity. Note that the payoff of a payer swaption with strike K at time T_0 is given by the maximum of the value of the swap at time T_0 and 0. Hence

$$\begin{aligned} \left(V_{0,m}^{pay}(T_0)\right)^+ &= \left[NP(T_0, T_0) - NP(T_0, T_m) - \sum_{i=1}^{m} P(T_0, T_i)N\tau_i K\right]^+ \\ &= N\left[P(T_0, T_0) - P(T_0, T_m) - K\sum_{i=1}^{m} P(T_0, T_i)\tau_i\right]^+ \\ &= N\left[S_{0,m}(T_0)P_{1,m}(T_0) - KP_{1,m}(T_0)\right]^+ \\ &= NP_{1,m}(T_0)\left[S_{0,m}(T_0) - K\right]^+. \end{aligned} \tag{2.19}$$

This can be seen as a payoff of a European call on the swap rate. If we take $P_{1,m}(t)$ as a numeraire with the corresponding martingale measure $\mathbb{Q}^{1,m}$, then the time t value of the payer swaption is given by

$$V_{0,m}^{pay}(t) = NP_{1,m}(t)\mathbb{E}^{\mathbb{Q}^{1,m}}\left[\frac{P_{1,m}(T_0)\left[S_{0,m}(T_0)-K\right]^+}{P_{1,m}(T_0)}\middle|\mathcal{F}_t\right] = NP_{1,m}(t)\mathbb{E}^{\mathbb{Q}^{1,m}}\left[\left[S_{0,m}(T_0)-K\right]^+\middle|\mathcal{F}_t\right]. \tag{2.20}$$

We will call this martingale measure the swap measure. See Appendix A.2.1 for further explanation on this topic.

To price swaptions with Monte Carlo simulation, it is convenient to derive the swaption price under the T_0-forward measure. If we take $P(t,T_0)$, the price of a zero-coupon bond at time t with maturity T_0, as a numeraire corresponding to the T_0-forward measure $\mathbb{Q}^{T_0}$, then the time t value of the payer swaption is given by

$$V_{0,m}^{pay}(t) = NP(t,T_0)\mathbb{E}^{\mathbb{Q}^{T_0}}\left[\left(1-P(T_0,T_m)-K\sum_{i=1}^{m}\tau_i P(T_0,T_i)\right)^+\middle|\mathcal{F}_t\right]. \tag{2.21}$$

Chapter 3

The one-factor Hull-White model

The one-factor Hull-White model is one of the most popular short rate models, that models a mathematical variable (not observed in the market), the instantaneous short rate. The Hull-White model belongs to the class of affine term structure models, hence the logarithm of the bond price is a linear function of the state variables. The state variables are Gaussian. Moreover the Hull-White model can be fitted perfectly to the initial yield curve. The model is analytic tractable and given that, closed form formulas can be obtained for basic interest rate products like bond options, caps and swaptions. But the model has also disadvantages, it gives an inaccurate fit to the swaption market volatility skew. That is why we are looking for new short rate models to overcome the drawbacks of Hull-White. This chapter discusses the following topics.

- The constant volatility Hull-White model, see Section 3.1.
- The piecewise constant volatility one-factor Hull-White model, see Section 3.2.
- Analytic pricing formula for swaptions, see Section 3.3.
- Calibration of the one-factor Hull-White model, see Section 3.4.
- Implied volatility skew under the Hull-White model, see Section 3.5.

3.1 The constant volatility Hull-White model

The dynamics of the instantaneous short rate under the risk neutral measure are given by

$$dr(t) = [\theta(t) - ar(t)]dt + \sigma dW^0(t) = a\left[\frac{1}{a}\theta(t) - r(t)\right]dt + \sigma dW^0(t), \tag{3.1}$$

where $\theta(t)$ is a parametric function that replicates the currect term structure observed in the market, a the mean reversion rate and σ the volatility. This model is mean reverting, a desired property in interest rate modelling. From Equation (3.1) we see that if at time t, the rate $r(t)$ is above (below) $\frac{\theta(t)}{a}$, then the drift term becomes negative (positive) and the rate is pushed to the level $\frac{\theta(t)}{a}$. The speed at which the rate is pushed back to $\frac{\theta(t)}{a}$ is a. That is why we call a the mean reversion rate.

Using Itô's formula we get

$$r(t) = r(0)e^{-at} + \int_0^t \theta(u)e^{-a(t-u)}du + \sigma\int_0^t e^{-a(t-u)}dW^0(u). \tag{3.2}$$

The Hull-White model has an affine term structure, hence the zero-coupon bond price is given by (see [5]).

$$\begin{aligned} P(t,T) &= A(t,T)e^{-B(t,T)r(t)}, \\ \log\left(A(t,T)\right) &= -\frac{\sigma^2}{2}\int_t^T B^2(u,T)du + \int_t^T \theta(u)B(u,T)du, \\ B(t,T) &= \frac{1}{a}\left(1-e^{-a(T-t)}\right). \end{aligned} \tag{3.3}$$

To fit the initial term structure we take

$$\theta(t) = \frac{\partial}{\partial t}f(0,t) + af(0,t) + \frac{\sigma^2}{2a}(1-e^{-2at}), \tag{3.4}$$

where $f(0,t)$ is given by (2.4). Substituting (3.4) into (3.2) we can write $r(t)$ as

$$r(t) = r(0)e^{-at} + g(t) - g(0)e^{-at} + \sigma\int_0^t e^{-a(t-u)}dW^0(u), \tag{3.5}$$

where

$$g(t) = f(0,t) + \frac{\sigma^2}{2a^2}\left(1-e^{-at}\right)^2. \tag{3.6}$$

With this explicit formulation of the short rate, we can conclude that[1]:

- For any $t > 0$, the short rate $r(t)$ in the Hull-White model, is normally distributed.
- For any $t > 0$, there is a positive probability that $r(t) < 0$.

Substituting (3.4) into the formula for $\log\left(A(t,T)\right)$ in (3.3), we can obtain an explicit formula for the zero-coupon bond price

$$P(t,T) = \frac{P(0,T)}{P(0,t)}\exp\left\{B(t,T)f(0,t) - \frac{\sigma^2}{4a}B^2(t,T)(1-e^{-2at}) - B(t,T)r(t)\right\}. \tag{3.7}$$

To get rid of $f(0,t)$ in the expression above, we consider the zero mean process

$$dx(t) = -ax(t) + \sigma dW^0(t), \tag{3.8}$$

$$x(0) = 0. \tag{3.9}$$

Using Itô's formula we derive

$$x(t) = x(0)e^{-at} + \sigma\int_0^t e^{-a(t-u)}dW^0(u). \tag{3.10}$$

One easily sees that

$$r(t) = x(t) + g(t),$$

where $g(t)$ is given by Equation (3.6). Substituting this identity in (3.7) eliminates the $f(0,t)$ term. In this case the zero-coupon bond price is given by

[1] For more details we refer to [5]

$$P(t,T) = \frac{P(0,T)}{P(0,t)} \exp\left\{-G(t,T) - B(t,T)x(t)\right\}, \tag{3.11}$$

where

$$G(t,T) = \frac{\sigma^2}{2a} B(t,T)(1-e^{-at}) \left\{ \frac{B(t,T)}{2}(1+e^{-at}) + \frac{(1-e^{-at})}{a} \right\}.$$

3.2 The piecewise constant volatility Hull-White model

In this section we discuss the zero-coupon bond price for the one-factor Hull-White model with piecewise constant volatility. We assume that the instantaneous short rate is modelled by

$$r(t) = x(t) + g(t), \tag{3.12}$$

with $g(t)$ a deterministic function of time, which allows an exact fit to the initial zero-coupon bond curve. $x(t)$ satisfies the following SDE under the risk-neutral measure:

$$\begin{aligned} dx(t) &= -ax(t)dt + \sigma(t)dW^{\mathbb{Q}^0}(t) \\ x(0) &= 0 \end{aligned} \tag{3.13}$$

where $\sigma(t)$ is piecewise constant on intervals between $0 = t_0 < t_1 < t_2 < \ldots < t_n = T$, e.g. $\sigma(t) = \sigma_j$ for $t \in (t_{j-1}, t_j]$.

The advantage of a piecewise constant volatility function $\sigma(t)$, with respect to a constant volatility function σ, is the extra degree of freedom in the calibration process. With $\sigma(t)$ piecewise constant, we can calibrate the model to n swaptions, with maturities $t_1 < t_2 < \cdots < t_n$. The values of the piecewise constant volatility function are chosen such that the model implied swaption prices match the market prices.

Proposition 3.1. Define the piecewise constant volatility function by $\sigma(t) = \sigma_j$ for any $t \in (t_{j-1}, t_j]$, $j \in \{1, 2, \ldots, n\}$. Then the price at time t of the zero-coupon bond with maturity $T(= t_n)$ under a piecewise constant volatility Hull-White model is given by

$$P(t,T) = \frac{P^M(0,T)}{P^M(0,t)} \exp\left(\frac{1}{2}\left(V(t,T) - V(0,T) + V(0,t)\right) - B(t,T)x(t) \right), \tag{3.14}$$

with

$$\begin{aligned} B(t,T) &= \frac{1}{a}\left(1 - e^{-a(T-t)}\right), \\ V(t,T) &= \bar{V}(t,t_j) + \sum_{k=j}^{n-1} \bar{V}(t_k, t_{k+1}), \end{aligned}$$

where for every $(l,u) \subseteq (t_k, t_{k+1}]$

$$\bar{V}(l,u) = \int_l^u \sigma_{k+1}^2 B(s,T)^2 ds = \frac{\sigma_{k+1}^2}{2a^3}\left(e^{-2aT}(e^{au} - e^{al})(e^{au} + e^{al} - 4e^{aT}) + 2a(u-l)\right).$$

Proof. The proof is given in Appendix B.1. □

3.3 Analytic pricing formula for swaptions

For the one-factor Hull-White model, with piecewise constant volatility, an analytic formula to price swaptions exists. In this section we give this formula for a European swaption, whose underlying is a payer interest rate swap with notional N and strike K. As before, let

$$\mathcal{T}_m := \{T_0, T_1, \ldots, T_m\},$$

be year fraction times related to the option on the swap and

$$\tau := \{\tau_1, \ldots, \tau_m\},$$

where $\tau_i = T_i - T_{i-1}$. We assume the option maturity to be T_0. We have to satisfy two conditions such that an analytic price exists. The first condition is that the dynamics of

$$Z_i(t) = \frac{P(t, T_i)}{P(t, T_{i-1})},$$

can be expressed as

$$dZ_i(t) = m_i(t)Z_i(t)dt + v_i(t)Z_i(t)dW^0(t),$$

with the volatility proces $v_i(t)$ deterministic. The second assumption is $\frac{\partial P}{\partial r} < 0$. Both assumptions are satisfied for the constant and the piecewise constant volatility H-W model, see [5]. Under these assumptions the value at time $t \leq T_0$ is given by

$$\textbf{PSwaption}(t, \mathcal{T}_m, N, K) = N \sum_{i=1}^{m} c_i \left[P(t, T_0)P(T_0, T_i, x_1)\mathcal{N}(d_1) - P(t, T_i)\mathcal{N}(d_2)\right], \tag{3.15}$$

where

$$\begin{aligned} c_i &= \tau_i K \text{ for } i = 1, 2, \ldots, m-1, \\ c_m &= 1 + \tau_m K, \\ \mathcal{N}(s) &= \frac{1}{\sqrt{2\pi}} \int_{-\infty}^{s} e^{-p^2/2} dp, \end{aligned}$$

and x_1 is defined as the value of $x(T_0)$ that satisfies

$$\sum_{i=1}^{m} c_i P(T_0, T_i, x_1) = 1,$$

where $P(T_0, T_i, x_1)$ is calculated using Equation (3.14) and

$$\begin{aligned} d_1(P(T_0, T_i, x_1), T_0, T_i, \vartheta) &= \frac{\log\left(\frac{P(t,T_0)P(T_0,T_i,x_1)}{P(t,T_i)}\right) + \frac{\vartheta^2(T_0)}{2}}{\vartheta(T_0)}, \\ d_2(P(T_0, T_i, x_1), T_0, T_i, \vartheta) &= d_1(P(T_0, T_i, x_1), T_0, T_i, \vartheta) - \vartheta(T_0). \end{aligned} \tag{3.16}$$

In this equation $\vartheta(T)$ is given by:

$$\vartheta^2(T) = \nu(t, t_j) + \sum_{s=j}^{n-1} \nu(t_s, t_{s+1}),$$

where for any $t \in (t_s, t_e] \subseteq (t_{j-1}, t_j]$,

$$\nu(t_s, t_e) = \int_{t_s}^{t_e} v^2(u)du,$$

and

$$v(u) = [B(u, T_{i-1}) - B(u, T_i)]\,\sigma_i.$$

3.4 Calibration of the one-factor Hull-White model

For an extensive motivation of the calibration of the piecewise Hull-White model we refer to [6]. In this section we give a summary of the main ideas. If we want to use the model for pricing purposes, we have to determine a and $\sigma(t)$. The process of determining parameters is called calibration. To calibrate a model one chooses a set of calibration instruments, for example a set of swaptions. The parameters of the model are choosen in such a way that the model generated prices match the market prices of the calibration instruments. In the Hull-White model with piecewise constant volatility, we have to determine the mean reversion and the piecewise volatility function $\sigma(t)$. In this case we do not calibrate the mean reversion rate a. This parameter is fixed, in most cases $a \in [0.01, 0.05]$.

When the mean reversion rate is fixed the piecewise constant volatility function is calibrated to the calibration instruments. For example, if we want to calibrate the model to the market data, one can choose the following calibration instruments.

Option Maturity	Tenor	Swap type	Strike
1Y	9Y	PAYER	ATM
4Y	6Y	PAYER	ATM
7Y	3Y	PAYER	ATM
9Y	1Y	PAYER	ATM

Table 3.1: Set of Swaption calibration instruments.

When a is chosen, one can calibrate the volatility step function in a bootstrap fashion, the function is piecewise constant between successive option maturities. So given the set of n swaptions, with maturities $S_1 < S_2 < \ldots < S_n$, then $\sigma(t) = \sigma_i$ for all $t \in [S_{i-1}, S_i]$. Given the first swaption, $\sigma(t) = \sigma_1$ is chosen such that

$$\textbf{PSwaption}(0, \mathcal{T}_m^1, N, \text{ATM})\{\sigma_1\} = V^1_{\text{P-swaption}}(0)\{\sigma^1_{\text{market}}\},$$

where $\textbf{PSwaption}(0, \mathcal{T}_m^1, N, \text{ATM})$ given by (3.16), the analytic pricing formula for swaptions under the one-factor Hull-White model and $V^1_{\text{P-swaption}}(0)$ given by (2.14), Black's pricing formula for swaptions. The superscript in $\mathcal{T}_m^1$ is to make clear that we have to take the set of payment dates of the underlying swap of the first swaption. Note that the volatility parameter σ which we use in Black's formula is not the same as σ_1. We take in Black's formula the volatility observed in the swaption market. Having $\sigma_1, \cdots, \sigma_{i-1}$, we determine σ_i by

$$\textbf{PSwaption}(0, \mathcal{T}_m^i, N, \text{ATM})\{\sigma_1, \cdots, \sigma_i\} = V^i_{\text{P-swaption}}(0)\{\sigma^i_{\text{market}}\}$$

This method is fast because at each step we have to solve one equation with one unknown and there exist fast and stable analytic or numerical methods to calculate the swaption prices in the one-factor Hull-White model.

3.5 Implied volatility skew under the Hull-White model.

In this section we show a couple of calibration results of the Hull-White model to market data. We illustrate that the Hull-White model is not able to fit the whole volatility skew, only the instrument to which we calibrate. This will be the starting point of this thesis. We try to find better short rate models which are more powerful in fitting the market volatility skew. In Chapter 4 we explain the Cheyette model and later on we discuss a stochastic volatility (SV) model.

The results in this section are based on the USD data for date 31 May 2010. Our set of calibration instruments contains nine payer at the money (ATM) swaptions such that maturity plus tenor equals ten years. We call this a strip of co-terminal swaptions. See Table 3.2.

Option Maturity	Tenor	Swap type	Strike
1Y	9Y	PAYER	ATM
2Y	8Y	PAYER	ATM
⋮	⋮	⋮	⋮
9Y	1Y	PAYER	ATM

Table 3.2: Set of Swaption calibration instruments.

The mean reversion is chosen to be $a = 0.03$. The calibration of the piecewise constant function $\sigma(t)$ is done as described in Section 3.4, using the analytic pricing formula for swaptions in the piecewise constant Hull-White model. In this case the set $[0 = S_0, S_1, \dots S_n]$ is given by $[0, 1, 2, \dots, 10]$. The result of the calibration process is given in Table 3.3.

$t \in (l, u]$	$(0,1]$	$(1,2]$	$(2,3]$	$(3,4]$	$(4,5]$	$(5,6]$	$(6,7]$	$(7,8]$	$(8,9]$	$(9,10]$
$\sigma_i \times 10^{-2}$	1.244	1.219	1.123	1.119	1.126	1.009	0.943	0.831	0.662	0.662

Table 3.3: Piecewise constant $\sigma(t)$, with mean reversion $a = 0.03$.

We can use this set of parameters to price interest rate products. For example, to price swaptions along a set of strikes, not necessarily ATM, using the analytic pricing formula for swaptions. Our choice is to show results for a X into Y year swaption for strikes

$$K \in \text{ATM} + \{-3\%, -2\%, -1\%, -0.25\%, 0, 0.25\%, 1\%, 2\%, 3\%\}\,.$$

To calculate the implied volatility we make use of Black's formula. Given a Hull-White model price for a swaption, we find the implied volatility σ that yields the same swaption price using Black's formula. If the Hull-White model has a satisfactory performance to fit the market skew, then the implied volatility skew should be close to the market volatility skew.

3.5.1 Results 1Y into 9Y swaption

In this subsection the results for a 1 year maturity swaption with 9 year tenor are given. In Table 3.4 the Hull-White price, model implied volatility and market volatility are summarized.

Strike	Hull-White Price	Implied Volatility	Market Volatility
ATM - 2%	1566.65	0.54187	0.371485
ATM - 1%	859.81	0.408656	0.346571
ATM - 0.25%	444.998	0.355662	0.341898
ATM	339.465	0.341999	0.342297
ATM + 0.25%	251.593	0.329736	0.342696
ATM + 1%	84.7359	0.299305	0.347294
ATM + 2%	12.1729	0.268851	0.356597
ATM + 3%	0.954037	0.245723	0.367135

Table 3.4: Results of a 1Y into 9Y swaption. ATM ≈ 0.0321581

In Figure 3.1 the implied volatility skew is drawn in comparison to the market skew.

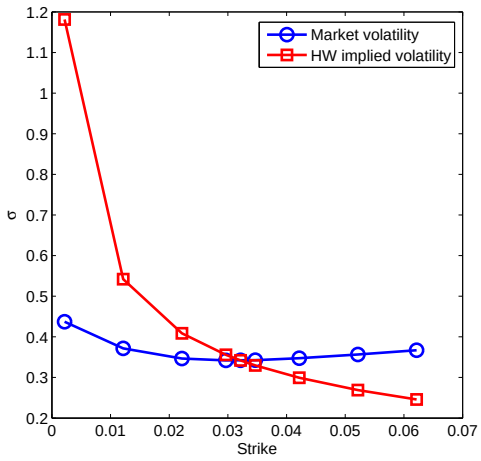

Figure 3.1: 1Y9Y: Model implied volatility skew compared to market skew.

3.5.2 Results 9Y into 1Y swaption

In this subsection the results for a 9 year maturity swaption with 1 year tenor are given. In Table 3.5 the Hull-White price, model implied volatility and market volatility are summarized.

Strike	Hull-White Price	Implied Volatility	Market Volatility
ATM - 3%	238.829	0.431434	0.313412
ATM - 2%	177.804	0.317207	0.265022
ATM - 1%	125.243	0.261441	0.238545
ATM - 0.25%	92.4272	0.234348	0.228753
ATM	82.8262	0.226973	0.227276
ATM + 0.25%	73.8975	0.220223	0.225798
ATM + 1%	51.0765	0.202977	0.225134
ATM + 2%	29.2048	0.185027	0.228503
ATM + 3%	15.4143	0.170939	0.234153

Table 3.5: Results of a 1Y into 9Y swaption. ATM ≈ 0.0419482

In Figure 3.2 the implied volatility skew is drawn in comparison to the market skew.

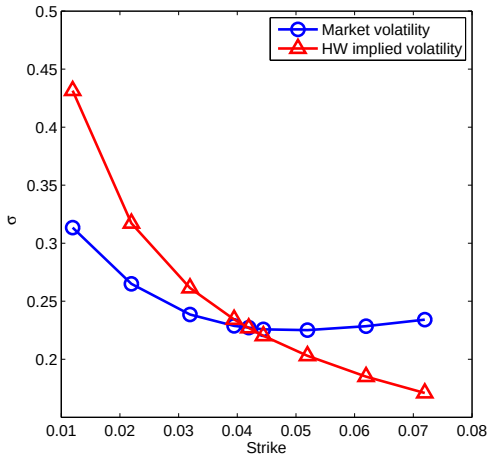

Figure 3.2: 9Y1Y: Model implied volatility skew compared to market skew.

3.5.3 Conclusion

From these results we see that Hull-White performs poorly when trying to fit the market volatility skew. As expected we matched the ATM-level, since we calibrated the model to this strike. For small strikes we have a big mismatch with the market skew. In this case the model overprices the swaption and for high strikes we underprice the swaption. This is one of the main drawbacks of the Hull-White model. The model performs bad in fitting the market volatility skew, as we have seen in the previous subsection. For this reason we look for other short rate models, to improve the fit to the market volatility skew. In Chapter 4 we start with a discussion of the Cheyette model with constant elasticity of variance and displaced diffusion formulation.

Chapter 4

The Cheyette model without Stochastic Volatility

In this chapter we give a formulation of the constant elasticity of variance and displaced diffusion formulation of the Ritchken-Sankarasubramanian model, without stochastic volatility. A stochastic volatility formulation will be discussed in Chapter 5. Another more convenient name for the Ritchken-Sankarasubramanian model is the Cheyette model. These models are embedded in the HJM framework for the instantaneous forward rates. The aim of introducing this kind of models is to get a better fit to the market skew of swaption volatilities. This chapter discusses the following topics.

- Theoretical background, see Section 4.1.
- CEV and DD formulation of the Cheyete model, see Section 4.2.
- Brief discussion of the CEV formulation, see Section 4.3.
- Displaced Diffusion model, see Section 4.4.

4.1 Theoretical background

In this section we give the main results without all proofs. For details about the derivations, we refer to [4].

The Cheyette model is an instantaneous short rate model embedded in the HJM-framework that models the instantaneous forward rates. In the HJM-framework we assume that the dynamics under the risk-neutral measure of the instantaneous forward rates are given by:

$$\begin{aligned} df(t,T) &= \alpha_f(t,T)dt + \sigma(t,T)dW^{\mathbb{Q}^0}(t), \\ f(0,T) &= f^{\text{mkt}}(0,T), \end{aligned} \tag{4.1}$$

where f^{mkt} represents the market instantaneous short rate at time $t = 0$, for maturity T. In order for this model to be arbitrage free, the drift term must be of the form:

$$\alpha_f(x,y) = \sigma(x,y)\int_x^y \sigma(x,s)ds.$$

Substituting this expression into the dynamics (4.1), and integrating both sides from 0 to t, yields

$$f(t,T) = f(0,T) + \int_0^t \sigma(u,T)\left(\int_u^T \sigma(u,s)ds\right)du + \int_0^t \sigma(u,T)dW^{\mathbb{Q}^0}(u).$$

Hence, since $r(t) = f(t,t)$, the instantaneous short rate given by the HJM-framework is

$$r(t) = f(0,t) + \int_0^t \sigma(u,t)\left(\int_u^t \sigma(u,s)ds\right)du + \int_0^t \sigma(u,t)dW^{\mathbb{Q}^0}(u). \tag{4.2}$$

From the equation above, we can see that the time variable t appears in the stochastic integral as an integration upper bound and as part of the integrand function, which in general is not a Markov process. For more information on this topic see [9]. In order to get a Markovian process, one needs a restriction on the volatilities $\sigma(x,y)$ of all forward rates. If we assume them to be of the form

$$\begin{aligned}\sigma(x,y) &= \eta(x,x)k(x,y),\\ k(x,y) &= \exp\left(-\int_x^y \kappa(v)dv\right),\end{aligned}$$

where $\eta(x,x)$ is the instantaneous volatility of the spot interest rate and $\kappa(v)$ is some deterministic function, then this will lead to a one- or two-state Markovian term-structure model. See also [9]. Calculating the differential of (4.2) with this choice of $\sigma(x,y)$ yields:

$$dr(t) = \left(\kappa(t)\left[f(0,t) - r(t)\right] + y(t) + \frac{\partial f(0,t)}{\partial t}\right)dt + \eta(t,t)dW^{\mathbb{Q}^0}(t), \tag{4.3}$$

$$dy(t) = \left(\eta^2(t,t) - 2\kappa(t)y(t)\right)dt, \tag{4.4}$$

where $y(t)$ represents the accumulated variance for the forward rate up to date t which captures the path dependence of the process, and has the form

$$y(t) = \int_0^t \sigma^2(u,t)du.$$

Note that $\sigma^2(u,t)$ is allowed to be non-deterministic. In order to avoid the computation of the derivative of the instantaneous forward rate we model:

$$x(t) = r(t) - f(0,t). \tag{4.5}$$

The differential is given by $dx(t) = dr(t) - \frac{\partial f(0,t)}{\partial t}dt$. Hence the dynamics of $x(t)$ are

$$\begin{aligned}dx(t) &= \left(y(t) - \kappa(t)x(t)\right)dt + \eta(t,t)dW^{\mathbb{Q}^0}(t),\\ dy(t) &= \left(\eta^2(t,t) - 2\kappa(t)y(t)\right)dt,\end{aligned} \tag{4.6}$$

with initial conditions $x(0) = y(0) = 0$. One can show that for this setup in the HJM framework, the price at time t of a zero-coupon bond, maturing at time T, is:

$$P(t,T) = \frac{P^M(0,T)}{P^M(0,t)}e^{-x(t)B(t,T) - \frac{1}{2}y(t)B^2(t,T)}, \tag{4.7}$$

with $P^M(0,t)$ the zero-coupon bond price observed in the market and $B(t,T) = \int_t^T k(t,x)dx$.

Proof. See Appendix B.2. □

Moreover when we assume the mean reversion parameter $\kappa(t)$ to be constant, $\kappa(t) = a$, then $B(t,T)$ is given by

$$B(t,T) = \int_t^T e^{-\int_t^x a dv} dx = \int_t^T e^{-a(x-t)} = \frac{1}{a}\left(1 - e^{-a(T-t)}\right). \tag{4.8}$$

For some purposes it is convenient to work with the dynamics of $x(t)$ under the T-forward measure, for example in a Monte Carlo implementation. This means that we have to change the martingale measure $\mathbb{Q}^0$, corresponding to the money market account, $M(t) = \exp\left(\int_0^t r(s)ds\right)$ as a numeraire, to a martingale measure $\mathbb{Q}^T$ corresponding to the zero-coupon bond with maturity T as a numeraire. We briefly describe the steps to derive the dynamics of $x(t)$ under the T-forward measure:

Denote the Radon Nikodym derivative process by $\zeta(t)^{0,T} = \frac{d\mathbb{Q}^T}{d\mathbb{Q}^0}$ in $\mathcal{F}_t$. In this case $\zeta(t)^{0,T} = \frac{M(0)}{P(0,T)}\frac{P(t,T)}{M(t)}$, which is a martingale under $\mathbb{Q}^0$. The differential is given by

$$d\zeta(t)^{0,T} = -\zeta(t)^{0,T} B(t,T)\eta(t,t) dW^{\mathbb{Q}^0}(t).$$

Solving this SDE yields

$$\zeta(t)^{0,T} = \exp\left(-\frac{1}{2}\int_0^t B^2(s,T)\eta(s,s)^2 ds - \int_0^t B(s,T)\eta(s,s) dW(s)\right).$$

Taking $B(t,T)\eta(t,t)$ as the Girsanov kernel and by defining

$$dW^{\mathbb{Q}^T}(t) := dW^{\mathbb{Q}^0}(t) + B(t,T)\eta(t,t)dt,$$

we find that $W^{\mathbb{Q}^T}(t)$ is a standard Brownian motion under $\mathbb{Q}^T$. This is a result from Girsanov's Theorem. Substituting $dW^{\mathbb{Q}^0}(t) = dW^{\mathbb{Q}^T}(t) - B(t,T)\eta(t,t)dt$ in Equation (4.9) gives the dynamics of $x(t)$ under the forward measure:

$$\begin{aligned} dx(t) &= \left(-\kappa(t)x(t) + y(t) - B(t,T)\eta^2(t,t)\right)dt + \eta(t,t)dW^{\mathbb{Q}^T}(t), \\ dy(t) &= \left(\eta^2(t,t) - 2\kappa(t)y(t)\right)dt. \end{aligned} \tag{4.9}$$

4.2 CEV and DD formulation of the Cheyete model

In this section we discuss the constant elasticity of variance (CEV) and displaced diffusion (DD) formulation of the Cheyette model. In the CEV formulation the instantaneous volatility $\eta(t,t)$[1] is given by:

$$\eta(t,x(t)) := \sigma(t)[r(t)]^{\gamma(t)}. \tag{4.10}$$

In the DD formulation the instantaneous volatility is given by

$$\eta(t,x(t)) := \sigma(t)[\gamma(t)r(t) + (1-\gamma(t))R_0], \tag{4.11}$$

where $\sigma(t)$ and $\gamma(t)$ are parameters which one has to calibrate to appropriate market data. We allow both to vary in a piecewise constant time-dependent manner. In the DD formulation R_0 is a constant.

[1]Note that we replace $\eta(t,t)$ by $\eta(t,x(t))$. Since $\eta(t,t)$ is allowed to depend on the state variable $x(t)$. Writing $\eta(t,x(t))$ instead of $\eta(t,t)$ makes this more clear.

4.3 Brief discussion of the CEV formulation

We will briefly discuss the CEV formulation of the Cheyette model. First, the term $r(t)^{\gamma(t)}$ can become a complex number if $r(t) < 0$. This creates numerical complications in the diffusion part. To avoid this, one can use a different formulation for the instantaneous volatility, such as

$$\eta(t, x(t)) = \sigma(t) \left| r(t) \right|^{\gamma(t)} .$$

This choice is valid, since under the HJM framework there is complete freedom on the choice of the instantaneous volatility.

Another inconvenience arrises if $r(t) \to 0$, since the term $|r(t)|^{\gamma(t)}$ might go to infinity. We can avoid this problem by setting $|r(t)|^{\gamma(t)} = 0$ for $r(t) \in [-\delta, \delta]$ and small values of δ. But then the empirical distribution of the forward rate has a spike near low levels. Another possibility is to set $|r(t)|^{\gamma(t)} = \delta^{\gamma(t)}$. In this case we get rid of this peak. Since we allow $\gamma(t)$ to take negative values. The drawback is that it is possible that we obtain a bi-model distribution for $x(t)$. So to avoid this, a domain for the pair (σ, γ) has to be defined on a regular basis such that this never happens. But this is not an easy task. Further details about this model and these issues can be found in [7].

The calibration of this model is done so far by Monte Carlo methods, a discussion of the calibration part can be found in [6]. The model can be calibrated to two swaptions with two different strike levels per maturity. For example, take a set of swaptions where for each maturity we have a payer swaption with strike ATM + 0.5% and a receiver swaption with strike ATM − 0.5%. Because the model has two degrees of freedom, we can choose $\gamma(t)$ and $\sigma(t)$ such that both options are priced back with the model. Hence a better fit around the ATM-level of the model implied volatility skew to the swaption market volatility skew is expected.

4.4 Displaced Diffusion model

Because of the drawbacks found in the CEV formulation of the Cheyette model we will investigate the DD formulation of the Cheyette model. In this model we take for the instantaneous volatility

$$\eta(t, x(t)) = \sigma(t) \left[\gamma(t) r(t) + (1 - \gamma(t)) R_0 \right] . \tag{4.12}$$

We restrict $\gamma(t)$ to take values in $[0, 1]$. In this section we discuss a pricing method to approximate the swaption prices under the DD model. We discuss the following topics:

- Dynamics of the swap rate under the swap measure.
- Approximation of the swap rate dynamics.
- Pricing formulas.
- Remarks on the approximations.
- Validation of the approximation method.

4.4.1 Dynamics of the swap rate under the swap measure

For the DD formulation of the Cheyette model, we want to derive the dynamics of the swap rate under the annuity measure (or equivalent swap measure). There is literature available [10] on how to do this for general dynamics under the risk-neutral measure. We refer the reader to Appendix A for more details. To apply what is discussed in Appendix A to the DD model, we note that the model can be written as

$$\begin{aligned} dx(t) &= a\left(\frac{y(t)}{a} - x(t)\right)dt + \eta(t, x(t))dW^{\mathbb{Q}^0}, \\ \eta(t, x(t)) &= \sigma(t)\left[\gamma(t)r(t) + (1-\gamma(t))R_0\right], \\ x(0) &= 0. \end{aligned}$$

where

$$y(t) = \int_0^t \eta(s, x(s))^2 e^{-2(t-s)}ds.$$

With the notation given in (A.1),

$$\begin{aligned} A &= a, \\ \theta &= \frac{1}{a}\int_0^t \eta(s, x(s)^2 e^{-2(t-s)}ds, \\ \alpha &= 1, \\ \beta &= 0, \\ \Sigma &= \eta(t, x(t)). \end{aligned} \tag{4.13}$$

Note that A, θ, Σ and $V(t) = 1$ are adapted processes to the filtration $\mathcal{F}$ generated by the Brownian motion under the risk-neutral measure $\mathbb{Q}^0$. The swap rate dynamics under the swap measure are given by

$$\begin{aligned} dS_{0,m}(t) &= \left\{\sum_{i=0}^{m} q_i^S(t)B(t, T_i)\right\}\sigma(t)\left[\gamma(t)r(t) + (1-\gamma(t))R_0\right]dW^{\mathbb{Q}^{1,m}}(t) \\ &= \frac{\partial S_{0,m}(t)}{\partial x}\sigma(t)\left[\gamma(t)r(t) + (1-\gamma(t))R_0\right]dW^{\mathbb{Q}^{1,m}}(t), \end{aligned} \tag{4.14}$$

with the coefficients $q_i^S(t)$ as in Equation (A.8).

4.4.2 Approximation of the swap rate dynamics

In this subsection we make some approximations to the derived swap rate dynamics for the DD model. The approximations are made to replace the non-deterministic terms by time-depenent terms. Once this is done, we can obtain closed form formulas of swaption prices.

Note that we can rewrite the swap rate dynamics in Equation (4.14) as

$$dS_{0,m}(t) = \left[\frac{\partial S_{0,m}(t)}{\partial x}\frac{\gamma(t)r(t) + (1-\gamma(t))R_0}{\gamma(t)S_{0,m}(t) + (1-\gamma(t))R_0}\right]\left(\gamma(t)S_{0,m}(t) + (1-\gamma(t))R_0\right)\sigma(t)dW^{\mathbb{Q}^{1,m}}(t), \tag{4.15}$$

see [11]. To remove part of the randomness we replace all $\mathbb{Q}^{1,m}$ martingale terms (and factors) by their time zero values. The only non-deterministic term which is not a martingale under the swap measure is $r(t)$. One can make several suggestions to remove the randomness. One possibility is to set $r(t) \approx \mathbb{E}^{\mathbb{Q}^{1,m}}[r(t)]$. Another, more crude estimate is to replace $r(t)$ by $r(t)|_{x(t)=0} = f(0,t)$ (see Equation (4.5)). Because replacing $r(t)$ by its expectation is non trivial, we choose the latter option. Hence we approximate the dynamics of the swap rate under the swap measure by the following SDE.

$$dS_{0,m}(t) \approx (\gamma(t)S_{0,m}(t) + (1-\gamma(t))R_0)\,\lambda(t)\sigma(t)dW^{\mathbb{Q}^{1,m}}(t), \tag{4.16}$$

with

$$\lambda(t) = \left[\left.\frac{\partial S_{0,m}(t)}{\partial x}\right|_{q_i^S(0)} \frac{\gamma(t)f(0,t) + (1-\gamma(t))R_0}{\gamma(t)S_{0,m}(0) + (1-\gamma(t))R_0} \right],$$

where

$$\left.\frac{\partial S_{0,m}(t)}{\partial x}\right|_{q_i^S(0)} = \sum_{i=0}^{m} q_i^S(0)B(t,T_i).$$

4.4.3 Pricing Formulas

If we assume the displacement parameter $\gamma(t)$ to be constant, then we can derive semi-exact pricing formulas. We distinguish two cases, $\gamma = 0$ and $\gamma > 0$.

Pricing formula for $\gamma > 0$

To derive the pricing formula we define

$$\overline{S}_{0,m}(t) = \gamma S_{0,m}(t) + (1-\gamma)R_0, \tag{4.17}$$
$$\overline{K} = \gamma K + (1-\gamma)R_0. \tag{4.18}$$

Now it is easy to see that $S_{0,m}(t) - K = \frac{1}{\gamma}\left[\overline{S}_{0,m}(t) - \overline{K}\right]$. The differential of $\bar{S}_{0,m}(t)$ is given by

$$\begin{aligned} d\bar{S}_{0,m} &= d\left(\gamma S_{0,m}(t)\right) + d\left((1-\gamma)R_0\right) \\ &= \gamma d\left(S_{0,m}(t)\right) \approx \gamma\lambda(t)\sigma(t)\bar{S}_{0,m}(t)dW^{\mathbb{Q}^{1,m}}(t). \end{aligned}$$

Hence $\bar{S}_{0,m}(t)$ has an (approximate) log-normal distribution. The price of the payer swaption in terms of the new variables is

$$V_{0,m}^{pay}(0) = P_{1,m}(0)\mathbb{E}^{\mathbb{Q}^{1,m}}\left[(S_{0,m}(T_0) - K)^+\right] = \frac{P_{1,m}(0)}{\gamma}\mathbb{E}^{\mathbb{Q}^{1,m}}\left[\left([\bar{S}_{0,m}(T_0) - \overline{K}]\right)^+\right].$$

If we solve the expectation, then we obtain Black's Formula with a specific volatility. To prove this Proposition 4.4.1 is helpful.

Proposition 4.4.1. Let $x(t)$ be some stochastic process with dynamics

$$\begin{aligned} dx(t) &= \nu(t)x(t)dW(t), \\ x(0) &= x_0, \end{aligned}$$

where $W(t)$ is a standard Brownian motion and $\nu(t)$ some deterministic function of time. Then

$$\mathbb{E}\left[(x(t)-K)^+\right] = x_0\mathcal{N}(d_1) - K\mathcal{N}(d_2),$$

where

$$\begin{aligned} d_1 &= \frac{\log(x_0/K) + \frac{1}{2}\bar{\sigma}^2}{\bar{\sigma}}, \\ d_2 &= d_1 - \bar{\sigma}, \\ \bar{\sigma}^2 &= \int_0^t \nu(s)^2 ds, \\ \mathcal{N}(x) &= \int_{-\infty}^x \frac{1}{\sqrt{2\pi}} e^{-\frac{1}{2}s^2} ds. \end{aligned}$$

This is Black's formula with Black's volatility $\sigma^2 = \bar{\sigma}^2/t$.

Proof. See Appendix B.3. □

Hence the price of a payer swaption at time 0 is given by the following formula

$$V_{0,m}^{pay}(0) = \frac{P_{1,m}(0)}{\gamma}\left(\bar{S}_{0,m}(0)\mathcal{N}(d_1) - \bar{K}\mathcal{N}(d_2)\right), \tag{4.19}$$

where

$$\begin{aligned} d_1 &= \frac{\log(\bar{S}_{0,m}(0)/\bar{K}) + \frac{1}{2}\bar{\sigma}^2}{\bar{\sigma}}, \\ d_2 &= d_1 - \bar{\sigma}, \\ \bar{\sigma}^2 &= \gamma^2 \int_0^t \sigma(s)^2\lambda(s)^2 ds. \end{aligned}$$

Note that we have derived a semi-analytic formula for the swaption price, since $\int_0^t \sigma(s)^2\lambda(s)^2 ds$ has no explicit expression. $\lambda(t)$ depends on the instantaneous forward rate $f(0,t)$ which we observe in the market. To calculate this integral numerically we propose to use the Trapezoidal rule. Divide $[0,t]$ in an equidistant grid with $N+1$ points and make the following approximation.

$$\int_0^t g(s)ds \approx \frac{t}{N}\left\{\frac{g(0)+g(t)}{2} + \sum_{i=1}^{N-1} g\left(i\frac{t}{N}\right)\right\}.$$

Pricing formula for $\gamma = 0$

If we take $\gamma = 0$ then (4.16) simplifies to

$$dS_{0,m}(t) \approx R_0\lambda(t)\sigma(t)dW^{\mathbb{Q}^{1,m}}(t),$$

with

$$\lambda(t) = \left.\frac{\partial S_{0,m}(t)}{\partial x}\right|_{q_i^S(0)} = \sum_{i=0}^m q_i^S(0)B(t,T_i).$$

In this case $S_{0,m}(t)$ has a normal distribution. To calculate the expectation and variance note that

$$S_{0,m}(t) = S_{0,m}(0) + \int_0^t \sigma(s)\lambda(s)R_0 dW^{\mathbb{Q}^{1,m}}(s).$$

Simple calculations show that

$$\bar{\mu} = S_{0,m}(0),$$

and

$$\bar{\sigma}^2 = R_0^2 \int_0^t \sigma(s)^2\lambda(s)^2 ds = R_0^2 \int_0^t \sigma(s)^2 \left(\sum_{i=0}^m q_i^S(0)B(s,T_i)\right)^2 ds.$$

Under the assumption of a piecewise constant $\sigma(t)$ this integral has an analytic solution. Suppose $\sigma(t)$ is piecewise constant on intervals $0 = s_0 < s_1 < s_2 < \ldots < s_p = t$, then

$$\begin{aligned}\int_0^t \sigma(s)^2\lambda(s)^2 ds &= \sum_{i=1}^p \sigma_i^2 \int_{s_{i-1}}^{s_i} \sum_{j,k=0}^m q_i^S(0)q_k^S(0)B(s,T_j)B(s,T_k)ds \\ &= \sum_{i=1}^p \sigma_i^2 \sum_{j,k=0}^m q_i^S(0)q_k^S(0) \int_{s_{i-1}}^{s_i} B(s,T_j)B(s,T_k)ds.\end{aligned}$$

Some calculus shows that

$$\begin{aligned}\int_l^u B(s,T_j)B(s,T_k)ds = \quad & \frac{1}{a^3}\Big(a(u-l) - e^{-a(T_k-u)} + e^{-a(T_k-l)} - e^{-a(T_j-u)} + e^{-a(T_j-l)} \\ & + \frac{1}{2}e^{-a(T_j+T_k-2u)} - \frac{1}{2}e^{-a(T_j+T_k-2l)}\Big).\end{aligned}$$

Hence we can calculate the expectation and variance of the corresponding normal distribution analytic.

The time zero price of a payer swaption is given by

$$\begin{aligned}V_{0,m}^{pay}(0) &= P_{1,m}(0)\mathbb{E}^{\mathbb{Q}^{1,m}}\left[(S_{0,m}(T_0) - K)^+\right] \\ &= P_{1,m}(0)\left[\bar{\sigma}\mathcal{N}'(\alpha) + (S_{0,m}(0) - K)\mathcal{N}(\alpha)\right],\end{aligned}$$

where

$$\begin{aligned}\alpha &= \frac{S_{0,m}(0) - K}{\bar{\sigma}} \\ \mathcal{N}'(x) &= \frac{1}{\sqrt{2\pi}}e^{-\frac{1}{2}x^2}\end{aligned}$$

Proposition 4.4.2 proves this result.

Proposition 4.4.2. Let X be a normally distributed random variable with expectation μ and standard deviation σ. Fix $K \in \mathbb{R}$ then

$$\mathbb{E}[(X-K)^+] = \sigma\mathcal{N}'(\alpha) + (\mu - K)\mathcal{N}(\alpha),$$

where

$$\alpha = \frac{\mu - K}{\sigma},$$
$$\mathcal{N}'(x) = \frac{1}{\sqrt{2\pi}} e^{-\frac{1}{2}x^2}.$$

Proof. Define Z to be a standard normal random variable and $f(x)$ the standard normal density then:

$$\begin{aligned}\mathbb{E}[(X-K)^+] = \mathbb{E}[(Z\sigma + \mu - K)^+] &= \int_{-\infty}^{\infty} (z\sigma + \mu - K)^+ f(z)dz \\ &= \sigma \int_{-\alpha}^{\infty} z f(z)dz + (\mu - K)\int_{-\alpha}^{\infty} f(z)dz \\ &= \sigma\mathcal{N}'(\alpha) + (\mu - K)\mathcal{N}(\alpha).\end{aligned}$$

□

4.4.4 Remarks on the approximations

We approximated the non-deterministic terms in the swap rate dynamics by deterministic, time-dependent terms. With these dynamics we derived (semi-)analytic formulas to price payer swaptions. In this subsection we discuss the quality of the approximations we made. Recall that we had to remove non-deterministic terms in

$$\frac{\partial S_{0,m}(t)}{\partial x} \frac{\gamma(t)r(t) + (1-\gamma(t))R_0}{\gamma(t)S_{0,m}(t) + (1-\gamma(t))R_0}.$$

We made the following approximations:

1. $S_{0,m}(t) \approx S_{0,m}(0)$.
2. $q_i^S(t) \approx q_i^S(0)$.
3. $r(t) \approx f(0,t)$.

The first approximation is equivalent to replacing the non-deterministic term by its expectation, because the swap rate is a martingale under the swap measure.

The second approximation deals with $\frac{\partial S_{0,m}(t)}{\partial x}$. By this we approximate:

$$\frac{\partial S_{0,m}(t)}{\partial x} = \sum_{i=0}^{m} q_i^S(t)B(t,T_i) \approx \sum_{i=0}^{m} q_i^S(0)B(t,T_i).$$

If we look at the expressions of $q_i^S(t)$, given in Equation (A.8), we see that the coefficients are products of $\mathbb{Q}^{1,m}$ martingales. This implies that we approximate all non-deterministic terms

by their expectations, or equivalent their time zero values. If we assume independence between $P(t,T_i)/P_{0,m}(t)$ and $S_{0,m}(t)$, we make an unbiased approximation i.e.:

$$\mathbb{E}^{\mathbb{Q}^{1,m}}\left(q_i^S(t)\right) = q_i^S(0), \quad \forall i \in \{0,1,\cdots,m\},$$

and hence

$$\mathbb{E}^{\mathbb{Q}^{1,m}}\left(\frac{\partial S_{0,m}(t)}{\partial x}\right) = \frac{\partial S_{0,m}(0)}{\partial x}.$$

The third approximation deals with the term $r(t)$. We noticed in Section 4.4.2 that this is a very crude estimate, because we do not take properties of $x(t)$ into account. The reason to ignore $x(t)$, is that its expectation is non-trivial. To see this note that:

$$x(t) = \int_0^t e^{-a(t-u)}y(u)du + \int_0^t e^{-a(t-u)}\eta(u,r(u))dW^{\mathbb{Q}^0}(u),$$

where

$$y(t) = \int_0^t \left[\sigma(s)\left(\gamma(s)r(s) + (1-\gamma(s))R_0\right)e^{-a(t-s)}\right]^2 ds.$$

If $\gamma(t) \neq 0$ then $y(t)$ is non-deterministic. This makes the Riemann integral, in the expression of $x(t)$, path-dependent, which makes the expectation of $x(t)$ non-trivial. If all randomness was captured in the Itô integral, then it is possible to find a deterministic expression for the expectation. Unfortunately this is not the case.

We expect that small values of the displacement parameter γ will minimize the effects of the third approximation. With small values we mean $\gamma \in (-\delta,\delta)$ for small $\delta \in \mathbb{R}^+$. We have good hope that the first approximation works quite well, under the assumption that the swap rate is a low variance martingale under the swap measure. If there is no independence between $P(t,T_i)/P_{0,m}(t)$ and $S_{0,m}(t)$, we expect a bias in the second approximation. Further we expect that small values of the volatility parameter σ reduces the effects of all the approximations we made.

In the next subsection we investigate how well these approximations work in practice.

4.4.5 Validation of the approximation method.

To investigate the approximations, we compare them with a Monte Carlo benchmark method, for different sets of parameters. In the DD model we have four parameters: a mean reversion parameter a, a displacement parameter γ, a scaling parameter R_0 and a volatility parameter σ. We assume the mean reversion parameter a and scaling parameter R_0 to be constant and set them equal to $a = 0.03$ and $R_0 = 0.02$. The displacement parameter γ and volatility parameter σ are varying.

In this subsection we discuss:

- Market data and implementation details.
- Test strategy.
- Criteria to determine the validity of Dirkmanns method.
- Pricing results and the impact on the implied volatility skew.
- Conclusion.

Market data and implementation details.

For the validation of the approximations we consider the market data from 31 May 2010. For the implementation we used Matlab, where we ignored day count conventions and all dates were given in year fractions. The tests were done for two different swaptions with maturities of 10-, and 20 years. We considered these swaptions on an underlying Pay IRS, with notional $N = 1$, swap tenor of 10, semi annual coupons and for different strikes K, where:

$$K \in \text{ATM} + \{-2\%, -1.5\%, -1\%, -50\text{bp}, -25\text{bp}, 0, 25\text{bp}, 50\text{bp}, 1\%, 1.5\%, 2\%\}. \tag{4.20}$$

We implemented two pricing methods:

1. A Monte Carlo method, where we use Euler discretization for the process given in (4.9).
2. The approximation method, described in Sections 4.4.1 - 4.4.3, proposed by Dirkmann [11]. We use the semi-analytic pricing formulas, given in Section 4.4.3. In the remainder of this chapter, we call this Dirkmann's method.

We take the Monte Carlo method as our benchmark method. We discretize the process in (4.9) with stepsize $dt = 0.01$. With this discretization we can obtain samples $(X(T_0), Y(T_0))$ and calculate realizations of (2.21). Taking the mean gives an approximation of the swaption price. We take $N = 50,000$ Monte Carlo samples to get an accurate price[2]. We assume that our benchmark method generates unbiased swaption prices and hence corresponding implied volatilities. Since we take a small time step and a large number of simulations, this is a safe assumption, since the mean is an unbiased estimator for the expectation.

Test strategy

To test the performance of Dirkmann's method for different sets of parameters (γ, σ), we perform the following steps.

1. Choose two parameters γ and σ, $\gamma \in \mathbb{R}$ and $\sigma > 0$.
2. Compute for all strike levels K, given in Equation (4.20), the swaption price via the Monte Carlo method to get a benchmark price.
3. Corresponding to each benchmark price compute Black's implied volatility.
4. Compute for all strike levels K, given in Equation (4.20), the swaption price via Dirkmann's method.
5. Corresponding to each Dirkmann price compute Black's implied volatility.
6. Compute the relative difference between the benchmark prices and the Dirkmann prices.

Criteria to determine the validity of Dirkmann's method

Dirkmann's method is a fast pricing method to price swaptions, because there are closed form pricing formulas available. This is one of the main advantages of Dirkmann's method, however Dirkmann's price is an approximation of the true swaption price. Here we define the 'true swaption price' as the swaption price implied by the DD model.

[2] $N = 50,000$: We compared benchmark prices generated with $dt = 0.01$ to benchmark prices with $dt = 0.005$. The relative difference between them is approximately 50bp. Prices are not sensitive to changes in dt anymore, hence we assume that $dt = 0.01$ is a sufficiently small timestep for testing.

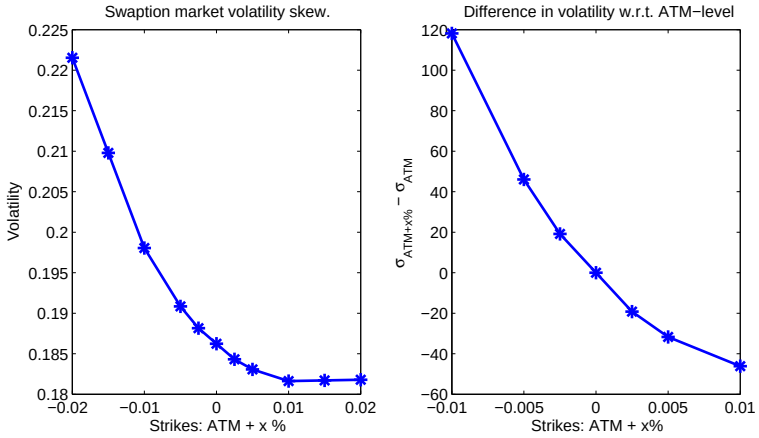

Figure 4.1: Market data: 31 May 2010. Swaption: 10Y10Y

Fast pricing methods are interesting for calibration purposes. Suppose that we calibrate the model to one option maturity. Then we need two swaptions with the same option maturity, but with different strikes since we have two degrees of freedom in the model, namely σ and γ. One choice is to take one strike to be ATM $+$ 100bp and the other ATM $-$ 100bp. From market experience it is known that the volatility at a strike of ATM$-$100bp is approximately 100bp higher than at the ATM-level. At a strike of ATM+100bp it is approximately 50bp lower than at the ATM-level. We illustrate this with a market data example. In the left plot of Figure 4.1, we show the swaption market volatility skew corresponding to a 10Y-10Y swaption. The right plot of Figure 4.1 shows the difference in basis points between the volatility at strike ATM $+ x\%$ and the volatility at strike ATM.

We assumed that our benchmark method generates unbiased swaption prices. This implies that for $dt \to 0$ and $N \to \infty$ the benchmark price converges to the true swaption price. Hence Black's implied volatility, corresponding to our benchmark price, converges to the true Black's implied volatility. In the calibration process we need a swaption pricer. If we use our benchmark method in the calibration process, then it is possible to match the market volatility skew at strike levels ATM $-$ 100bp and ATM $+$ 100bp, for some set of parameters (γ, σ). For N sufficiently large and dt sufficiently small, we assume to have an accurate approximation of the true swaption price. Hence with this set of parameters the model is calibrated perfectly to the market volatility skew at strike levels $K =$ ATM $\pm$ 100bp . A drawback is that this pricing method is slow compared to Dirkmann's method.

To speed up the calibration we can choose Dirkmann's method in the calibration process. Since Dirkmann's method approximates the true swaption price, the question is how much confidence we have in the resulting parameters. To decide whether Dirkmann's method is a satisfactory pricing method for calibration purposes or not, we make the following analysis.

- Choose an arbitrary set of parameters (σ, γ). We assume these are the values obtained when calibrating to strike levels ATM $\pm$ 100bp, using Dirkmann's method.

- For strike level ATM + 100bp, calculate the difference between Black's implied volatility corresponding to Dirkmann's method and Black's implied volatility corresponding to the benchmark method. We denote the absolute difference by d_+.

- For strike level ATM − 100bp, calculate the difference between Black's implied volatility corresponding to Dirkmann's method and Black's implied volatility corresponding to the benchmark method. We denote the absolute difference by d_-.
- If d_+ or d_- are larger then 100bp, or 50bp respectively, we do not have much confidence in the set of parameters (σ, γ).

Assume that σ and γ are calibrated. We are then able to use these calibrated parameters to price, with the DD benchmark model, the instruments that were used for calibration. We denoted the difference between both methods d_+ and d_- for the ATM+100bp and ATM−100bp swaption, respectively. Finally d_+ and d_- are compared to 100bp and 50bp respectively to determine the reliability of the parameters.

As we have mentioned before, in Section 4.4.4, we expect Dirkmann's method to work quite well for small values of the displacement parameter γ and volatility parameter σ.

Pricing results and the impact on the implied volatility skew

After performing the steps described in the test strategy section, we discuss the results corresponding to a 10Y-10Y swaption and a 20Y-10Y swaption. We show the results for the following choice of parameters:

- Swaption 10Y-10Y: $\gamma = 0.2$, $\sigma = 0.2$.
- Swaption 10Y-10Y: $\gamma = 0.8$, $\sigma = 0.2$.
- Swaption 20Y-10Y: $\gamma = 0.2$, $\sigma = 0.1$.

Results for the 10Y-10Y swaption, with parameters $\gamma = 0.2$, $\sigma = 0.2$

Strikes around ATM	Benchmark price	Dirkmann price	Relative difference	Benchmark implied volatility	Dirkmann implied volatility	Difference in implied volatility
-2%	0.12128	0.12121	-0.050%	0.11528	0.11326	-20.2 bp
-1%	0.0661	0.06620	0.115%	0.09754	0.09800	4.6bp
-50bp	0.04374	0.04381	0.143%	0.09261	0.0928	2.5bp
-25bp	0.03445	0.03449	0.121%	0.09052	0.09067	1.5bp
0	0.02655	0.0265	-0.01%	0.0887	0.08868	-0.16bp
+25bp	0.01999	0.0199	-0.188%	0.08700	0.08687	-1.2bp
+50bp	0.01473	0.01464	-0.593%	0.08551	0.08521	-3.0bp
+1%	0.0075	0.0073	-2.533%	0.08310	0.08227	-8.3bp
+2%	0.00157	0.00139	-11.871%	0.07953	0.07753	-20.0bp

Table 4.1: 10Y-10Y: $\gamma = 0.2$, $\sigma = 0.2$, ATM-level $\approx$ 0,0394

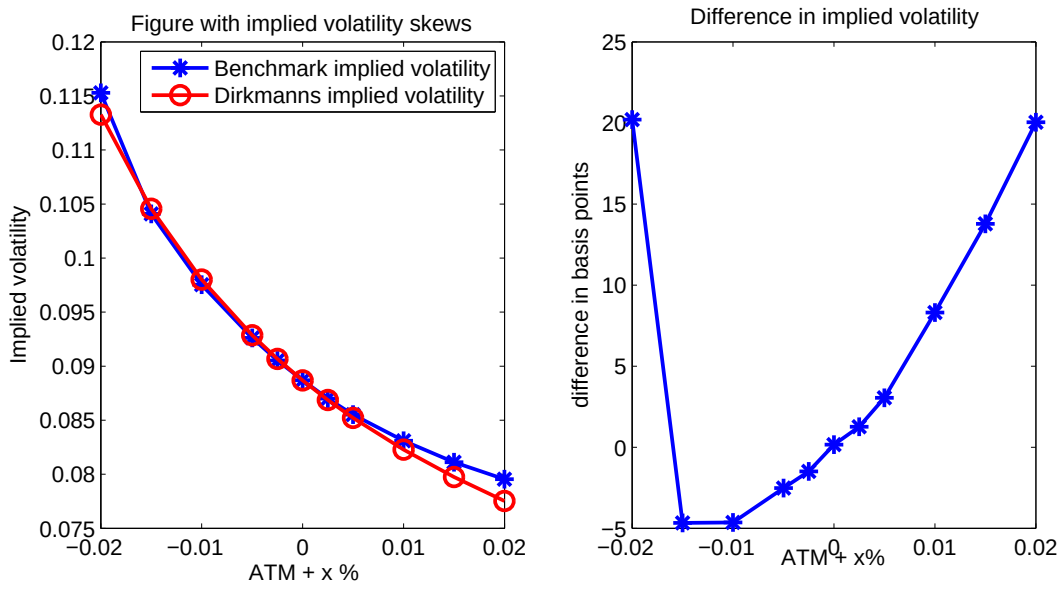

Figure 4.2: 10Y-10Y: $\gamma = 0.2$, $\sigma = 0.2$, ATM-level $\approx$ 0.0394

Figure 4.2 looks quite promissing, although there is a relative pricing mismatch of at most 2.5% for strikes between ATM $-$ 100bp and ATM $+$ 100bp. If we look to strike levels ATM $\pm$ 100bp, we see an absolute difference of at most 8.3bp in the implied volatility. Hence, if we get these parameters from the calibration process, we have to include an uncertainty region of approximately 10bp around the implied volatility at strike ATM $+$ 100bp and an uncertainty region of 5bp at strike ATM $-$ 100bp .

Results for the 10Y-10Y swaption, with parameters $\gamma = 0.8$, $\sigma = 0.2$

Strikes around ATM	Benchmark price	Dirkmann price	Relative difference	Benchmark implied volatility	Dirkmann implied volatility	Difference in implied volatility
-2%	0.1213	0.1217	0.36 %	0.115	0.1265	115.6 bp
-1%	0.0694	0.0706	1.83%	0.1159	0.1226	67.3bp
-50bp	0.0499	0.0511	2.28%	0.117	0.1214	44.1bp
-25bp	0.042	0.043	2.25%	0.1175	0.1209	33.6 bp
0	0.0352	0.0359	2.04%	0.118	0.1204	24.3bp
+25bp	0.0294	0.0299	1.66%	0.1184	0.12	16.2bp
+50bp	0.0245	0.0247	1.02%	0.1188	0.1196	8.3bp
+1%	0.0169	0.0167	0.91%	0.1195	0.119	-5.5bp
+2%	0.008	0.0074	-7.5%	0.1209	0.118	-29.9bp

Table 4.2: 10Y-10Y: $\gamma = 0.8$, $\sigma = 0.2$, ATM-level $\approx$ 0,0394

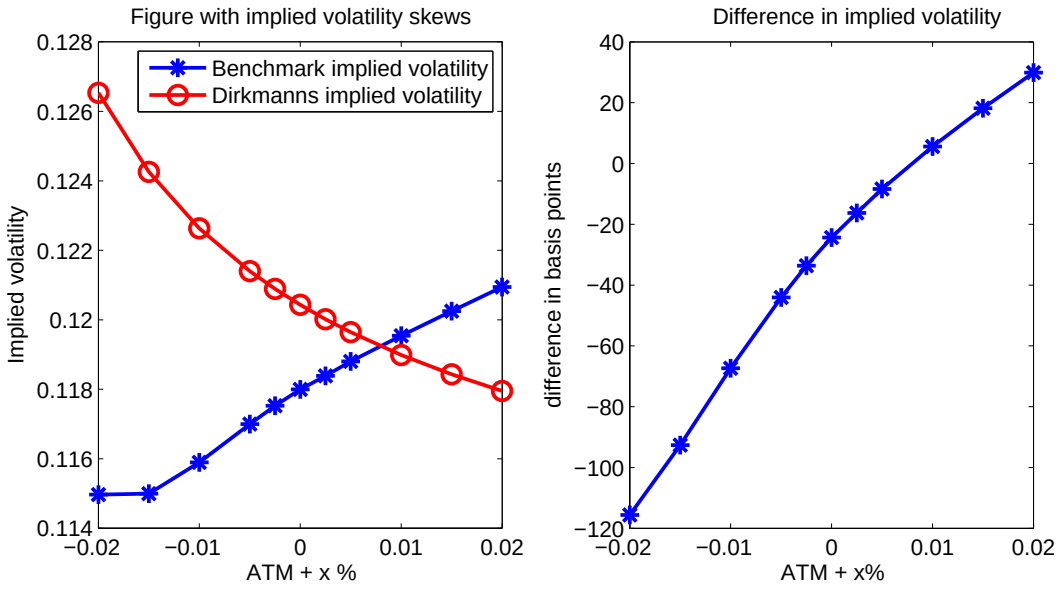

Figure 4.3: 10Y-10Y: $\gamma = 0.8$, $\sigma = 0.2$, ATM-level $\approx$ 0.0394

From Figure 4.3 we see that the approximation method performs poorly for this set of parameters. The shape of the implied volatility skew is different from that of our benchmark method. Although we have a relative pricing mismatch of at most 2.28% for strikes between ATM$-$100bp and ATM$+$100bp. If we look to strike level ATM$-$100bp, we see an absolute error of 67.3bp in the implied volatility. Hence, if we get these parameters from the calibration process, we have to include an uncertainty region of approximately 70bp, around the implied volatility at strike ATM $-$ 100bp. This uncertainty is clearly greater than the 50bp difference observed at strike levels at ATM+100bp.

Results for the 20Y-10Y swaption, with parameters $\gamma = 0.2$, $\sigma = 0.1$

Strikes around ATM	Benchmark price	Dirkmann price	Relative difference	Benchmark implied volatility	Dirkmann implied volatility	Difference in implied volatility
-1.5%	0.0654	0.0654	0.09%	0.074	0.0816	75.9bp
-1%	0.0443	0.0444	0.23%	0.0693	0.0713	19.9bp
-50bp	0.0258	0.0259	0.46%	0.0636	0.0645	8.4bp
-25bp	0.0182	0.0183	0.55%	0.0613	0.0618	5.5bp
0	0.0122	0.0123	0.53%	0.0592	0.0596	3.2bp
+25bp	0.0077	0.0077	0.23%	0.0575	0.0576	0.9bp
+50bp	0.0046	0.0045	-0.28%	0.0559	0.0558	-0.7bp
+1%	0.0013	0.0013	-2.82%	0.0532	0.0529	-3.9bp
+2%	5.76E-5	4.92E-5	-14.52%	0.0492	0.0484	-8.4bp

Table 4.3: 20Y-10Y: $\gamma = 0.2$, $\sigma = 0.1$, ATM-level ≈ 0.0266

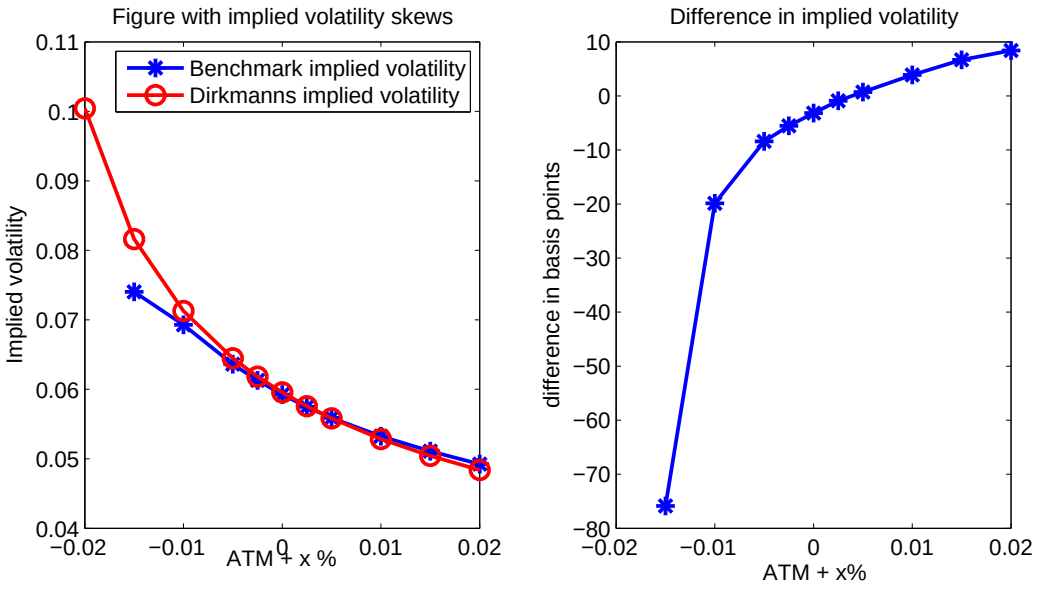

Figure 4.4: 20Y-10Y: $\gamma = 0.2$, $\sigma = 0.1$, ATM-level ≈ 0.0266

Again, like in the 10Y-10Y case, we have for a small γ and small σ quite good pricing results for the 20Y-10Y swaption. For strikes between ATM $\pm$ 100bp we have at most a mismatch in the price of 2.82%. However, at strike level ATM $-$ 100bp we have a mismatch of 19.9bp in the implied volatility. This means, if we calibrate to a strike level of ATM $-$ 100bp, we have to include an uncertainty region of approximately 20bp.

Conclusion

From the results we have shown, we can draw several conclusions.

1. We saw that we can obtain approximations of the swaption price, up to an accuracy of 2% with respect to our benchmark price, given small values of the displacement parameter γ and volatility σ. The implied volatility skews from Dirkmann's method and our benchmark method have the same shape and match each other closely.

2. For calibration purposes Dirkmann's method may not work satisfactory. As we saw earlier, if we calibrate to a 20Y-10Y swaption with strikes ATM $\pm$ 100bp and the resulting parameters are $(\bar{\gamma}, \bar{\sigma}) = (0.2, 0.1)$, then we have to include an uncertainty region of 20bp around the implied volatility.

   Only for short maturities and calibration to strikes close around the ATM level, say $\pm$25bp, it may give an acceptable uncertainty window. So even in the case where we have a small σ and γ, it does not imply that this approximation method works well satisfactory for calibration.

3. From the case of a 10Y-10Y swaption and a displacement parameter $\gamma = 0.8$ in the model, we observed that the errors obtained in the approximations become more visible than in case of small values for the displacement γ. This is something we already expected in paragraph 4.4.4. The implied volatility skew of the approximation method has a totally different shape than our benchmark implied volatility skew, see Figure 4.3. This directly implies that we have to include a larger uncertainty window than with a small displacement parameter.

4. The uncertainty regions we have to include are relatively large with respect to an expected increase or decrease of 100bp respectively 50bp in the market volatility skew at strike levels ATM $\pm$ 100bp. Even for a small displacement and a small volatility, where we expect a good performance of Dirkmann's method, we have to include a significant error window. As we have seen from the 20Y-10Y swaption with displacement $\gamma = 0.2$ and $\sigma = 0.1$ an error window of 20bp.

These effects will have more impact in case of longer maturities, larger displacement parameters γ, and larger volatility parameters σ. Even in case of small values of γ and σ, we see that Dirkmann's method is not suitable as a swaption pricer in the calibration process. For the DD model, Dirkmann's method has a limiting scope of applicability. If we want to apply this method in the calibration process, we have to make several restrictions:

1. A short option maturity T.

2. Strike levels, to which we want to calibrate the model, should be close to the ATM-level.

3. $\gamma \in [0, \delta]$ with $\delta \in \mathbb{R}^+$ small.

4. $\sigma \in [0, \epsilon]$ with $\epsilon \in \mathbb{R}^+$ small.

Only under these conditions and the assumption that there exists a pair of parameters (γ, σ), $\gamma \in [-\delta, \delta]$ and $\sigma \in [0, \epsilon]$, such that Dirkmann's method matches the market skew at the strike levels to which we calibrate the model, we may expect a sufficiently small error window around the implied volatily. But for general calibration purposes we do not choose for Dirkmann's method.

Chapter 5

Displaced Diffusion model with Stochastic Volatility

In Chapter 4 we discussed the DD formulation of the Cheyette model without stochastic volatility. In this model the instantaneous short rate $r(t)$ is modelled by the one-factor model:

$$r(t) = f(0,t) + x(t)$$

Recall that the differential of $x(t)$, under the risk-neutral measure, is given by;

$$\begin{aligned} dx(t) &= (y(t) - ax(t))\, dt + \eta(t, x(t)) dW^{\mathbb{Q}^0}(t), \\ dy(t) &= \left(\eta^2(t, x(t)) - 2ay(t)\right) dt, \end{aligned}$$

where the instantaneous volatility function is given by:

$$\eta(t, x(t)) = \left[\gamma(t) r(t) + (1 - \gamma(t)) R_0\right] \sigma(t). \tag{5.1}$$

In this formulation there are no stochastic terms involved that are driven by some other random process than the Brownian motion driving $x(t)$. Up to now, the instantaneous volatility function depends on two deterministic functions of time, one constant and the state variable $x(t)$. To extend the DD model to a displaced diffusion model with stochastic volatility (DDSV), we make the instantaneous volatility function dependent on some stochastic process, $V(t)$, driven by a different Brownian motion process than the Brownian motion driving $x(t)$.

In this chapter we consider the following topics

- Formulation of the DDSV model, see Section 5.1.
- The dynamics of the swap rate under the annuity measure, see Section 5.2.
- Approximation of the swaption price under the DDSV model, see Section 5.3.
- Parameter averaging, see Section 5.4.
- Efficient implementation method, see Section 5.5.
- Simulation of the DDSV model under the T-forward measure, see Section 5.6.
- The case of non zero correlation, $\rho \neq 0$, see Section 5.7.
- Numerical results, see Section 5.8.

5.1 Formulation of the DDSV model

To formulate the DDSV model, which is the main focus of the present thesis, we have to specify a variance process, $V(t)$, on which our instantaneous volatility function will depend. We choose a Cox-Ingersoll-Ross (CIR) model to model $V(t)$, hence the dynamics of $V(t)$ are given by:

$$dV(t) = \beta(V(0) - V(t))dt + \epsilon(t)\sqrt{V(t)}dW_V(t). \tag{5.2}$$

With β constant, $\epsilon(t)$ a deterministic function of time and $W_V(t)$ a standard Brownian motion. This process has a unique solution if the well-known Feller condition holds

$$\frac{2\beta V(0)}{\epsilon(t)^2} > 1, \forall t \geq 0.$$

To make the instantaneous volatility function of the $x(t)$ process dependent on the process $V(t)$, we choose to multiply (5.1) by $\sqrt{V(t)}$:

$$\bar{\eta}(t, x(t)) = \eta(t, x(t))\sqrt{V(t)}. \tag{5.3}$$

It is a trivial exercise to show that $\mathbb{E}(V(t)) = V(0)$. Since we multiply $\eta(t, x(t))$ by the square root of $V(t)$, a common choice is to set:

$$V(0) = 1.$$

We take (5.3) as the instantaneous volatility function in the DDSV formulation of the Cheyette model. A complete formulation of the dynamics under the risk-neutral measure of this model is given by:

Model 1: The DDSV model

$$\boxed{\begin{aligned} dx(t) &= (y(t) - ax(t))dt + \eta(t, x(t))\sqrt{V(t)}dW_x^{\mathbb{Q}^0}(t), \\ dy(t) &= (\eta^2(t, x(t))V(t) - 2ay(t))dt, \\ dV(t) &= \beta(V(0) - V(t))dt + \epsilon(t)\sqrt{V(t)}dW_V^{\mathbb{Q}^0}(t), \end{aligned}} \tag{5.4}$$

with $\eta(t, x(t))$ given by Equation (5.1) and initial conditions $x(0) = 0, y(0) = 0$. To summarize, we have the following parameters in our model:

- a the mean reversion rate of the $x(t)$ process.
- $\gamma(t)$ the piecewise constant skew function.
- $\sigma(t)$ the piecewise constant volatility function.
- R_0 a scaling parameter in (5.1).
- β the mean reversion of the variance process.
- $\epsilon(t)$ the piecewise constant volatility of volatility function.

Our first analysis will consider the case of uncorrelated Brownian motions, hence:

$$dW_x^{\mathbb{Q}^0}(t) \cdot dW_V^{\mathbb{Q}^0}(t) = 0. \tag{5.5}$$

In Section 5.7 we discuss the case of non-zero correlations.

Like in the DD model, the zero-coupon bond price is given by,

$$P(t,T) = \frac{P^M(0,T)}{P^M(0,t)} e^{-x(t)B(t,T) - \frac{1}{2}y(t)B^2(t,T)}, \tag{5.6}$$

with

$$B(t,T) = \frac{1}{a}\left(1 - e^{-a(T-t)}\right).$$

This is because the zero-coupon bond price, in the Cheyette model, is independent of the choice of the instantaneous volatility function. To formulate a stochastic volatility model we only made a change in the instantaneous volatility function in the $x(t)$-dynamics. Hence we can follow the same proof, given in Appendix B.2, for the Cheyette zero-coupon bond price without stochastic volatility.

Following the same ideas as in Section 4.1 and using the assumption made in Equation (5.5), we can derive the dynamics of the process, given by Equation (5.4), under the T-forward measure.

Model 1b: The DDSV model under the T-forward measure

$$\boxed{\begin{aligned} dx(t) &= \left[y(t) - ax(t) - B(t,T)\eta^2(t,x(t))V(t)\right]dt + \eta(t,x(t))\sqrt{V(t)}dW_x^{\mathbb{Q}^T}(t), \\ dy(t) &= (\eta^2(t,x(t))V(t) - 2ay(t))dt, \\ dV(t) &= \beta(V(0) - V(t))dt + \epsilon(t)\sqrt{V(t)}dW_V^{\mathbb{Q}^T}(t), \end{aligned}} \tag{5.7}$$

with $\eta(t,x(t))$ given by Equation (5.1) and initial conditions $x(0) = 0, y(0) = 0$. These dynamics are convenient if we want to use Monte Carlo methods to price interest rate products.

5.2 The dynamics of the swap rate under the annuity measure.

To derive the dynamics of the swap rate under the swap measure, we take a similar approach as in Section 4.4.1. The only difference is the choice of Σ in (4.13). From the dynamics of $x(t)$, given in Equation (5.4), we see that:

$$\Sigma = \eta(x(t),t)\sqrt{V(t)}.$$

After a change of measure, from $\mathbb{Q}^0$ to $\mathbb{Q}^{1,m}$ and due to the zero correlation between $W_x^{\mathbb{Q}^0}(t)$ and $W_v^{\mathbb{Q}^0}(t)$ so that the drift term of $V(t)$ remains unchanged, we derive the following system of SDEs which models the swap rate under the annuity measure:

$$dS_{0,m}(t) = \left\{\sum_{i=0}^{m} q_i^S(t)B(t,T_i)\right\}\eta(x(t),t)\sqrt{V(t)}dW_1^{\mathbb{Q}^{1,m}}(t), \tag{5.8}$$

$$dV(t) = \beta(V(0) - V(t))dt + \epsilon(t)\sqrt{V(t)}dW_2^{\mathbb{Q}^{1,m}}(t). \tag{5.9}$$

For a derivation we refer to Appendix A. The initial conditions are given by $S_{0,m}(0)$, the swap rate corresponding to the underlying swap at time zero.

We approximate the swap rate dynamics given by Equation (5.8) by making the volatility term deterministic

$$\left\{\sum_{i=0}^{m} q_i^S(t)B(t,T_i)\right\}\eta(x(t),t).$$

We make the same approximations as in Section 4.4.2, yielding:

Model 2: The swap rate model

$$\boxed{\begin{aligned} dS_{0,m}(t) &= [\gamma(t)S_{0,m}(t) + (1-\gamma(t))R_0]\,\lambda(t)\sqrt{V(t)}dW_1^{\mathbb{Q}^{1,m}}(t), \\ dV(t) &= \beta(V(0)-V(t))dt + \epsilon(t)\sqrt{V(t)}dW_2^{\mathbb{Q}^{1,m}}(t), \end{aligned}} \tag{5.10}$$

with

$$\lambda(t) := \left\{\sum_{i=0}^{m} q_i^S(0)B(t,T_i)\right\}\left(\frac{\gamma(t)f(0,t) + (1-\gamma(t))R_0}{\gamma(t)S_{0,m}(0) + (1-\gamma(t))R_0}\right)\sigma(t), \tag{5.11}$$

the deterministic part of the volatility function and $f(0,t)$ the instantaneous forward rate at time 0 with maturity t.

5.3 Approximation of the swaption price under the DDSV model

In this section we discuss how to calculate the price of a payer and receiver swaption, using the swap rate model given by (5.10), under the same settings as those described in Section 2.3. To derive a semi-analytic formula for the swaption price, we need a constant displacement parameter $\gamma(t)$. For now, assume $\gamma(t) \equiv \gamma$ to be constant, hence we consider the following model:

$$\begin{aligned} dS_{0,m}(t) &= (\gamma S_{0,m}(t) + (1-\gamma)R_0)\lambda(t)\sqrt{V(t)}dW_1^{\mathbb{Q}^{1,m}}(t), \\ dV(t) &= \beta(V(0)-V(t))dt + \epsilon(t)\sqrt{V(t)}dW_2^{\mathbb{Q}^{1,m}}(t), \end{aligned}$$

with $\lambda(t)$ defined in (5.11). For convenience we omitted the $\approx$ sign in the dynamics of $S_{0,m}(t)$. From Formula (2.20) we know that the price of a payer swaption is given by:

$$V_{0,m}^{pay}(0) = P_{1,m}(0)\mathbb{E}^{\mathbb{Q}^{1,m}}\left[(S_{0,m}(T_0) - K)^+\right], \tag{5.12}$$

with $P_{1,m}(0)$ the annuity.

Under the assumption that $\gamma > 0$ and defining

$$\begin{aligned} \bar{S}_{0,m}(t) &:= \gamma S_{0,m}(t) + (1-\gamma)R_0, \\ \bar{K} &:= \gamma K + (1-\gamma)R_0, \end{aligned}$$

we obtain

$$\boxed{V_{0,m}^{pay}(0) = \frac{P_{1,m}(0)}{\gamma}\mathbb{E}^{\mathbb{Q}^{1,m}}\left[\left(\bar{S}_{0,m}(T_0) - \bar{K}\right)^+\right].} \tag{5.13}$$

The dynamics of $\bar{S}_{0,m}$, under the annuity measure $\mathbb{Q}^{1,m}$, are given by

$$\begin{aligned} d\bar{S}_{0,m}(t) &= \gamma\lambda(t)\bar{S}_{0,m}(t)\sqrt{V(t)}dW_1^{\mathbb{Q}^{1,m}}(t), \\ dV(t) &= \beta(V(0)-V(t))dt + \epsilon(t)\sqrt{V(t)}dW_2^{\mathbb{Q}^{1,m}}(t). \end{aligned} \tag{5.14}$$

With initial condition:

$$\bar{S}_{0,m}(0) = \gamma S_{0,m}(0) + (1-\gamma)R_0. \tag{5.15}$$

The random variable $\bar{S}_{0,m}$ is then modelled by the well-known Heston dynamics. There are several methods to calculate the expectation in (5.13). We call this the Heston part of the option value:

$$\boxed{\text{Heston}(\bar{S}_{0,m}(T_0), \bar{K}) := \mathbb{E}^{\mathbb{Q}^{1,m}}\left[\left(\bar{S}_{0,m}(T_0) - \bar{K}\right)^+\right]} \tag{5.16}$$

The problem of pricing payer swaptions is reduced to solving Equation (5.16). This equation can be solved using the so called fundamental transform. This method will be discussed in Section 5.3.1. Before we explain this method, we derive the price of a receiver swaption. Note that the price is given by:

$$V^{rec}_{0,m}(0) = P_{1,m}(0)\mathbb{E}^{\mathbb{Q}^{1,m}}\left[(K - \bar{S}_{0,m}(T_0))^+\right], \tag{5.17}$$

and that the following relation holds:

$$(S_{0,m}(T_0) - K)^+ - (K - S_{0,m}(T_0))^+ = S_{0,m}(T_0) - K. \tag{5.18}$$

Taking expectations on both sides of Equation (5.18) and using the fact that the swap rate is a martingale under the swap measure yields:

$$\mathbb{E}^{\mathbb{Q}^{1,m}}\left[(K - S_{0,m}(T_0))^+\right] = \mathbb{E}^{\mathbb{Q}^{1,m}}\left[(S_{0,m}(T_0) - K)^+\right] - S_{0,m}(0) + K. \tag{5.19}$$

Substituting (5.19) in (5.17) yields:

$$\begin{aligned} V^{rec}_{0,m}(0) &= P_{1,m}(0)\mathbb{E}^{\mathbb{Q}^{1,m}}\left[(S_{0,m}(T_0) - K)^+\right] + P_{1,m}(0)(K - S_{0,m}(0)) \\ &= V^{pay}_{0,m}(0) + P_{1,m}(0)(K - S_{0,m}(0)). \end{aligned}$$

Hence the relationship, between the price of a payer swaption and a receiver swaption, is given by the following put-call parity:

$$\boxed{V^{rec}_{0,m}(0) = V^{pay}_{0,m}(0) + P_{1,m}(0)(K - S_{0,m}(0)).} \tag{5.20}$$

5.3.1 Fundamental transform

In this subsection we state a result from Lewis, to calculate the Heston part in Equation (5.16). For more information about the fundamental transform, we refer to [14]. The Heston part can be calculated by the following inverse Fourier integral,

$$\text{Heston}(\bar{S}_{0,m}(T_0), \bar{K}) = \bar{S}_{0,m}(0) - \frac{\bar{K}}{2\pi}\int_{-\infty}^{\infty} \frac{e^{-(i\omega+\alpha)\log\left(\bar{K}/\bar{S}_{0,m}(0)\right)}}{(\alpha+i\omega)(1-\alpha-i\omega)}\psi_X(\alpha+i\omega, T_0)d\omega, \tag{5.21}$$

where α defines the integration contour in the complex plane, a common choice is $\alpha = \frac{1}{2}$. $\psi_X(u, T_0)$ is given by (see [21] for more details):

$$\psi_X(u,T) := \exp(A(0,T_0) + V(0)B(0,T_0)),$$

where $A(t,T_0)$ and $B(t,T_0)$ satisfy the following Riccati ODEs

$$\begin{aligned}
\frac{d}{dt}A(t,T_0) &= -\beta V(0)B(t,T_0),\\
\frac{d}{dt}B(t,T_0) &= -\frac{1}{2}\gamma^2 u(u-1)\lambda^2(t) + \beta B(t,T_0) - \frac{\epsilon^2(t)}{2}B^2(t,T_0),
\end{aligned}$$

with terminal conditions $(A(T_0,T_0), B(T_0,T_0)) = (0,0)$.

Special case $\epsilon(t) \equiv 0$

We can apply this result to the SV model with $\epsilon(t) \equiv 0$. Under this assumption our SV model is given by:

$$d\bar{S}_{0,m}(t) = \sqrt{V(0)}\gamma\lambda(t)\bar{S}_{0,m}dW^{\mathbb{Q}^{1,m}}(t),$$

since

$$dV(t) = \beta(V(0) - V(t))dt,$$

implies $V(t) \equiv V(0)$. This is a trivial exercise left to the reader. To show this, apply Itô's product rule to $e^{\beta t}V(t)$ to solve the equation for $V(t)$. Hence the dynamics of $\bar{S}_{0,m}(t)$ are log-normal and we can solve the Heston part using the results from Section 4.4.3.

$$\mathbb{E}^{\mathbb{Q}^{1,m}}\left[(\bar{S}_{0,m}(T_0) - \bar{K})^+\right] = \bar{S}_{0,m}(0)\mathcal{N}(d_1) - \bar{K}\mathcal{N}(d_2),$$

with

$$\begin{aligned}
\nu^2 &= \gamma^2 V(0)\int_0^{T_0}\lambda^2(t)dt,\\
d_1 &= \frac{\log(\bar{S}_{0,m}(0)/\bar{K}) + \frac{1}{2}\nu^2}{\nu}.\\
d_2 &= d_1 - \nu
\end{aligned}$$

Or equivalent in terms of Black's formula:

$$\mathbb{E}^{\mathbb{Q}^{1,m}}\left[(\bar{S}_{0,m}(T_0) - \bar{K})^+\right] = \text{Black}(\bar{S}_{0,m}(0), \bar{K}, 0, T_0, \xi), \tag{5.22}$$

with Black's volatility

$$\xi = \frac{\nu}{\sqrt{T_0}}.$$

Another way to solve the Heston part is to use Equation (5.21):

$$\text{Heston}_{\epsilon(t)\equiv 0}(\bar{S}_{0,m}(T_0), \bar{K}) = \bar{S}_{0,m}(0) - \frac{\bar{K}}{2\pi}\int_{-\infty}^{\infty}\frac{e^{-(i\omega+\alpha)\log\left(\bar{K}/\bar{S}_{0,m}(0)\right)}}{(\alpha+i\omega)(1-\alpha-i\omega)}\psi_X^0(\alpha+i\omega,T_0)d\omega, \tag{5.23}$$

with $\psi_X^0(u;T_0)$ given by (see [21] for more details).

$$\psi_X^0(u;T_0) = e^{\frac{1}{2}\nu^2(u^2-u)},$$

Since (5.22) and (5.23) yield the same value, we have that:

$$\text{Black}(\bar{S}_{0,m}(0),\bar{K},0,T_0,\xi) - \bar{S}_{0,m}(0) + \frac{\bar{K}}{2\pi}\int_{-\infty}^{\infty} \frac{e^{-(i\omega+\alpha)\log\left(\bar{K}/\bar{S}_{0,m}(0)\right)}}{(\alpha+i\omega)(1-\alpha-i\omega)}\psi_X^0(\alpha+i\omega,T_0)d\omega = 0. \tag{5.24}$$

Fourier integral with control variate

We add the identity in (5.24) to the result in Equation (5.21), i.e. we use the case $\epsilon(t) \equiv 0$ as a control variate for integration, then the Heston part is given by:

$$\begin{aligned}\text{Heston}(\bar{S}_{0,m}(T_0),\bar{K}) &= \text{Black}(\bar{S}_{0,m}(0),\bar{K},0,T_0,\xi)\\ &\quad - \frac{\bar{K}}{2\pi}\int_{-\infty}^{\infty} \frac{e^{-(i\omega+\alpha)\log\left(\bar{K}/\bar{S}_{0,m}(0)\right)}}{(\alpha+i\omega)(1-\alpha-i\omega)}(\psi_X(\alpha+i\omega,T_0) - \psi_X^0(\alpha+i\omega,T_0))d\omega.\end{aligned}$$

Substituting $\alpha = 1/2$ and the definitions of $\psi_X(u,T_0)$ and $\psi_X^0(u,T_0)$ into this expression yields:

$$\begin{aligned}\text{Heston}(\bar{S}_{0,m}(T_0),\bar{K}) &= \text{Black}(\bar{S}_{0,m}(0),\bar{K},0,T_0,\xi)\\ &\quad - \frac{\bar{K}}{2\pi}\int_{-\infty}^{\infty} \frac{e^{\left(i\omega+\frac{1}{2}\right)\log\left(\bar{S}_{0,m}(0)/\bar{K}\right)}}{\omega^2+\frac{1}{4}}\left(e^{A_\omega(0,T_0)+V(0)B_\omega(0,T_0)} - e^{-\frac{1}{2}\nu^2\left(\omega^2+\frac{1}{4}\right)}\right)d\omega,\end{aligned} \tag{5.25}$$

with

$$\begin{aligned}\nu^2 &= \gamma^2\ V(0)\int_0^{T_0}\lambda^2(t)dt,\\ \xi &= \frac{\nu}{\sqrt{T_0}},\end{aligned} \tag{5.26}$$

and $A_\omega(t,T_0)$, $B_\omega(t,T_0)$ satisfying:

$$\begin{aligned}\frac{d}{dt}A_\omega(t,T_0) &= -\beta V(0)B_\omega(t,T_0),\\ \frac{d}{dt}B_\omega(t,T_0) &= \left(\frac{1}{8}+\frac{1}{2}\omega^2\right)\gamma^2\lambda^2(t) + \beta B_\omega(t,T_0) - \frac{\epsilon^2(t)}{2}B_\omega^2(t,T_0),\end{aligned} \tag{5.27}$$

Simplification of the integral

The integral in (5.25) can be simplified if we note that:

$$\begin{aligned}
&\int_{-\infty}^{\infty} \frac{e^{\left(i\omega+\frac{1}{2}\right)\log\left(\bar{S}_{0,m}(0)/\bar{K}\right)}}{\omega^2+\frac{1}{4}} \left(e^{A_\omega(0,T_0)+V(0)B_\omega(0,T_0)} - e^{-\frac{1}{2}\nu^2\left(\omega^2+\frac{1}{4}\right)}\right) d\omega = \\
&\int_{-\infty}^{\infty} \frac{\cos\left(\omega\log\left(\frac{\bar{S}_{0,m}(0)}{\bar{K}}\right)\right)\sqrt{\frac{\bar{S}_{0,m}(0)}{\bar{K}}}}{\omega^2+\frac{1}{4}} \left(e^{A_\omega(0,T_0)+V(0)B_\omega(0,T_0)} - e^{-\frac{1}{2}\nu^2\left(\omega^2+\frac{1}{4}\right)}\right) d\omega + \\
&i\int_{-\infty}^{\infty} \frac{\sin\left(\omega\log\left(\frac{\bar{S}_{0,m}(0)}{\bar{K}}\right)\right)\sqrt{\frac{\bar{S}_{0,m}(0)}{\bar{K}}}}{\omega^2+\frac{1}{4}} \left(e^{A_\omega(0,T_0)+V(0)B_\omega(0,T_0)} - e^{-\frac{1}{2}\nu^2\left(\omega^2+\frac{1}{4}\right)}\right) d\omega = \\
&2\int_{0}^{\infty} \frac{\cos\left(\omega\log\left(\frac{\bar{S}_{0,m}(0)}{\bar{K}}\right)\right)\sqrt{\frac{\bar{S}_{0,m}(0)}{\bar{K}}}}{\omega^2+\frac{1}{4}} \left(e^{A_\omega(0,T_0)+V(0)B_\omega(0,T_0)} - e^{-\frac{1}{2}\nu^2\left(\omega^2+\frac{1}{4}\right)}\right) d\omega,
\end{aligned}$$

where we used:

- $(A_\omega(0,T_0), B_\omega(0,T_0)) = (A_{-\omega}(0,T_0), B_{-\omega}(0,T_0))$, this follows from the Riccati ODEs.
- The integrand with the sine is odd and vanishes.
- The integrand with the cosine is even and the region of integration is symmetric around 0.

Using this result, the Heston part simplifies to

$$\boxed{\text{Heston}(\bar{S}_{0,m}(T_0),\bar{K}) = \text{Black}(\bar{S}_{0,m}(0),\bar{K},0,T_0,\xi) - \frac{\sqrt{\bar{S}_{0,m}(0)\bar{K}}}{\pi}\int_0^\infty f(\omega)d\omega.} \tag{5.28}$$

with

$$f(\omega) := \frac{\cos\left(\omega\log\left(\bar{S}_{0,m}(0)/\bar{K}\right)\right)}{\omega^2+\frac{1}{4}} \left(e^{A_\omega(0,T_0)+V(0)B_\omega(0,T_0)} - e^{-\frac{1}{2}\nu^2\left(\omega^2+\frac{1}{4}\right)}\right),$$

where

$$\begin{aligned}
\nu^2 &= \gamma^2\ V(0)\int_0^{T_0}\lambda^2(t)dt, \\
\xi &= \frac{\nu}{\sqrt{T_0}},
\end{aligned}$$

and $A_\omega(t,T_0)$, $B_\omega(t,T_0)$ satisfying:

$$\begin{aligned}
\frac{d}{dt}A_\omega(t,T_0) &= -\beta V(0)B_\omega(t,T_0), \\
\frac{d}{dt}B_\omega(t,T_0) &= \left(\frac{1}{8}+\frac{1}{2}\omega^2\right)\gamma^2\lambda^2(t) + \beta B_\omega(t,T_0) - \frac{\epsilon^2(t)}{2}B_\omega^2(t,T_0),
\end{aligned}$$

Solutions of the Riccati ODEs for constant $\lambda(t)$ and $\epsilon(t)$

Assume that we are in the case that $\lambda(t) \equiv \lambda$ and $\epsilon(t) \equiv \epsilon$ are both constant. Then the system of Riccati ODEs, given by Equation (5.27), has an analytic solution. We state the following general result

Result 5.1. Consider the following set of ordinary differential equations

$$\frac{dx(t)}{dt} = dy(t), \tag{5.29}$$

$$\frac{dy(t)}{dt} = a + by(t) + cy^2(t), \tag{5.30}$$

with terminal conditions $(x(T), y(T)) = (0, 0)$. Assume that a, b, c and d are constants, satisfying $ac < 0$, $b \geq 0$ and $d \in \mathbb{R}$. Then the solutions for $x(t)$ and $y(t)$ are given by:

$$y(t) = \frac{1}{2c}\left[-b + \frac{1 + \left(\frac{b-\eta}{b+\eta}\right)e^{-\eta(T-t)}}{1 + \left(\frac{\eta-b}{b+\eta}\right)e^{-\eta(T-t)}}\eta\right], \tag{5.31}$$

$$x(t) = \frac{bd(T-t)}{2c} - \frac{d}{2c}\log\left(\frac{\left[1 + \frac{\eta-b}{\eta+b}e^{-\eta(T-t)}\right]^2}{4\frac{\eta^2-b^2}{(\eta+b)^2}e^{-\eta(T-t)}}\left(1 - \frac{b^2}{\eta^2}\right)\right), \tag{5.32}$$

where we defined:

$$\eta := \sqrt{-4ac + b^2}.$$

Proof. For a proof of this result, we refer to Appendix B.4 . □

To get the analytic solutions of the Riccati ODEs, given by Equation (5.27), take in Result 5.1

$$x(t) = A_\omega(t, T_0), \quad y(t) = B_\omega(t, T_0)$$

and

$$a = \left(\frac{1}{8} + \frac{1}{2}\omega^2\right)\gamma^2\lambda^2, \quad b = \beta, \quad c = -\frac{1}{2}\epsilon^2, \quad d = -\beta V(0).$$

This implies two restrictions

1. $c \neq 0$ implies $\epsilon > 0$.
2. $a \neq 0$ implies $\gamma > 0, \lambda > 0$. Note that $\gamma > 0$ is satisfied by assumption.

Implementation

In this subsection we discuss some implementation details. We have to calculate the improper integral in Equation (5.28) numerically. For a sufficiently accurate numerical integration we need:

- $u \in \mathbb{R}^+$ sufficiently large to truncate the region of integration, such that

$$\left| \int_u^\infty f(\omega) d\omega \right| < TOL,$$

for some tolerance level TOL. Then we get an initial estimate of the improper integral. Hence

$$\int_0^\infty f(\omega) d\omega \approx \int_0^u f(\omega) d\omega.$$

We have to truncate the region of integration, since numerical integration schemes can not handle infinite domains.

- A numerical integration rule to approximate proper integrals:

$$\int_a^b g(x) dx, \quad [a, b] \subset \mathbb{R}.$$

- A numerical ODE solver, to solve the Riccati ODEs when $\epsilon(t)$ and $\lambda(t)$ are time-dependent.

Truncation of the region of integration

We restrict our analysis to the constant coefficient case i.e.: $\lambda(t)$ and $\epsilon(t)$ constant. For now we assume that $A_\omega(0, T_0) \leq 0$ and $B_\omega(0, T_0) \leq 0$

$$\begin{aligned}
\left| \int_u^\infty f(\omega) d\omega \right| &\leq \int_u^\infty |f(\omega)| \, d\omega \\
&\leq \int_u^\infty \frac{\left| \cos\left(\omega \log\left(\frac{\bar{S}_{0,m}(0)}{K} \right) \right) \right|}{\omega^2 + \frac{1}{4}} \left(\left| e^{A_\omega(0,T_0) + B_\omega(0,T_0) V(0)} \right| + \left| e^{-\left(\omega^2 + \frac{1}{4}\right)\nu^2/2} \right| \right) d\omega \\
&\leq 2 \int_u^\infty \frac{1}{\omega^2 + \frac{1}{4}} d\omega.
\end{aligned} \tag{5.33}$$

To show that for an arbitrary ω both $A_\omega(0, T_0) \leq 0$ and $B_\omega(0, T_0) \leq 0$ hold in the constant coefficient case, we use the following steps:

1. We can show that $\frac{dy(t)}{dt} \geq 0$ for all $t \in [0, T]$, with $y(t)$ given by Equation (5.31).
2. We use the terminal condition $y(T) = 0$ and the fact that $y(t)$ is increasing in t on $[0, T]$. This proves $y(t) \leq 0$ for all $t \in [0, T]$. Hence $B_\omega(t, T_0) \leq 0$ for all $t \in [0, T_0]$.
3. We use in Equation (5.29) that $y(t) \leq 0$ for all $t \in [0, T]$, this proves that $\frac{dx(t)}{dt} \geq 0$ if $d < 0$ hence $x(t)$ is increasing in t on $[0, T]$. Note that $d < 0$ is satisfied, since $d = -\beta V(0)$.
4. Since $x(t)$ is increasing and $x(T) = 0$ we have shown that $x(t) \leq 0$ for all $t \in [0, T]$. Hence $A_\omega(t, T_0) \leq 0$ for all $t \in [0, T_0]$.

Solving for u in the inequality

$$2 \int_u^\infty \frac{1}{\omega^2 + \frac{1}{4}} d\omega \leq TOL,$$

yields

$$u \geq \frac{1}{2}\tan\left(\frac{\pi}{2} - \frac{TOL}{4}\right), \text{ with } 0 < \text{TOL}/4 < \pi.$$

If we choose our integration region to be $[0, u]$ with u equal to:

$$u = \frac{1}{2}\tan\left(\frac{\pi}{2} - \frac{TOL}{4}\right), \tag{5.34}$$

then we are sure that:

$$\left|\int_u^\infty f(\omega)d\omega\right| \leq TOL$$

For example, if we take $TOL = 0.005$ then $u = 400$.

We make some remarks on the choice of u.

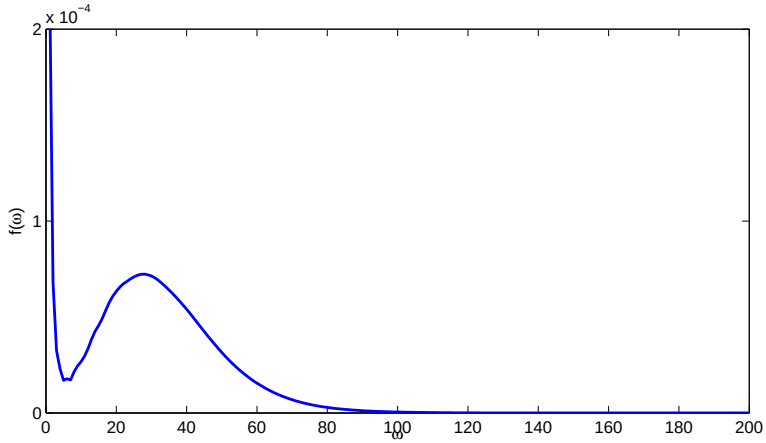

Figure 5.1: Fundamental transform integrand with model parameters $\gamma = 0.1$, $\epsilon = 0.80$ and $\sigma = 0.20$ with numerical ODE solutions.

- We made very crude estimations to derive (5.34). We do not take the exponential decay into account:

  $$e^{-(\omega^2+1/4)\nu^2/2} \to 0 \text{ if } \omega \to \infty,$$

  and

  $$e^{A_\omega(0,T_0)+B_\omega(0,T_0)V(0)} \to 0 \text{ if } \omega \to \infty.$$

  The latter limit is not difficult to prove in the constant coefficient case. We already showed $A_\omega(0, T_0) \leq 0$ and $B_{\omega,T_0}(0) \leq 0$. It is thus sufficient to prove $A_\omega(0, T_0) \to -\infty$ if $\omega \to \infty$. This is equivalent to showing that $x(0) \to -\infty$ if $a \to \infty$, with $x(t)$ given by Equation (5.32). This is a trivial calculus exercise left to the reader.

- If we take $u = 500$, this corresponds to $TOL = 0.004$. Then we expect a much higher accuracy, since the integrand decays to zero exponentially. We illustrate this in Figure 5.1.

Numerical integration rule to approximate $\int_a^b g(x)dx$

To compute the improper integral $\int_0^\infty f(\omega)d\omega$, we have to compute a proper integral of the form

$$\int_a^b g(x)dx$$

numerically, we propose an adaptive Simpson quadrature. For a detailed explanation of adaptive integration rules we refer to [17]. There are Matlab and C++ libraries available to perform an adaptive Simpson quadrature with a desired level of accuracy.

Numerical ODE solver

If $\epsilon(t)$ and $\lambda(t)$ are time-dependent, we have to solve the Riccati ODEs given by Equation (5.27) numerically. We choose a Runge Kutta scheme to solve the Riccati ODEs.

5.4 Parameter averaging

In this section we start with the swap rate model, given by Equation (5.10). We state it once again for convenience:

Model 2: The swap rate model

$$\boxed{\begin{aligned} dS_{0,m}(t) &= [\gamma(t)S_{0,m}(t) + (1-\gamma(t))R_0]\,\lambda(t)\sqrt{V(t)}dW_1^{\mathbb{Q}^{1,m}}(t), \\ dV(t) &= \beta(V(0)-V(t))dt + \epsilon(t)\sqrt{V(t)}dW_2^{\mathbb{Q}^{1,m}}(t), \end{aligned}} \tag{5.35}$$

where $\epsilon(t), \gamma(t)$ and $\lambda(t)$ are time-dependent functions. We wish to find appropriate time-homogeneous parameters $\bar{\epsilon}, \bar{\gamma}$ and $\bar{\lambda}$ for the functions $\epsilon(t), \gamma(t)$ and $\lambda(t)$, to obtain an approximating system of SDEs:

Model 3: The time-homogeneous swap rate model

$$\boxed{\begin{aligned} d\tilde{S}_{0,m}(t) &= (\bar{\gamma}\tilde{S}_{0,m}(t) + (1-\bar{\gamma})R_0)\bar{\lambda}\sqrt{\tilde{V}(t)}dW_1^{\mathbb{Q}^{1,m}}(t), \\ d\tilde{V}(t) &= \beta(V(0)-\tilde{V}(t))dt + \bar{\epsilon}\,\sqrt{\tilde{V}(t)}dW_2^{\mathbb{Q}^{1,m}}(t), \end{aligned}} \tag{5.36}$$

with $\tilde{S}_{0,m}(0) = S_{0,m}(0)$ and $\tilde{V}(0) = V(0)$, so that the terminal distribution of the swap rate model, is approximated by the terminal distribution of the time-homogeneous swap rate model. Once we derived a time-homogeneous swap rate model the form (5.36), we approximate the swaption price by:

$$V_{0,m}^{pay}(0) \approx P_{1,m}(0)\mathbb{E}^{\mathbb{Q}^{1,m}}\left[\left(\tilde{S}_{0,m}(T_0) - K\right)^+\right]. \tag{5.37}$$

Using this model, we can apply the concepts given in Section 5.3 to calculate the expectation in Equation (5.37).

Note that it is sufficient to find an appropriate constant skew parameter γ, to replace the time-dependent skew function $\gamma(t)$. Then we can apply the techniques from Section 5.3 to compute an approximation of the swaption price. A drawback is that the Riccati ODEs have to be solved numerically. This is computationally expensive. If we are able to derive the time-homogeneous swap rate model, given by Equation (5.36), then there exists an analytic solution for the Riccati ODEs. This will speed up the computation of the fundamental transform integral.

Hence the pricing problem is reduced to finding appropriate time-averaged values of the time-dependent functions $\gamma(t)$, $\epsilon(t)$ and $\lambda(t)$. This is the main topic in the subsequent subsections.

5.4.1 Averaging the volatility of volatility function $\epsilon(t)$

In this subsection we discuss a method to calculate a time-averaged value $\bar{\epsilon}$ for $\epsilon(t)$ over a time horizon $[0, T_0]$, so that we can replace the process $V(t)$ by a process $\tilde{V}(t)$ with dynamics:

$$\begin{aligned} d\tilde{V}(t) &= \beta(V(0) - \tilde{V}(t))dt + \bar{\epsilon}\sqrt{\tilde{V}(t)}dW_2^{\mathbb{Q}^{1,m}}(t), \\ \tilde{V}(0) &= V(0). \end{aligned} \tag{5.38}$$

Recall that the swap rate dynamics are approximated by:

$$dS_{0,m}(t) = [\gamma(t)S_{0,m}(t) + (1-\gamma(t))R_0]\,\lambda(t)\sqrt{V(t)}dW_1(t),$$

with:

$$\gamma(t)S_{0,m}(t) + (1-\gamma(t))R_0,$$

the skew function and $\sqrt{V(t)}\lambda(t)$ the volatility function. The volatility of volatility parameter $\bar{\epsilon}$ allows us to control the curvature of the implied volatility skew. In stochastic volatility models this is controlled by the variance of the quantity [21]:

$$\int_0^{T_0} \lambda^2(t)V(t)dt, \tag{5.39}$$

which depends on the path of $V(t)$. If we replace the process of $V(t)$ by $\tilde{V}(t)$, with dynamics given by (5.38), then the accumulated variance is given by:

$$\int_0^{T_0} \lambda^2(t)\tilde{V}(t)dt, \tag{5.40}$$

which depends on the path of $\tilde{V}(t)$. The quantities in Equations (5.39) and (5.40) are both stochastic, hence random variables, with some unknown distribution. To get an appropriate value for $\bar{\epsilon}$, we choose it so that the first and second moments of (5.39) and (5.40) are the same[1]. This is an obvious choice, since the variance of this quantity controls the curvature. Therefore we state the following theorem.

Theorem 5.2. Given the process

$$dS_{0,m}(t) = [\gamma(t)S_{0,m}(t) + (1-\gamma(t))R_0]\,\lambda(t)\sqrt{V(t)}dW_1(t),$$

and let $V(t)$ and $\tilde{V}(t)$ be two stochastic processes with dynamics

$$\begin{aligned} dV(t) &= \beta(V(0) - V(t))dt + \epsilon(t)\sqrt{V(t)}dW_2(t), \\ d\tilde{V}(t) &= \beta(V(0) - \tilde{V}(t))dt + \bar{\epsilon}\sqrt{\tilde{V}(t)}dW_2(t), \end{aligned}$$

where $\bar{\epsilon}$ is given by:

[1] If the first and second moments are the same, then the variances of both distributions are the same.

$$\bar{\epsilon}^2 = \frac{\int_0^{T_0} e^{2\beta r}\epsilon^2(r)\rho_{T_0}(r)dr}{\int_0^{T_0} e^{2\beta r}\rho_{T_0}(r)dr}, \tag{5.41}$$

and

$$\rho_{T_0}(r) = \int_r^{T_0} e^{-\beta s}\lambda^2(s)\int_s^{T_0}\lambda^2(t)e^{-\beta t}dtds.$$

Then the following holds:

$$\mathbb{E}\left[\int_0^{T_0}\lambda^2(t)\tilde{V}(t)dt\right] = \mathbb{E}\left[\int_0^{T_0}\lambda^2(t)V(t)dt\right]$$

and

$$\mathbb{E}\left[\left(\int_0^{T_0}\lambda^2(t)\tilde{V}(t)dt\right)^2\right] = \mathbb{E}\left[\left(\int_0^{T_0}\lambda^2(t)V(t)dt\right)^2\right].$$

Proof. For a proof of this theorem we refer to Appendix B.5. □

5.4.2 Averaging the time varying displacement $\gamma(t)$

As already noticed, we need a constant displacement parameter $\gamma(t)$ to derive the Heston part (5.16). Since we allow $\gamma(t)$ to be a piecewise constant function in the model, we have to find an appropriate time-averaged displacement parameter $\bar{\gamma}$. For this, we state a theorem from Piterbarg [13].

Theorem 5.3. For the SDE with a time-dependent displacement $\gamma(t)$:

$$dS(t) = (\gamma(t)S(t) + (1-\gamma(t))S(0))\lambda(t)\sqrt{\tilde{V}(t)}dW_1(t),$$

with the dynamics of $\tilde{V}(t)$ given by:

$$d\tilde{V}(t) = \beta(V(0) - \tilde{V}(t))dt + \bar{\epsilon}\sqrt{\tilde{V}(t)}dW_2(t),$$

the effective skew parameter $\bar{\gamma}$ over a time horizon $[0, T_0]$ is given by:

$$\bar{\gamma} = \frac{\int_0^{T_0}\gamma(t)v(t)\lambda^2(t)dt}{\int_0^{T_0}v(t)\lambda^2(t)dt}, \tag{5.42}$$

where $v(t)$ is given by:

$$v(t) = V(0)^2\int_0^t\lambda^2(s)ds + \frac{V(0)\bar{\epsilon}^2e^{-\beta t}}{2\beta}\int_0^t\lambda^2(s)(e^{\beta s} - e^{-\beta s})ds. \tag{5.43}$$

Using this $\bar{\gamma}$, we define a new stochastic process $\bar{S}$, whose dynamics are given by:

$$d\bar{S}(t) = (\bar{\gamma}\bar{S}(t) + (1-\bar{\gamma})S(0))\lambda(t)\sqrt{\tilde{V}(t)}dW_1(t),$$

with $\bar{S}(0) = S(0)$. This choice of $\bar{\gamma}$, minimizes the difference of the second and third moment between the distribution of $S(T_0) - S(0)$ and $\bar{S}(T_0) - \bar{S}(0)$.

Proof. For a detailed proof we refer to [13]. □

We summarize the results we have up to this point. In Subsection 5.4.1 we derived an appropriate time-averaged volatility of volatility parameter $\bar{\epsilon}$, so that the first and second moments of the processes given in Equations (5.39) and (5.40) match. Using a result from Piterbarg, we derived an effective displacement parameter $\bar{\gamma}$, so that the differences between the second and third moment of the distributions:

$$S(T_0) - S(0) \text{ and } \bar{S}(T_0) - \bar{S}(0)$$

are minimized. With this choice of $\bar{\gamma}$ we can base our pricing on the ideas of Section 5.3.1.

Hence we transformed the swap rate model, given in Equation (5.35), to an approximating model:

Model 2a: Swap rate model with time-homogeneous skew

$$\boxed{\begin{aligned} d\hat{S}_{0,m}(t) &= (\bar{\gamma}\hat{S}_{0,m}(t) + (1-\bar{\gamma})R_0)\lambda(t)\sqrt{\tilde{V}(t)}dW_1^{\mathbb{Q}^{1,m}}(t), \\ d\tilde{V}(t) &= \beta(V(0) - \tilde{V}(t))dt + \bar{\epsilon}\sqrt{\tilde{V}(t)}dW_2^{\mathbb{Q}^{1,m}}(t), \end{aligned}} \tag{5.44}$$

with intial conditions: $\hat{S}_{0,m}(0) = S_{0,m}(0)$ and $\tilde{V}(0) = V(0)$. We call this model from now on 'swap rate model with time-homogeneous skew'. With this model we can solve the Heston part with the fundamental transform. The drawback is that the Riccati ODEs, given by Equation (5.27), have to be solved numerically. This can be computationally time consuming. We call this the ODE fundamental transform solution. In order to overcome this inconvenience we model $\lambda(t)$ to be constant and use analytic solutions for the Riccatti equations. We call this the analytic fundamental transform solution. This is the topic of the next subsection.

5.4.3 Averaging the time-dependent volatility function $\lambda(t)$

To obtain an appropriate time-averaged parameter $\bar{\lambda}$ for the time-dependent function $\lambda(t)$ over a time horizon $[0, T_0]$, we use a result from Piterbarg. This result derives a time-homogeneous parameter $\bar{\lambda}$, to replace the time-dependent volatility function $\lambda(t)$, so that the price of an at the money swaption is preserved to satisfactory approximation. Before we state this result as a theorem, we sketch the main ideas underlying the result. Up to this moment we have a system of the following form.

$$\begin{aligned} dS(t) &= [\gamma S(t) + (1-\gamma)S(0)]\,\lambda(t)\sqrt{V(t)}dW_1^{\mathbb{Q}^{1,m}}(t), \\ dV(t) &= \beta(V(0) - V(t))dt + \epsilon\sqrt{V(t)}dW_2^{\mathbb{Q}^{1,m}}(t), \end{aligned} \tag{5.45}$$

For convenience we omited tildes and other confusing symbols. Recall from Equation (5.12), that for an ATM swaption we have to compute the following expectation:

$$\mathbb{E}^{\mathbb{Q}^{1,m}}\left[(S(T_0) - S(0))^+\right] = \mathbb{E}^{\mathbb{Q}^{1,m}}\left[\mathbb{E}^{\mathbb{Q}^{1,m}}\left[(S(T_0) - S(0))^+ \middle| \{V(t)\}_{0\le t\le T_0}\right]\right].$$

This equality follows from the tower property for conditional expectations. Because the Brownian motion that drives $V(t)$ is independent of the Brownian motion that drives $S(t)$, the distribution of $S(T_0)$ is displaced log-normal when conditioned on a particular path of $V(t)$. Using techniques from Chapter 4.4.3, we can derive an expression for the inner expectation.

$$\mathbb{E}^{\mathbb{Q}^{1,m}}\left((S(T_0)-S(0))^+\middle|\,\{V(t)\}_{0\leq t\leq T_0}\right)=\frac{S(0)}{\gamma}\left(2\mathcal{N}(d_1)-1\right),$$

with

$$\begin{aligned}d_1&=\frac{1}{2}\bar{\sigma},\\ \bar{\sigma}^2&=\gamma^2\int_0^{T_0}\lambda^2(s)V(s)ds.\end{aligned}$$

Hence:

$$\mathbb{E}^{\mathbb{Q}^{1,m}}\left[(S(T_0)-S(0))^+\right]=\mathbb{E}^{\mathbb{Q}^{1,m}}\left[h\left(\int_0^{T_0}\lambda^2(s)V(s)ds\right)\right],\tag{5.46}$$

with $h(x)$ given by

$$h(x):=\frac{S(0)}{\gamma}\left(2\mathcal{N}(\gamma\sqrt{x}/2)-1\right).\tag{5.47}$$

We can derive a similar result if we have a constant volatility function $\lambda(t)\equiv\bar{\lambda}$ in our system of SDEs (5.45). Then we obtain:

$$\mathbb{E}^{\mathbb{Q}^{1,m}}\left[(S(T_0)-S(0))^+\right]=\mathbb{E}^{\mathbb{Q}^{1,m}}\left[h\left(\bar{\lambda}^2\int_0^{T_0}V(s)ds\right)\right].$$

Hence we can reformulate the problem of finding the effective time-homogeneous parameter $\bar{\lambda}$ in the following way. Solve $\bar{\lambda}$ from the following equation:

$$\mathbb{E}^{\mathbb{Q}^{1,m}}\left[h\left(\bar{\lambda}^2\int_0^{T_0}V(s)ds\right)\right]=\mathbb{E}^{\mathbb{Q}^{1,m}}\left[h\left(\int_0^{T_0}\lambda^2(s)V(s)ds\right)\right].\tag{5.48}$$

We expect that this choice of $\bar{\lambda}$ preserves accurate approximations of the ATM-level swaption prices. The problem with both expectations in Equation (5.48) is that they are not available in closed form. However the moment-generating functions of the following random variables

$$\int_0^{T_0}\lambda^2(s)V(s)ds\text{ and }\int_0^{T_0}\bar{\lambda}^2V(s)ds,$$

are known in closed form, see [21]. Recall that the moment-generating function of a random variable X is defined as

$$\mathbb{E}\left[\exp(tX)\right],t\in\mathbb{R}.$$

This suggests to approximate $h(x)$ with an exponential function of the form

$$h(x)\approx c_1+c_2e^{c_3x}=g(x).$$

We choose the coefficients c_1,c_2 and c_3 to get a second-order accurate fit around the mean ζ_{T_0} of $\int_0^{T_0}\lambda^2(s)V(s)ds$:

$$\zeta_{T_0} := \mathbb{E}\left[\int_0^{T_0} \lambda^2(s)V(s)ds\right] = V(0)\int_0^{T_0} \lambda^2(s)ds. \tag{5.49}$$

Writing out the Taylor expansions yields:

$$\begin{aligned} g(x) &\approx g(\zeta_{T_0}) + g'(\zeta_{T_0})(x-\zeta_{T_0}) + \frac{1}{2}g''(\zeta_{T_0})(x-\zeta_{T_0})^2, \\ h(x) &\approx h(\zeta_{T_0}) + h'(\zeta_{T_0})(x-\zeta_{T_0}) + \frac{1}{2}h''(\zeta_{T_0})(x-\zeta_{T_0})^2. \end{aligned}$$

To get a second order accurate approximation around $x = \zeta_{T_0}$ we have to satisfy:

$$\begin{aligned} h(\zeta_{T_0}) &= c_1 + c_2 e^{c_3\zeta_{T_0}}, \\ h'(\zeta_{T_0}) &= c_2 c_3 e^{c_3\zeta_{T_0}}, \\ h''(\zeta_{T_0}) &= c_2 c_3 c_3 e^{c_3\zeta_{T_0}}, \end{aligned}$$

from which we derive

$$c_3 = \frac{h''(\zeta_{T_0})}{h'(\zeta_{T_0})}.$$

with $h(x)$ given by (5.47) and ζ_{T_0} given by Equation (5.49). Note that the coefficients c_1 and c_2 are not relevant. With this choice of c_3 we replace the problem, given by Equation (5.46), by the following problem:

$$\mathbb{E}^{\mathbb{Q}^{1,m}}\left[c_1 + c_2\exp\left(\frac{h''(\zeta_{T_0})}{h'(\zeta_{T_0})}\int_0^{T_0}\bar{\lambda}^2 V(s)ds\right)\right] = \mathbb{E}^{\mathbb{Q}^{1,m}}\left[c_1 + c_2\exp\left(\frac{h''(\zeta_{T_0})}{h'(\zeta_{T_0})}\int_0^{T_0}\lambda^2(s)V(s)ds\right)\right],$$

or equivalently

$$\mathbb{E}^{\mathbb{Q}^{1,m}}\left[\exp\left(\kappa\bar{\lambda}^2\int_0^{T_0} V(s)ds\right)\right] = \mathbb{E}^{\mathbb{Q}^{1,m}}\left[\exp\left(\kappa\int_0^{T_0}\lambda^2(s)V(s)ds\right)\right], \tag{5.50}$$

where we defined

$$\kappa := \frac{h''(\zeta_{T_0})}{h'(\zeta_{T_0})}.$$

We can solve $\bar{\lambda}$ from Equation (5.50), since the moment-generating functions are known. The moment-generating function of $\int_0^{T_0}\lambda^2(s)V(s)ds$ is given by:

$$\mathbb{E}^{\mathbb{Q}^{1,m}}\left[\exp\left(\kappa\int_0^{T_0}\lambda^2(s)V(s)ds\right)\right] = \exp\left(A(0,T_0) + B(0,T_0)V(0)\right),$$

where $A(t,T_0)$ and $B(t,T_0)$ satisfy the following system of Riccati ODEs.

$$\begin{aligned} \frac{d}{dt}A(t,T_0) &= -\beta V(0)B(t,T_0), \\ \frac{d}{dt}B(t,T_0) &= -\kappa\lambda^2(t) + \beta B(t,T_0) - \frac{\epsilon^2}{2}B^2(t,T_0), \end{aligned}$$

with terminal conditions $(A(T_0,T_0), B(T_0,T_0)) = (0,0)$. To obtain the moment-generating function of $\int_0^{T_0}\bar{\lambda}^2 V(s)ds$, replace $\lambda(t)$ by $\bar{\lambda}$ in the sytem of Riccati ODEs. We summerize this result in the following theorem.

Theorem 5.4. A second-order accurate effective volatility parameter $\bar{\lambda}$, over a time horizon $[0, T_0]$, is given as a solution to the equation

$$\varphi_0\left(\frac{h''(\xi)}{h'(\xi)}\bar{\lambda}^2\right) = \varphi\left(\frac{h''(\xi)}{h'(\xi)}\right), \tag{5.51}$$

with

$$\begin{aligned}\xi &:= V(0)\int_0^{T_0}\lambda^2(t)dt,\\ h(x) &:= \frac{S_{0,m}(0)}{\bar{\gamma}}\left(2\mathcal{N}\left(\frac{\bar{\gamma}}{2}\sqrt{x}\right)-1\right).\end{aligned}$$

φ_0 is given by

$$\varphi_0(\mu) := \exp\left(C_\mu(0,T_0) + V(0)\cdot D_\mu(0,T_0)\right),$$

with $C_\mu(t,T_0)$, $D_\mu(t,T_0)$ satisfying the following system of Riccati ODEs

$$\begin{aligned}\frac{dC_\mu(t,T_0)}{dt} &= -\beta\cdot V(0)\cdot D_\mu(t,T_0),\\ \frac{dD_\mu(t,T_0)}{dt} &= -\mu + \beta D_\mu(t,T_0) - \frac{1}{2}\bar{\epsilon}^2 D_\mu^2(t,T_0),\end{aligned}$$

and terminal condition $(C_\mu(T_0,T_0), D_\mu(T_0,T_0)) = (0,0)$.

Function φ is given by:

$$\varphi(\mu) = \exp(A_\mu(0,T_0) + V(0)\cdot B_\mu(0,T_0)).$$

The functions $A_\mu(t,T_0)$ and $B_\mu(t,T_0)$ satisfy the Riccati system of ODEs:

$$\begin{aligned}\frac{dA_\mu(t,T_0)}{dt} &= -\beta\cdot V(0)\cdot B_\mu(t,T_0)\\ \frac{dB_\mu(t,T_0)}{dt} &= -\mu\lambda^2(t) + \beta B_\mu(t,T_0) + \frac{1}{2}\bar{\epsilon}^2 B_\mu^2(t,T_0),\end{aligned}$$

subject to the terminal conditions $(A_\mu(T_0,T_0), B_\mu(T_0,T_0)) = (0,0)$.

Note the following:

1. ξ in (5.51) is a constant, obtained by numerical integration of $\lambda^2(.)$, hence $\kappa = \frac{h''(\xi)}{h'(\xi)}$ is constant.
2. $h'(x)$ and $h''(x)$ are given by:

$$\begin{aligned}h'(x) &= \frac{S_{0,m}(0)}{\sqrt{8\pi x}}e^{-\frac{1}{8}\bar{\gamma}^2 x},\\ h''(x) &= -\frac{S_{0,m}(0)}{16x\sqrt{2\pi x}}\left(4+x\bar{\gamma}^2\right)e^{-\frac{1}{8}\bar{\gamma}^2 x}.\end{aligned}$$

   For any $x > 0$, $h'(x)$ and $h''(x)$ have opposite signs, which implies $\kappa < 0$.

3. $\varphi_0(.)$ is known in closed form. The analytic solution is obtained by an application of Result 5.1, with

$$a = \kappa\bar{\lambda}^2, b = \beta, c = -\frac{1}{2}\bar{\epsilon}^2 \text{ and } d = -\beta V(0).$$

4. We have to solve one system of Riccati ODEs numerically, with $\mu = \frac{h''(\xi)}{h'(\xi)}$, to obtain φ.

Hence the problem of solving $\bar{\lambda}^2$, from Equation (5.51), is a simple root-finding problem.

A Newton iteration scheme to solve Equation (5.51)

Using the notation and symbols from Theorem 5.4, we see that the equation given by (5.51), is equivalent to

$$\log(\varphi_0(\kappa\bar{\lambda}^2)) = \log(\varphi(\kappa)), \tag{5.52}$$

The right-hand side of Equation (5.52) is constant. We use the second-order Newton scheme to solve the non-linear equation (5.52) for the unknown $\bar{\lambda}^2$. If we write $\rho = \bar{\lambda}^2$, then the iteration scheme reads:

$$\rho_{i+1} = \rho_i - \Delta_i,$$

with

$$\Delta_i := \frac{\log(\varphi_0(\kappa\rho_i)) - \log(\varphi(\kappa))}{\frac{\partial \log(\varphi_0)}{\partial \rho}(\kappa\rho_i)}.$$

Stopping criterion Newton iteration

We propose the following rule to terminate the iteration scheme:

Stop the iteration scheme if the following condition is satisfied:

$$|\rho_{i+1} - \rho_i| = |\Delta_i| \leq \overline{TOL}$$

for some tolerance level $\overline{TOL} > 0$.

Initial guess Newton iteration

As an initial guess we propose

$$\rho_0 := \frac{\int_0^{T_0} \lambda^2(t)dt}{T_0}, \tag{5.53}$$

and assume it to be in the ball of attraction. This choice is arbitrary, but we give the following motivation for this choice of ρ_0. We solve the equation for $\rho = \bar{\lambda}^2$, which will be some average value of $\lambda^2(t)$ on the interval $[0, T_0]$. It is well-known from calculus that the definition of ρ_0, given by (5.53), is a measure for the average value of a function $\lambda^2(t)$ on a closed interval $[0, T_0]$. Hence we expect that ρ_0 is sufficiently close to $\bar{\lambda}^2$ so that Newton's method converges.

Summary

We summarize the steps we have to take to price payer swaptions with the concepts from Section 5.3. We assume time-dependent functions $\gamma(t), \epsilon(t)$ and $\lambda(t)$ in the swap rate model given by Equation (5.10).

- Apply Theorem 5.2 to obtain a time-averaged parameter $\bar{\epsilon}$ for the piecewise constant volatility of volatility function $\epsilon(t)$. Use this parameter to define the variance process $\tilde{V}(t)$, given by Equation (5.38). Replace the variance process $V(t)$ in the swap rate model, by the proces $\tilde{V}(t)$ to obtain the following system:

$$\begin{aligned} dS^*_{0,m}(t) &= (\gamma(t)S^*_{0,m}(t) + (1-\gamma(t))R_0)\lambda(t)\sqrt{\tilde{V}(t)}dW_1^{\mathbb{Q}^{1,m}}(t), \\ d\tilde{V}(t) &= \beta(V(0) - \tilde{V}(t))dt + \bar{\epsilon}\sqrt{\tilde{V}(t)}dW_2^{\mathbb{Q}^{1,m}}(t). \end{aligned} \tag{5.54}$$

- Apply Theorem 5.3, using the model given by Equation (5.54), to obtain a time-averaged parameter $\bar{\gamma}$ for the piecewise constant skew function $\gamma(t)$. With this parameter define a new stochastic process $\hat{S}_{0,m}(t)$, with dynamics given by:

$$d\hat{S}_{0,m}(t) = (\bar{\gamma}\hat{S}_{0,m}(t) + (1-\bar{\gamma})R_0)\lambda(t)\sqrt{\tilde{V}(t)}dW_1^{\mathbb{Q}^{1,m}}.$$

  With this random variable we approximate the model, given by Equation (5.54), by the swap rate model with time-homogeneous skew:

$$\begin{aligned} d\hat{S}_{0,m}(t) &= (\bar{\gamma}\hat{S}_{0,m}(t) + (1-\bar{\gamma})R_0)\lambda(t)\sqrt{\tilde{V}(t)}dW_1^{\mathbb{Q}^{1,m}}, \\ d\tilde{V}(t) &= \beta(V(0) - \tilde{V}(t))dt + \bar{\epsilon}\sqrt{\tilde{V}(t)}dW_2^{\mathbb{Q}^{1,m}}(t). \end{aligned} \tag{5.55}$$

  This system approximates the terminal distribution of $S_{0,m}(T_0)$ driven by the swap rate model (5.10).

- Apply the theory of Section 5.3 to the swap rate model with time-homogeneous skew, given by Equation (5.55), to derive the Heston part of the option value.

- Solve the Heston part, using the fundamental transform, described in Section 5.3.1. This can be done in two ways:

  1. Solve the Heston part, derived from the system defined in Equation (5.55) where $\lambda(t)$ is time-dependent with the ODE fundamental transform. This is computationally time-consuming, since the Riccati ODEs have to be solved numerically. To avoid this, use the second method.
  2. Apply Theorem 5.4, to obtain a time-averaged parameter $\bar{\lambda}$ for the time-dependent function $\lambda(t)$. Using this parameter define a stochastic process $\tilde{S}_{0,m}$ with dynamics:

$$d\tilde{S}_{0,m}(t) = (\bar{\gamma}\tilde{S}_{0,m}(t) + (1-\bar{\gamma})R_0)\bar{\lambda}\sqrt{\tilde{V}(t)}dW_1^{\mathbb{Q}^{1,m}}.$$

     With this stochastic process we approximate the swap rate model with time-homogeneous skew, given by Equation (5.55), by the time-homogeneous swap rate model:

$$\begin{aligned} d\tilde{S}_{0,m}(t) &= (\bar{\gamma}\tilde{S}_{0,m}(t) + (1-\bar{\gamma})R_0)\bar{\lambda}\sqrt{\tilde{V}(t)}dW_1^{\mathbb{Q}^{1,m}}, \\ d\tilde{V}(t) &= \beta(V(0) - \tilde{V}(t))dt + \bar{\epsilon}\sqrt{\tilde{V}(t)}dW_2^{\mathbb{Q}^{1,m}}(t). \end{aligned} \tag{5.56}$$

Derive the Heston part for this system and solve it with the analytic fundamental transform. This is faster than the ODE fundamental transform, since there are analytic solutions for the Riccati Equations available.

5.5 Efficient implementation method

In this section we propose an efficient method to implement the closed form swaption price, to speed up the swaption pricing in the stepwise calibration process. A detailed discussion of the stepwise calibration process is postponed until Chapter 6. If one is not familiar with the stepwise calibration process, we recommend the reader to read Section 6.1 before this section. We propose this implementation method, since a naive implementation of the closed form swaption price slows down the stepwise calibration process considerably.

We start with a discussion of the problem. Assume that we calibrated to the nth set of calibration instruments, this means that the piecewise constant functions are defined on the interval $[0, S_{n-1}]$. When the optimizer solves the nth optimization problem, it evaluates the objective function. One function evaluation of the objective function requires the computation of three swaption prices. There are two steps involved. In the first step we average the piecewise constant functions $\epsilon(t), \gamma(t)$ and $\lambda(t)$, over a time-horizon $[0, S_n]$, with S_n the option maturity. In the second step we apply the fundamental transform (Equation 5.28), with the averaged values $\bar{\epsilon}, \bar{\gamma}$ and $\bar{\lambda}$, to obtain an approximation of the swaption price.

First of all, the time-homogeneous values of the piecewise constant functions do not depend on the strike of the swaption. They are only dependent on the option maturity and the piecewise constant functions. Secondly, if we take a closer look to the $\epsilon(t)-$ and $\gamma(t)$-averaging formulas, both formulas contain multidimensional integrals. In the $\epsilon(t)$ averaging formula it is a three-dimensional integral, in the $\gamma(t)$-averaging formula a two-dimensional integral. The drawback of multidimensional integrals is that they are computationally expensive to evaluate numerically. Hence for a longer option maturity, the computation of the homogenized parameters requires more time. For every evaluation of the objective function, with at each time a different extension of the piecewise constant functions on $(S_{n-1}, S_n]$, we have to apply the averaging formulas before we can use the closed form solution.

To reduce the work that has to be done with the averaging formulas, we store information after calibration to a previous option maturity S_{n-1}. At this moment we know the values of $\epsilon(t), \gamma(t)$ and $\sigma(t)$ on $[0, S_{n-1}]$. Hence if we store the correct information up to time S_{n-1}, then we only have to compute multidimensional integrals over $[S_{n-1}, S_n]^d$ instead of $[0, S_n]^d$. In combination with the information up to time S_{n-1} we can compute the homogenized parameters over the time-horizon $[0, S_n]$.

5.5.1 Implementation of the averaging formulas

$\epsilon(t)$ averaging formula

Here we show how we implement the $\epsilon(t)$ averaging formula to speed up the homogenization of the volatility of volatility parameter.

Assume that we calibrate the model to the calibration instruments with maturity S_n and that N evaluations of the objective function are necessary to determine the optimal set of parameters. Then we have priced the calibration instruments, by extending the piecewise constant functions $(\epsilon(t), \gamma(t), \sigma(t))$ on $(S_{n-1}, S_n]$ with N different triplets

$$(\epsilon_n^1, \gamma_n^1, \sigma_n^1), \quad (\epsilon_n^2, \gamma_n^2, \sigma_n^2), \cdots, (\epsilon_n^N, \gamma_n^N, \sigma_n^N).$$

For every triplet $i \in \{1, 2, \cdots, N\}$, we have to apply the parameter-averaging procedure for $\epsilon(t)$ to price the calibration instruments. Hence we have to compute for every triplet:

$$\bar{\epsilon}^2 = \frac{\int_0^{S_n} e^{2\beta r} \epsilon^2(r) \rho_{S_n}(r) dr}{\int_0^{S_n} e^{2\beta r} \rho_{S_n}(r) dr}, \tag{5.57}$$

with

$$\rho_{S_n}(r) = \int_r^{S_n} e^{-\beta s} \lambda^2(s) \int_s^{S_n} \lambda^2(t) e^{-\beta t} dt ds. \tag{5.58}$$

The numerator and denominator in Equation (5.57) are both three-dimensional integrals. They are computationally expensive to evaluate numerically. The numerator in Equation (5.57) can however be written as:

$$\begin{aligned}
\int_0^{S_n} e^{2\beta r} \epsilon^2(r) \rho_{S_n}(r) dr = \quad & (\epsilon_n^i)^2 \int_{S_{n-1}}^{S_n} e^{2\beta r} \int_r^{S_n} \int_s^{S_n} e^{-\beta(s+t)} \lambda^2(s) \lambda^2(t) dt ds dr + \\
& \int_0^{S_{n-1}} e^{2\beta r} \epsilon^2(r) \int_r^{S_{n-1}} \int_s^{S_{n-1}} e^{-\beta(s+t)} \lambda^2(s) \lambda^2(t) dt ds dr + \\
& \int_0^{S_{n-1}} e^{2\beta r} \epsilon^2(r) \int_r^{S_{n-1}} e^{-\beta s} \lambda^2(s) ds dr \int_{S_{n-1}}^{S_n} e^{-\beta t} \lambda^2(t) dt + \\
& \frac{1}{2} \left(\int_0^{S_{n-1}} e^{2\beta r} \epsilon^2(r) dr \right) \left(\int_{S_{n-1}}^{S_n} e^{-\beta t} \lambda^2(t) dt \right)^2.
\end{aligned} \tag{5.59}$$

The denominator in Equation (5.57) can be written as:

$$\begin{aligned}
\int_0^{S_n} e^{2\beta r} \rho_{S_n}(r) dr = \quad & \int_{S_{n-1}}^{S_n} e^{2\beta r} \int_r^{S_n} \int_s^{S_n} e^{-\beta(s+t)} \lambda^2(s) \lambda^2(t) dt ds dr + \\
& \int_0^{S_{n-1}} e^{2\beta r} \int_r^{S_{n-1}} \int_s^{S_{n-1}} e^{-\beta(s+t)} \lambda^2(s) \lambda^2(t) dt ds dr + \\
& \int_0^{S_{n-1}} e^{2\beta r} \int_r^{S_{n-1}} e^{-\beta s} \lambda^2(s) ds dr \int_{S_{n-1}}^{S_n} e^{-\beta t} \lambda^2(t) dt + \\
& \frac{1}{2} \left(\int_0^{S_{n-1}} e^{2\beta r} dr \right) \left(\int_{S_{n-1}}^{S_n} e^{-\beta t} \lambda^2(t) dt \right)^2.
\end{aligned} \tag{5.60}$$

The integrals in Equations (5.59) and (5.60) with upper bounds S_{n-1} can be computed after calibrating to maturity S_{n-1}. If we store these values, then the problem of averaging $\epsilon(t)$ is reduced to:

- Compute for every triplet $(\epsilon_n^i, \gamma_n^i, \sigma_n^i)$,

$$\int_{S_{n-1}}^{S_n} e^{2\beta r} \int_r^{S_n} \int_s^{S_n} e^{-\beta(s+t)} \lambda^2(s)\lambda^2(t) dt ds dr, \tag{5.61}$$

  and

$$\int_{S_{n-1}}^{S_n} e^{-\beta t} \lambda^2(t) dt, \tag{5.62}$$

  since $\lambda(t)$ depends on (γ_n^i, σ_n^i).

- Substitute ϵ_n^i and the values of the integrals, given by Equations (5.61) and (5.62) in Equations (5.59) and (5.60).

- Since all other terms are known, the integrals in Equations (5.59) and (5.60) are known numerically. Hence we can calculate $\bar{\epsilon}$.

This strategy to apply the parameter averaging procedure for $\epsilon(t)$ saves a lot of work for the nth optimization problem.

$\gamma(t)$ averaging formula

Here we propose a method to implement the $\gamma(t)$-averaging procedure in the stepwise calibration process, we follow the same ideas as described in the previous paragraph. We note that:

$$\bar{\gamma} = \frac{\int_0^{S_n} \gamma(t)v(t)\lambda^2(t)dt}{\int_0^{S_n} v(t)\lambda^2(t)dt} = \frac{\int_0^{S_{n-1}} \gamma(t)v(t)\lambda^2(t)dt + \gamma_n^i \int_{S_{n-1}}^{S_n} v(t)\lambda^2(t)dt}{\int_0^{S_{n-1}} v(t)\lambda^2(t)dt + \int_{S_{n-1}}^{S_n} v(t)\lambda^2(t)dt}, \tag{5.63}$$

with $v(t)$ given by Equation (5.43). The S_{n-1} integrals in Equation (5.63) are known after calibrating to maturity S_{n-1}. Hence the new part, which depends on the values of the parameters on $(S_{n-1}, S_n]$, is:

$$\int_{S_{n-1}}^{S_n} v(t)\lambda^2(t)dt.$$

Time decomposition

In this subsection we investigate the speed we gain from the described implementation method. In the test we calibrate to co-terminal[2] swaptions

$$1\text{Y}10\text{Y}, 2\text{Y}9\text{Y}, \ldots 10\text{Y}1\text{Y}.$$

Assume that the model is calibrated to the 9Y2Y swaptions and we calibrate to the last option maturity. In the calibration process we price swaptions with a 10Y maturity. In our test we compare the computation time to compute the time homogenous parameters with two different methods. First of all we measure the time it takes to compute $\bar{\epsilon}$ with Equation (5.41) and $\bar{\gamma}$ with Equation (5.42). Secondly, we measure the time to compute $\bar{\epsilon}$ and $\bar{\gamma}$ with the proposed implementation method. In Table 5.1 we show the results. Hence we speed up the parameter averaging procedure with a factor 10.
Note that this becomes more important if we calibrate to a strip of swaptions with expiries beyond 10Y.

[2]Co-terminal swaptions are a series of European swaptions whose expiry plus tenor is equal.

	Slow method	Fast method	Speed up factor
$\bar{\epsilon}$	2.025	0.206	9.8
$\bar{\gamma}$	0.0650	0.007	9.8

Table 5.1: Time decomposition in seconds for the calculation time of the time homogeneous parameters.

5.5.2 Instantaneous forward rate

Another time consuming operation is the computation of the instantaneous forward rate $f(0,t)$ from market data. The instantaneous forward rate is a term in the swap rate volatility function $\lambda(t)$, given by Equation (5.11). The forward rate $f(0,t)$ is computed by the following formula:

$$f(0,t) := R(0,t) + t\frac{\partial}{\partial t}R(0,t),$$

where $R(0,t)$ is the yield. The yield is computed from the available market data. However, only for a finite number of $t > 0$ there is a quoted value $R(0,t)$. The missing values are interpolated between these quotes. We use cubic spline interpolation to interpolate between the market quotes.

If we look at the definition of the instantaneous forward rate, we see the derivative of $R(0,t)$ with respect to t, which is approximated by a second order central difference approximation:

$$f(0,t) \approx R(0,t) + t\frac{R(0,t+h) - R(0,t-h)}{2h}. \tag{5.64}$$

For one value of the instantaneous forward rate we have to compute three yield values from the market data. Cubic spline interpolation is computationally expensive compared to linear interpolation. If we implement the instantaneous forward rate in a naive way, then the computation of the closed form swaption price slows down. If we apply the $\epsilon(t)$ and $\gamma(t)$ averaging formulas, then the n-dimensional adaptive integration routines require many $\lambda(t)$ function evaluations. The same holds for the numerical ODE solver, which is used when we apply the $\lambda(t)$ averaging formula.

Since it is not known a priori for which values $t \geq 0$ the numerical routines require the value $f(0,t)$, it is not possible to precompute them. Hence to speed up the computation of $f(0,t)$ we have to find a different approach. We propose the following method.

Assume that we compute the closed form swaption price for a swaption with maturity T. Discretize the interval $[0,T]$ with a time-step $dt = 0.01$. Hence we define a grid[3]

$$0 < 0.01 < 0.02 < \ldots < T.$$

Define N the number of nodes, on this grid we precalculate the values of $f(0,t)$. Hence we obtain a vector:

$$\mathbf{f} = (f_0, f_1, \ldots, f_{N-1})^T,$$

with

[3]We assume that $T/0.01 \in \mathbb{N}$. If $T/0.01 \notin \mathbb{N}$, then we define the last interval of the grid to be: $[\lfloor T/0.01 \rfloor \times 0.01, T]$

$$f_i := f(0, i \times 0.01).$$

Any missing value of the instantaneous forward rate $f(0,t)$, which is required for the computations, is linearly interpolated between the values of $\mathbf{f}$. To illustrate the performance, we assume piecewise constant parameters and price a 10Y1Y swaption with two different methods. First of all we compute the instantaneous forward rate with Formula (5.64). Secondly, we precompute the instantaneous forward rates and use linear interpolation to compute the missing forward rates. In Table 5.2 we show the results. From this table we conclude that we maintain the same accuracy, hence we do not expect a significant bias in the option price if we use this method to compute the forward rates. Furthermore, we conclude that this method is 8 times faster.

	Swaption price	Computation time
Formula (5.64)	52.1659	26.5 sec
Linear interpolation	52.1659	3.3 sec

Table 5.2: Pricing results of an ATM-swaption on a notional of $10,000$.

5.6 Simulation of the DDSV model under the T-forward measure.

In this section we discuss how to simulate the process, given by Equation (5.7), by Monte Carlo methods. A naive approach would be to discretize the whole system using the Euler discretization. Theoretically the variance process cannot yield $V(t) < 0$. Unfortunately, using an Euler discretization to simulate the variance process can yield $V(t) < 0$. This happens especially if the Feller condition is violated. There are several ways to overcome this inconvenience.

1. Sampling from a non-central χ^2 distribution, this is a result from Broadie and Kaya [18]. An advantage is that we have an exact simulation of the process. Under the assumption that
$$\frac{4\beta V(0)}{\epsilon^2} > 1,$$
a fast implementation is possible. Hence if this condition is violated, then simulation of the variance process is slow. For more information see [18], this is the main drawback of this method.

2. Use a moment-matched, log-normal approximation [19]:
$$\begin{aligned} V(t+\Delta t) &= \left(V(0) + [V(t) - V(0)]e^{-\beta \Delta t}\right) \exp\left(-\frac{1}{2}\Gamma(t)^2 + \Gamma(t) Z_t\right), \\ \Gamma(t)^2 &= \log\left(1 + \frac{\epsilon^2 V(t)(1 - \exp(-2\beta\Delta t))}{2\beta(V(0) + [V(t) - V(0)]\exp(-\beta\Delta t))^2}\right), \end{aligned} \tag{5.65}$$
with Z_t a Gaussian sample. An advantage is that, without restrictions on the parameters, a fast implementation is possible. Since sampling from a standard normal distribution is relative cheap with respect to sampling from a non-central χ^2 distribution. It is also possible to work with antithetic variables. The scheme cannot yield $V(t) < 0$. This is clear from Equation (5.65), since $V(t) > 0$ implies $V(t + \Delta t) > 0$. A drawback is that we sample from an approximating distribution and we need a sufficiently small timestep Δt to get convergence to the true distribution. If the Feller condition is violated this method has a poor performance.

3. The Quadratic-Exponential (QE) scheme. This is a moment-matched scheme, based on a combination of a squared Gaussian and an exponential distribution. For large values of $V(t)$ we use a moment-matched squared Gaussian distribution. For small values of $V(t)$ we approximate the conditional distribution of $V(t+\Delta t)$ given $V(t)$ by an exponential distribution. We summarize the entire sampling algorithm step-by-step. For further details we refer to [20].

   (a) Conditional on $V(t)$ compute the first and second moments of $V(t+\Delta t)$:

   $$m := \mathbb{E}\left[V(t+\Delta t)|\, V(t)\right] = V(0) + [V(t) - V(0)]e^{-\beta\Delta t},$$
   $$s^2 := \mathrm{Var}\left(V(t+\Delta t)|\, V(t)\right) = \frac{V(t)\epsilon^2(t)e^{-\beta\Delta t}}{\beta}\left(1-e^{-\beta\Delta t}\right) + \frac{V(0)\epsilon^2(t)}{2\beta}\left(1-e^{-\beta\Delta t}\right)^2.$$

   (b) Compute $\psi = \frac{s^2}{m^2}$.

   (c) Fix an arbitrary $\psi_c \in [1,2]$.

   (d) **If** $\psi \leq \psi_c$

      i. Compute

      $$c^2 = \frac{2}{\psi} - 1 + \sqrt{\frac{2}{\psi}}\sqrt{\frac{2}{\psi} - 1},$$
      $$d = \frac{m}{1+c^2}.$$

      ii. Set $V(t+\Delta t) \approx d(c+Z)^2$ with $Z \sim \mathcal{N}(0,1)$.

      With this choice of c and d, the first and second moments of $d(c+Z)^2$ and $V(t+\Delta t)$ are equal.

   (e) **Otherwise**, if $\psi > \psi_c$:

      i. Compute

      $$p = \frac{\psi - 1}{\psi + 1},$$
      $$q = \frac{2}{m(\psi+1)}.$$

      ii. Set $V(t+\Delta t) \approx \psi^{-1}(U;p;q)$ with $\psi^{-1}(u;p;q)$ given by

      $$\psi^{-1}(u;p;q) = \begin{cases} 0 & 0 \leq u \leq p \\ \frac{1}{q}\log\left(\frac{1-p}{1-u}\right) & p < u \leq 1 \end{cases}$$

      and $U \sim U(0,1)$.

      With this choice of p and q, the first and second moments of $\psi^{-1}(U;p;q)$ and $V(t+\Delta t)$ are equal.

We wish to use a scheme that approximates the distribution of $V(t+\Delta t)$ given $V(t)$ accurately, without restrictions on the parameters. Note that the variance process cannot reach zero (theoretically) if the Feller condition is satisfied. Recall that the Feller condition is given by:

$$\frac{2\beta V(0)}{\epsilon^2} > 1.$$

It may happen that under certain market conditions the Feller condition is violated, for example with a small β and a high ϵ is required. In this case $V(t)$ can reach zero with non-zero probability. By construction the log-normal scheme cannot give a value
$V(t+\Delta t)=0$, but the QE scheme can yield $V(t+\Delta t)=0$. Hence if the Feller condition is violated, this argues in favor of the QE scheme and it seems more obvious to use this discretization method. To illustrate the performance of the discretization schemes we present some figures with the sampled distribution of $V(t+\Delta t)$ given $V(t)$. We show two extreme cases, one in which the Feller condition is satisfied and another in which the Feller condition is violated. In our tests we compare the sampled distributions to the exact distributions.

In Figures 5.2(a) and 5.2(b) we show the results for $V(t)=0.09$, $t\in[0,T]$ and $\Delta t=0.10$. We see that the QE scheme has a satisfactory performance in both cases, we have almost a perfect match with the true distribution. We see that the moment-matched log-normal scheme has difficulties to approximate the true distribution if the Feller condition is violated, which is clear from Figure 5.2(a). If the Feller condition is satisfied, then the log-normal method exhibits an improved performance but not better than the QE scheme.

It is known from the literature that the log-normal scheme requires a small time step to get convergence to the true distribution. Hence we can take a smaller timestep, $\Delta t=0.01$ and do the same excercise. If we look to Figures 5.3(a) and 5.3(b), we can conclude that the QE scheme replicates the true distribution in both cases quite accurately, but the log-normal scheme has still a poor perfomance when the Feller condition is violated. It is better than using a timestep $\Delta t=0.10$, but it is still not as accurate as the QE scheme.

These results give us confidence to use the QE scheme. For any β,ϵ and $V(0)$, we expect that this method gives us a more accurate simulation of the variance process than the log-normal scheme.

To simulate the $x(t)$ and $y(t)$ dynamics we use the Milstein scheme.

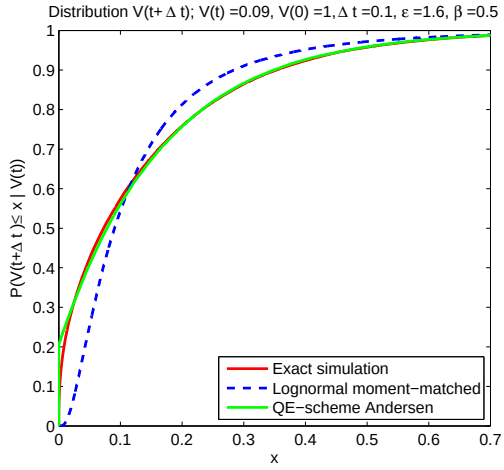

(a) $\frac{2\beta V(0)}{\epsilon^2} = 0.3906 < 1$, Feller condition violated.

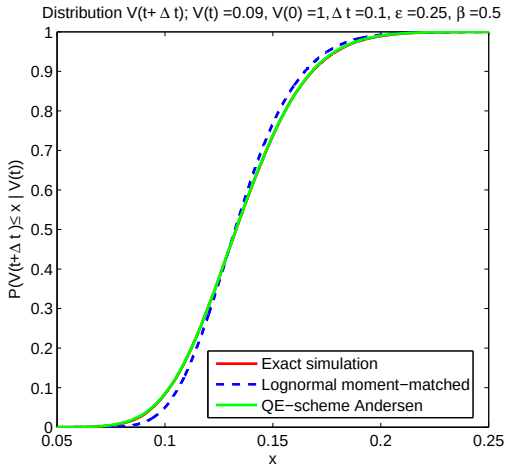

(b) $\frac{2\beta V(0)}{\epsilon^2} = 16 \gg 1$, Feller condition satisfied.

Figure 5.2: $\Delta t = 0.10$: Performance of the QE-scheme and the lognormal scheme, compared to exact simulation.

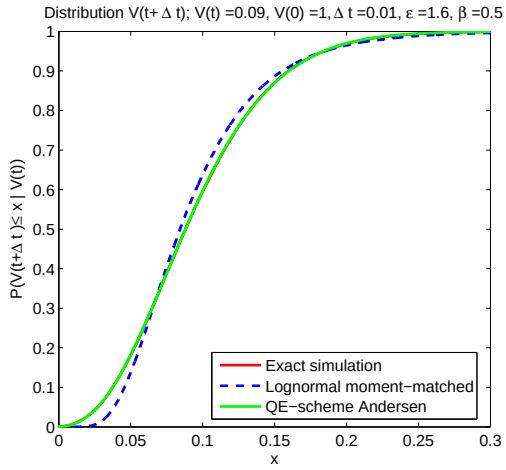

(a) $\frac{2\beta V(0)}{\epsilon^2} = 0.3906 < 1$, Feller condition violated.

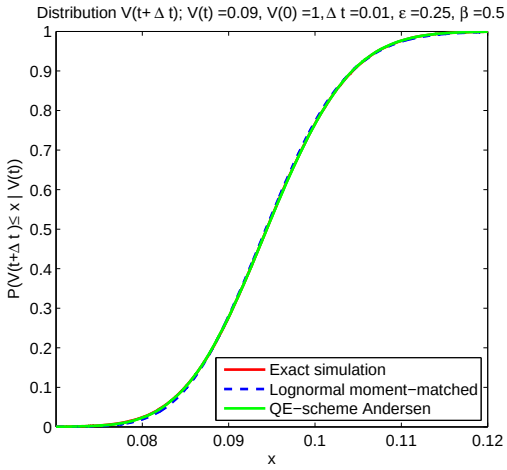

(b) $\frac{2\beta V(0)}{\epsilon^2} = 16 \gg 1$, Feller condition satisfied.

Figure 5.3: $\Delta t = 0.01$: Performance of the QE-scheme and the lognormal scheme, compared to exact simulation.

5.7 The case of non zero correlation, $\rho \neq 0$.

In this section we discuss the influence of a non-zero correlation coefficient ρ between the Brownian motion processes $W_V^{\mathbb{Q}^0}(t)$ and $W_x^{\mathbb{Q}^0}(t)$, in the dynamics of $(x(t), y(t), V(t))$, given by Equation (5.4). A correlation ρ between both Brownian motions can be written as:

$$dW_x^{\mathbb{Q}^0}(t) \cdot dW_V^{\mathbb{Q}^0}(t) = \rho dt. \tag{5.66}$$

5.7.1 The dynamics of the $x(t)$ process under $\mathbb{Q}^0$.

We use Cholesky decomposition to decouple the correlated Brownian motions, given in (5.66), into two independent Brownian motions under the same measure. Note that the correlation matrix Σ is defined by:

$$\Sigma = \begin{pmatrix} 1 & \rho \\ \rho & 1 \end{pmatrix}.$$

The Cholesky decompostion $\Sigma = CC^T$ of the correlation matrix is given by:

$$C = \begin{pmatrix} 1 & 0 \\ \rho & \sqrt{1-\rho^2} \end{pmatrix}.$$

Using matrix C to decouple the correlated Brownian motions under $\mathbb{Q}^0$ gives:

$$\begin{bmatrix} dW_x^{\mathbb{Q}^0}(t) \\ dW_V^{\mathbb{Q}^0}(t) \end{bmatrix} = \begin{pmatrix} 1 & 0 \\ \rho & \sqrt{1-\rho^2} \end{pmatrix} \begin{bmatrix} dW_1^{\mathbb{Q}^0}(t) \\ dW_2^{\mathbb{Q}^0}(t) \end{bmatrix},$$

where $W_1^{\mathbb{Q}^0}(t)$ and $W_2^{\mathbb{Q}^0}(t)$ are independent Brownian motions under $\mathbb{Q}^0$. With this notation we can rewrite the dynamics in (5.4) as a system of SDEs with independent Brownian motions:

$$\begin{aligned} dx(t) &= (y(t) - ax(t))dt + \eta(t, x(t))\sqrt{V(t)}dW_1^{\mathbb{Q}^0}(t), \\ dy(t) &= (\eta^2(t, x(t))V(t) - 2ay(t))dt, \\ dV(t) &= \beta(V(0) - V(t))dt + \rho\epsilon(t)\sqrt{V(t)}dW_1^{\mathbb{Q}^0}(t) + \sqrt{1-\rho^2}\epsilon(t)\sqrt{V(t)}dW_2^{\mathbb{Q}^0}(t). \end{aligned} \tag{5.67}$$

5.7.2 The dynamics of $x(t)$ and $S_{0,m}(t)$ under the annuity measure

Recall that the instantaneous short rate $r(t)$ is modelled by:

$$r(t) = f(0,t) + x(t).$$

We apply a change of measure, from the risk-neutral measure $\mathbb{Q}^0$ to the annuity measure $\mathbb{Q}^{1,m}$, to derive the dynamics of $x(t)$ under the swap measure. This will affect the drift term in the $x(t)$- and variance process. From Appendix A we derive:

$$W_1^{\mathbb{Q}^{1,m}}(t) = W_1^{\mathbb{Q}^0}(t) + \int_0^t \phi(s)ds,$$

with

$$\phi(s) = \eta(s, x(s))\sqrt{V(s)} \sum_{i=1}^{m} \frac{P(s,T_i)}{P_{1,m}(s)} \tau_i B(s,T_i).$$

The dynamics of the $x(t)$ process are given by:

$$dx(t) = (y(t) - ax(t) - \phi(t)\eta(t, x(t))\sqrt{V(t)})dt + \eta(t, x(t))\sqrt{V(t)}dW_1^{\mathbb{Q}^{1,m}}(t),$$

with

$$dy(t) = (\eta^2(t, x(t))V(t) - 2ay(t))dt,$$

and

$$\begin{aligned} dV(t) = &\left[\beta(V(0) - V(t)) - \rho\epsilon(t)\phi(t)\sqrt{V(t)}\right]dt + \rho\epsilon(t)\sqrt{V(t)}dW_1^{\mathbb{Q}^{1,m}}(t) \\ &+ \sqrt{1-\rho^2}\epsilon(t)\sqrt{V(t)}dW_2^{\mathbb{Q}^{1,m}}(t). \end{aligned} \tag{5.68}$$

The system of SDEs, to model the swap rate under the annuity measure, is given by:

$$\begin{aligned} dS_{0,m}(t) &= \left(\sum_{i=0}^{m} q_i^S(t)B(t, T_i)\right)\eta(t, x(t))\sqrt{V(t)}dW_1^{\mathbb{Q}^{1,m}}(t), \\ dV(t) &= \left[\beta(V(0) - V(t)) - \rho\epsilon(t)\eta(t, x(t))V(t)\sum_{i=1}^{m}\frac{P(t, T_i)}{P_{1,m}(t)}B(t, T_i)\right]dt \\ &\quad + \rho\epsilon(t)\sqrt{V(t)}dW_1^{\mathbb{Q}^{1,m}}(t) + \sqrt{1-\rho^2}\epsilon(t)\sqrt{V(t)}dW_2^{\mathbb{Q}^{1,m}}(t). \end{aligned} \tag{5.69}$$

Note that we substituted the definition of $\phi(t)$ in the dynamics of the variance process $V(t)$. As we expect for $\rho = 0$ the system in (5.69) reduces to the system given in Equations (5.8) and (5.9), which we derived in the zero correlation case.

5.7.3 Implications for the solvability

We can approximate the swap rate dynamics, in the same way as we did in Section 5.2. In addition, we have to approximate the non-deterministic terms in the variance process. We use similar approximations, the martingale terms under the annuity measure are approximated by their time zero values and $x(t)$ by $x(0)$. Then, we obtain

$$\begin{aligned} dS_{0,m}(t) &\approx (\gamma(t)S_{0,m}(t) + (1-\gamma(t))R_0)\lambda(t)\sqrt{V(t)}dW_1^{\mathbb{Q}^{1,m}}(t), \\ dV(t) &\approx [\beta(V(0) - V(t)) + f(t)V(t)]\,dt + \rho\epsilon(t)\sqrt{V(t)}dW_1^{\mathbb{Q}^{1,m}}(t) \\ &\quad + \sqrt{1-\rho^2}\epsilon(t)\sqrt{V(t)}dW_2^{\mathbb{Q}^{1,m}}(t). \end{aligned} \tag{5.70}$$

with $\lambda(t)$ defined by (5.11) and $f(t)$ by:

$$f(t) := -\rho\epsilon(t)\eta(t, x(0))\left(\sum_{i=1}^{m}\frac{P(0, T_i)}{P_{1,m}(0)}B(t, T_i)\right).$$

To derive the Heston part, given by Equation (5.16), we have to transform the system given by Equation (5.70) to a system with a constant skew parameter γ.

Assume that $\gamma(t) = \gamma$ is constant in the system given by Equation (5.70). In this case we can derive Equation (5.16) by defining the random variable $\bar{S}_{0,m}(t)$:

$$\bar{S}_{0,m}(t) := \gamma S_{0,m}(t) + (1-\gamma)R_0.$$

The system, given by Equation (5.70), in terms of the new stochastic process $\bar{S}_{0,m}(t)$ reads:

$$\begin{aligned} d\bar{S}_{0,m}(t) &\approx \gamma\lambda(t)\bar{S}_{0,m}(t)\sqrt{V(t)}dW_1^{\mathbb{Q}^{1,m}}(t), \\ dV(t) &\approx [\beta(V(0)-V(t)) + f(t)V(t)]\,dt + \rho\epsilon(t)\sqrt{V(t)}dW_1^{\mathbb{Q}^{1,m}}(t) \\ &\quad + \sqrt{1-\rho^2}\epsilon(t)\sqrt{V(t)}dW_2^{\mathbb{Q}^{1,m}}(t). \end{aligned} \tag{5.71}$$

A transformation to log-space, $x(t) := \log(\bar{S}_{0,m}(t))$, makes the process affine.

$$\begin{aligned} dx(t) &\approx -\frac{1}{2}\gamma^2\lambda^2(t)V(t)dt + \gamma\lambda(t)\sqrt{V(t)}dW_1^{\mathbb{Q}^{1,m}}(t), \\ dV(t) &\approx [\beta(V(0)-V(t)) + f(t)V(t)]\,dt + \rho\epsilon(t)\sqrt{V(t)}dW_1^{\mathbb{Q}^{1,m}}(t) \\ &\quad + \sqrt{1-\rho^2}\epsilon(t)\sqrt{V(t)}dW_2^{\mathbb{Q}^{1,m}}(t). \end{aligned} \tag{5.72}$$

Equation (5.16), in terms of $x(t)$, reads:

$$\text{Heston}(\bar{S}_{0,m}(T_0), \bar{K}) = \text{Heston}(x(T_0), \bar{K}) = \mathbb{E}^{\mathbb{Q}^{1,m}}\left[\left(\exp(x(T_0)) - \bar{K}\right)^+\right] \tag{5.73}$$

Since $x(t)$ is modelled by an affine process, Equation (5.73) can be solved using Fourier techniques, for example the COS method [15] or fundamental transform [21]. Hence we can calculate an approximation of the swaption price.

To obtain the system, given by Equation (5.71), we have to find an appropriate time averaged value for the piecewise constant function $\gamma(t)$ over a time horizon $[0, T_0]$. To apply the result from Piterbarg, given by Theorem 5.3, for an effective skew parameter γ, we require that $V(t)$ is modelled by a Cox-Ingersoll-Ross process with dynamics:

$$dz(t) = \theta(z(0) - z(t))dt + \eta z(t)dW(t), \tag{5.74}$$

with θ and η constant. If we look at the process, given by Equation (5.70), we see that the variance process $V(t)$ is not of the form (5.74). We have two Brownian motions in the dynamics of the variance process, so that it is impossible to transform the process to a CIR-process of the form (5.74). This implies that we cannot apply Theorem 5.3 to derive an effective skew parameter γ.

The formulation of a theorem to compute an effective skew parameter γ over a time horizon $[0, T_0]$, for the system with dynamics given by Equation (5.70), is an issue for future research. Once this problem is solved, we can calculate an approximation of the swaption price in the case of non-zero correlation.

Another possibility is to fix the skew parameter γ. But then we loose control of the skewness of the implied volatility skew. At this moment we do not see any reason to include correlation into our model, since our volatility of volatility parameter $\epsilon(t)$ gives us control of the curvature, $\gamma(t)$ control of the skewness and $\sigma(t)$ control of the level. We expect that this is sufficient to obtain accurate fits to the market skews. Adding correlation makes things more complicated in the sense of making additional approximations.

5.8 Numerical results

In this section we give numerical results based on the topics we discussed in the previous sections. There are three questions we would like to answer in this section:

- The impact of the different model parameters on the implied volatility skew?
- The performance of the averaging formulas?
- Which restrictions on the parameters are necessary to obtain accurate results.

To answer these questions we subdivide this section in three parts, in each part we show corresponding numerical test results. In the numerical tests we use Monte Carlo simulation to price swaptions. We use the Monte Carlo method as described in Section 5.6. Unless otherwise stated the Monte Carlo parameters are: discretization step $dt = 0.005$ and $N = 100,000$ simulations.

5.8.1 The impact of the model parameters on the implied volatility skew

In this subsection we discuss the impact of the parameters $R_0, \beta, \sigma, \gamma$ and ϵin the DDSV model on the implied volatility skew. We illustrate our arguments with a simulation experiment. In the experiment we take a 10Y into 1Y swaption and simulate the $x(t)$ process under the T-forward measure, given by Equation (5.7). When we illustrate the impact of a certain parameter, we fix the remaining parameters and price the swaption for a vector of strikes. The fixed values of the parameters are:

$$a = 0.03, R_0 = 0.04, \beta = 0.40, \epsilon = 0.80, \gamma = 0.15, \sigma = 0.20.$$

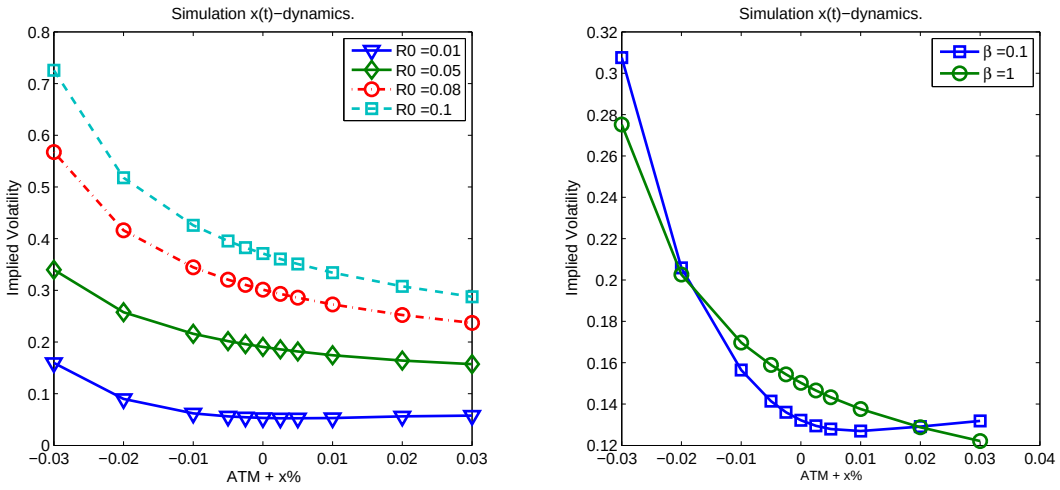

(a) Impact scaling parameter R_0.

(b) Impact parameter β.

Figure 5.4: Impact of parameter R_0 and β on the implied volatility skew.

We start the discussion with parameters R_0. This parameter has impact on the level of the skew. In Figure 5.4(a) we see the impact of R_0. Increasing R_0 implies higher swaption prices and hence a shift in the implied volatility skew. To explain this behaviour we give the following argument. R_0 is part of the instantaneous volatility function. If R_0 increases, then we have larger values in the instantaneous volatility function:

$$\eta(t, x(t)) = \gamma(t)r(t) + (1 - \gamma(t))R_0.$$

Hence this explains why the resulting swaption prices are higher. Note that the effect of R_0 is controlled by parameter γ. For values of γ close to zero, R_0 has larger impact.

Next we discuss the mean reversion of variance parameter β. It is known from the literature [21] that β controls the speed of decay of the volatility smile convexity. In Figure 5.4(b) we illustrate this behaviour. We can explain this behaviour by looking to the long-term variance of the variance process. Recall that the long-term variance is given by:

$$\frac{V(0)\epsilon^2}{2\beta}.$$

Increasing β decreases the long-term variance of $V(t)$ and limits the effect of the stochastic variance process on the volatility skew for long-dated maturities. Since this parameter is assumed to be constant in the model, we have to fix this parameter before we calibrate the model. From market observations and [21] we expect that for major interest rate markets, $\beta \in [0.05, 0.20]$ is a typical setting.

In the model we have three time-dependent parameters, $\sigma(t), \gamma(t)$ and $\epsilon(t)$. We calibrate these parameters to market data. Hence it is interesting to discuss the impact of these parameters on the implied volatility skew.

The volatility parameter σ controls the level of the skew. This is clear from Figure 5.5(a). It is straight forward to explain this behaviour. Larger values in the instananeous volatility function, imply larger prices and hence a shift in the implied volatility skew.

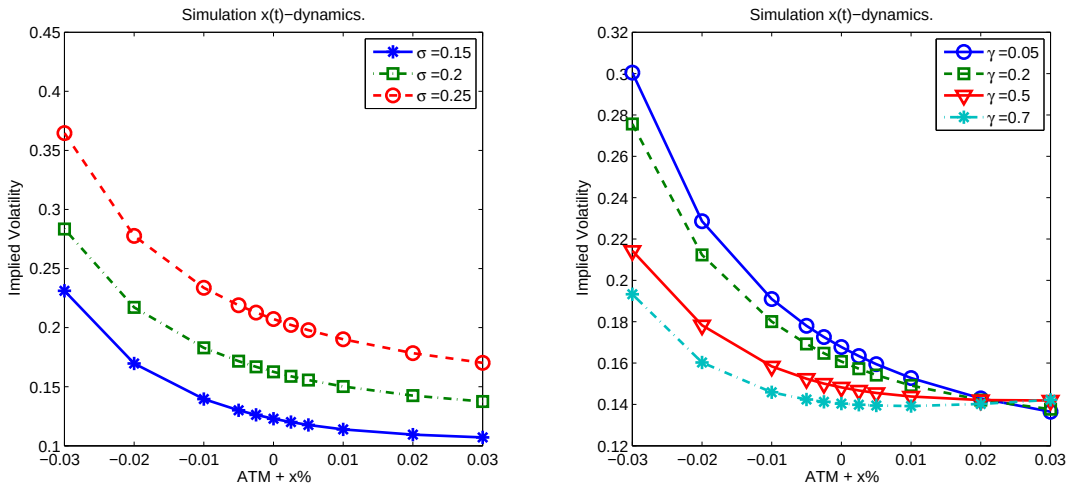

(a) Impact volatility parameter σ.

(b) Impact skew parameter γ.

Figure 5.5: Impact of parameter σ and γ on the implied volatility skew.

Parameter γ is the skew parameter. This parameter controls the slope of the implied volatility skew. We illustrate this in Figure 5.5(b). From this figure we see that a small γ implies a steeper skew than γ close to one. We can explain this if we look to the dynamics $x(t)$. If $\gamma \equiv 0$, then our state variable $x(t)$ is normally distributed. If $\gamma \to 1$ then we are close to a log-normal model and it is well-known that a log-normal model implies a flat implied volatility skew.

The last parameter we discuss is the volatility of volatility parameter ϵ. In the literature this parameter is also known as the smile parameter. As the name suggests this parameters controls the convexity of the implied volatility skew. In Figure 5.6 we illustrate this behaviour.

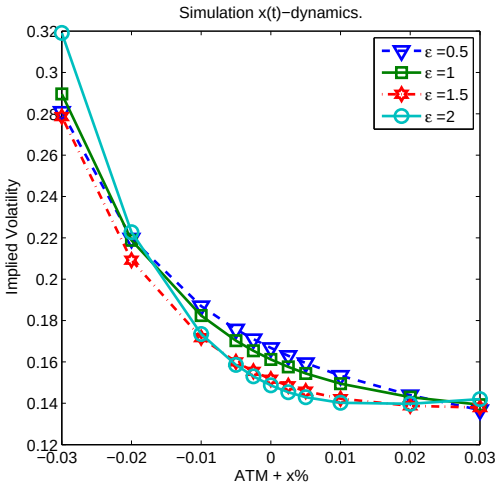

Figure 5.6: Impact of parameter ϵ on the implied volatility skew.

To understand this, we can give a similar argument as for parameter β. Looking to the long-term variance of the CIR process, we see that increasing ϵ increases the long-term variance. Decreasing ϵ decreases the long-term variance and hence limits the effects of the variance process on the implied volatility skew. This immediately explains why it is sufficient to calibrate ϵ and fix β. Both parameters have the same effect on the implied volatility skew. A good choice of β will be sufficient for the parameter ϵ to do the job of adding the required convexity to the implied volatility skew to match the market skew.

Note that there is another constant parameter in the model, which we did not discuss in this section: the initial condition $V(0)$ of the variance process. For scaling reasons we take $V(0) = 1$. This implies $\mathbb{E}[V(t)] = 1$ for every $t \geq 0$. To motivitate this choice note that we multiply the DD instantaneous volatility function $\eta(t, x(t))$ by $\sqrt{V(t)}$. Due to this multiplication, the most obvious choice to keep a proper scaling of the problem is $V(0) = 1$. Note that we do not multiply by a random variable with expected value one, since by Jensen's inequality for concave functions we get:

$$\mathbb{E}[\sqrt{V(t)}] \leq \sqrt{\mathbb{E}[V(t)]} = 1.$$

5.8.2 Performance of the averaging formulas

In this subsection we discuss the performance of the averaging formulas from Section 5.4. Recall that we derived averaging formulas for the time-dependent parameters $\epsilon(t), \gamma(t)$ and $\lambda(t)$ in order to obtain a fast pricing formula for swaptions. To illustrate the performance of these formulas we did the following test. (For an extensive test we refer the reader to [13].)

We take a 10Y into 10Y swaption. We assume piecewise constant functions $\gamma(t), \sigma(t)$ and $\epsilon(t)$ and we keep the remaining parameters constant. The piecewise constant functions are assumed to be constant on the following intervals:

$$S_0 = 0 < S_1 = 1 < S_2 = 2 < \ldots < S_9 = 9 < S_{10} = 10,$$

and are defined as

$$\begin{aligned}\epsilon(t) &= \sum_{j=0}^{9} \mathbb{I}_{t\in(S_j,S_{j+1}]}\,(2.2-0.2j)\,,\\ \gamma(t) &= \sum_{j=0}^{9} \mathbb{I}_{t\in(S_j,S_{j+1}]}\,(1.0-0.1j)\,,\\ \sigma(t) &\equiv 0.15.\end{aligned}$$

For the constant parameters we take:

$$\beta = 0.40, \quad V(0) = 1, \quad a = 0.03, \quad R(0) = S_{0,m}(0).$$

We use these parameters to price the swaption for the following vector of strikes

$$ATM + \{-0.02, -0.01, -0.005, 0, 0.005, 0.01, 0.02\}.$$

To get a good understanding of how well the averaging formulas perform, we compare the fundamental transform pricing results to Monte Carlo results. To avoid additional errors from the approximations we made to derive the swap rate model, we simulate the swap rate model instead of the DDSV model. To test the averaging formulas we take the following approach.

- To test the $\epsilon(t)$-averaging formula we set $\gamma(t) \equiv 0.15$. We apply the averaging formula to derive the swap rate model with constant skew. Note that swap rate volatility function $\lambda(t)$ is still time-dependent. We do not average $\lambda(t)$, but solve the Riccati ODEs numerically. Hence we use the ODE fundamental transform to price the swaptions. In the second step we price the same instruments using the Monte Carlo method.
- To test the $\gamma(t)$-averaging formula we do exactly the same test as for the $\epsilon(t)$-averaging formula. But in this case we fix $\epsilon(t) \equiv 1$ and keep the skew function piecewise constant.
- The third test is to keep $\gamma(t)$ and $\epsilon(t)$ piecewise constant and perform the same test as in the previous cases.
- To test the $\lambda(t)$-averaging formula, we price the instruments with the analytic fundamental transform. I.e. we average the time-dependent volatility function $\lambda(t)$ so that we obtain the time-homogeneous swap rate model.

Results
In Figure 5.7 we present the results for the $\epsilon(t)$ averaging formula. From this figure we conclude that the averaging formula has a satisfactory convergence. The difference between the ODE fundamental transform solution and the Monte Carlo solution is at most 25 basis points. At the ATM-level we are fewer than 5bp off.

In Figure 5.8 we present the results for the $\gamma(t)$ averaging formula. From this figure we conclude that the averaging formula has a satisfactory performance too. The difference between the ODE fundamental transform solution and the Monte Carlo solution is at most 5 basis points. The analytic fundamental transform has a good performance around the ATM-level. By construction of this averaging formula this is exactly what we expect. We have more inaccuracy if we are far of the ATM level, but we stay within a range of 40 basis points accuracy.

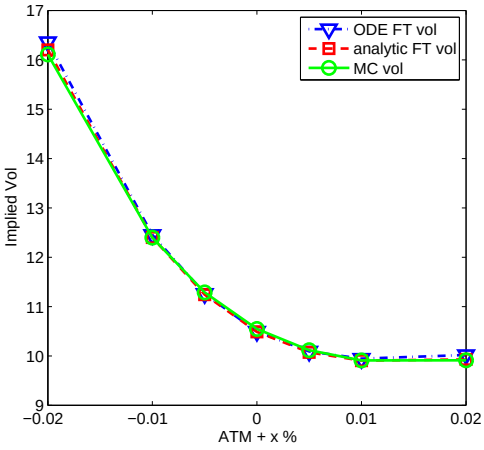

(a) Implied volatility skews

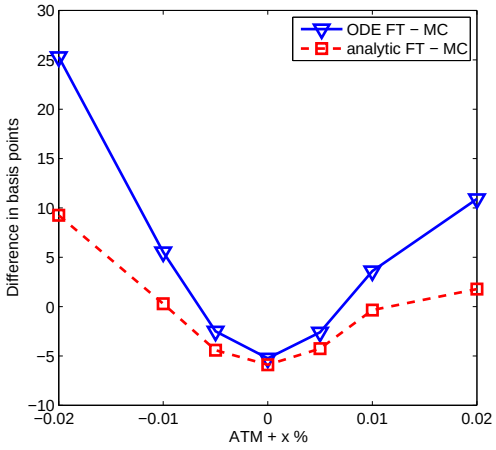

(b) Difference in basis points

Figure 5.7: Performance of the $\epsilon(t)$ averaging formula.

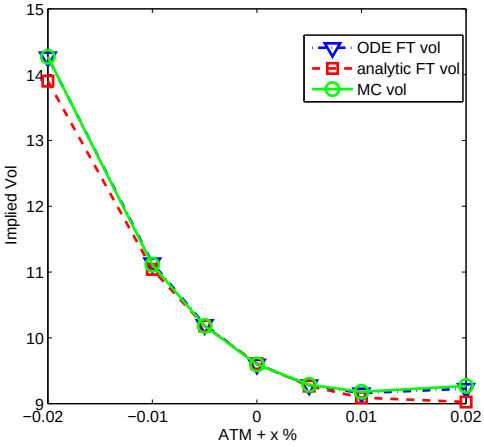

(a) Implied volatility skews

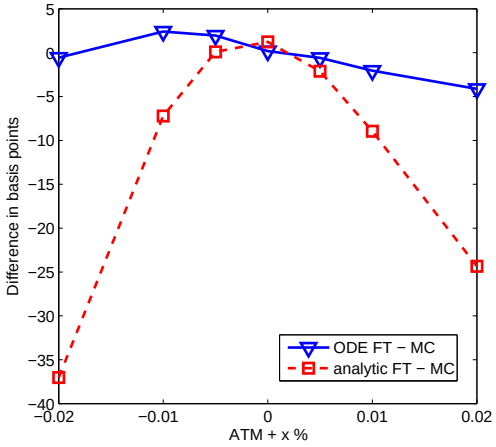

(b) Difference in basis points

Figure 5.8: Performance of the $\gamma(t)$ averaging formula.

In Figure 5.9 we present the results where we combine all averaging formulas. This figure shows the power of the formulas. If we use the ODE fundamental transform solution we see that we stay within a range of 35 bp accuracy. If we average the volatility function $\lambda(t)$ then there is more inaccuracy, but there is still an accurate price around the ATM-level.

We did the same tests for other parameter sets. From these tests we draw the same conclusions. In general we expect similar results to the results we have shown in this section.

5.8.3 Restrictions on the parameters

In this subsection we discuss the approximations in the swap rate dynamics. All approximations are made in the swap rate volatility function to derive $\lambda(t)$, the volatility function of the swap rate model. Recall that we approximate $r(t) \approx f(0,t)$. The effects of this approximation are

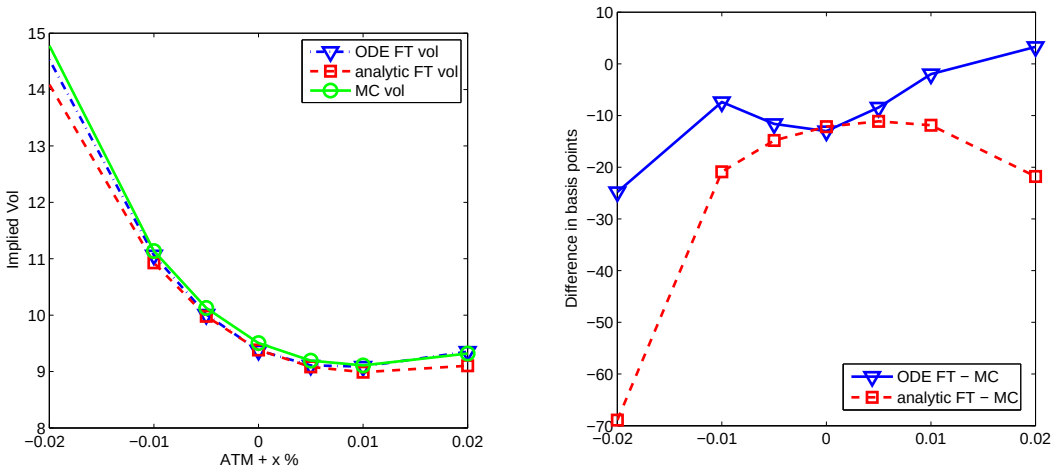

(a) Implied volatility skews

(b) Difference in basis points

Figure 5.9: Joint performance of the $\epsilon(t)$ and $\gamma(t)$ averaging formulas.

small if γ is close to zero. The overall effect of all approximations is affected by the value of σ, since σ is a factor in the swap rate volatility function $\lambda(t)$.

We wish to use the closed form swaption price formula to calibrate the model, hence we are interested for which parameter domains the approximation formulas are accurate. With a test we determine the restriction on both parameters. The approximation error increases when the option maturity increases, hence we choose a 10Y into 1Y swaption. We test based on trial and error, we fix all parameters and vary σ and γ. Then we price a 10Y into 1Y swaption with the closed form solution and the Monte Carlo method. We price the instrument for the following strikes

$$\text{ATM} + \{-0.03, -0.02, -0.01, -0.0050, -0.0025, 0, 0.0025, 0.0050, 0.01, 0.02, 0.03\}.$$

after pricing we compare the implied volatility skews. We assume that the closed form solution works well, if the difference between the Monte Carlo skew and the one obtained from the closed form solution is at most 100bp. Indeed, this value is quite arbitrary, but our goal is to improve the fit to the whole market skew. With Hull-White's model we match only one instrument perfectly. The difference between the model implied skew and the market skew, was in some cases 500 bp or more. (See Figure 3.2.)

In Cheyette's model we have three parameters per option maturity to which we calibrate the model. Theoretically this implies that we can fit three strike levels perfectly. Hence we expect that we are able to fit the other points on the market skew more accurately than with Hull-White. Assume that the Cheyette model is calibrated to a set of swaptions and we price back the calibration instruments with Monte Carlo simulation, if skew implied by this method deviates at most 100bp from the skew implied by the closed form solution (and hence market skew), then we expect in many cases a better fit to the market skew than calibration with Hull-White. This is our motivation why an overall error of 100bp is acceptable[4].

[4]If we allow an overall error of 100 bp we expect a better performance around the ATM level, since our $\lambda(t)$ averaging formula is by construction more accurate around the ATM level.

We did the following trial and error experiment on multiple market data sets. We take two intervals, for γ we define $[0, u_1]$ and for σ we define $[0, u_2]$. Then both, the skew and volatility parameters are fixed to the worst case scenario i.e. $\gamma = u_1$ and $\sigma = u_2$ for all $t \in [0, 10]$. Finally we compute the implied volatility skews. By increasing u_1 and u_2 we derived a safe upperbound on the parameters, so that we have confidence that the overall error between both skews is smaller than 100bp.

We derived that $u_1 = 0.30$ and $\sigma = 0.30$ are safe upperbounds for the intervals. In Figure 5.10 we show the results. In Figure 5.11 we show that increasing both upperbounds to 0.35 exceeds an overall error of 100bp.

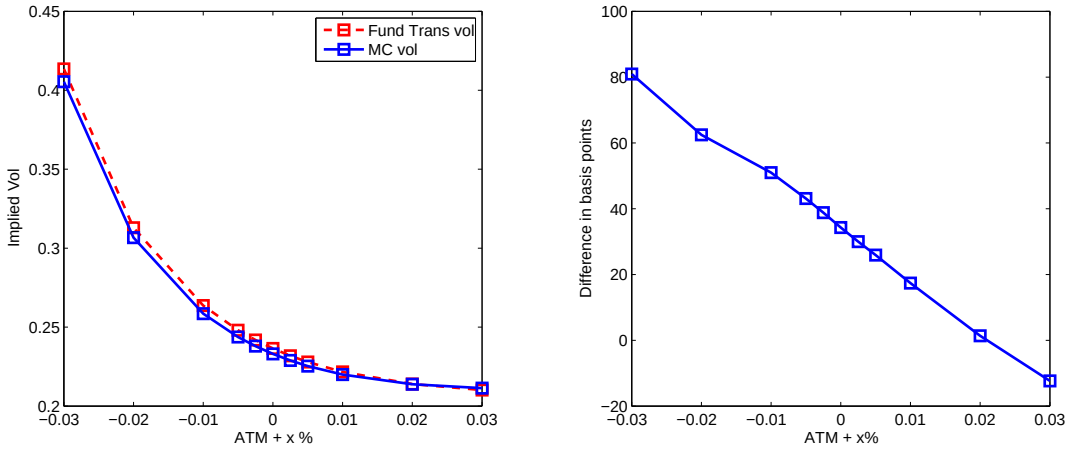

(a) Implied volatility skews

(b) Difference in basis points

Figure 5.10: $\sigma = 0.3$, $\gamma = 0.3$: Accuracy of the closed form solution for a 10Y into 1Y swaption.

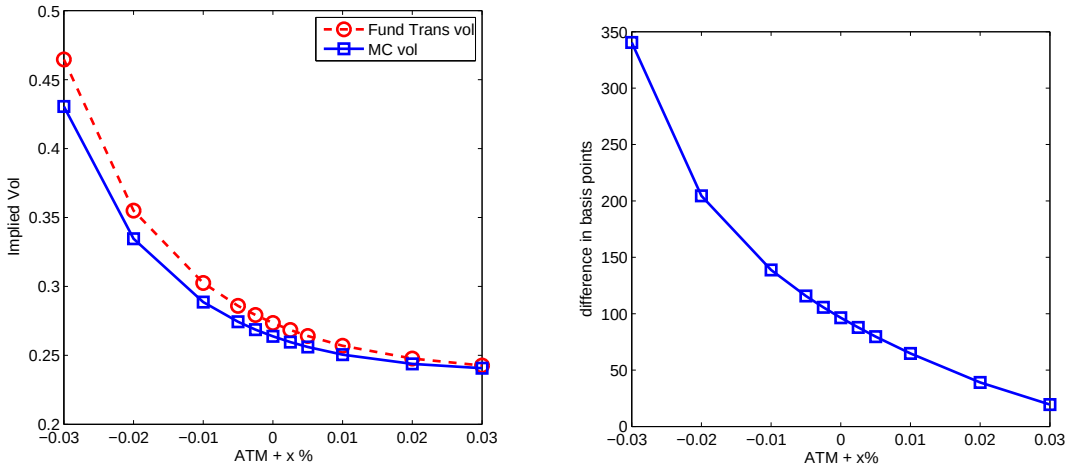

(a) Implied volatility skews

(b) Difference in basis points

Figure 5.11: $\sigma = 0.35$, $\gamma = 0.35$: Accuracy of the closed form solution for a 10Y into 1Y swaption.

Chapter 6

Calibration of the DDSV model

In order to be able to use the model for option pricing, we have to determine the model parameters. The model parameters are chosen in such a way that the model prices match the market prices of a certain set of market instruments as close as possible. The process of finding the set of optimal parameters is called calibration. In practice it is common to calibrate to European style products. In our analysis we are interested in calibration to the swaption market. The way we calibrate the DDSV model to the swaption market is the main topic of this chapter. We subdivide this chapter into the following sub-topics.

- Stepwise calibration of the DDSV model, see Section 6.1.
- Minimization problem, see Section 6.2.
- Calibration to market data, see Section 6.3.
- Calibration results, see Section 6.4.

6.1 Stepwise calibration of the DDSV model.

We calibrate the DDSV model parameters with a bootstrap method. This means that we calibrate the parameters in a piecewise constant fashion for subsequent option maturities. The mean reversion rate a of the $x(t)$ proces, the mean reversion rate β of the variance process and the scaling parameter R_0 are fixed in advance. Hence we calibrate the skew function $\gamma(t)$, the volatility function $\sigma(t)$ and the volatility of volatility function $\epsilon(t)$. To calibrate these piecewise constant functions to the swaption market, we apply the following general algorithm. Details of the algorithm are explained later.

1. Choose a set of option maturities $0 < S_1 < S_2 < \ldots < S_p$.
2. Per option maturity S_i choose three payer swaptions with the same option maturity[1] S_i, but different strike levels, K_1, K_2 and K_3.
3. Start with the calibration instruments corresponding to the first option maturity S_1. Calibrate parameters σ, ϵ and γ so that the model prices match the market prices as close as possible. (In Subsection 6.2 we go into more detail on this.) Once the optimal set of parameters $\sigma_1^*, \gamma_1^*, \epsilon_1^*$ is found, define:

[1] Note that it is allowed to take swaptions with a different underlying swap. Unless otherwise stated we assume three swaptions with the same underlying, but a different fixed rate K on the fixed leg.

$$\sigma(t) \equiv \sigma_1^*, \quad \epsilon(t) \equiv \epsilon_1^*, \quad \gamma(t) \equiv \gamma_1^*,$$

for all $t \in [0, S_1]$. This defines the first parts of the piecewise constant functions $\gamma(t)$, $\sigma(t)$ and $\epsilon(t)$, kept constant on this interval.

4. To calibrate the parameters to the other maturities, proceed as follows. Assume that we have knowledge of the piecewise constant functions up to time S_n, $n \in \{1, 2, \cdots, p-1\}$ i.e. the model is calibrated to the first n sets of calibration instruments. To calibrate the model to the set of calibration instruments corresponding to maturity S_{n+1}, find $\sigma_{n+1}^*, \gamma_{n+1}^*, \epsilon_{n+1}^*$ on interval $(S_n, S_{n+1}]$, such that the model prices match the market prices. Once the optimal set of parameters $\sigma_{n+1}^*, \gamma_{n+1}^*, \epsilon_{n+1}^*$ is found, define

$$\sigma(t) \equiv \sigma_{n+1}^*, \quad \epsilon(t) \equiv \epsilon_{n+1}^*, \quad \gamma(t) \equiv \gamma_{n+1}^*,$$

for all $t \in (S_n, S_{n+1}]$.

5. Repeat the previous step until the model is calibrated to the last maturity.

Note that this is a very general description of the calibration algorithm. In Section 6.2 we explain the minimization problem (objective function and constraints) and the minimization algorithm we use to calibrate the model.

6.2 Minimization problem.

In general we minimize the difference between the model prices and the corresponding market prices. A common choice is to minimize this distance in the $\|.\|_2$-norm. Since we calibrate with the stepwise calibration algorithm, explained in Subsection 6.1, we have p minimization problems. Before we state the nth minimization problem, we introduce definitions and notations.

The option maturity corresponding to the nth minimization problem is S_n. The market prices of the three calibration instruments with maturity S_n are denoted by:

$$\{C_{n,i}^{mkt}, \quad i = 1, 2, 3\}.$$

We denote the current state of the model by χ_{n-1}:

$$\chi_{n-1} := \{\sigma(.), \epsilon(.), \gamma(.)\},$$

the elements of this set are the calibrated piecewise constant functions up to maturity S_{n-1}. The model prices of the swaptions are denoted by

$$\{C_{n,i}(\chi; \sigma_n, \epsilon_n, \gamma_n), \quad i = 1, 2, 3\},$$

We use the time-homogeneous swap rate model, given by (5.36), to compute an approximation of the swaption price for the DDSV model. For this model there exists a closed-form solution for the swaption price. For the nth optimization problem this price is computed conditional on the current state χ_{n-1} of the model and an extension of the piecewise constant function with values $\sigma_n, \epsilon_n, \gamma_n$ on $(S_{n-1}, S_n]$. w_i, $i \in \{1, 2, 3\}$, is the weight factor of the corresponding calibration instrument.

Using this notation, we define the nth minimization problem as:

$$\begin{aligned} &\min_{\sigma_n,\epsilon_n,\gamma_n} \sum_{i=1}^{3} w_i \left(C_{n,i}(\chi_{n-1};\sigma_n,\epsilon_n,\gamma_n) - C_{n,i}^{mkt} \right)^2, \\ &\text{subject to: } \delta \leq \sigma_n \leq 0.30, \\ &\qquad\qquad \delta \leq \gamma_n \leq 0.30, \\ &\qquad\qquad \delta \leq \epsilon_n \leq 5.00. \end{aligned} \tag{6.1}$$

Unless otherwise stated, we take $\delta = 0.01$. We do not allow our parameters to be zero, due to numerical complications, for example, division by zero and the validity of the closed form solution, since the closed form solution is only valid for $\gamma > 0$. Since there is no closed form formula for the implied volatility, we calibrate to market prices and not to market volatilities. If we calibrate to market volatilities, then we have to solve three nonlinear equations after pricing the calibration instruments to evaluate the objective function. This is computationally more expensive. Another drawback is that, for some sets of the parameters, there is no solution for the implied volatility. For these sets the prices are too small, or too large, so that there is no solution for the implied volatility.

To solve the p minimization problems we choose a Sequential Quadratic Programming method, which is an iterative method for nonlinear optimization problems. For unconstrained problems this method resembles the Newton method. Similar to the steepest gradient method, the SQP method defines at every iterate $\mathbf{x}_k$ an appropriate search direction $\mathbf{d}_k$ as a solution to a quadratic programming subproblem and performs a line minimization in the direction of this search direction to obtain a scalar λ_k. Once λ_k is obtained, the next iterate is defined as $\mathbf{x}_{k+1} = \mathbf{x}_k + \lambda \mathbf{d}_k$. This method converges in general to a local minimizer in the neighborhood of the initial guess.

For an extensive description of the SQL method, we refer the reader to [22].

6.3 Calibration to market data.

In the previous sections we discussed in a very general way the calibration of the DDSV model. In this section we discuss the test setup and we calibrate the model to market data. The calibration of the DDSV model is implemented in an existing C++ library. To implement the calibration in C++ we need numerical algorithms. We use functions available in the NAG[2] library.

6.3.1 Choice of the constant parameters.

In the DDSV model we fix parameters a, R_0, and β, before we calibrate the piecewise constant functions. We give a discussion of how we choose these constant parameters. Recall from Section 3.1 that $a \in [0.01, 0.05]$ is a common choice. Unless otherwise stated we define $a = 0.03$. With parameter R_0 we can shift the level of the skew. From our experience $R_0 \in [0.04, 0.07]$ is a common choice. To investigate wheter a suitable R_0 is chosen, it is useful to look at the calibration results. Recall that for accuracy reasons, σ is restricted to $[0, 0.30]$. If there are boundary solutions for σ obtained, then it is better to increase R_0 and recalibrate the model.

In Section 5.8.1 we mentioned that from the literature [21] and market observations it is known that $\beta \in [0.05, 0.20]$ is a common choice. We propose the following method to find the most

[2]For more information about NAG we refer to http://www.nag.co.uk/numeric/CL/CLdescription.asp

suitable β. Before calibrating the model, we investigate the market skews. If there is a strong curvature in the market skews for medium- and long-dated maturities, we expect that a small beta is required. In this case we define $\beta = 0.10$ and we calibrate the DDSV model. If the market skews are flatting out for medium- and long dated maturities, $\beta = 0.20$ is more suitable. If there is no strong curvature in the market skews, even for short-dated maturities, $\beta \in [0.60, 1.00]$ is a suitable choice.

Recall that β and ϵ have a similar impact on the implied volatility skew. To investigate whether a suitable choice for β is made, we look at the interplay of β and ϵ. If the piecewise constant function $\epsilon(t)$ is strongly fluctuating in time, then we may have chosen a suboptimal β. In this case we recommend to recalibrate the DDSV model with a different choice of β.

6.3.2 Choice of calibration instruments.

We need three calibration instruments (payer swaptions), for each option maturity to which we calibrate the model. We take the same underlying swap, but different strike levels. In this paragraph we discuss the choice of calibration instruments in our test. To decide which swaptions to take, there are two important issues to take into account. First of all, which part of the market skew do we wish to fit with the model? Secondly, how liquid are the calibration instruments in the swaption market?

One choice is to calibrate to swaptions with the following strikes

$$\text{ATM} + \{-0.03, 0, 0.03\}.$$

The problem with this choice is that we calibrate to two points of the market skew, ATM-0.03 and ATM$+0.03$, which are in general not liquid in the swaption market. The corresponding quoted market prices are in general obtained by extrapolation. If a swaption is liquid in the market, then we can have more confidence in the quoted market price. It is known from market experience that the most liquid swaptions have strikes between:

$$[\text{ATM} - 150\text{bp}, \text{ATM} + 150\text{bp}].$$

Hence it makes more sense to calibrate to swaptions with strike levels within this range. To capture the whole market skew in this range we choose for each option maturity, unless otherwise stated, swaptions with strike levels:

$$\{\text{ATM} - 1.5\%, \text{ATM}, \text{ATM} + 1.5\%\}.$$

With this choice of calibration instruments we expect to have a good fit to the most liquid instruments of the market skew.

6.3.3 The choice of weight factors w_1, w_2 and w_3.

In the objective function from the optimization problems, given by Equation (6.1), we see weight factors w_1, w_2 and w_3. Defining $w_1 = w_2 = w_3 \equiv 1$ assigns equal weight to the calibration instruments. If we want to assign more weight to one particular calibration instrument, we can assign unequal weights. Unless otherwise stated we choose:

$$w_1 = w_2 = w_3 = 1.$$

6.3.4 Initial guess for the model parameters.

The optimization routine requires an initial guess for the parameters. Since it is possible that the optimization routine can converge to a local minimizer, one needs in general a good initial guess close to the global minimizer of the optimization problem. If the initial guess is far away from the global minimizer, then there is a chance that the optimizer will not reach the global minimizer.

One way to obtain an initial guess, is to use a global optimization algorithm to obtain a start solution for the SQP optimization algorithm. Global minimization schemes are in general based on a stochastic algorithm. The drawback is that they are computationally expensive and slower than local algorithms. We expect that a combination of a global minimization algorithm for the initial guess and a local optimization algorithm has a better accuracy than restricting ourselves to local algorithms. Since calibration is a trade-off between speed and accuracy and we are focussing on a fast calibration, we restrict ourselves to local optimization algorithms to calibrate the model.

Because we use the SQP algorithm, we have to define an initial guess for the p optimization problems. We define them as follows, if we calibrate to the first set of calibration instruments, or equivalently to the first option maturity S_1, we define the following initial guess:

$$\sigma_1^{init} = \frac{1}{2}(\sigma_{min} + \sigma_{max}), \quad \gamma_1^{init} = \frac{1}{2}(\gamma_{min} + \gamma_{max}), \quad \epsilon_1^{init} = \frac{1}{2}(\epsilon_{min} + \epsilon_{max}),$$

where $\sigma_{min}, \ldots, \epsilon_{max}$ are the lower- and upperbounds on the corresponding parameters. Assume that for some n, $n \in \{1, 2, \ldots, p-1\}$, the optimization problem is solved and we obtained the optimal parameters $\sigma_n^*, \gamma_n^*, \epsilon_n^*$ on $(S_{n-1}, S_n]$, then we define

$$\sigma_{n+1}^{init} = \sigma_n^*, \quad \gamma_{n+1}^{init} = \gamma_n^*, \quad \epsilon_{n+1}^{init} = \epsilon_n^*,$$

as an initial guess for the parameters on $(S_n, S_{n+1}]$ for optimization problem $n+1$. Defining the optimal parameters from the previous optimization problem as an initial guess for the next optimization problem is a good choice for parameter stability reasons.

6.3.5 Calibration of the DDSV model to real market data.

In this subsection we discuss the calibration results for real market data of three different currencies and three different dates. We show the results for the EURO, (European Union), USD (United States) and KRW (Korean Won) market. For each currency we take the historical data for 19 November 2009, 9 August 2010 and 15 April 2011. We calibrate the model to the following set of co-terminal swaptions, $\{1\text{Y}10\text{Y}, 2\text{Y}9\text{Y}, \ldots, 10\text{Y}1\text{Y}\}$. To validate the calibration we perform the following analysis.

We use the calibrated parameters to price back the co-terminal swaptions for the following vector of strikes,

$$\text{ATM} + \{-250, -200, -150, -100, -50, -25, 0, 25, 50, 100, 150, 200, 250\}\text{bp}.$$

The instruments are priced back in two different ways. First of all we price the instruments with the closed form formula, hence we obtain fits to the market skew using the time-homogeneous swap rate model. Secondly, we price the instruments using the full-scale DDSV model, with the Monte Carlo method described in Section 5.6. For convergence of the Monte Carlo method, we need a sufficiently large N and sufficiently small timestep dt. In the Monte Carlo simulation we

take $N = 100,000$ and $dt = 1/365$. These settings were obtained by decreasing the time step and increasing the number of simulations, so that the difference between the swaption prices, for a swaption with notional of $10,000$, was less than one basis point.

To compare the DDSV calibration to the Hull-White results, we calibrate the Hull-White model to the same co-terminal swaptions. Since there is only one degree of freedom, we take ATM swaptions. In the Hull-White calibration process we use the analytic swaption formula to price swaptions. We use the calibrated Hull-White parameters and the analytic formula to price back the co-terminal swaptions for the same vector of strikes. Once the calibration instruments are priced back, using the three different models, we compare the results.

At the end of this chapter, in Section 6.4, we present the calibration results for the market data from 15 April 2011. In Appendix C we present the other calibration results, for the market data from 10 November 2009 and 9 August 2010. The appendix is subdivived into three parts. In Sections C.1 through C.2 we present the results for the EURO market. In Sections C.3 through C.4 we present the results for the KRW market. And finally, in Sections C.5 through C.6 we present the results for the USD market.

For each currency and date, we present here the following results. We include one table with calibration results, in which we show for each calibration instrument the observed market price and the time-homogeneous swap rate model price after calibration. With these two prices we can compute the relative difference and the corresponding Black's implied volatility. The difference between the model implied volatility and the market volatility is given in basis points.

$$\text{difference in bp} = 10000 \times (\sigma_{model} - \sigma_{market}) .$$

Furthermore we present one table with the calibrated piecewise constant parameters and the values of the constant parameters. Finally we include for the 1Y10Y, 3Y8Y, 6Y5Y, 7Y4Y, 9Y2Y and 10Y1Y swaption, a figure in which we give the fits to the corresponding market skew. In each figure we show the fit with DDSV model to the market skew (DDSV Monte Carlo line), the fit with the time-homogeneous swap rate model (DDSV Closed formula line) and the fit with the Hull-White model (H&W analytic line). In the caption of each figure we give information about the accuracy of the closed form solution. With

Accuracy, ATM x bp, max y bp.

we mean the following. The difference between the DDSV Monte Carlo and DDSV Closed formula is x bp at the ATM level and the maximum difference between ATM $+[-150\text{bp}, 150\text{bp}]$ is y bp. In the remaining part of this subsection we discuss the results for each market.

The market of 15 April 2011

We start with the market conditions of 15 April 2011 for the EURO, KRW and USD markets. In Figure 6.1 we show the yield curves and in Figure 6.2 we show the market volatility skews for the 1Y10Y and the 10Y1Y swaptions. From the market skews we conclude that the USD market is more volatile than the EURO and KRW markets. To obtain free σ parameters in the calibration, we expect that a larger scaling parameter R_0 is required for the USD market. Furthermore we see that the EURO market has a steeper skew than the KRW and USD markets. Hence we expect that the skew parameter γ is smaller for the EURO market than for the KRW and USD markets. For the KRW market we observe a strong curvature in the market skews, also for the 10Y maturity. We expect that a small mean reversion of variance parameter β, e.g. $\beta \approx 10\%$, is a proper choice to fit these market skews.

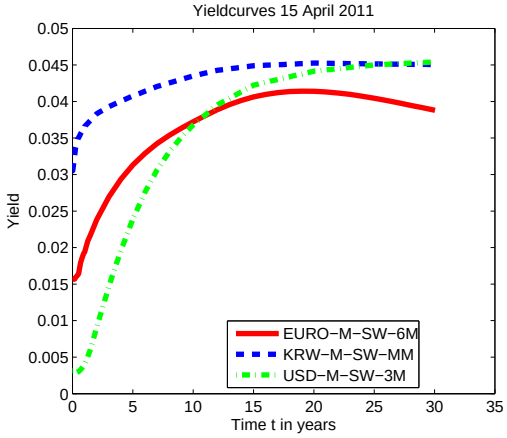

Figure 6.1: Yieldcurves for the EURO, KRW and USD market.

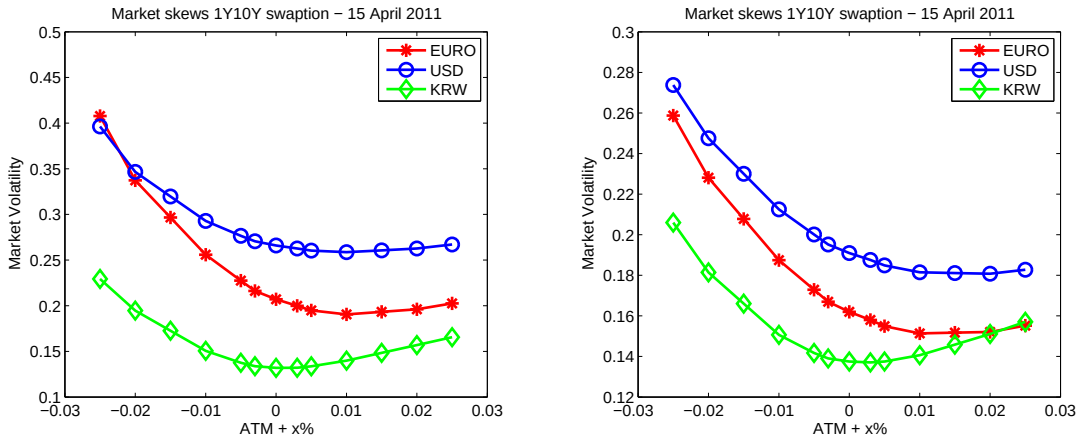

(a) (b)

Figure 6.2: Market skews for the 1Y10Y swaption and 10Y1Y swaption in the three different currencies.

EURO swaption market

For the EURO market we use the EUR-M-SW-6M yield curve. For this market we have an improvement in comparison to the Hull-White model. In general the skew function $\gamma(t)$ is well below 0.30. This implies a high accuracy between the closed form solution and the Monte Carlo

method. We observe that the calibrated parameters are free[3], but there are a few exceptions. For the market of 19 November 2009 we obtain one boundary solution for γ and one boundary solution for σ. For the market of 9 August 2010 we obtain two boundary solutions for γ, for the 9Y and 10Y maturity swaptions. These boundary solutions are obtained after a jump from $\gamma = 0.068$ to $\gamma = 0.30$ and a jump from $\epsilon = 1.12$ to $\epsilon = 0.116$. This tells us that the calibration became unstable for the 9Y and 10Y maturities. Which is reflected in the results for the 10Y maturity swaptions.

If we restrict the calibration to the 10Y maturity swaptions, then we obtain an accurate calibration without any boundary solutions. In Table 6.1 we present the calibration results. The calibrated parameters are given by $\gamma = 0.1688$, $\sigma = 0.2384$ and $\epsilon = 1.0299$. To explain why the calibration to the 10Y1Y swaption is less accurate, when we calibrate to co-terminal swaptions in a bootstrap fashion, is explained by the following argument. For the 10Y1Y skew we require a skew parameter $\gamma = 0.1688$. Since we calibrate to one option maturity we need to satisfy $\gamma(t) \equiv \bar{\gamma}$, the time-averaged skew parameter over a time-horizon $[0, 10]$. We investigated the calibration process for the co-terminal swaptions into more detail. After calibration to the 10Y maturity, we observed that the averaged skew parameter $\bar{\gamma}$ was 0.1772. This is larger than 0.1688, which is required for an accurate match. We expect that the optimizer converged to a local optimum. The use of a global optimizer, to obtain an initial guess for the SQP method, may give a better performance.

Maturity in years	Tenor in years	Strike	Model price	Market price	Relative diff.	Model impl vol.	Market vol.	Diff in bp
10	1	0.0263	132.77	132.77	1e-4	21.67	21.67	0
10	1	0.0413	61.53	61.53	3e-4	16.5	16.5	0
10	1	0.0563	27.25	27.25	4e-4	15.58	15.58	0

Table 6.1: Euro market 9 August 2010: Calibration to 10Y1Y calibration instruments, $\beta = 0.10$ and $R_0 = 0.04$.

If we look at the constant parameters, we conclude the following. For all dates $R_0 = 0.04$ gives a satisfactory performance, since the calibrated σ parameter is always free. Depending on the curvature in the market skews, choosing $\beta \in [0.10, 0.20]$ gives a stable behaviour for the volatility of volatility function $\epsilon(t)$. In general there is no strong curvature in the EURO market, hence there is no need to choose $\beta < 0.10$.

The overall conclusion regarding the EURO market is that we are able to calibrate this market well. We can improve the fit to the market skew in comparison to Hull-White.

KRW swaption market

For the KRW market we use the KRW-M-SW-MM yield curve. From the market skews we observe that the KRW market has more curvature than the EURO market. This market is more difficult to calibrate with the DDSV model than the EURO market. We have a better accuracy at the ATM instruments, than the in-the-money and out-of-the-money instruments.

In general the calibrated parameters are stable. There is one exception for the market of 19 November 2009. There we observe a jump in the volatility of volatility function $\epsilon(t)$. There are

[3]With free we mean that there is no boundary solution obtained.

two arguments to explain this behaviour. First of all, the choice of β is not optimal. Secondly the calibration becomes unstable due to the boundary solutions for γ. Calibrating the model with different values of β did not improve the stability in time of $\epsilon(t)$, hence we expect that the instability is a result from the boundary solutions for γ.

If we look at the calibrated skew function $\gamma(t)$, we observe many boundary solutions. This tells us that we may require a larger skew parameter γ than we allow for accuracy reasons, which suggests us that it is important to improve the crude approximation $r(t) \approx f(0,t)$, in a way that we can loosen the restriction on parameter γ.

For the three dates we observe that for short-dated maturities the fits of the DDSV model to the market skews are more accurate than the Hull-White fits. For the 9Y and 10Y maturities, the fits are less accurate. For these maturities the Hull-White model is closer to the in-the-money swaptions. Only for out of the money swaptions the DDSV is closer to the market skew. The first observation is explained by the boundary solutions for γ. We expect that a larger γ is required to improve the fit to the in-the-money swaptions, since increasing γ decreases the steepness of the skew, see Figure 5.5(b). The second observation is explained by the fact that the DDSV model has control on the curvature of the implied volatility skew. Hence we can obtain a better fit to the out of the money swaptions, where the market skew has a strong curvature.

The overall conclusion for the KRW market is that the DDSV model is able to calibrate the short-dated maturity swaption smiles more accurately than Hull-White. The KRW market requires a larger skew parameter γ than we allow for accuracy reasons. This results in inaccurate calibration results for the long-dated maturity swaptions.

USD swaption market
For the USD market we use the USD-M-SW-3M yield curve. We observe that the calibration to this market is less accurate than the calibration to the EURO market.

We observe that the USD market is more volatile than the EURO and KRW markets. The market skews are approximately 8% higher. This implies that we require $R_0 \in [0.06, 0.08]$ to shift the implied volatility skew, so that we obtain free σ parameters in the calibration process. Secondly, we observe that the market skews have little curvature. Hence $\beta \in [0.20, 0.40]$ is a proper choice and the volatility of volatility function has a stable behaviour in time.
We observe many boundary solutions for the skew parameter. We see this particular in the results for the market data of 9 August 2010 and 19 November 2009. The market skews of 19 November 2009 are relatively flat, which implies that a large skew parameter γ is required. Since we restrict this parameter to the interval $[0, 0.30]$ it is not possible to fit these market skews. For this date the calibration failed. To improve the calibration we propose to investigate a better approximation for the short rate $r(t)$, so that we can loosen the restriction on γ. To illustrate why this is important, we calibrate the time-homogeneous swap rate model without restrictions on the parameters. Hence we allow $\gamma \in [0, 1]$. In this case we are able to match the calibration instruments accurately. In Table 6.2 we show the calibration results. The calibrated parameters are $\gamma = 0.7221$, $\sigma = 0.5138$ and $\epsilon = 0.9647$.

If we price back the instruments with the DDSV model, we obtain an inaccurate fit, see Figure 6.3. This is what we expect and illustrates why γ should be restricted to $[0, 0.30]$. Since for both models, the time-homogeneous swap rate model and the DDSV model, we obtain a flatter implied volatility skew if γ increases, we expect that improving the approximation of the short rate will improve the accuracy of the calibration to USD markets.

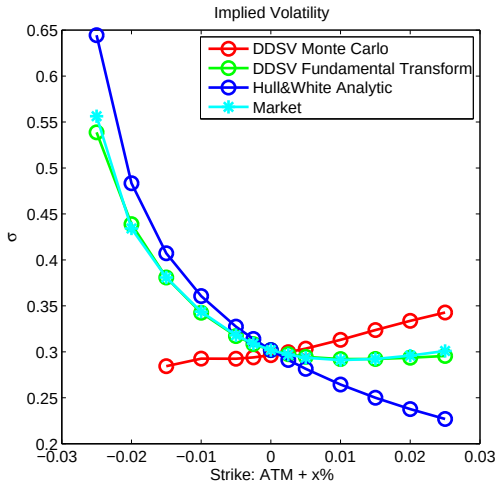

Figure 6.3: USD market 9 August 2010: Fit to the 1Y10Y market skew without restrictions on the parameters.

Maturity in years	Tenor in years	Strike	Model price	Market price	Relative diff.	Model impl vol.	Market vol.	Diff in bp
1	10	0.0171	1325.58	1325.58	3e-4	38.08	38.08	0
1	10	0.0321	337.22	337.22	1e-4	30.19	30.19	0
1	10	0.0471	44.12	44.12	7e-4	29.22	29.22	0

Table 6.2: USD market 9 August 2010: Calibration to 1Y10Y calibration instruments, $\beta = 0.40$ and $R_0 = 0.07$.

We also recommend to investigate the effects of introducing correlation between the Brownian motions. This may give some additional control in the calibration process, such that we can increase the accuracy of the calibration to the USD market. The conclusion for the USD market is that, with the current knowledge, we are not able to calibrate the market skews accurately.

We have seen that the calibration is not perfect in the sense of accuracy. This is something that we can also not expect, as there are many approximations involved to derive the time-homogeneous swap rate model. There is a mismatch between the closed form solution prices and the DDSV prices computed byMonte Carlo. We are interested in the skew and curvature impact on exotic interest rate derivatives. Therefore we investigate the price impact between the Hull-White model and the DDSV model on digitals, range accrual swaps and callable range accruals. To investigate the impact, we restrict the test cases to dates for which we have confidence in an accurate calibration. This will be the main topic of the next chapter, Chapter 7.

6.4 Calibration results

6.4.1 EURO swaption market 15 April 2011.

Maturity in years	Tenor in years	Strike	Model price	Market price	Relative diff.	Model impl vol.	Market vol.	Diff in bp
1	10	0.0252	1224.18	1225.90	-0.14	0.2906	0.2966	-60
1	10	0.0402	267.20	267.20	0.00	0.2070	0.2070	0
1	10	0.0552	17.29	15.58	10.94	0.1975	0.1933	42
2	9	0.0267	1128.48	1130.63	-0.19	0.2852	0.2882	-30
2	9	0.0417	346.45	346.48	-0.01	0.2080	0.2080	0
2	9	0.0567	64.98	62.87	3.36	0.1965	0.1945	20
3	8	0.0279	1025.12	1027.40	-0.22	0.2749	0.2773	-24
3	8	0.0429	369.53	369.67	-0.04	0.2029	0.2030	-1
3	8	0.0579	100.83	101.81	-0.97	0.1913	0.1920	-7
4	7	0.0288	910.25	911.30	-0.11	0.2639	0.2649	-10
4	7	0.0438	358.82	358.06	0.21	0.1954	0.1950	4
4	7	0.0588	119.10	120.22	-0.93	0.1849	0.1856	-7
5	6	0.0296	782.03	782.73	-0.09	0.2494	0.2500	-7
5	6	0.0446	325.26	325.30	-0.01	0.1859	0.1859	0
5	6	0.0596	120.43	121.57	-0.94	0.1767	0.1774	-7
6	5	0.0302	652.05	652.49	-0.07	0.2389	0.2393	-4
6	5	0.0452	283.19	284.77	-0.55	0.1789	0.1799	-10
6	5	0.0602	113.76	114.77	-0.88	0.1704	0.1711	-7
7	4	0.0308	521.50	521.47	0.00	0.2310	0.2310	0
7	4	0.0458	234.86	236.66	-0.76	0.1736	0.1750	-14
7	4	0.0608	100.46	101.38	-0.90	0.1654	0.1662	-7
8	3	0.0314	389.26	389.60	-0.09	0.2225	0.2230	-5
8	3	0.0464	180.71	182.47	-0.97	0.1683	0.1700	-17
8	3	0.0614	81.14	81.60	-0.56	0.1605	0.1609	-5
9	2	0.0320	257.59	257.81	-0.08	0.2153	0.2157	-4
9	2	0.0470	122.90	124.63	-1.39	0.1640	0.1663	-24
9	2	0.0620	57.38	57.77	-0.67	0.1561	0.1567	-5
10	1	0.0326	127.68	127.64	0.03340	0.2079	0.2078	2
10	1	0.0476	62.32	63.31	-1.57	0.1594	0.1612	-26
10	1	0.0626	29.95	30.03	-0.28	0.1515	0.1517	-2

Table 6.3: EURO market 15 April 2011: Calibration results.

$\sigma(t)$	0.2484	0.2840	0.2888	0.2911	0.2646	0.2718	0.2787	0.2663	0.2593	0.2401
$\gamma(t)$	0.0100	0.0100	0.0100	0.0100	0.0511	0.0438	0.0354	0.0618	0.0610	0.0445
$\epsilon(t)$	1.1541	1.1190	1.9676	1.8181	2.4517	2.4431	2.4394	2.4392	2.4395	2.3739

Table 6.4: EURO market 15 April 2011: $R_0 = 0.04, \beta = 0.20, a = 0.03, V(0) = 1$.

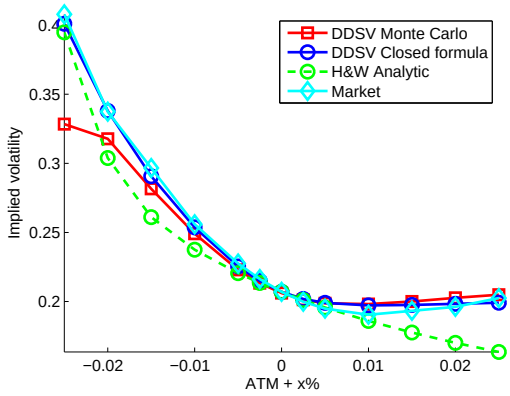

(a) 1Y10Y: Accuracy, ATM -9 bp, max. 90 bp.

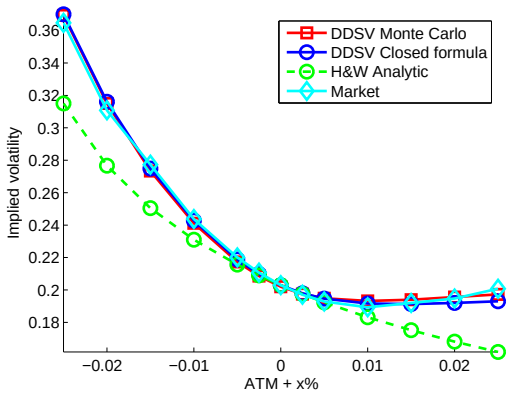

(b) 3Y8Y: Accuracy, ATM -9 bp, max. 27 bp.

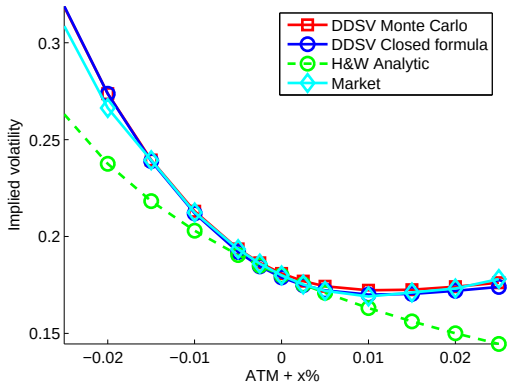

(c) 6Y5Y: Accuracy, ATM 20bp, max. 22bp.

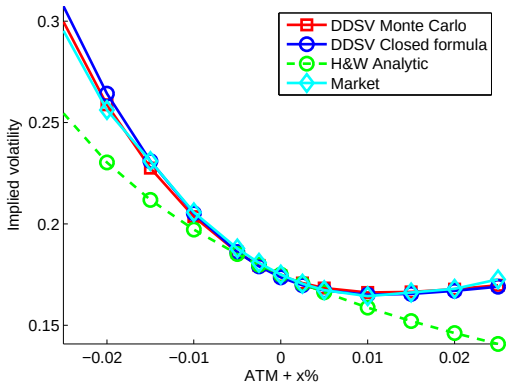

(d) 7Y4Y: Accuracy, ATM 8 bp, max. 11 bp.

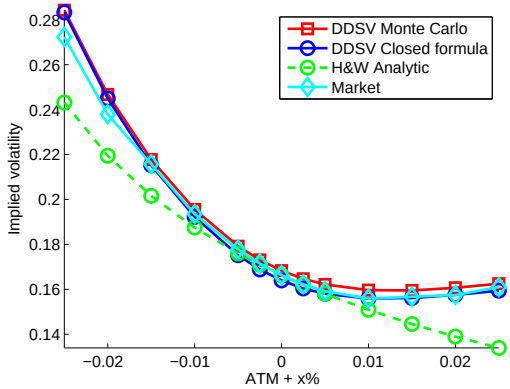

(e) 9Y2Y: Accuracy, ATM 43bp, max. 43 bp.

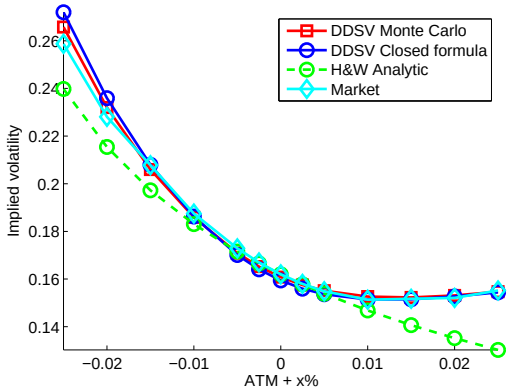

(f) 10Y1Y: Accuracy, ATM 14 bp, max. 20bp.

Figure 6.4: EURO market 15 April 2011: Figures with Cheyette and Hull-White fits to the market skew.

6.4.2 KRW swaption market 15 April 2011.

Maturity in years	Tenor in years	Strike	Model price	Market price	Relative diff.	Model impl vol.	Market vol.	Diff in bp
1	10	0.0413	934.64	932.96	0.18	17.93	17.26	67
1	10	0.0563	183.15	183.13	0.01	13.20	13.20	0
1	10	0.0713	12.45	13.83	-10.01	14.51	14.84	-32
2	9	0.0407	863.65	859.43	0.49	17.32	16.66	67
2	9	0.0557	222.97	224.29	-0.59	12.78	12.86	-8
2	9	0.0707	38.09	38.30	-0.56	13.97	13.99	-2
3	8	0.0401	786.70	783.26	0.44	16.74	16.34	40
3	8	0.0551	236.09	240.40	-1.79	12.58	12.82	-23
3	8	0.0701	55.60	61.82	-10.07	13.45	13.94	-49
4	7	0.0394	705.75	700.95	0.68	16.60	16.10	50
4	7	0.0544	238.28	237.57	0.30	12.74	12.70	4
4	7	0.0694	68.07	73.98	-7.99	13.26	13.68	-42
5	6	0.0386	620.12	617.25	0.46	16.68	16.39	29
5	6	0.0536	230.36	229.00	0.59	13.04	12.96	8
5	6	0.0686	76.06	82.06	-7.31	13.31	13.73	-42
6	5	0.0378	526.76	525.36	0.27	16.58	16.44	15
6	5	0.0528	207.51	208.64	-0.54	13.08	13.15	-7
6	5	0.0678	74.65	83.99	-11.12	13.19	13.88	-70
7	4	0.0368	427.60	423.93	0.87	16.47	16.02	45
7	4	0.0518	175.22	175.74	-0.30	13.04	13.08	-4
7	4	0.0668	66.64	76.94	-13.39	13.03	13.91	-88
8	3	0.0361	327.70	323.62	1.26	16.75	16.13	62
8	3	0.0511	141.13	140.05	0.77	13.30	13.20	10
8	3	0.0661	57.00	65.61	-13.12	13.11	14.02	-91
9	2	0.0352	222.03	219.42	1.19	16.95	16.39	56
9	2	0.0502	99.66	98.82	0.86	13.55	13.43	12
9	2	0.0652	42.53	48.69	-12.66	13.25	14.16	-91
10	1	0.0338	112.56	110.90	1.50	17.30	16.61	69
10	1	0.0488	52.10	51.77	0.64	13.84	13.75	9
10	1	0.0638	23.09	27.20	-15.10	13.42	14.59	-117

Table 6.5: KRW market 15 April 2011: Calibration results.

$\sigma(t)$	0.1139	0.1224	0.1280	0.1422	0.1613	0.1613	0.1613	0.1867	0.2005	0.2005
$\gamma(t)$	0.3000	0.2988	0.2897	0.2692	0.2919	0.2919	0.2919	0.2318	0.2981	0.2981
$\epsilon(t)$	1.4138	0.8390	0.8128	0.9944	0.9817	0.9817	0.9816	1.0349	0.7242	0.7250

Table 6.6: KRW market 15 April 2011: : $R_0 = 0.06, \beta = 0.10, a = 0.03, V(0) = 1$.

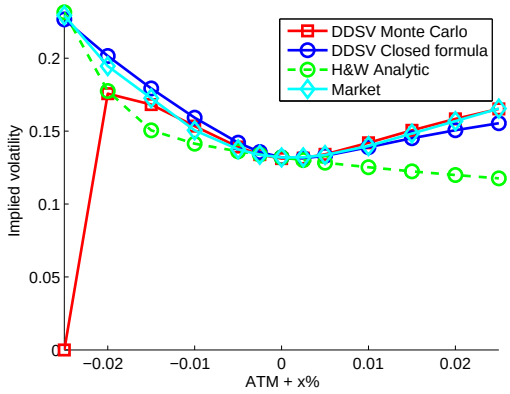

(a) 1Y10Y: Accuracy, ATM -8 bp, max. 110 bp.

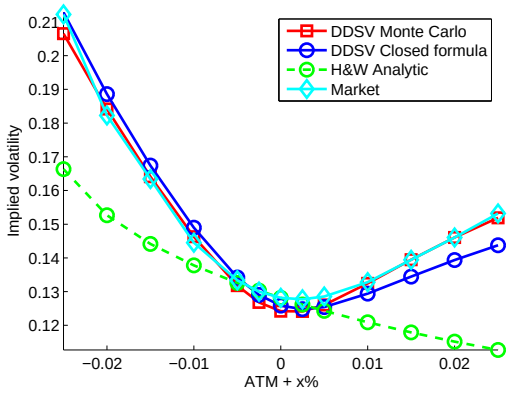

(b) 3Y8Y:: Accuracy, ATM -16 bp, max. 50 bp.

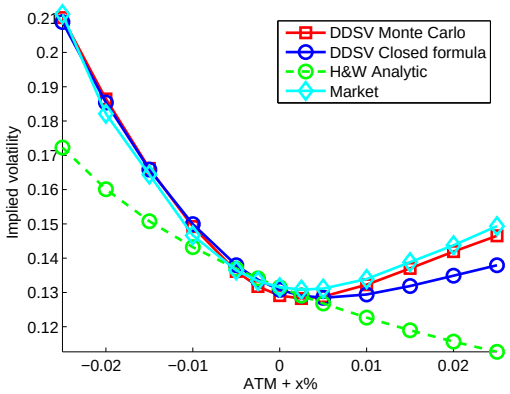

(c) 6Y5Y: Accuracy, ATM -17 bp, max. 51 bp.

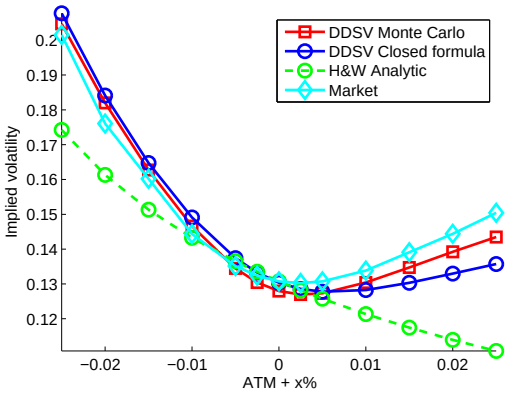

(d) 7Y4Y: Accuracy, ATM -24 bp, max. 44 bp.

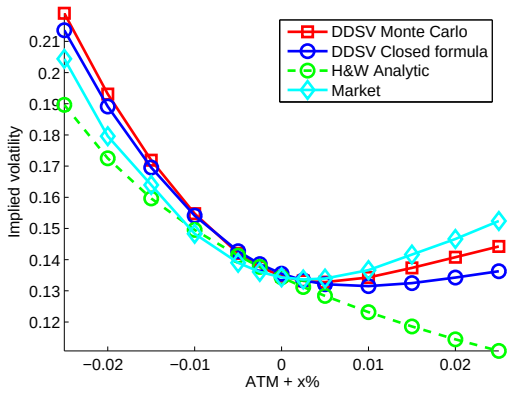

(e) 9Y2Y: Accuracy, ATM -7 bp, max. 48 bp.

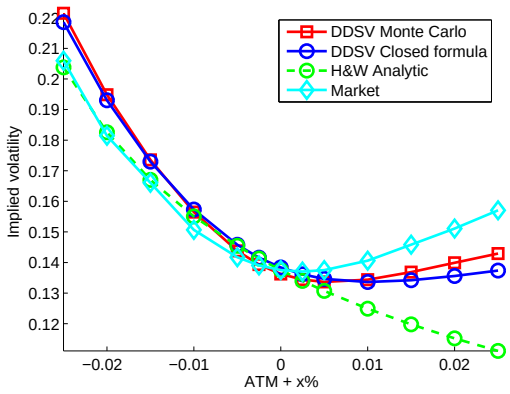

(f) 10Y1Y: Accuracy, ATM -21 bp, max. 26 bp.

Figure 6.5: KRW market 15 April 2011: Figures with Cheyette and Hull-White fits to the market skew.

6.4.3 USD swaption market 15 April 2011.

Maturity in years	Tenor in years	Strike	Model price	Market price	Relative diff.	Model impl vol.	Market vol.	Diff in bp
1	10	0.0255	1292.95	1283.61	0.727678417	34.28	31.97	232
1	10	0.0405	360.18	359.81	0.101438668	26.63	26.60	3
1	10	0.0555	48.78	57.32	-14.89816248	24.91	26.06	-116
2	9	0.0291	1219.44	1207.41	0.996331723	31.89	30.61	128
2	9	0.0441	465.14	464.14	0.216606061	25.45	25.40	6
2	9	0.0591	134.12	149.72	-10.41884144	23.82	24.88	-107
3	8	0.0319	1123.36	1114.82	0.765737804	29.61	28.92	69
3	8	0.0469	495.63	496.53	-0.180003299	24.05	24.10	-4
3	8	0.0619	185.91	206.11	-9.800168992	22.47	23.57	-110
4	7	0.0340	1011.84	1001.31	1.051493093	28.23	27.46	76
4	7	0.0490	492.59	489.29	0.675306166	23.26	23.10	16
4	7	0.0640	215.70	232.40	-7.186516983	21.69	22.53	-84
5	6	0.0355	879.55	867.80	1.353595927	26.86	26.01	85
5	6	0.0505	455.97	453.69	0.50324497	22.41	22.29	11
5	6	0.0655	219.39	233.45	-6.024150189	20.92	21.64	-72
6	5	0.0364	737.15	731.47	0.776000665	25.80	25.36	44
6	5	0.0514	398.35	397.30	0.26363044	21.65	21.60	6
6	5	0.0664	202.80	215.96	-6.095081598	20.19	20.92	-73
7	4	0.0370	589.28	586.42	0.486846564	24.92	24.66	26
7	4	0.0520	328.03	325.28	0.843541909	20.98	20.80	18
7	4	0.0670	173.35	181.02	-4.241547305	19.51	20.00	-50
8	3	0.0374	440.81	440.27	0.124660556	24.28	24.22	6
8	3	0.0524	251.89	249.06	1.135438393	20.50	20.27	24
8	3	0.0674	137.39	141.99	-3.236731959	19.01	19.39	-38
9	2	0.0377	291.36	291.86	-0.169607759	23.64	23.72	-8
9	2	0.0527	169.82	167.59	1.328675648	20.00	19.73	27
9	2	0.0677	94.75	97.35	-2.672302392	18.50	18.80	-31
10	1	0.0375	143.01	143.43	-0.293468201	22.87	23.00	-13
10	1	0.0525	84.03	82.95	1.29494734	19.35	19.10	26
10	1	0.0675	47.29	48.37	-2.233152609	17.86	18.11	-25

Table 6.7: USD market 15 April 2011: Calibration results.

$\sigma(t)$	0.2603	0.2645	0.2390	0.2401	0.2315	0.2049	0.1847	0.1815	0.1619	0.1185
$\gamma(t)$	0.3000	0.2816	0.2544	0.2500	0.3000	0.2652	0.2321	0.2311	0.2081	0.2198
$\epsilon(t)$	1.0058	0.9927	1.1338	1.1225	1.2833	1.1306	0.9914	0.9818	0.8521	0.4306

Table 6.8: USD market 15 April 2011: $R_0 = 0.07, \beta = 0.20, a = 0.03, V(0) = 1$.

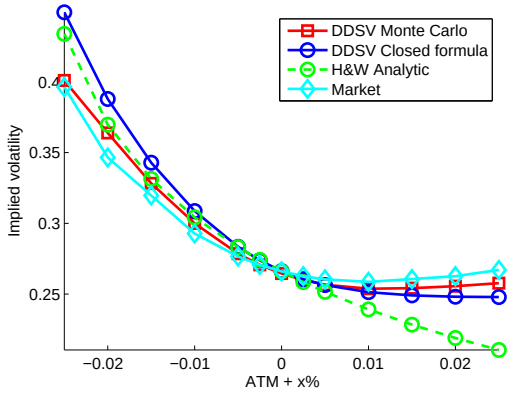

(a) 1Y10Y: Accuracy, ATM -17 bp, max. 145 bp.

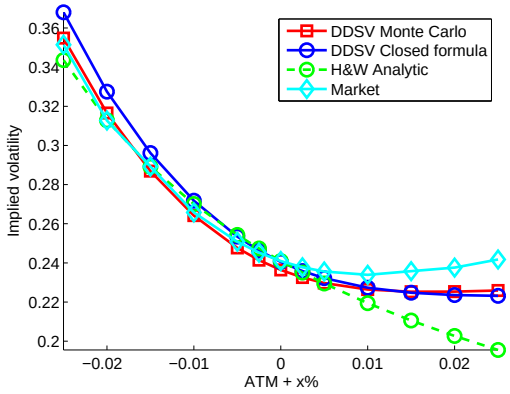

(b) 3Y8Y: Accuracy, ATM -41 bp, max. 92 bp.

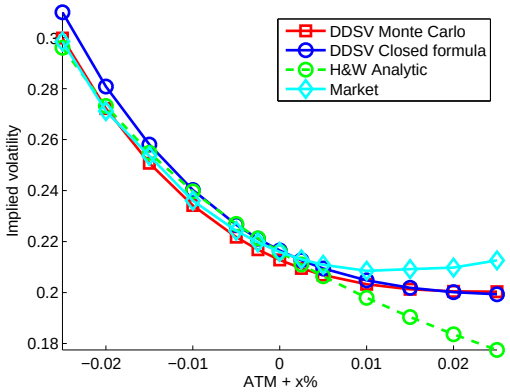

(c) 6Y5Y: Accuracy, ATM -37 bp, max. 73 bp.

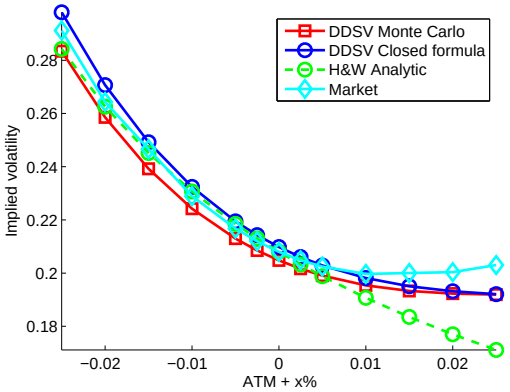

(d) 7Y4Y: Accuracy, ATM -50 bp, max. 100 bp.

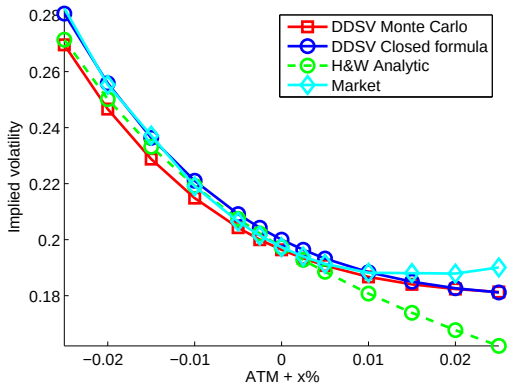

(e) 9Y2Y swaption: Accuracy, ATM -36 bp, max. 76 bp.

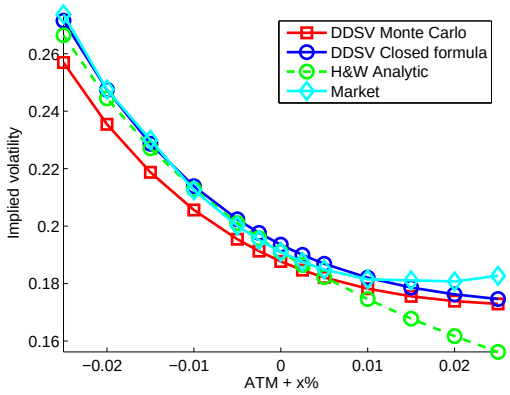

(f) 10Y1Y swaption: Accuracy, ATM -58 bp, max. 99 bp.

Figure 6.6: USD market 15 April 2011: Figures with Cheyette and Hull-White fits to the market skew.

Chapter 7

Pricing of exotic IR derivatives

In this chapter we investigate the skew and curvature impact on interest rate derivatives. We consider digital caplets, digital caps, range accrual swaps, callable range acrruals and a callable remaining maturity swap. We price these derivatives with the Hull-White model and the DDSV model. We analyze the difference between the Hull-White and the DDSV prices, which is the skew and curvature impact of the DDSV model. We subdivide this chapter into the following sections.

- Definitions and pricing of the interest rate derivatives, see Section 7.1.
- Test strategy, see Section 7.2.
- Test results, see Section 7.3.

7.1 Definitions and pricing of the interest rate derivatives

In this section we give the definitions of the interest rate derivatives that are in the present analysis. Define by $\mathcal{T} := \{T_0, T_1, \ldots, T_m\}$ the set of coupon dates. We assume T_0 to be the start date and $T_1, T_2 \ldots T_m$ to be the pay dates. For convenience of notation we assume that the fixing date of the LIBOR rate, or any other reference rate, coincides with the start date of the coupon. In general there is a fixing lag between the fixing date of the rate and the start date of the coupon. Secondly, we assume that the pay date coincides with the end date of the coupon. We define $\tau(T_{i-1}, T_i)$ the year fraction between date T_{i-1} and T_i. Recall that this distance depends on the market conventions.

7.1.1 Digital caps and digital floors

A digital cap (digital floor) is the sum of a number of basic contracts, knows as digital caplets (digital floorlets), which are defined as follows. A digital is a derivative with a non-linear discontinuous payoff function. Given two dates T_0 and T_1, a notional amount N, a fixed rate K and a floating interest rate, in general the LIBOR rate $L(T_0, T_1)$. A digital floorlet with barrier B is an instrument whose coupon payment at time T_1 is given by:

$$V_{d-floorlet}(T_1) := N\tau(T_0, T_1)K\mathbb{I}_{L(T_0,T_1)<B}.$$

Where $\mathbb{I}$ is the indicator function, i.e.

$$\mathbb{I}_{L(T_0,T_1)<B} := \begin{cases} 1 & L(T_0, T_1) < B \\ 0 & L(T_0, T_1) > B \end{cases}.$$

Using the zero-coupon bond $P(t,T_1)$ as a numeraire and assuming Black's model for the LIBOR rate $L(T_0,T_1)$, the value at time $t \leq T_0$ of the digital floorlet is given by:

$$V_{d-floorlet}(t) = P(t,T_1)N\tau(T_0,T_1)K\mathbb{E}^{\mathbb{Q}^{T_1}}\left[\mathbb{I}_{L(T_0,T_1)<B}\middle|\mathcal{F}(t)\right] = P(t,T_1)N\tau(T_0,T_1)1K\mathcal{N}(-d_2), \tag{7.1}$$

where d_2 is given by (2.16). A similar definition holds for the digital caplet. In this case the coupon payment at time T_1 is given by:

$$V_{d-caplet}(T_1) := N\tau(T_0,T_1)K\mathbb{I}_{L(T_0,T_1)>B}.$$

The value at time $t \leq T_0$ of a digital caplet is given by:

$$V_{d-caplet}(t) = P(t,T_1)N\tau(T_0,T_1)K\mathcal{N}(d_2). \tag{7.2}$$

Static replication (SR)

One can show that the payoff of a digital floorlet can be written as:

$$\mathbb{I}_{L(T_0,T_1)<B} = \lim_{\delta\to 0}\frac{(B+\delta-L(T_0,T_1))^+ - (B-\delta-L(T_0,T_1))^+}{2\delta},$$

and the payoff of a digital caplet as:

$$\mathbb{I}_{L(T_0,T_1)>B} = \lim_{\delta\to 0}\frac{(L(T_0,T_1)-(B-\delta))^+ - (L(T_0,T_1)-(B+\delta))^+}{2\delta}.$$

Hence we can decompose the digital floorlet into two floorlets with different strikes and the digital caplet into two caplets with different strikes. The strikes of the floorlets, respectively caplets, are given by $B+\delta$ and $B-\delta$, with $\delta > 0$, called the call spread. The decomposition of the digital, into a set of more simple payoffs is called *static replication* (SR). To value the digital floorlet or digital caplet with SR at any time $t < T_0$, we can value the corresponding caplets and floorlets by assuming Black's model for the LIBOR rate. We refer to Section 2.2.7 for the formulas. In practice, SR of a digital is applied to take the market skew into account. If the digital is priced using Formula (7.1) or (7.2), then we assume a constant volatility. If we price the digital with SR, then we take the market volatilities for strikes $B-\delta$ and $B+\delta$ to value the caplets or floorlets. Hence, we take the local skewness around the barrier of the market skew into account. The market price of a digital is in general computed with static replication. For this reason it is important that for the valuation of interest rate derivatives, whose coupon payments consist of digital payoffs, the short rate models give a consistent price compared to the SR price.

A digital cap, respectively a digital floor, is defined as a contract with coupon dates

$$\{T_0, T_1, \ldots, T_m\},$$

so that the coupon with start date T_i and end date T_{i+1} is given by a digital caplet, respectively digital floorlet. The value at time $t < T_0$ with SR, is given by the sum of the time t values of the digitals.

7.1.2 Range Accrual

A range accrual is a structured coupon. This coupon is defined as given a rate, in the simplest case fixed[1], that only accrues when a different reference rate, for example the LIBOR rate, is inside a given interval $[l, u] \subset \mathbb{R}$. We denote the payment rate by $R_n(t)$ and the reference rate by $X_n(t)$. At all payment dates $T_i \in \mathcal{T}_m \backslash T_0$ there is a cashflow equal to:

$$C_i = N\tau(T_{i-1}, T_i)R_i(T_{i-1})\frac{\sum_{t\in\mathcal{T}^i_{obs}} \mathbb{I}_{X_n(t)\in[l,u]}}{\#\{t \in \mathcal{T}^i_{obs}\}},$$

with $\mathcal{T}^i_{obs}$ the set of observation dates between T_{i-1} and T_i. $\#\{.\}$ is used to denote the number of days that a given criteria is satisfied. The most common choice of the reference rate $X_n(t)$ is the LIBOR rate, but a CMS rate (or any other rate) is also occasionally used. We note that a range accrual coupon is a sum of digital payoffs. The value at time $t < T_0$ of the range accrual coupon payoff C_i, using the T_i forward measure as a numeraire, is given by:

$$V^i_{rac-coupon}(t) := P(t, T_i)\mathbb{E}^{\mathbb{Q}^{T_i}}\left[C_i|\,\mathcal{F}(t)\right].$$

Hence the value at time t of the range accrual is given by:

$$V_{rac}(t) := \sum_{i=1}^{m} P(t, T_i)\mathbb{E}^{\mathbb{Q}^{T_i}}\left[C_i|\,\mathcal{F}(t)\right]. \tag{7.3}$$

In general, we need Monte Carlo methods to compute the expectations in Equation (7.3).

7.1.3 Callable structured swap

In a structured swap, a regular plain vanilla floating LIBOR leg is swapped against a structured leg. The plain vanilla floating leg is called the funding leg, the leg paying the structured coupon is called the structured leg. A plain vanilla swap is a trivial example where the structured coupon pays the fixed rate. Assume that the structured coupon pays a coupon C_i at time T_i. The value of a structured swap[2] at any time $t < T_0$ is given by:

$$V_{struct-swap}(t) := \sum_{i=1}^{m} P(t, T_i)\mathbb{E}^{\mathbb{Q}^{T_i}}\left[(C_i - L(T_{i-1}, T_i))|\,\mathcal{F}(t)\right]. \tag{7.4}$$

A callable structured swap is a structured swap with a Bermudan style option to cancel the deal on a schedule of exercise dates. Typically this call schedule will coincide with the coupon dates. Hence if we define the set of call dates by:

$$\mathcal{E} := \{E_1, E_2, \ldots E_s\},$$

then we have $\mathcal{E} \subset \mathcal{T}$. A callable structured swap can be seen as a structured swap, plus a Bermudan-style right to cancel the structured swap. For valuation purposes it is convenient to represent a callable structured swap as a structured swap plus a Bermudan-style option to enter at any exercise date E_i a reverse structured swap with start date E_i and end date T_m. Hence a structured swap with the same market conventions, day count conventions, observation index, observation frequency and payment index, but where legs are reversed relative to the original one.

[1] LIBOR, CMS or CMS spread are also allowed.

[2] We assume the same coupon dates on the funding and structured leg.

For pricing callable structured swaps within a Monte Carlo framework an additional approximation is introducted to approximate the exercise decision, in the literature well-known as the Longstaff & Schwarz (LS) method. We do not give a detailed description of this method, since this method has been described extensively in the literature [23]. In this method the early exercise boundary is determined based on a regression for the hold value of the Bermudan and the immediate exercise value along a path. The key attributes controlling the performance of this method are the choice of the explanatory variables and the degree of the polynomials.

Callable range accrual on LIBOR

A callable range accrual on LIBOR is a callable structured swap, where the underlying structured swap has range accrual coupons on the structured leg with the LIBOR rate as the observation rate (RAC). RAC we use as an abbreviation for range accrual on LIBOR. For the valuation of this option we compare at each exercise date the immediate exercise value (the path- and time-specific value of the RAC swap) to the continuation value (that is the value of holding the option and not to exercise). As Longstaff and Schwarz proposed, the continuation value along the path is approximated by regression, where the discounted path-specific future cashflows are regressed on basis functions. The value of the RAC swap given the path- and state variables, cannot be calculated analytically without introducing additional approximations. Therefore a regression is performed in order to approximate the immediate exercise value. As discussed before, the choice of explanatory variables and the degree of polynomials is crucial for the performance. This choice has extensively been discussed in [8], for consistency we use the same regression variables. This implies that for the immediate exercise value we use the model state variables and the analytic cap floor prices as regression variables. The latter two variables contain information about the sum of digital caplet and floorlet prices corresponding to the upper u and lower l boundaries. The relative position of the LIBOR rate with respect to the observation range is embedded in those prices. For the continuation value we use the model state variables and the value of the RAC swap that is approximated in the underlying instrument regression.

The Hull-White model is analytically tractable and given that, closed form formulas for caps and floors exist. We do not have a closed form formula to compute the cap and floor prices in the DDSV model. This implies that we cannot compute the cap floor regression variables in the DDSV model analytically. Since these regression variables are computed a large number of times, it is not a good idea to compute them using Monte Carlo methods. This will slow down the Longstaff and Schwartz algorithm dramatically. Fortunately, we do not need to be all that exact in trying to match the exercise values with the explanatory variables. Piterbarg [24] proposes that a rough estimate will give already satisfactory results. For example, one can use Black's formula to value the caps and floors, even in models where it does not exactly apply. For the DDSV model, we propose to use the Hull-White cap floor analytic prices to compute the regression variables.

Callable RMS

A callable remaining maturity swap (callable RMS) is a callable structured swap. The structured leg of the underlying structured swap is given by a RMS range accrual. The reference rate of the range accrual is defined as follows. For coupon i with start date T_{i-1}, define a plain vanilla swap with start date T_{i-1} and the end date T_m, hence the end date coincides with the end date of the deal. Then the reference rate of the range accrual is the swap rate of this plain vanilla swap, denoted by:

$$S(T_{i-1}, [T_{i-1}, T_m]). \tag{7.5}$$

Hence if we run over the coupons, the tenors of the swaps are decreasing and are equal to the length of the remaining lifetime of the deal.

7.2 Test strategy

This section consists of the following aspects. We discuss which models are in scope to value the interest rate derivatives and to which calibration instruments these models are calibrated. Secondly, we discuss which numerical methods we apply to value the interest rate derivatives. In the last subsection we give the characteristics of the deals.

7.2.1 Models and calibration

All the interest rate derivatives are priced using the Hull-White and the DDSV models. Before we can use the models for option valuation, we have to calibrate the models. We calibrate the models in a bootstrap fashion to the swaption market. For a digital caplet, the models are calibrated to swaptions with maturity T_0 and tenor $\tau(T_0, T_1)$. For a digital cap, we calibrate the models to the following swaption strip:

$$\{(T_0, \tau(T_0, T_1)), (T_1, \tau(T_1, T_2)), \ldots, (T_{m-1}, \tau(T_{m-1}, T_m))\},$$

where $(T_i, \tau(T_i, T_{i+1})$ is defined as the swaption with maturity T_i and tenor $\tau(T_i, T_{i+1})$. To value the RACs, callable RACs and RMS we calibrate to co-terminal swaptions. This implies that the models are calibrated to the following swaption strip:

$$\{(T_0, \tau(T_0, T_m)), (T_1, \tau(T_1, T_m)), \ldots, (T_{m-1}, \tau(T_{m-1}, T_m))\}.$$

7.2.2 Valuation

To value the interest rate derivatives with the Hull-White and the DDSV model, we use Monte Carlo methods. For the DDSV model we use the Milstein discretization for the $x(t)$ and $y(t)$ dynamics and the QE scheme to discretize the variance process, see Section 5.6. For the Hull-White model we use an exact simulation method without discretization error. In this method we use the exact solution of the SDE under the T-forward measure, see [1]. We use $100,000$ simulations for both models and a time step of $dt = 1/365$ for the DDSV model. For the callable RAC the Monte Carlo methods are based on the LS algorithm.

7.2.3 Trade characteristics

In Table 7.1 we give the characteristics of the test deals we have in scope. For the digital caps, the RACs and the callable RACs, we use the market data of:

13 April 2011, 16 December 2010 and 30 June 2010.

We restrict the analysis of the digital caplet and the callable RMS to the market data of 13 April 2011. In Table 7.1 we show the characteristics of the test deals. Next, we give for each derivative information about the fixed rates, barriers of the observation range and other information that is not listed in the table.

	Digital caplet	Digital cap	RAC & callable RAC	callable RMS
notional	10,000	10,000	10,000	10,000
start date in	4Y or 10Y	5Y	1Y	1Y
tenor	1Y	5Y	10Y	10Y
swap type	n/a	n/a	structured receiver	structured receiver
Structured leg				
market convention	EURIB12M	EURIB12M	EURIB12M	EURIB12M
coupon type	digital caplet	digital caplet	range acr	range acr
payment index	fixed	fixed	fixed	fixed
coupon frequency	annual	annual	annual	annual
day count conventions	Actual 360	Actual 360	Actual 360	Actual 360
observation index	LIBOR	LIBOR	LIBOR	$S(T_{i-1};[T_{i-1},T_m])$
observation frequency	Annual	Annual	Annual	Annual
observation index tenor	12 months	12 months	12 months	12 months
exercise schedule callable	n/a	n/a	Annual	Annual
# of coupons	1	5	10	10
Funding leg				
market convention	n/a	n/a	EURIB12M	EURIB12M
coupon type	n/a	n/a	floating	floating
payment index	n/a	n/a	LIBOR	LIBOR
coupon frequency	n/a	n/a	annual	annual
day count conventions	n/a	n/a	Actual 360	Actual 360
# of coupons	n/a	n/a	10	10

Table 7.1: Trade characteristics

Digital caplet
The fixed rate K of the payment rate is 4%. Note that the value of K is not relevant for the price of the digital caplet, it has only a linear scaling impact since it is a constant factor in the payoff function. For the digital caplet starting in four years we take the following barriers B:

$$B \in \{0.02, 0.025, 0.03, 0.035, 0.04, 0.045, 0.05, 0.055, 0.06\}.$$

For the digital starting in ten years we take barriers B:

$$B \in \{0.025, 0.03, 0.035, 0.04, 0.045, 0.05, 0.055, 0.065\}.$$

Digital cap
Define by S the swap rate of the corresponding plain vanilla interest rate swap. Hence the swap has the same start date and end date as the digital cap. Then we take the following barriers B:

$$B \in S + \{-2, -1.5, -1, -0.5, 0, 0.5, 1, 1.5, 2\}\%.$$

The fixed rate K of the payment rate is 4%.

RAC and callable RAC
The observation range for the LIBOR rate is $(-\infty, B]$. We take three different values B, related to the swap rate of the corresponding plain vanilla interest rate swap. Hence we define S the swap rate of the plain vanilla interest rate swap with the same start date and end date as the deal. We value the RAC and callable RAC for the following barriers B:

$$B \in S + \{-1, 0, 1\}\%.$$

The fixed rate K of the payment index is defined as follows. Define K_{atm} the fixed payment rate, such that the Hull-White price of the RAC is approximately zero (at the money). We value the RAC and callable RAC for the following fixed payment rates K:

$$K \in K_{atm} + \{-1, 0, 1\}\%.$$

RMS
The observation range for the observation index is $(-\infty, B]$. We value the callable RMS for the following barriers B:

$$B \in \{3, 4, 5, 6, 7, 8, 9, 10\}\%.$$

The fixed rate K of the payment index is 5%.

7.3 Test results

In this section we show the test results for the test deals we described in Section 7.2. In Subsection 7.3.1 we give the results for the digital caplets, in Subsection 7.3.2 the results for the digital caps, in Subsection 7.3.3 the results for the RACs and the callable RACs and finally in Subsection 7.3.4 the results for the callable RMS. In the main text we include the results for the market data of 13 April 2011. For the other results we refer to Appendix D. These other results are in correspondence with the results of April 2011.

7.3.1 Digital caplets

In Table 7.2 we show the pricing results for the digital caplet starting in 4 years and in Table 7.3 we show the pricing results for the digital caplet starting in 10 years. In Figure 7.1 we plot the Hull-White, DDSV and SR prices in a graph. For the calibration results we refer the reader to Appendix D.1.1.

B - ATM %	B	SR	H&W price	H&W - SR	DDSV price	DDSV - SR
-2.11	0.02	310.98	299.86	-11.12	304.19	-6.80
-1.61	0.025	275.63	276.74	1.11	286.85	11.22
-1.11	0.03	263.92	247.90	-16.01	260.72	-3.20
-0.61	0.035	221.14	215.49	-5.65	223.38	2.24
-0.11	0.04	169.91	179.86	9.95	174.51	4.60
0.39	0.045	128.29	144.08	15.80	124.48	-3.81
0.89	0.05	92.04	109.96	17.92	86.59	-5.46
1.39	0.055	60.34	79.80	19.46	61.36	1.02
1.89	0.06	44.89	55.47	10.57	44.61	-0.29

Table 7.2: Pricing results: 13 April 2011, digital caplet starting in 4Y. The ATM level of the 4Y1Y swaption is 4.11%.

B - ATM %	B	SR	H&W price	H&W - SR	DDSV price	DDSV - SR
-2.30	0.025	220.50	218.71	-1.79	226.81	6.31
-1.80	0.03	201.35	203.74	2.39	215.21	13.86
-1.30	0.035	194.91	185.54	-9.37	198.76	3.85
-0.80	0.04	171.42	165.22	-6.20	176.48	5.06
-0.30	0.045	147.30	143.63	-3.68	147.84	0.54
0.20	0.05	121.58	121.78	0.21	116.29	-5.29
0.70	0.055	89.19	100.48	11.30	87.36	-1.83
1.20	0.06	61.26	80.82	19.56	65.14	3.88
1.70	0.065	48.70	62.77	14.06	49.04	0.34

Table 7.3: Pricing results: 13 April 2011, digital caplet starting in 10Y. The ATM level of the 10Y1Y swaption is 4.80%.

From these results we conclude that the SR prices are better matched by the DDSV model than by the Hull-White model. We expected this for two reasons. First of all, the DDSV model has a better fit to the market skew than the Hull-White model, see Appendix D.1.1. Secondly, we use the same market volatility skew to price the digital caplet with SR, hence we use Black volatilities from the market skew to which we have calibrated the short rate models.

In both results, we see an unstable behavior in the SR prices for small strikes. We think that these instabilities are explained by extrapolation errors in the swaption market volatility data. Recall that only for a finite number of strikes there is a quoted swaption price available. This implies that the missing values are obtained by interpolation or extrapolation between the existing quotes. This can explain the instabilities we observe in the SR prices for small strikes. From these results we expect that the SR prices of a digital cap are better matched by the DDSV model than by the Hull-White model. These results are discussed in the next subsection.

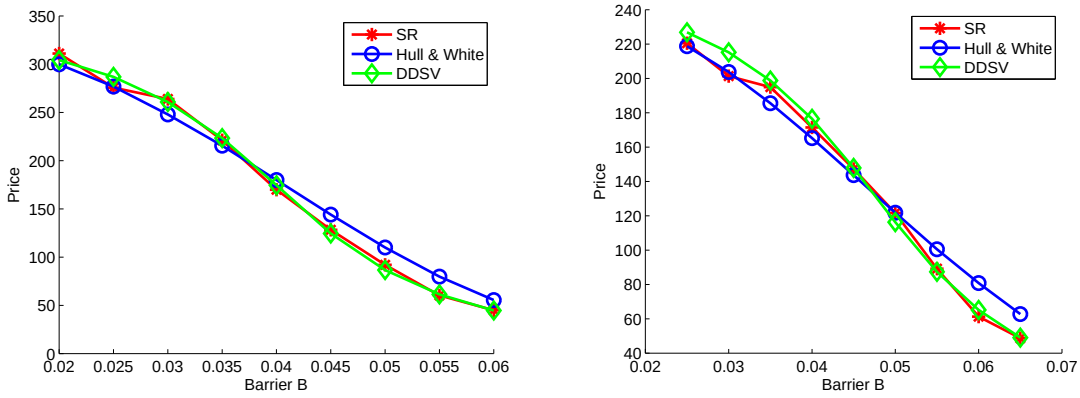

(a) Digital caplet starting in 4Y.

(b) Digital caplet starting in 10Y.

Figure 7.1: Pricing results for the digital caplets.

7.3.2 Digital cap

In Table 7.4 we show the pricing results for a digital cap. The digital cap starts in five years and pays five annual digital coupons, hence the end date of the contract is in ten years. In Figure 7.2(a) we plot the Hull-White, DDSV and SR prices in a graph. In Figure 7.2(b) we show a plot of the difference between the model prices and the SR prices.

The tables with the pricing results for 30 June 2010 and 16 December 2010 are given in Appendix D.2. In Appendix D.1.2 we show the calibration results for the market data of 13 April 2011 and in Appendix D.1.3 we show the calibration results for the market data of 30 June 2010. To obtain the calibration results for 16 December 2010, we refer the reader to the author.

B - ATM	B	SR	H&W price	H&W - SR	DDSV price	DDSV - SR
-0.02	0.0248	1265.37	1240.70	-24.67	1291.47	26.10
-0.015	0.0298	1170.27	1137.69	-32.58	1208.16	37.89
-0.01	0.0348	1073.61	1018.59	-55.02	1088.15	14.54
-0.005	0.0398	910.59	887.05	-23.54	922.65	12.07
0	0.0448	723.62	749.54	25.92	721.40	-2.21
0.005	0.0498	537.94	613.48	75.55	529.52	-8.42
0.01	0.0548	381.80	485.43	103.63	381.05	-0.75
0.015	0.0598	269.07	371.46	102.39	277.53	8.47
0.02	0.0648	195.31	273.59	78.28	208.43	13.12

Table 7.4: Pricing results: 13 April 2011, digital cap. The ATM level of the 5Y5Y swaption is 4.48%. H&W 99% confidence interval width, < 8.9. DDSV 99% confidence interval width, < 13.3.

From the results in Table 7.4 and Figure 7.2, we conclude that the SR prices are better matched by the DDSV model than by the Hull-White model. We expected this for two reasons, first of all from the results that we have obtained for a single digital caplet. Secondly, since we calibrate the model in a bootstrap fashion to the 5Y1Y, 6Y1Y, 7Y1Y, 8Y1Y and 9Y1Y swaption skews. From the calibration results in Appendix D.1.2, we conclude that the DDSV model has better fits to the market skews than the Hull-White model. If we price the digital cap with SR, then we price each digital caplet of the series with SR. For example, if we price the digital starting

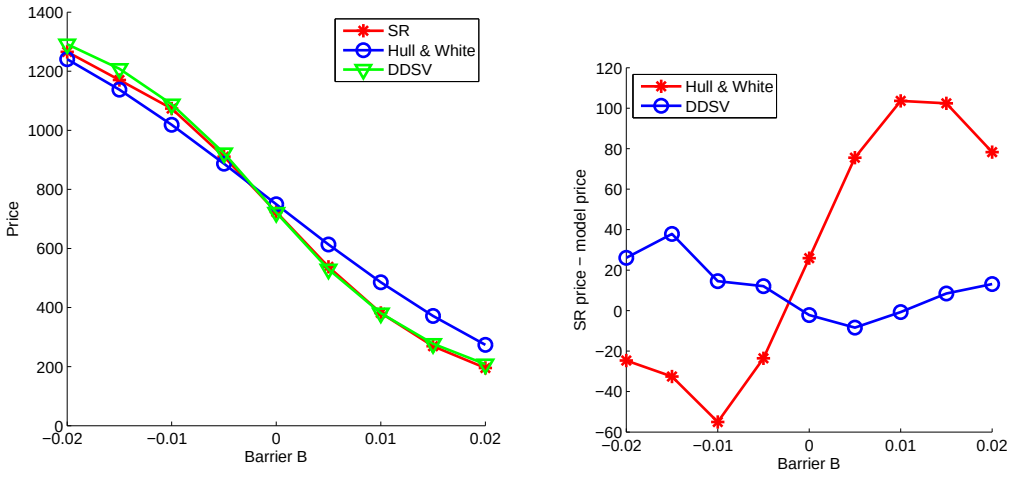

(a) Prices

(b) Difference to SR.

Figure 7.2: 13 April 2011: Pricing results for a digital cap.

in 7 years and paying the coupon in 8 years, we use the volatilities from the 7Y1Y swaption market skew to price the caplets with Black's formula. This is also the market skew to which we have calibrated the model. From the test for a digital caplet we conclude that the SR price of a digital caplet is better matched by the DDSV model, hence we expect that the same holds for the sum of n digital caplets, the digital cap. This is reflected in the results for 13 April 2011, but also in the results given in Appendix D.2 for the other two historical dates.

Furthermore, from the results in the appendix, we conclude that there are some exceptions. In Table D.2 with the results for 30 June 2010, we have for barriers B smaller than the 5Y5Y swap rate a closer match with the Hull-White model to the SR price. Note that the 5Y5Y swap rate is in general not equal to the ATM levels of the swaptions to which we calibrate the models, which is clear from Table 7.5. From this table we conclude that the ATM level for the 5Y5Y swap is at most 27 bp smaller than the ATM levels of the swaptions to which we calibrate. This implies that for all the maturities and all the barriers B from our results with $B - ATM > 0.005$, we are in the out of the money region.

	13 April 2011	16 December 2010	30 June 2010
5Y5Y	4.48%	4.41%	3.90%
5Y1Y	4.28%	4.18%	3.58%
6Y1Y	4.43%	4.33%	3.80%
7Y1Y	4.49%	4.45%	3.97%
8Y1Y	4.58%	4.51%	4.04%
9Y1Y	4.69%	4.63%	4.17%

Table 7.5: For each historical date the swap rates of the swaptions to which we calibrate the models.

From the calibration results we conclude that the DDSV model has a better fit to the out of the money swaptions than the Hull-White model. Hence we expect that for the large barriers, the SR prices are better matched by the DDSV model than by the Hull-White model. This is indeed confirmed by the results in Table 7.4 and Appendix D.2. We have seen that for some small barriers the SR price is better matched by the Hull-White model than by the DDSV model.

We can explain this by the following argument. From the calibration results for 30 June 2010, given in Appendix D.1.3, we conclude that the Hull-White model has an 'accurate' fit to the in-the-money swaptions. For some market skews the fits are even more accurate than the DDSV fits. This explains why for the small barriers the SR price is better matched by the Hull-White model. Hence the results for 30 June 2010 are well explained by the calibration results.

7.3.3 RAC and callable RAC

In this section we show the results for the RACs and the callable RACs. From the trade characteristics, given in Section 7.2.3, it is clear that we consider elementary range accruals. We have one observation date per coupon, which coincides with the start date of the coupon and we pay a fixed rate K if the LIBOR rate is less than some barrier B. Hence, we consider a series of digital floorlets. For the RACs we consider the holder receives the structured leg. The callable RACs have these RACs as underlying structured swaps. We choose these elementary RACs, since they will give us relevant information about the pricing of the callable range accruals.

The callable RACs we consider have an annual exercise schedule. These exercise dates coincide with the start dates of the coupons. Hence in this case the exercise dates are in one year, two years up to ten years. At the evaluation date, the holder has a basket of options to enter at any exercise date into a RAC, where the legs are reversed relative to the underlying RAC of the option. We expect that the market volatilities of the co-terminal swaptions, 1Y10Y, 2Y9Y, 3Y8Y, ..., 10Y1Y, reflect information about the value of the options in this basket. This motivates why we calibrate the short rate models to co-terminal swaptions. In Table 7.6 we show the pricing results for the RACs and in Table 7.7 we show the pricing results for the callable RACs. We use the following abbreviations in the tables, K is the fixed rate of the underlying RAC and B is the barrier of the digitals in the payoff function.

K	B	SR price	H&W price	H&W − SR	DDSV price	DDSV − SR
0.0659	0.0311	-1600.87	-1558.94	41.93	-1719.67	-118.80
0.0659	0.0411	-367.72	-433.21	-65.49	-460.36	-92.64
0.0659	0.0511	742.07	523.38	-218.69	653.07	-89.01
0.0759	0.0311	-1345.23	-1296.94	48.29	-1482.11	-136.88
0.0759	0.0411	75.03	-0.40	-75.43	-31.71	-106.74
0.0759	0.0511	1353.22	1101.34	-251.88	1250.67	-102.55
0.0859	0.0311	-1089.59	-1034.95	54.64	-1244.54	-154.95
0.0859	0.0411	517.78	432.41	-85.38	396.94	-120.84
0.0859	0.0511	1964.38	1679.30	-285.08	1848.27	-116.11

Table 7.6: 13 April 2011: Hull-White and DDSV prices for the RAC, compared to the static replication price. H&W 99% confidence interval width, < 58. DDSV 99% confidence interval width, < 59.

From Table 7.6, we conclude the following for both models. The value of the underlying RAC is not consistent with the SR price and we can explain this as follows. We calibrated the models to different market skews than the market skews we use to price with SR. To price the underlying RAC coupons with SR, which are digital floorlets with a one year tenor, we use the volatilities from the 1Y1Y, 2Y1Y, ... , 10Y1Y market skews. These market skews are in general not equal to the 1Y10Y, 2Y9Y, ..., 10Y1Y market skews, i.e. the skews to which we calibrated the models. We illustrate this in Appendix D.1.4, where we show the calibration results for 13 April 2011.

Moreover, we show for each option maturity to which we calibrate the corresponding market skew we use to price with SR. For the other calibration results we refer the reader to the author. From these results it is clear that we cannot expect that the DDSV prices have a good match to the SR prices, since we use different market volatilities to price with SR. Hence both models are not able to price back the underlying range accrual. So, we need a two-factor model to perform a joint calibration to both, the co-terminal swaptions and the 1 year LIBOR volatilities market skews. Since both, the Hull-White and the DDSV model are one-factor short rate models, we have for both models the issue of joint calibration. We cannot expect that these models are able to price back the underlying RAC, even for the DDSV model which is able to give accurate fits to the market skews. We can draw the same conclusions from the results for the market data of 30 June 2010 and 16 December 2010, given in Appendix D.3.2.

K	B	RAC HW	RAC DDSV	C-RAC H&W	C-RAC DDSV	C-RAC DDSV − C-RAC H&W
0.0659	0.0311	-1558.94	-1719.67	521.04	522.97	1.93
0.0659	0.0411	-433.21	-460.36	809.34	826.45	17.11
0.0659	0.0511	523.38	653.07	1139.85	1260.06	120.21
0.0759	0.0311	-1296.94	-1482.11	676.32	660.57	-15.75
0.0759	0.0411	-0.40	-31.71	1083.87	1100.35	16.48
0.0759	0.0511	1101.34	1250.67	1568.80	1738.87	170.07
0.0859	0.0311	-1034.95	-1244.54	844.65	807.59	-37.06
0.0859	0.0411	432.41	396.94	1386.45	1403.08	16.63
0.0859	0.0511	1679.30	1848.27	2037.88	2249.97	212.09

Table 7.7: 13 April 2011: The Hull-White and DDSV prices for the callable RAC.

Next, we discuss the skew and curvature impact of the DDSV model on the callable RACs. The pricing results for the callable RACs, with the Hull-White and the DDSV models, are given in Table 7.7. We conclude from these results that the largest skew and curvature impact is for callable RACs where the underlying RAC is in-the-money. We see small price impact if the underlying RAC is out-of-the-money for both models. We see a similar behavior in the results for 30 June 2010 and 16 December 2010, given in Appendix D.3.

7.3.4 Callable RMS

In this subsection we show the pricing results for the callable RMS deal. In Table 7.8, we show the Hull-White and DDSV prices of the callable RMS and the value of the underlying RMS range accrual. In Figure 7.3, we show a plot with the pricing results.

For the callable RMS we can use the same argument as for the callable RAC, to explain why we calibrate to co-terminal swaptions. Note that the i-th coupon of the structured leg has a payoff given by:

$$C_i := K\tau(T_{i-1}, T_i)\mathbb{I}_{S(T_{i-1},[T_{i-1},T_m])<B}, \tag{7.6}$$

with $S(T_{i-1}, [T_{i-1}, T_m])$ the swap rate defined in Section 7.1.3. To value these digital coupon payments with static replication, we have to use the co-terminal swaption market skews. These are exactly the skews to which we calibrate the models. We see that this differs from the callable RACs, as in that case the coupon payment depends on the one year LIBOR rate. This implies that we need the market skews with a one year tenor to compute the SR price. Hence for the RMS we have consistency between the skews to which we calibrate and the skews we use to price

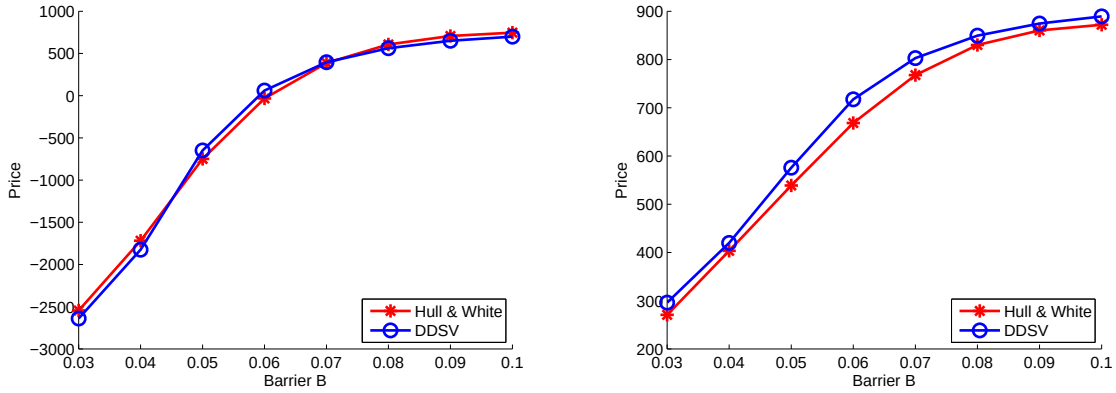

(a) Prices of the underlying RMS range accrual

(b) Prices of the callable RMS

Figure 7.3: Pricing results: 13 April 2011, (callable) RMS range accrual deal.

the RMS range accrual with SR. This implies that we do not have the issue of joint calibration for a RMS.

We have confidence from the test on a digital cap, that the DDSV model is able to give a consistent price compared to the SR price, if we have consistency between the skews to which we calibrate and the skews we use for SR. Hence we expect that this also holds for the RMS range accrual, since it is a series of digital floorlets but with a different reference rate. For this reference rate, we cannot compute the SR price analytically. To see this, note that we can write the digital in Equation (7.6) as:

$$\mathbb{I}_{S(T_{i-1},[T_{i-1},T_m])<B} = \lim_{\delta\to 0} \frac{(B+\delta - S(T_{i-1},[T_{i-1},T_m]))^+ - (B-\delta - S(T_{i-1},[T_{i-1},T_m]))^+}{2\delta}.$$

In this expression we cannot value the two put options under the T_i forward measure using Black's formula, since the swap rate is not a martingale under the T_i forward measure. This implies that the forward price of the swap rate $S(T_{i-1},[T_{i-1},T_m])$ under the T_i forward measure is unknown. Hence we cannot compare the DDSV price of the RMS range accrual to the analytic SR price like we have done for the digital cap, but from the experience with the digital cap we assume that the DDSV model is close to the SR price.

B	RMS rac H&W	RMS rac DDSV	Difference	callable RMS H&W	callable RMS DDSV	Difference
0.03	-2545.03	-2640.37	-95.34	270.56	296.00	25.44
0.04	-1717.86	-1824.26	-106.40	403.41	419.79	16.37
0.05	-749.47	-648.56	100.92	538.93	575.69	36.77
0.06	-32.58	60.60	93.18	668.39	717.42	49.04
0.07	387.64	396.23	8.58	767.62	802.89	35.27
0.08	606.66	562.43	-44.24	829.98	849.36	19.38
0.09	706.76	650.22	-56.54	860.21	874.47	14.26
0.10	746.48	699.20	-47.28	872.04	889.30	17.26

Table 7.8: 13 April 2011: The Hull-White and DDSV RMS prices.

From the results in Table 7.8 we conclude that for all barriers the DDSV prices of the callable RMS are larger than the Hull-White prices. This implies an underestimate of the option price if

we do not take the skew and the curvature of the volatility skews into account. On deals with a large notional, that are priced with the Hull-White model, this can have a large impact on the option value. If we look at the pricing result for $B = 0.07$, then we observe that the Hull-White and DDSV price of the underlying RMS range accrual are approximately equal. Hence we expect that the Hull-White model price of the RMS range accrual is close to the SR price. That for this barrier the Hull-White model gives a consistent price compared to the SR price, does not imply that we have consistency between the option values. We see a skew and curvature impact of 35.27 in the option values.

Chapter 8

Conclusion

In this thesis we considered two short rate models, the Hull-White model and the Cheyette model. We derived a displaced diffusion stochastic volatility (DDSV) formulation of the Cheyette model. We implemented this model with three piecewise constant parameters to incorporate the term structure, these parameters are included in the calibration. The mean reversion of variance, the mean reversion of the short rate and the scaling parameter R_0 are not included in the calibration. We have seen in Chapter 5 that the piecewise constant parameters can control the curvature, skewness and level of the implied volatility skew. We assumed that these are the key ingredients to improve the fit to the market volatility skew compared to the Hull-White fit, since the Hull-White model is not able to control the skewness and curvature of the implied volatility skew.

We showed how the DDSV model can be calibrated to the swaption market in an efficient way. We have to change measure to obtain the dynamics of the swap rate under the swap measure. Then there are several approximations involved to obtain a time-dependent volatility function $\lambda(t)$. To obtain a closed-form solution for the swaption price we use averaging theorems from Piterbarg. Applying these theorems on the swap rate model, transforms the swap rate model into the time-homogeneous swap rate model. The time-homogeneous swap rate model allows for the derivation of a closed-form formula to compute the swaption price, which is computed using the fundamental transform with a control variate for the integration. This swaption price is an approximation of the true model implied swaption price, since there are approximations involved. One of the approximations is the approximation of the short rate with the forward rate. Since this is a crude approximation, we have to restrict the skew parameter γ. In Section 5.8.3 we derived an upperbound on the parameters, such that we conserve accuracy between the closed-form swaption price and the Monte Carlo swaption price. Due to the closed-form swaption price formula and the efficient implementation of the averaging formulas, we are able to calibrate the model in an efficient way to the swaption market.

In Chapter 6 we discussed the calibration of the DDSV model on the market data for the EURO, USD and KRW markets. We have seen that we calibrate the EURO market skews accurately. For this market we obtain a major improvement with respect to the Hull-White model. For the KRW market we improve the calibration to the short-dated maturities, but the USD markets are in general difficult to calibrate. We observe that for the KRW market and the USD market we obtain many boundary solutions for the skew parameter γ. This suggests that for both markets larger values of the skew parameter are required to improve the calibration. At this moment we can not weaken the restriction on γ, since γ deals with the crude approximation of the short rate. We expect that improving this approximation will improve the accuracy of the calibration. It is also worthwhile to investigate the case of non-zero correlation and compare the calibration

results from the DDSV model with non-zero correlation to the results from the DDSV model with zero correlation. This is adressed for future research. The choice of the constant parameters β and R_0 is crucial for the stability of the calibration. The choice of β is crucial for stability in the volatility of volatility function. If there is no knowledge of this parameter, it may happen that the model has to be calibrated for several choices of β to obtain an accurate calibration result with a stable volatility of volatility function. The same holds for parameter R_0. As a result we note that calibration of the DDSV model is not robust. A methodology to define optimal constant parameters is adressed for future research.

In Chapter 7 we investigated the skew and curvature impact on interest rate derivatives. We have seen for a digital cap that the DDSV model price is close to the SR price, this is explained by the accurate fit of the DDSV model to the market skew. In general the SR prices for digitals are better matched by the DDSV model prices than the Hull-White model prices. For the valuation of the callable range accrual on LIBOR, it is important that the model gives a consistent price of a series of digitals, since the underlying structured swap of a callable RAC is a series of digitals. The problem with the valuation of a callable RAC is that the models are calibrated to co-terminal swaptions. We have seen that both models are not able to give a consistent price of the underlying RAC, since we use different market volatilities to price the underlying RAC with SR. We cannot calibrate one-factor short rate models to two different market skews per swaption maturity, we recommend to investigate a multi-factor DDSV model. If we are able to calibrate to both market skews per maturity, we expect that we will overcome this issue.

Future research direction

We recommend the following issues for future research.

- In this thesis we approximated the short rate $r(t)$ by $f(0,t)$, to derive a closed form swaption price for the DDSV model. This is a crude approximation, since we do not take properties of $x(t)$ into account. (Recall that the short rate is given by $r(t) = x(t) + f(0,t)$.) This crude approximation implies a constraint on the skew parameter γ. For accuracy reasons we have to restrict the skew parameter to $\gamma \in [0, 0.30]$. We have seen that this interval is not always sufficient for the calibration, for some markets this restriction is too severe. We have seen this for the USD and KRW markets, there we obtain a lot of boundary solutions for γ. The EURO market skews are steeper, hence for this market $[0, 0.30]$ is sufficient. We propose to improve the approximation of the short rate, such that we can improve the calibration to USD and KRW markets.

- We assume zero correlation ρ between the Brownian motion of the variance process and the Brownian motion of the interest rate process. In Section 5.7 we showed that we complicate the derivation of the closed-form swaption price if $\rho \neq 0$, since the averaging formulas do not apply in this case and the drift term in the variance process changes. We propose to investigate how the DDSV model can be calibrated in an efficient way, if the correlation between the Brownian motions is non-zero.

- We have seen that the calibration of the DDSV model is not robust, the stability of the calibration strongly depends on the choice of the constant model parameters. Given the market data, the choice of the constant model parameters is non-trivial. We propose to do future research on the optimal choice of the constant model parameters, such that we can improve the robustness of the calibration.

- We have seen that the valuation of callable range accruals on LIBOR depends on the joint calibration of the model to co-terminal swaptions and the LIBOR rate market volatilities. We propose to extend the DDSV model to a two-factor short rate model, so that we can calibrate to two market skews per option maturity. Furthermore we propose to investigate the skew and curvature impact on callable range accruals on LIBOR with a two-factor model.

Bibliography

[1] D. Brigo and F. Mercurio: *Interest Rate Models - Theory and Practice; with smile, inflation and credit*, second edition, 2007.

[2] S.E. Shreve: *Stochastic Calculus for Finance; Continuous-time Models*, first edition, 2004.

[3] T. Bjork: *Arbitrage Theory in Continuous Time*, second edition, 2004.

[4] C. González Sterling, ING Bank Quantitative Analytics Team CMRM Trading.

[5] C. González Sterling and N. Hári: *Short Rate Models Theory, The one- and two-factor Hull-White Model*, ING Bank Quantitative Analytics Team CMRM Trading, November 16, 2009.

[6] C. González Sterling, N. Hári and D. Kandhai: *Short Rate Models Calibration, the 1-factor Hull-White Model The Ritchken-Sankarasubramanian Model*, ING Bank Quantitative Analytics Team CMRM Trading, November 17, 2009.

[7] C. González Sterling, D. Kandhai and N. Hári, *Short Rate Models - Theory, CEV formulation of the Ritchken-Sankarasubramanian Model*, ING Bank Quantitative Analytics Team CMRM Trading, November 16, 2009.

[8] N. Hári, D. Kandhai and C. González Sterling, *Validation of Callable Range Accrual Swaps on LIBOR*, ING Bank Quantitative Analytics Team CMRM Trading, November 25, 2009.

[9] P. Ritchken and L. Sankarasubramanian: *Volatility Structures of Forward Rates and the Dynamics of the Term Structure* , Mathematical Finance, Vol. 5, No. 1, pp. 55-72, January 1995.

[10] D.F. Schrager and A.A.J. Pelsser, *Pricing Swaptions and Coupon Bond Options in Affine Term Structure Models*, October 14, 2004.

[11] M. Dirkmann, *A multifactor, stochastic volatility HJM model in a low dimensional markov representation; theory overview and implementation details*, 2006

[12] L. Andersen and J. Andreasen, *Volatile Volatilities*, Risk, December 1, 2002.

[13] V. Piterbarg, *Stochastic Volatility Model with Time-dependent skew*, Applied Mathematical Finance, Vol.12, No.2, 147-185, June 2005.

[14] A. Lewis, *Option Valuation under Stochastic Volatility*, Finance Press, February 1, 2000.

[15] F. Fang and C.W. Oosterlee, *A novel pricing method for european options based on fourier-cosine series expansions*, SIAM Journal on Scientific Computing. 31: 826-848, 2008.

[16] D. Duffie, J. Pan and K. Singleton, *Transform Analysis and Asset Pricing for Affine Jump-Diffusions*, Econometrica, November 1999.

[17] W. Gander and W. Gautschi, *Adaptive Quadrature Revisited*, BIT Numerical Mathematics, 40, pp. 84-101, 2000.

[18] M. Broadie and Ö. Kaya *Exact Simulation of Stochastic Volatility and other Affine Jump Diffusion Processes*, September 29, 2004.

[19] L. Andersen, R. Brotherton-Ratcliff, *Extended Libor Market Models with Stochastic Volatility*, December 31, 2001.

[20] L. Andersen, *Efficient simulation of the Heston Stochastic Volatility Model*, Banc of America securities, January 23, 2007.

[21] L. Andersen and V. Piterbarg, *Interest Rate Modeling, Volume I: Foundations and Vanilla Models*, Atlantic Financial Press, 1st edition, 2010.

[22] U Faigle, W Kern and G Still, *Algorithmic Priciples of Mathematical Programming*, Kluwer Academic Publishers, 2002.

[23] F.A. Longstaff and E.S. Schwartz, *Valuing American options by simulation: A Simple Least-Squares approach*, The Review of Financial Studies, Vol. 14, No. 1, pp. 113-147, Spring 2001.

[24] V. Piterbarg, *A practitioner's guide to pricing and hedging callable libor exotics in forward LIBOR models*, June 25, 2003.

Delft University of Technology
Faculty of Electrical Engineering, Mathematics and Computer Science
Delft Institute of Applied Mathematics

Appendix

On the Cheyette short rate model with stochastic volatility

A thesis submitted to the
Delft Institute of Applied Mathematics
in partial fulfillment of the requirements

for the degree

MASTER OF SCIENCE
in
APPLIED MATHEMATICS

by

Bart Hoorens

Delft, the Netherlands
June 2011

Appendix A

Swap rate under the swap measure

In this appendix we derive for a general class of models the dynamics of the swap rate under the so called swap measure. Fur further reading we refer to [10].

A.1 General setup

Our goal is to derive the dynamics of the swap rate under the swap measure. We derive these dynamics for a general affine term structure model. In these models the short rate is modelled as an affine function of state variables $\mathbf{X}(t) = (x_1(t), \ldots, x_n(t))^T$.

$$r(t) = g(t) + \mathbf{w}^T \mathbf{X}(t)$$

Where $g(t)$ is a scalar function of time and $\mathbf{w}^T$ an n-vector. The n-dimensional factor dynamics are given by the following diffusion process

$$d\mathbf{X}(t) = A(\theta - \mathbf{X}(t))dt + \Sigma\sqrt{V(t)}d\mathbf{W}^{\mathbb{Q}^0}(t) \tag{A.1}$$

where $\mathbf{W}^{\mathbb{Q}^0}(t)$ is an n-dimensional Brownian motion under the risk neutral measure, θ is an n-vector, A and Σ are $n \times n$ matrices. The entries of θ, A and Σ are adapted to the filtration $\mathcal{F}_t$ generated by the Brownian motion. The matrix $V(t)$ is a diagonal $(n \times n)$ matrix holding the diffusion coefficients of the factors on the diagonal, hence

$$V_{ii}(t) = \alpha_i + \beta_i^T \mathbf{X}(t)$$

with α_i a scalar and β_i an n-vector. In the affine term structure models the zero-coupon bond prices have the following form:

$$P(t,T) = \exp\left(C(t,T) - \mathbf{B}(t,T) \cdot \mathbf{X}(t)\right) \tag{A.2}$$

The coefficients $C(t,T)$ and $\mathbf{B}(t,T)$ can be obtained by solving the Riccati equations. A simple application of Itô's Lemma to $P(t,T)$ gives the dynamics under the risk neutral measure.

$$dP(t,T) = r(t)P(t,T)dt - P(t,T)\mathbf{B}(t,T)^T\Sigma\sqrt{V_t}d\mathbf{W}^{\mathbb{Q}^0}(t). \tag{A.3}$$

A.2 The dynamics of the swap rate under the swap measure

In this Subsection we derive the dynamics of the swap rate under the swap measure. First we derive the Radon Nikodym process for a general ATSM and construct the corresponding

martingale measure $\mathbb{Q}^{1,m}$. Second we derive the swap rate and factor dynamics under the new martingale measure.

A.2.1 The Radon Nikodym process to change measure and Brownian motion

In this subsection we derive the Radon-Nikodým derivative, such that we can change the risk-neutral measure $\mathbb{Q}^0$, to the martingale measure $\mathbb{Q}^{1,m}$ with $P_{1,m}(t)$ as a numeraire. The Radon-Nikodým derivative of $\mathbb{Q}^{1,m}$ with respect to $\mathbb{Q}^0$ is a $\mathcal{F}_{T_0}$-measurable random variable, defined by:

$$\zeta(T_0) := \frac{d\mathbb{Q}^0}{d\mathbb{Q}^{1,m}}, \text{ on } \mathcal{F}_{T_0}.$$

For all sufficiently integrable T_0-claims, $\zeta(T_0)$ is given by:

$$\zeta(T_0) = \frac{P_{1,m}(T_0)/P_{1,m}(t)}{M(T_0)/M(t)}.$$

For any $s \in [t, T_0]$, the induced likelihood process is given by:

$$\zeta(s) := \mathbb{E}^{\mathbb{Q}^0}\left[\zeta(T_0)|\mathcal{F}_s\right] = \frac{P_{1,m}(s)/P_{1,m}(t)}{M(s)/M(t)},$$

since the process $P_{1,m}(s)/M(s)$ is a martingale under $\mathbb{Q}^0$. Under these conditions, the measure $\mathbb{Q}^{1,m}$ defined by:

$$\mathbb{Q}^{1,m}(A) = \int_A \zeta(T_0) d\mathbb{Q}^0, \text{ for all } A \in \mathcal{F}_{T_0}, \tag{A.4}$$

is a martingale measure for $P_{1,m}(t)$. Using the martingale property of $\zeta(s)$ under $\mathbb{Q}^0$ we can derive its differential.

$$\begin{aligned} d\zeta(s) &= d\left(\frac{P_{1,m}(s)}{M(s)} \underbrace{\frac{M(t)}{P_{1,m}(t)}}_{\text{constant}}\right) = \frac{M(t)}{P_{1,m}(t)} d\left(\frac{P_{1,m}(s)}{M(s)}\right) \\ &= \frac{M(t)}{P_{1,m}(t)} \left\{ \frac{1}{M(s)} dP_{1,m}(s) + P_{1,m}(s) d\left(\frac{1}{M(s)}\right) + \underbrace{dP_{1,m}(s) d\left(\frac{1}{M(s)}\right)}_{=0} \right\} \end{aligned} \tag{A.5}$$

One easily shows that

$$d\left(\frac{1}{M(s)}\right) = -r(s)\frac{1}{M(s)} ds$$

and

$$\begin{aligned} d(P_{1,m}(s)) &= \sum_{i=1}^{m} \tau_i d(P(s,T_i)) \\ &= \sum_{i=1}^{m} \tau_i r(s) P(s,T_i) ds - \tau_i P(s,T_i) \mathbf{B}(s,T_i)^T \Sigma \sqrt{V(s)} d\mathbf{W}^{\mathbb{Q}^0}(s) \end{aligned}$$

Where we used Equation (A.3) for the differential of the bond price under the risk neutral measure. Substituting these results in (A.5) yields

$$\begin{aligned}
d\zeta(s) &= -\frac{M(t)}{P_{1,m}(t)}\frac{1}{M(s)}\sum_{i=1}^{m}\tau_i P(s,T_i)\mathbf{B}(s,T_i)^T\Sigma\sqrt{V(s)}d\mathbf{W}^{\mathbb{Q}^0}(s)\\
&= -\frac{M(t)}{P_{1,m}(t)}\frac{P_{1,m}(s)}{M(s)}\sum_{i=1}^{m}\tau_i\frac{P(s,T_i)}{P_{1,m}(s)}\mathbf{B}(s,T_i)^T\Sigma\sqrt{V(s)}d\mathbf{W}^{\mathbb{Q}^0}(s)\\
&= -\zeta(s)\sum_{i=1}^{m}\tau_i\frac{P(s,T_i)}{P_{1,m}(s)}\mathbf{B}(s,T_i)^T\Sigma\sqrt{V(s)}d\mathbf{W}^{\mathbb{Q}^0}(s)\\
&= -\zeta(s)\underbrace{\left[\sqrt{V(s)}\Sigma^T\sum_{i=1}^{m}\tau_i\frac{P(s,T_i)}{P_{1,m}(s)}\mathbf{B}(s,T_i)\right]}_{\boldsymbol{\phi}(s):=}\cdot d\mathbf{W}^{\mathbb{Q}^0}(s)
\end{aligned}$$

Where $\boldsymbol{\phi}(s)$ defined above is an n dimensional vector with all entries adapted processes to $\mathcal{F}_s$. We can solve this SDE with an easy application of Itô's Lemma to $f(x) = \log(x)$.

$$\zeta(s) = \exp\left(-\int_t^s \boldsymbol{\phi}(p)\cdot d\mathbf{W}^{\mathbb{Q}^0}(t) - \frac{1}{2}\int_t^s \|\boldsymbol{\phi}(p)\|^2 dp\right).$$

Now by taking $\boldsymbol{\phi}(s)$ as the Girsanov's Kernel in the n- dimensional Girsanov's Theorem[1] we get:

$$\mathbf{W}^{\mathbb{Q}^{1,m}}(s) = \mathbf{W}^{\mathbb{Q}^0}(s) + \int_t^s \boldsymbol{\phi}(p)dp,$$

a n-dimensional standard Brownian motion under the swap measure given in (A.4). In differential notation

$$d\mathbf{W}^{\mathbb{Q}^0}(s) = d\mathbf{W}^{\mathbb{Q}^{1,m}}(s) - \boldsymbol{\phi}(s)ds. \tag{A.6}$$

A.2.2 Swap rate and factor dynamics under $\mathbb{Q}^{1,m}$

Using the previous results we easily derive the factor dynamics under the swap measure. By substituting (A.6) in (A.1) we get

$$\begin{aligned}
d\mathbf{X}(t) &= \left[A(\theta - \mathbf{X}(t)) - \Sigma\sqrt{V(t)}\boldsymbol{\phi}(t)\right]dt + \Sigma\sqrt{V(t)}d\mathbf{W}^{\mathbb{Q}^{1,m}}(s)\\
&= \left[A(\theta - \mathbf{X}(t)) - \Sigma V(t)\Sigma^T\sum_{i=1}^{m}\tau_i\frac{P(t,T_i)}{P_{1,m}(t)}\mathbf{B}(t,T_i)\right]dt + \Sigma\sqrt{V(t)}d\mathbf{W}^{\mathbb{Q}^{1,m}}(s)\\
&= \left[A(\theta - \mathbf{X}(t)) + \Sigma V(t)\Sigma^T\nabla\log P_{1,m}(t)\right]dt + \Sigma\sqrt{V(t)}d\mathbf{W}^{\mathbb{Q}^{1,m}}(s).
\end{aligned}$$

The gradient in the last line is taken with respect to the state variables $\mathbf{X}(t) = (X_1(t), \cdots X_n(t))^T$:

[1] under the assumption that $\mathbb{E}^{\mathbb{Q}^0}\left[\int_0^{T_0}\boldsymbol{\phi}(s)^2\zeta(s)^2 ds\right] < \infty$

$$\begin{aligned}\nabla \log P_{1,m}(t) &= \left(\frac{\partial}{\partial X_1}\log P_{1,m}(t), \cdots, \frac{\partial}{\partial X_n}\log P_{1,m}(t)\right)^T \\ &= \frac{1}{P_{1,m}(t)}\left(\frac{\partial}{\partial X_1}P_{1,m}(t), \cdots, \frac{\partial}{\partial X_n}P_{1,m}(t)\right)^T \\ &= -\frac{1}{P_{1,m}(t)}\sum_{i=1}^{m}\tau_i P(t,T_i)\left(B_1(t,T_i), \cdots, B_n(t,T_i)\right)^T \\ &= -\frac{1}{P_{1,m}(t)}\sum_{i=1}^{m}\tau_i P(t,T_i)\mathbf{B}(t,T_i),\end{aligned}$$

where we used:

$$\frac{\partial}{\partial X_j}P_{1,m}(t) = -\sum_{i=1}^{m}\tau_i P(t,T_i)B_j(t,T_i), \text{ for all } j \in \{1,\cdots,n\}.$$

The derivation of the dynamics of the swap rate under the swap measure is more complicated. But to simplify things we use the fact that the swap rate is a martingale under the swap measure. This is because the swap rate is given by a difference of two bonds divided by the numeraire, see (2.13), hence a martingale under $\mathbb{Q}^{1,m}$. So if we calculate the differential of $S_{0,m}(t)$ under this measure we can ignore all dt-terms.

First we calculate:

$$d\left(\frac{P(t,T)}{P_{1,m}(t)}\right) = \frac{1}{P_{1,m}(t)}d\left(P(t,T)\right) + P(t,T)d\left(\frac{1}{P_{1,m}(t)}\right) + \underbrace{d\left(P(t,T)\right)d\left(\frac{1}{P_{1,m}(t)}\right)}_{\text{Only } dt\text{-terms}}$$

We have to calculate two differentials under the swap measure. The first one is given by:

$$d\left(P(t,T)\right) = \{\cdots\}dt - P(t,T)\mathbf{B}^T(t,T)\Sigma\sqrt{V(t)}d\mathbf{W}^{\mathbb{Q}^{1,m}}(t)$$

Where we used Equation (A.1) in combination with Equation (A.6). An application of Itô's Lemma to $f(x) = \frac{1}{x}$ shows

$$d\left(\frac{1}{P_{1,m}(t)}\right) = -\frac{1}{P_{1,m}(t)^2}d\left(P_{1,m}(t)\right) + \underbrace{\frac{1}{P_{1,m}(t)^3}\left[d\left(P_{1,m}(t)\right)\right]^2}_{\text{Only } dt\text{-terms}}$$

The latter term will contain only dt-terms. For the first term we have to substitute

$$d\left(P_{1,m}(t)\right) = \sum_{i=1}^{m}\tau_i d\left(P(t,T_i)\right) = \{\ldots\}dt - \sum_{i=1}^{m}\tau_i P(t,T_i)\mathbf{B}^T(t,T_i)\Sigma\sqrt{V(t)}d\mathbf{W}^{\mathbb{Q}^{1,m}}(t)$$

When we substitute this we get

$$d\left(\frac{1}{P_{1,m}(t)}\right) = \{\ldots\}dt + \frac{1}{P_{1,m}(t)^2}\sum_{i=1}^{m}\tau_i P(t,T_i)\mathbf{B}^T(t,T_i)\Sigma\sqrt{V(t)}d\mathbf{W}^{\mathbb{Q}^{1,m}}(t)$$

Collecting all $d\mathbf{W}^{\mathbb{Q}^{1,m}}(t)$ together we get

$$
\begin{aligned}
d\left(\frac{P(t,T)}{P_{1,m}(t)}\right) = \quad & \{\ldots\}dt \\
& - \frac{P(t,T)}{P_{1,m}(t)}\mathbf{B}^T(t,T)\Sigma\sqrt{V(t)}d\mathbf{W}^{\mathbb{Q}^{1,m}}(t) \\
& + \frac{P(t,T)}{P_{1,m}(t)^2}\sum_{i=1}^{m}\tau_i P(t,T_i)\mathbf{B}^T(t,T_i)\Sigma\sqrt{V(t)}d\mathbf{W}^{\mathbb{Q}^{1,m}}(t),
\end{aligned}
$$

where we do not specify the dt-term. The previous result for the cases $T = T_0$ and $T = T_m$ gives:

$$
\begin{aligned}
d\left(S_{0,m}(t)\right) = \quad & d\left(\frac{P(t,T_0)}{P_{1,m}(t)}\right) - d\left(\frac{P(t,T_m)}{P_{1,m}(t)}\right) \\
= & -\frac{P(t,T_0)}{P_{1,m}(t)}\mathbf{B}^T(t,T_0)\Sigma\sqrt{V(t)}d\mathbf{W}^{\mathbb{Q}^{1,m}}(t) \\
& + \frac{P(t,T_m)}{P_{1,m}(t)}\mathbf{B}^T(t,T_m)\Sigma\sqrt{V(t)}d\mathbf{W}^{\mathbb{Q}^{1,m}}(t) \\
& + \underbrace{\frac{P(t,T_0)-P(t,T_m)}{P_{1,m}(t)^2}}_{S_{0,m}(t)/P_{1,m}(t)}\sum_{i=1}^{m}\tau_i P(t,T_i)\mathbf{B}^T(t,T_i)\Sigma\sqrt{V(t)}d\mathbf{W}^{\mathbb{Q}^{1,m}}(t)
\end{aligned}
$$

Or simplified

$$
d\left(S_{0,m}(t)\right) = \sum_{i=0}^{m} q_i^S(t)\mathbf{B}^T(t,T_i)\Sigma\sqrt{V(t)}d\mathbf{W}^{\mathbb{Q}^{1,m}}(t) \tag{A.7}
$$

with

$$
q_i^S(t) = \begin{cases} -P(t,T_0)/P_{1,m}(t) & i = 0 \\ \tau_i S_{0,m}(t)P(t,T_i)/P_{1,m}(t) & i \in \{1,2,\ldots,m-1\} \\ (1+\tau_m S_{0,m}(t))P(t,T_m)/P_{1,m}(t) & i = m \end{cases} \tag{A.8}
$$

Appendix B

Proofs of Propositions and Theorems

In this Appendix we list the proofs, which we have ommited in the main text.

B.1 Zero coupon bond price in the piecewise Hull-White model

Proposition B.1. Define the piecewise constant volatility $\sigma(t) = \sigma_j$ for any $t \in (t_{j-1}, t_j]$, $j \in \{1, 2, \ldots, n\}$. The price at time t of the zero-coupon bond with maturity $T(= t_n)$ under a piecewise constant volatility Hull-White model is given by

$$P(t,T) = \frac{P^M(0,T)}{P^M(0,t)} \exp\left(\frac{1}{2}\left(V(t,T) - V(0,T) + V(0,t)\right) - B(t,T)x(t),\right)$$

with

$$B(t,T) = \frac{1}{a}\left(1 - e^{-a(T-t)}\right),$$
$$V(t,T) = \bar{V}(t,t_j) + \sum_{k=j}^{n-1} \bar{V}(t_k, t_{k+1}),$$

where for every $(l,u) \subseteq (t_k, t_{k+1}]$

$$\bar{V}(l,u) = \int_l^u \sigma_{k+1}^2 B(s,T)^2 ds = \frac{\sigma_{k+1}^2}{2a^3}\left(e^{-2aT}(e^{au} - e^{al})(e^{au} + e^{al} - 4e^{aT}) + 2a(u-l)\right).$$

Proof. From Equation (3.12) we derive that the dynamics of the instantaneous short rate under the risk neutral measure are

$$dr(t) = dx(t) + \frac{\partial g}{\partial t}dt = \underbrace{\left(g'(t) + ag(t) - ar(t)\right)}_{b(t,r(t)):=} dt + \underbrace{\sigma(t)}_{c(t,r(t)):=} dW^{\mathbb{Q}^0}(t),$$

with $g(t)$ an unknown, deterministic, differentiable function of time. The coefficients $b(t,r(t))$ and $c(t,r(t))^2$ are affine functions of $r(t)$. I.e. they can be written as:

$$b(t,r(t)) = \lambda(t)r(t) + \eta(t) \quad c(t,r(t))^2 = \gamma(t)r(t) + \delta(t).$$

In this case:

$$\begin{aligned}\eta(t) &= g'(t) + ag(t),\\ \lambda(t) &= -a,\\ \delta(t) &= \sigma^2(t),\\ \gamma(t) &= 0.\end{aligned}$$

Hence for an Affine Term Structure model, the zero-coupon bond price is given by:

$$P(t,T) = A(t,T)e^{-B(t,T)r(t)}. \tag{B.1}$$

Where functions $A(t,T)$ and $B(t,T)$ can be obtained from the coefficients, λ, η, γ and δ by solving the following ordinary differential equations:

$$\begin{aligned}\frac{\partial}{\partial t}B(t,T) &= aB(t,T) - 1,\\ \frac{\partial}{\partial t}\left[\log(A(t,T))\right] &= (g'(t) + ag(t))B(t,T) - \frac{1}{2}\sigma(t)^2B(t,T)^2.\end{aligned}$$

subject to final conditions $B(T,T) = 0$ and $A(T,T) = 1$. The solution for $B(t,T)$ is:

$$B(t,T) = \frac{1}{a}\left(1 - e^{-a(T-t)}\right). \tag{B.2}$$

To solve for $A(t,T)$, we integrate both sides of the second differential equation.

$$\int_t^T \frac{\partial}{\partial s}\log(A(s,T))ds = \int_t^T (g'(s) + ag(s))B(s,T)ds - \frac{1}{2}\int_t^T \sigma(s)^2B(s,T)^2ds.$$

Using the final condition $A(T,T) = 1$ we get

$$A(t,T) = \exp\left\{\frac{1}{2}\int_t^T \sigma(s)^2B(s,T)^2ds - \int_t^T (g'(s) + ag(s))B(s,T)ds\right\}. \tag{B.3}$$

Since we assume a piecewise constant function $\sigma(t) = \sigma_j$, for $t \in (t_{j-1}, t_j]$ we define

$$V(t,T) := \int_t^T \sigma(s)^2B(s,T)^2ds = \bar{V}(t,t_j) + \sum_{k=j}^{n-1}\bar{V}(t_k,t_{k+1}), \tag{B.4}$$

where for every $(l,u) \subseteq (t_k, t_{k+1}]$

$$\bar{V}(l,u) := \int_l^u \sigma_{k+1}^2B(s,T)^2ds = \frac{\sigma_{k+1}^2}{2a^3}\left(e^{-2aT}(e^{au} - e^{al})(e^{au} + e^{al} - 4e^{aT}) + 2a(u-l)\right).$$

With this definition we can rewrite $A(t,T)$:

$$A(t,T) = \exp\left\{\frac{1}{2}V(t,T) - \int_t^T \underbrace{(g'(s) + ag(s))B(s,T)}_{\phi(s):=}\,ds\right\}. \tag{B.5}$$

Where we defined $\phi(s)$ for abbreviation. Substitution of $A(t,T)$ and $B(t,T)$ in Equation (B.1) yields

$$\begin{aligned} P(t,T) &= \exp\left(\frac{1}{2}V(t,T) - \int_t^T \phi(s)ds - B(t,T)r(t)\right) \\ &= \exp\left(\frac{1}{2}V(t,T) - \int_t^T \phi(s)ds - B(t,T)g(t) - B(t,T)x(t)\right) \\ &= \exp\left(\frac{1}{2}V(t,T) + h(t,T) - B(t,T)x(t)\right). \end{aligned} \tag{B.6}$$

where we defined

$$h(t,T) := -\int_t^T \phi(s)ds - B(t,T)g(t). \tag{B.7}$$

$h(t,T)$ depends on, the still unknown, function $g(t)$. We are going to use this unknown function to fit the zero-coupon bond price to the initial zero-coupon bond curve observed in the market. This means, that the model zero-coupon bond price satisfies:

$$P(0,t) = P^M(0,t), \quad \forall t \geq 0, \tag{B.8}$$

with $P(0,t)$ the model zero-coupon bond price and $P^M(0,t)$ the market zero-coupon bond price. To get an expression for $g(t)$, such that we get an exact fit to the initial zero-coupon curve, we require that:

$$P^M(0,T) = P(0,T) = \exp\left(\frac{1}{2}V(0,T) + h(0,T)\right),$$

and

$$P^M(0,t) = P(0,t) = \exp\left(\frac{1}{2}V(0,t) + h(0,t)\right).$$

From these Equations, $h(0,T)$ and $h(0,t)$ must satisfy:

$$h(0,t) = \log\left(P^M(0,t)\right) - \frac{1}{2}V(0,t),$$

and

$$h(0,T) = \log\left(P^M(0,T)\right) - \frac{1}{2}V(0,T).$$

Subtract the second equation from the first to obtain:

$$h(0,T) - h(0,t) = \log\left(\frac{P^M(0,T)}{P^M(0,t)}\right) - \frac{1}{2}V(0,T) + \frac{1}{2}V(0,t). \tag{B.9}$$

Substituting the definition of $h(0,t)$ and $h(0,T)$, given in Equation (B.7), yields:

$$\begin{aligned} h(0,T) - h(0,t) &= -\int_t^T \phi(s)ds - B(0,T)g(0) + B(0,t)g(0) \\ &= -\int_t^T \phi(s)ds + g(0)\left(B(0,t) - B(0,T)\right). \end{aligned} \tag{B.10}$$

Now we are going to derive a condition on $g(t)$ such that: $h(0,T) - h(0,t) = h(t,T)$. Writing out the second term in the right hand side of (B.10) yields:

$$\begin{aligned} g(0)(B(0,t) - B(0,t)) &= g(0)\left(\frac{1}{a}(1-e^{-at}) - \frac{1}{a}(1-e^{-aT})\right) \\ &= g(0)\frac{1}{a}\left(-e^{-at} + e^{-aT}\right) \\ &= -g(0)e^{-at}\frac{1}{a}\left(1 - e^{-a(T-t)}\right) \\ &= -g(t)B(t,T) \end{aligned} \tag{B.11}$$

where we defined $g(t)$as:

$$g(t) = g(0)e^{-at} \quad \text{and} \quad g(0) = r(0). \tag{B.12}$$

With this choice of $g(t)$, substitution of (B.11) in (B.10) yields

$$h(0,T) - h(0,t) = -\int_t^T \phi(s)ds - g(t)B(t,T) = h(t,T). \tag{B.13}$$

Hence combining Equations (B.13) and (B.9) yields

$$h(t,T) = \log\left(\frac{P^M(0,T)}{P^M(0,t)}\right) - \frac{1}{2}V(0,T) + \frac{1}{2}V(0,t). \tag{B.14}$$

To finish the proof, substitute (B.14) in (B.6). Then we get the price of a zero-coupon bond under the piecewise constant volatility Hull-White model:

$$\begin{aligned} P(t,T) &= \exp\left(\frac{1}{2}V(t,T) + \log\left(\frac{P^M(0,T)}{P^M(0,t)}\right) - \frac{1}{2}V(0,T) + \frac{1}{2}V(0,t) - B(t,T)x(t)\right) \\ &= \frac{P^M(0,T)}{P^M(0,t)}\exp\left(\frac{1}{2}\left(V(t,T) - V(0,T) + V(0,t)\right) - B(t,T)x(t)\right). \end{aligned}$$

One easily sees that the model implied zero-coupon bond price satisfies the required condition (B.8). □

B.2 Zero coupon bond price in the Cheyette model

Proposition B.2. Under the same settings as those described in Section 4.1 the price at time t of a zero-coupon bond, maturing at time T, is given by:

$$P(t,T) = \frac{P^M(0,T)}{P^M(0,t)}e^{-x(t)B(t,T) - \frac{1}{2}y(t)B^2(u,T)},$$

with $P^M(0,t)$ the zero-coupon bond price observed in the market and $B(t,T) = \int_t^T k(t,x)dx$.

Proof. The instantaneous forward rate given by the HJM-framework is:

$$f(t,T) = f(0,T) + \int_0^t \sigma(u,T)\left(\int_u^T \sigma(u,s)ds\right)du + \int_0^t \sigma(u,T)dW^{\mathbb{Q}^0}(u),$$

with $0 \leq t \leq T$, under the assumption that

$$\sigma(x,y) = \eta(x,x)k(x,y),$$

and

$$k(x,y) = \exp\left(-\int_x^y \kappa(v)dv\right).$$

Note that:

$$\sigma(x,y) = \eta(x,x)k(x,y) = \eta(x,x)k(x,s)k(s,y) = \sigma(x,s)k(s,y), \quad 0 \leq x \leq s \leq y.$$

We use this expression twice in the derivation below. Using these identities in the equation for $f(t,T)$ yields:

$$\begin{aligned}
f(t,T) &= f(0,T) + \int_0^t \sigma(u,t)k(t,T)\left(\int_u^T \sigma(u,s)ds\right)du + \int_0^t \sigma(u,t)k(t,T)dW^{\mathbb{Q}^0}(u) \\
&= f(0,T) + k(t,T)\left\{\int_0^t \sigma(u,t)\left(\int_u^t \sigma(u,s)ds + \int_t^T \sigma(u,s)ds\right)du \right. \\
&\quad \left. + \int_0^t \sigma(u,t)dW^{\mathbb{Q}^0}(u)\right\} \\
&= f(0,T) + k(t,T)\left\{\underbrace{\int_0^t \sigma(u,t)\int_u^t \sigma(u,s)dsdu + \int_0^t \sigma(u,t)dW^{\mathbb{Q}^0}(u)}_{=f(t,t)-f(0,t)}\right\} \\
&\quad + k(t,T)\int_0^t \sigma(u,t)\left(\int_t^T \sigma(u,s)ds\right)du \\
&= f(0,T) + k(t,T)\left\{f(t,t) - f(0,t) + \int_0^t \sigma(u,t)\left(\int_t^T \sigma(u,s)ds\right)du\right\} \\
&= f(0,T) + k(t,T)\left\{r(t) - f(0,t) + \int_0^t \sigma(u,t)^2\left(\int_t^T k(t,s)ds\right)du\right\} \\
&= f(0,T) + k(t,T)x(t) + k(t,T)\underbrace{\int_0^t \sigma(u,t)^2 du}_{y(t)}\int_t^T k(t,s)ds \\
&= f(0,T) + x(t)\frac{\partial}{\partial T}\int_t^T k(t,s)ds + \frac{1}{2}y(t)\frac{\partial}{\partial T}\left(\int_t^T k(t,s)ds\right)^2.
\end{aligned}$$

Hence we derived the following equation

$$f(t,T) = f(0,T) + \frac{\partial}{\partial T}\left\{x(t)\int_t^T k(t,s)ds + \frac{1}{2}y(t)\left(\int_t^T k(t,s)ds\right)^2\right\}. \tag{B.15}$$

Using the definition of the instantaneous forward rate, see Equation (2.4), we derive:

$$P(t,T) = \exp\left(-\int_t^T f(t,s)ds\right).$$

Using the identity for $f(t,s)$, given in Equation (B.15), yields

$$\begin{aligned}
P(t,T) &= \exp\left(-\int_t^T f(0,s) + \frac{\partial}{\partial s}\left\{x(t)\int_t^s k(t,u)du + \frac{1}{2}y(t)\left(\int_t^s k(t,u)du\right)^2\right\}ds\right) \\
&= \exp\left(-\int_t^T f(0,s)ds\right)\exp\left(-x(t)\int_t^T k(t,u)du - \frac{1}{2}y(t)\left(\int_t^T k(t,u)du\right)^2 ds\right) \\
&= \frac{P(0,T)}{P(0,t)}\exp\left(-x(t)B(t,T) - \frac{1}{2}y(t)B(t,T)^2 ds\right),
\end{aligned}$$

with

$$B(t,T) = \int_t^T k(t,u)du,$$

as to be shown.

□

B.3 Proof of Proposition 4.4.1

Proposition B.3. Let $x(t)$ be some stochastic process with dynamics:

$$\begin{aligned}
dx(t) &= \nu(t)x(t)dW(t), \\
x(0) &= x_0,
\end{aligned}$$

where $W(t)$ is a standard Brownian motion and $\nu(t)$ some deterministic function of time. Then

$$\mathbb{E}\left[(x(t)-K)^+\right] = x_0\mathcal{N}(d_1) - K\mathcal{N}(d_2),$$

where

$$\begin{aligned}
d_1 &= \frac{\log(x_0/K) + \frac{1}{2}\bar{\sigma}^2}{\bar{\sigma}}, \\
d_2 &= d_1 - \bar{\sigma}, \\
\bar{\sigma}^2 &= \int_0^t \nu(s)^2 ds, \\
\mathcal{N}(x) &= \int_{-\infty}^x \frac{1}{\sqrt{2\pi}} e^{-\frac{1}{2}s^2} ds.
\end{aligned}$$

This is Black's formula with Black's volatility $\sigma^2 = \bar{\sigma}^2/t$.

Proof. Using Itô's formula on $f(x) = \log(x)$ yields

$$\log(x(t)) = \log(x_0) + \int_0^t \nu(s)dW(s) - \frac{1}{2}\int_0^t \nu(s)^2 ds,$$

hence the log of $x(t)$ has a normal distribution at time t. The expectation at time t is trivial since Itô integrals are martingales and the other terms are non random. (We assume $\nu(t)$ to be deterministic.)

$$\bar{\mu} := \mathbb{E}[\log(x(t))] = \log(x_0) - \frac{1}{2}\int_0^t \nu(s)^2 ds.$$

To compute the second moment note that

$$\begin{aligned}[\log(x(t))]^2 = &\left[\log(x_0) - \frac{1}{2}\int_0^t \nu(s)^2 ds\right]^2 \\ &+ 2\left[\log(x_0) - \frac{1}{2}\int_0^t \nu(s)^2 ds\right]\int_0^t \nu(s)dW(s) \\ &+ \left(\int_0^t \nu(s)dW(s)\right)^2.\end{aligned}$$

Taking expectations together with Itô's Isometry yields

$$\mathbb{E}\left[\log(x(t))^2\right] = \left[\log(x_0) - \frac{1}{2}\int_0^t \nu(s)^2 ds\right]^2 + \int_0^t \nu(s)^2 ds.$$

Now we easily obtain the variance at time t

$$\bar{\sigma}^2 := \mathrm{Var}(x(t)) = \mathbb{E}\left[\log(x(t))^2\right] - \mathbb{E}\left[\log(x(t))\right]^2 = \int_0^t \nu(s)^2 ds.$$

With this information and defining Z a standard normal random variable, we can calculate $\mathbb{E}\left[(x(t) - K)^+\right]$.

$$\begin{aligned}\mathbb{E}\left[(x(t) - K)^+\right] &= \mathbb{E}\left[(\exp(\log(x(t))) - K)^+\right] = \mathbb{E}\left[(\exp(Z\bar{\sigma} + \bar{\mu}) - K)^+\right] \\ &= \exp(\bar{\mu})\mathbb{E}\left[(\exp(Z\bar{\sigma}) - K\exp(-\bar{\mu}))^+\right] \\ &= e^{\bar{\mu}}\int_{(\log(K)-\bar{\mu})/\bar{\sigma}}^{\infty}\left(e^{z\bar{\sigma}} - Ke^{-\bar{\mu}}\right)\frac{1}{\sqrt{2\pi}}e^{-\frac{1}{2}z^2}dz \\ &= e^{\bar{\mu}}\int_{-\alpha}^{\infty}\frac{1}{\sqrt{2\pi}}e^{z\bar{\sigma}-\frac{1}{2}z^2}dz - K\int_{-\alpha}^{\infty}\frac{1}{\sqrt{2\pi}}e^{-\frac{1}{2}z^2}dz,\end{aligned} \tag{B.16}$$

where we defined:

$$\alpha = (\bar{\mu} - \log(K))/\bar{\sigma}. \tag{B.17}$$

Expressions for the integrals are:

$$\begin{aligned}&\int_{-\alpha}^{\infty}\frac{1}{\sqrt{2\pi}}e^{-\frac{1}{2}z^2}dz = \mathbb{P}(Z \geq -\alpha) = \mathbb{P}(Z \leq \alpha) = \mathcal{N}(\alpha) \\ &\int_{-\alpha}^{\infty}\frac{1}{\sqrt{2\pi}}e^{z\bar{\sigma}-\frac{1}{2}z^2}dz = e^{\frac{1}{2}\bar{\sigma}^2}\int_{-\alpha-\bar{\sigma}}^{\infty}\frac{1}{\sqrt{2\pi}}e^{\frac{1}{2}p^2}dp = e^{\frac{1}{2}\bar{\sigma}^2}\mathcal{N}(\bar{\sigma} + \alpha)\end{aligned} \tag{B.18}$$

Hence, a combination of formulas (B.16), (B.17), (B.18), definitions of $\bar{\mu}$, $\bar{\sigma}$ and the fact that $\bar{\mu} + \frac{1}{2}\bar{\sigma}^2 = \log(x_0)$ yields:

$$\begin{aligned}\mathbb{E}\left[(x(t) - K)^+\right] &= e^{\bar{\mu}+\frac{1}{2}\bar{\sigma}^2}\mathcal{N}(\bar{\sigma} + \alpha) - K\mathcal{N}(\alpha) \\ &= x_0\mathcal{N}\left(\frac{\log(x_0/K) + \frac{1}{2}\bar{\sigma}^2}{\bar{\sigma}}\right) - K\mathcal{N}\left(\frac{\log(x_0/K) - \frac{1}{2}\bar{\sigma}^2}{\bar{\sigma}}\right),\end{aligned}$$

as to be shown. □

B.4 Analytic solution of the Riccati ODEs

Result B.4. Consider the following set of ordinary differential equations

$$\frac{dx(t)}{dt} = dy(t), \tag{B.19}$$

$$\frac{dy(t)}{dt} = a + by(t) + cy^2(t), \tag{B.20}$$

$$\tag{B.21}$$

with terminal conditions $(x(T), y(T)) = (0, 0)$. Assume that a, b, c and d are constants, satisfying $ac < 0$, $b \geq 0$ and $d \in \mathbb{R}$. Then the solutions for $x(t)$ and $y(t)$ are given by:

$$y(t) = \frac{1}{2c}\left[-b + \frac{1 + \left(\frac{b-\eta}{b+\eta}\right)e^{-\eta(T-t)}}{1 + \left(\frac{\eta-b}{b+\eta}\right)e^{-\eta(T-t)}}\eta\right], \tag{B.22}$$

$$x(t) = \frac{bd(T-t)}{2c} - \frac{d}{2c}\log\left(\frac{\left[1 + \frac{\eta-b}{\eta+b}e^{-\eta(T-t)}\right]^2}{4\frac{\eta^2-b^2}{(\eta+b)^2}e^{-\eta(T-t)}}\left(1 - \frac{b^2}{\eta^2}\right)\right). \tag{B.23}$$

where we defined:

$$\eta := \sqrt{-4ac + b^2}.$$

Proof. Using standard techniques for solving Riccati Equations, we obtain the solution for $y(t)$.

$$y(t) = \frac{1}{2c}\left[-b + \tanh\left(\frac{1}{2}(T-t)\eta + \operatorname{arctanh}\left(\frac{b}{\eta}\right)\right)\eta\right] \tag{B.24}$$

Rewriting the hyperbolic functions, using the identities:

$$\begin{aligned}\tanh(x) &= \frac{e^{2x} - 1}{e^{2x} + 1}, \\ \operatorname{arctanh}(x) &= \frac{1}{2}\log\left(\frac{1+x}{1-x}\right), |x| < 1,\end{aligned} \tag{B.25}$$

yields the closed form solution for $y(t)$. Since the derivation is tedious, we omit it here. One can verify the solution by showing that $y(t)$ satisfies the differential equation, given by Equation

(B.20) and $y(T) = 0$. To show that the solution is well defined, we have to show that $\frac{b}{\eta} \in (-1, 1)$, since $\operatorname{arctanh}(z)$ is only defined for $z \in (-1, 1)$. Under the assumptions made, we satisfy

$$0 \leq b < \sqrt{-4ac + b^2} = \eta \Rightarrow \frac{b}{\eta} \in [0, 1).$$

We concentrate on the solution for $x(t)$. Integrating both sides of Equation (B.19) from t to T and using $x(T) = 0$ yields:

$$\begin{aligned} x(t) &= -d \int_t^T \frac{1}{2c} \left[-b + \tanh\left(\frac{1}{2}(T-s)\eta + \operatorname{arctanh}\left(\frac{b}{\eta}\right)\right)\eta \right] ds \\ &= -d \left(\frac{b(t-T)}{2c} + \frac{\eta}{2c} \int_t^T \tanh\left(-\frac{1}{2}\eta s + \frac{1}{2}\eta T + \operatorname{arctanh}\left(\frac{b}{\eta}\right)\right) ds \right). \end{aligned} \tag{B.26}$$

To work out the solution for $x(t)$, we have to compute the following integral

$$\int_t^T \tanh\left(\rho s + \kappa\right) ds, \quad \{\rho, \kappa\} \in \mathbb{R}. \tag{B.27}$$

The integrand is given by:

$$\int \tanh(\rho s + \kappa) ds = -\frac{1}{2}\frac{\log(\zeta(s) - 1)}{\rho} - \frac{1}{2}\frac{\log(\zeta(s) + 1)}{\rho} + C, \quad C \in \mathbb{R},$$

where we defined:

$$\zeta(s) := \tanh(\rho s + \kappa).$$

Hence

$$\int_t^T \tanh\left(\rho s + \kappa\right) = \frac{1}{2\rho}\left(-\log(\zeta(T) - 1) - \log(\zeta(T) + 1) + \log(\zeta(t) - 1) + \log(\zeta(t) + 1)\right). \tag{B.28}$$

Note that we have to be careful with $\log(x)$, for negative values of x. We define for any $x \in (-\infty, 0)$:

$$\log(x) = \log(|x| \exp(i\pi)) = \log(|x|) + i\pi. \tag{B.29}$$

Observe that for any $\{\rho, \kappa, t\} \subset \mathbb{R}$ we satisfy:

$$\tanh(\rho t + \kappa) \in (-1, 1) \Rightarrow \begin{cases} \tanh(\rho t + \kappa) - 1 \in (-2, 0) \\ \tanh(\rho t + \kappa) + 1 \in (0, 2) \end{cases} \tag{B.30}$$

With the definition given in Equation (B.29) and the observations made in Equation (B.30), we can rewrite Equation (B.28) as:

$$\int_t^T \tanh\left(\rho s + \kappa\right) = \frac{1}{2\rho}\left(-\log(\zeta(T) + 1) + \log(\zeta(t) + 1) + \log(|\zeta(t) - 1|) - \log(|\zeta(T) - 1|)\right).$$

Taking ρ and κ in Equation (B.26) equal to:

$$\begin{aligned} \rho &:= -\frac{1}{2}\eta, \\ \kappa &:= \frac{1}{2}\eta T + \operatorname{arctanh}\left(\frac{b}{\eta}\right), \end{aligned}$$

yields, after some simplification, the solution for $x(t)$:

$$\begin{aligned}
x(t) &= \frac{bd(T-t)}{2c} - \frac{d}{2c}\left(\log(1+b/\eta) + \log(1-b/\eta) - \log(1-\zeta(t)) - \log(\zeta(t)+1)\right) \\
&= \frac{bd(T-t)}{2c} - \frac{d}{2c}\log\left(\frac{1-b^2/\eta^2}{1-\zeta^2(t)}\right) \\
&= \frac{bd(T-t)}{2c} - \frac{d}{2c}\log\left(\frac{1-b^2/\eta^2}{1-\varphi^2(t)}\right) \\
&= \frac{bd(T-t)}{2c} - \frac{d}{2c}\log\left(\frac{\left(e^{\eta(T-t)}(\eta+b)+\eta-b\right)^2}{4(\eta^2-b^2)e^{(T-t)\eta}}\left(1-\frac{b^2}{\eta^2}\right)\right) \\
&= \frac{bd(T-t)}{2c} - \frac{d}{2c}\log\left(\frac{\left[1+\frac{\eta-b}{\eta+b}e^{-\eta(T-t)}\right]^2}{4\frac{\eta^2-b^2}{(\eta+b)^2}e^{-\eta(T-t)}}\left(1-\frac{b^2}{\eta^2}\right)\right).
\end{aligned}$$

with $\varphi(t)$ defined by:

$$\varphi(t) := \frac{e^{\eta(T-t)}(\eta+b)+b-\eta)}{e^{\eta(T-t)}(\eta+b)+\eta-b}$$

The step from the second to the third line is easily verified by writing out the hyperbolic functions with the identities given by Equation (B.25). The step from the third line to the fourth line is justified by some algebraic manipulations. The last step is made for numerical stability.

□

B.5 Effective volatility of volatility parameter $\bar{\epsilon}$

Proposition B.5. Given the process

$$dS_{0,m}(t) = (\gamma(t)S_{0,m}(t) + (1-\gamma(t))R_0)\lambda(t)\sqrt{V(t)}dW_1(t),$$

and let $V(t)$ and $\tilde{V}(t)$ be two stochastic processes with dynamics

$$\begin{aligned}
dV(t) &= \beta(V(0)-V(t))dt + \epsilon(t)\sqrt{V(t)}dW_2(t), \\
d\tilde{V}(t) &= \beta(V(0)-\tilde{V}(t))dt + \bar{\epsilon}\sqrt{\tilde{V}(t)}dW_2(t),
\end{aligned}$$

where $\bar{\epsilon}$ is given by:

$$\bar{\epsilon}^2 = \frac{\int_0^{T_0} e^{2\beta r}\epsilon^2(r)\rho(r)dr}{\int_0^{T_0} e^{2\beta r}\rho(r)dr}, \tag{B.31}$$

and

$$\rho(r) = \int_r^{T_0} e^{-\beta s}\lambda^2(s)\int_s^{T_0}\lambda^2(t)e^{-\beta t}dtds.$$

Then we satisfy:

$$\mathbb{E}\left[\int_0^{T_0}\lambda^2(t)\tilde{V}(t)dt\right] = \mathbb{E}\left[\int_0^{T_0}\lambda^2(t)V(t)dt\right]$$

and

$$\mathbb{E}\left[\left(\int_0^{T_0}\lambda^2(t)\tilde{V}(t)dt\right)^2\right] = \mathbb{E}\left[\left(\int_0^{T_0}\lambda^2(t)V(t)dt\right)^2\right].$$

Hence the first and second moment of the realized volatility of $S_{0,m}(t)$, generated by the two variance processes $V(t)$ and $\tilde{V}(t)$, are equal for this choice of $\bar{\epsilon}$.

Proof. To prove that the first moments are equal, i.e.:

$$\mathbb{E}\left[\int_0^{T_0}\lambda^2(t)\tilde{V}(t)dt\right] = \mathbb{E}\left[\int_0^{T_0}\lambda^2(t)V(t)dt\right],$$

we have to notice that:

$$\mathbb{E}(V(t)) = V(0) \text{ and } \mathbb{E}(\tilde{V}(t)) = V(0).$$

We prove this for $V(t)$, it is literally the same for $\tilde{V}(t)$. Define the process

$$x(t) := e^{\beta t}(V(t) - V(0)) \text{ with } x(0) = 0.$$

The differential and solution of $x(t)$ are given by:

$$dx(t) = e^{\beta t}\epsilon(t)\sqrt{V(t)}dW(t) \Rightarrow x(t) = \int_0^t e^{\beta s}\epsilon(s)\sqrt{V(s)}dW(s)$$

hence the expectation of $x(t)$ is given by

$$\mathbb{E}(x(t)) = 0.$$

Using the definition of $x(t)$ we derive the expecation of $V(t)$.

$$V(t) = x(t)e^{-\beta t} + V(0) \Rightarrow \mathbb{E}[V(t)] = V(0)$$

Now we see that

$$\mathbb{E}\left[\int_0^{T_0}\lambda^2(t)\tilde{V}(t)dt\right] = \int_0^{T_0}\lambda^2(t)\mathbb{E}\left[\tilde{V}(t)\right]dt = V(0)\int_0^{T_0}\lambda^2(t)dt$$

and

$$\mathbb{E}\left[\int_0^{T_0}\lambda^2(t)V(t)dt\right] = \int_0^{T_0}\lambda^2(t)\mathbb{E}\left[V(t)\right]dt = V(0)\int_0^{T_0}\lambda^2(t)dt$$

This proves that, for every choice of $\bar{\epsilon}$, the first moments are equal. Now we derive a condition on $\bar{\epsilon}$ such that the second moments are equal i.e.:

$$\mathbb{E}\left[\left(\int_0^{T_0}\lambda^2(t)V(t)dt\right)^2\right] = \mathbb{E}\left[\left(\int_0^{T_0}\lambda^2(t)\tilde{V}(t)dt\right)^2\right] \tag{B.32}$$

In Equation (B.33) we work out the left hand side of Equation (B.32), the right hand side is literally the same.

$$\begin{aligned}\mathbb{E}\left[\left(\int_0^{T_0}\lambda^2(t)V(t)dt\right)^2\right] &= \mathbb{E}\left[\int_0^{T_0}\int_0^{T_0}\lambda^2(s)\lambda^2(t)V(s)V(t)dsdt\right]\\ &= \int_0^{T_0}\int_0^{T_0}\lambda^2(s)\lambda^2(t)\mathbb{E}\left[V(s)V(t)\right]dsdt\\ &= 2\int_0^{T_0}\int_0^{t}\lambda^2(s)\lambda^2(t)\mathbb{E}\left[V(s)V(t)\right]dsdt\\ &= \cdots\end{aligned} \tag{B.33}$$

To work this equation, we derive an expression for $\mathbb{E}\left[V(s)V(t)\right]$ under the condition that $s \leq t$. Therefor it is convenient to calculate $\mathbb{E}\left[x(s)x(t)\right]$ for $s \leq t$. Defining:

$$\phi(a,b) := \int_a^b e^{\beta r}\epsilon(r)\sqrt{V(r)}dW(r),$$

and using previous results gives:

$$\begin{aligned}\mathbb{E}\left[x(s)x(t)\right] &= \mathbb{E}\left[\int_0^s e^{\beta r}\epsilon(r)\sqrt{V(r)}dW(r)\cdot\int_0^t e^{\beta r}\epsilon(r)\sqrt{V(r)}dW(r)\right]\\ &= \mathbb{E}\left[\left(\int_0^s e^{\beta r}\epsilon(r)\sqrt{V(r)}dW(r)\right)^2 + \phi(0,s)\cdot\phi(s,t)\right]\\ &= \mathbb{E}\left[\left(\int_0^s e^{\beta r}\epsilon(r)\sqrt{V(r)}dW(r)\right)^2\right] + \mathbb{E}\left[\phi(0,s)\right]\cdot\mathbb{E}\left[\phi(s,t)\right]\\ &= \mathbb{E}\left[\int_0^s e^{2\beta r}\epsilon^2(r)V(r)dr\right]\\ &= \int_0^s e^{2\beta r}\epsilon^2(r)\mathbb{E}\left[V(r)\right]dr\\ &= V(0)\int_0^s e^{2\beta r}\epsilon^2(r)dr\end{aligned}$$

In the third line we use the property of independent increments of the Brownian motion on disjointness intervals. In the fourth line we use that Itô integrals are martingales and Itô's Isometry. Substitution of $x(t) = e^{\beta t}(V(t) - V(0)$ into the expression for $\mathbb{E}\left[x(s)x(t)\right]$ yields

$$\mathbb{E}\left[V(s)V(t)\right] = V(0)^2 + V(0)e^{-\beta(t+s)}\int_0^s e^{2\beta r}\epsilon^2(r)dr. \tag{B.34}$$

Substituting (B.34) in (B.33) yields:

$$\begin{aligned}\cdots =& 2\int_0^{T_0}\int_0^t \lambda^2(s)\lambda^2(t)\left(V(0)^2 + V(0)e^{-\beta(t+s)}\int_0^s e^{2\beta r}\epsilon^2(r)dr\right)dsdt\\ =& 2\int_0^{T_0}\int_0^t \lambda^2(s)\lambda^2(t)V(0)^2 dsdt +\\ & 2\int_0^{T_0}\int_0^t\int_0^s V(0)e^{-\beta(t+s)}\lambda^2(s)\lambda^2(t)e^{2\beta r}\epsilon^2(r)drdsdt\end{aligned}$$

Note that the triple integral above can be writen as:

$$\int_0^{T_0}\int_r^{T_0}\int_s^{T_0} V(0)e^{-\beta(t+s)}\lambda^2(s)\lambda^2(t)e^{2\beta r}\epsilon^2(r)dtdsdr =$$
$$V(0)\int_0^{T_0} e^{2\beta r}\epsilon^2(r)\int_r^{T_0}\lambda^2(s)e^{-\beta s}\int_s^{T_0} e^{-\beta t}\lambda^2(t)dtdsdr =$$
$$V(0)\int_0^{T_0} e^{2\beta r}\epsilon^2(r)\rho(r)dr$$

with

$$\rho(r) = \int_r^{T_0}\lambda^2(s)e^{-\beta s}\int_s^{T_0} e^{-\beta t}\lambda^2(t)dtds. \tag{B.35}$$

Using this notation, the second moment of the realized volatility is given by:

$$\mathbb{E}\left[\left(\int_0^{T_0}\lambda^2(t)V(t)dt\right)^2\right] = 2V(0)^2\int_0^{T_0}\int_0^t \lambda^2(s)\lambda^2(t)dsdt + 2V(0)\int_0^{T_0} e^{2\beta r}\epsilon^2(r)\rho(r)dr$$

A similar derivation, with variance process $\tilde{V}(t)$ process, gives:

$$\mathbb{E}\left[\left(\int_0^{T_0}\lambda^2(t)V(t)dt\right)^2\right] = 2V(0)^2\int_0^{T_0}\int_0^t \lambda^2(s)\lambda^2(t)dsdt + 2V(0)\bar{\epsilon}^2\int_0^{T_0} e^{2\beta r}\rho(r)dr$$

Equating both second moments yields $\bar{\epsilon}^2$:

$$\bar{\epsilon}^2 = \frac{\int_0^{T_0}\epsilon^2(r)e^{2\beta r}\rho(r)dr}{\int_0^{T_0} e^{2\beta r}\rho(r)dr},$$

with $\rho(r)$ defined by Equation (B.35), as to be shown.

□

Appendix C

Calibration results

C.1 EURO swaption market 9 August 2010.

Maturity in years	Tenor in years	Strike	Model price	Market price	Relative diff.	Model impl vol.	Market vol.	Diff in bp
1	10	0.0159	1291.54	1291.47	0.01	36.28	36.22	5
1	10	0.0309	254.93	254.93	0	24.2	24.2	0
1	10	0.0459	12.58	12.64	-0.48	22.87	22.89	-2
2	9	0.0179	1183.66	1183.66	0	34.85	34.85	0
2	9	0.0329	333.85	333.86	0	23.79	23.79	0
2	9	0.0479	54.9	54.92	-0.05	22.39	22.4	0
3	8	0.0198	1069.68	1069.51	0.02	31.96	31.94	2
3	8	0.0348	352.95	353.24	-0.08	22.27	22.28	-2
3	8	0.0498	84.7	84.58	0.14	20.94	20.93	1
4	7	0.0213	942.51	943	-0.05	29.18	29.24	-6
4	7	0.0363	338.28	337.78	0.15	20.63	20.6	3
4	7	0.0513	96.72	97.21	-0.5	19.42	19.46	-4
5	6	0.0225	805.77	806.44	-0.08	26.53	26.61	-8
5	6	0.0375	306.24	307.47	-0.4	19.22	19.3	-8
5	6	0.0525	100.12	102.32	-2.15	18.33	18.5	-17
6	5	0.0235	673.59	674.61	-0.15	25.32	25.45	-13
6	5	0.0385	271.08	270.38	0.26	18.55	18.5	5
6	5	0.0535	97.54	98.54	-1.01	17.64	17.72	-8
7	4	0.0242	538.93	539.64	-0.13	24.27	24.37	-10
7	4	0.0392	225.46	224.69	0.34	17.86	17.8	6
7	4	0.0542	85.91	86.71	-0.91	16.91	16.98	-7
8	3	0.0249	405.26	404.41	0.21	23.69	23.55	14
8	3	0.0399	176.92	175.56	0.77	17.54	17.4	14
8	3	0.0549	71.42	71.74	-0.45	16.49	16.52	-4
9	2	0.0256	267.18	267.44	-0.1	22.32	22.38	-6
9	2	0.0406	119.33	119.64	-0.26	16.75	16.8	-4
9	2	0.0556	50.29	50.25	0.07	15.85	15.84	1
10	1	0.0263	131.8	132.77	-0.73	21.25	21.68	-42
10	1	0.0413	60.3	61.53	-1.99	16.16	16.5	-34
10	1	0.0563	26.41	27.25	-3.07	15.34	15.58	-24

Table C.1: Euro market 9 August 2010: Calibration results.

$\sigma(t)$	0.2573	0.2808	0.2589	0.2276	0.2234	0.2356	0.2139	0.2394	0.1890	0.1890
$\gamma(t)$	0.1810	0.1343	0.1047	0.0850	0.2826	0.1503	0.0878	0.0680	0.3000	0.3000
$\epsilon(t)$	1.0372	0.9627	0.8939	1.1192	1.1425	1.1358	1.1416	1.1287	0.1160	0.1160

Table C.2: Euro market 9 August 2010: $R_0 = 0.04, \beta = 0.10, a = 0.03, V(0) = 1$.

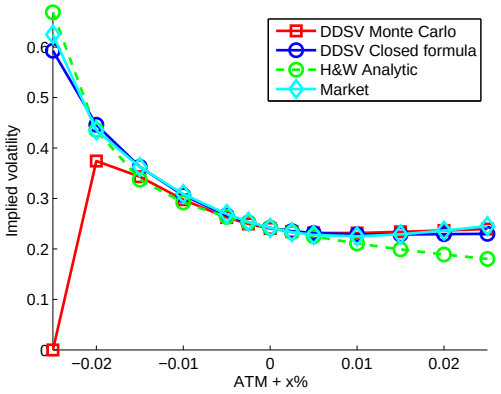

(a) 1Y10Y: Accuracy, ATM -14 bp, max. 195 bp.

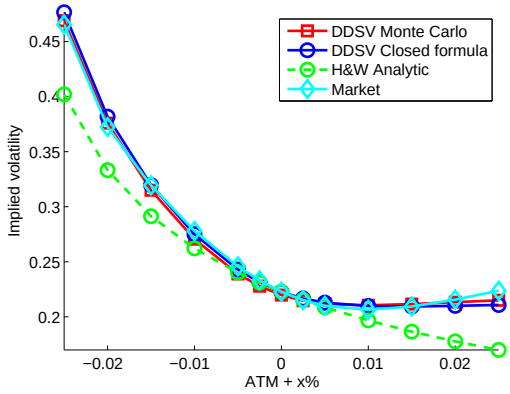

(b) 3Y8Y: Accuracy, ATM -29 bp, max. 47 bp.

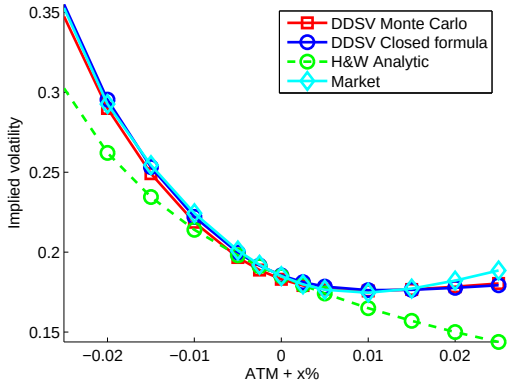

(c) 6Y5Y: Accuracy, ATM -25 bp, max. 41 bp.

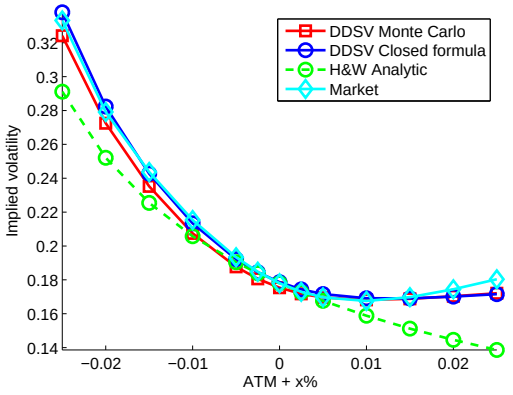

(d) 7Y4Y: Accuracy, ATM -32bp, max. 74 bp.

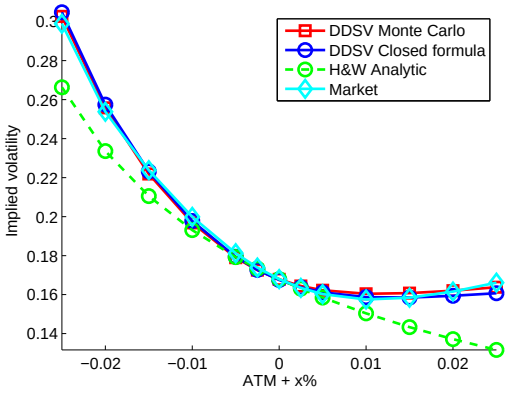

(e) 9Y2Y: Accuracy, ATM 3 bp, max. 23 bp.

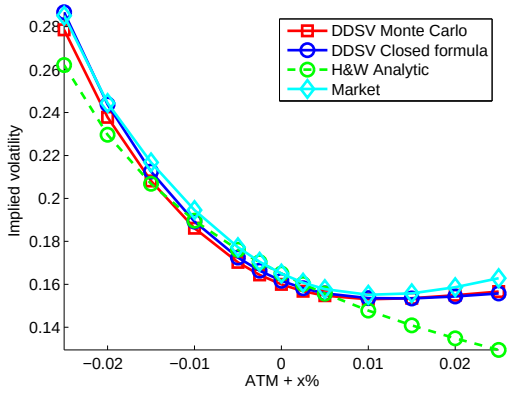

(f) 10Y1Y: Accuracy, ATM -17 bp, max. 44bp.

Figure C.1: Euro market 9 August 2010: Figures with Cheyette and Hull-White fits to the market skew.

C.2 EURO swaption market 19 November 2009.

Maturity in years	Tenor in years	Strike	Model price	Market price	Relative diff.	Model impl vol.	Market vol.	Diff in bp
1	10	0.0239	1260.21	1260.21	0.00	34.31	34.31	0
1	10	0.0389	291.80	291.80	0.00	22.89	22.89	0
1	10	0.0539	31.96	31.96	0.00	23.21	23.21	0
2	9	0.0262	1165.08	1167.14	-0.18	30.98	31.25	-27
2	9	0.0412	357.20	356.83	0.10	21.32	21.30	2
2	9	0.0562	82.80	84.46	-1.97	21.38	21.53	-14
3	8	0.0278	1048.12	1048.18	-0.01	27.75	27.76	-1
3	8	0.0428	357.56	357.89	-0.09	19.28	19.30	-2
3	8	0.0578	106.22	106.35	-0.12	19.41	19.42	-1
4	7	0.0291	917.49	915.34	0.23	25.11	24.90	20
4	7	0.0441	332.72	337.77	-1.49	17.63	17.90	-27
4	7	0.0591	116.42	113.78	2.32	18.07	17.90	17
5	6	0.0301	778.14	772.38	0.75	22.75	22.20	55
5	6	0.0451	294.75	301.81	-2.34	16.30	16.70	-40
5	6	0.0601	111.79	108.55	2.99	16.78	16.57	21
6	5	0.0309	643.93	640.89	0.47	21.38	21.07	31
6	5	0.0459	257.30	261.53	-1.62	15.69	15.95	-26
6	5	0.0609	104.39	101.65	2.70	16.03	15.84	19
7	4	0.0315	508.33	506.28	0.40	20.06	19.82	24
7	4	0.0465	209.45	211.67	-1.05	14.94	15.10	-16
7	4	0.0615	87.41	86.05	1.59	15.14	15.04	11
8	3	0.0320	378.28	376.87	0.37	19.29	19.09	20
8	3	0.0470	162.84	163.38	-0.33	14.65	14.70	-5
8	3	0.0620	70.61	70.26	0.49	14.67	14.64	3
9	2	0.0327	249.20	248.33	0.35	18.46	18.28	18
9	2	0.0477	110.71	110.69	0.02	14.24	14.23	0
9	2	0.0627	49.14	49.22	-0.15	14.12	14.13	-1
10	1	0.0334	123.26	123.08	0.14	17.73	17.67	7
10	1	0.0484	56.44	56.13	0.56	13.88	13.80	8
10	1	0.0634	25.61	25.48	0.50	13.64	13.60	3

Table C.3: EURO market 19 November 2009: Calibration results.

$\sigma(t)$	0.2878	0.3000	0.2652	0.2595	0.2025	0.2180	0.1752	0.1981	0.1747	0.1689
$\gamma(t)$	0.0427	0.0359	0.0292	0.1617	0.3000	0.2689	0.2163	0.2311	0.2036	0.1910
$\epsilon(t)$	1.6502	1.4572	3.5047	0.0101	0.0103	0.0122	0.0117	0.0112	0.0112	0.0112

Table C.4: EURO market 19 November 2009: $R_0 = 0.04, \beta = 0.20, a = 0.03, V(0) = 1$.

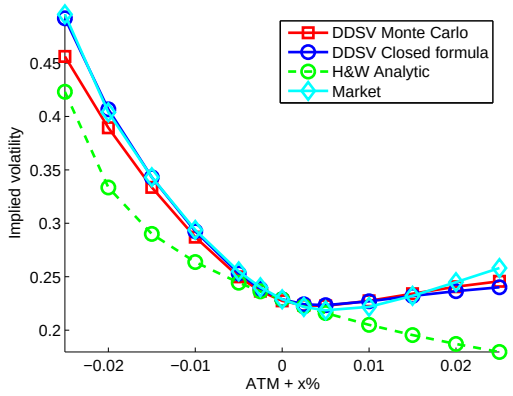

(a) 1Y10Y: Accuracy, ATM -14 bp, max. 90 bp.

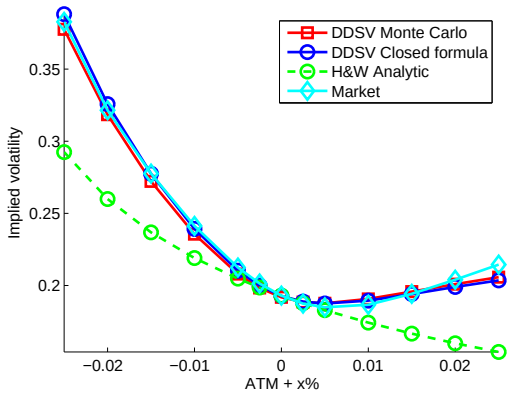

(b) 3Y8Y: Accuracy, ATM -9 bp, max. 52 bp.

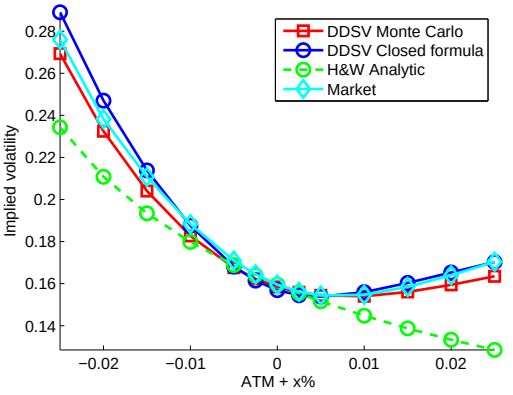

(c) 6Y5Y: Accuracy, ATM 15 bp, max. 97 bp.

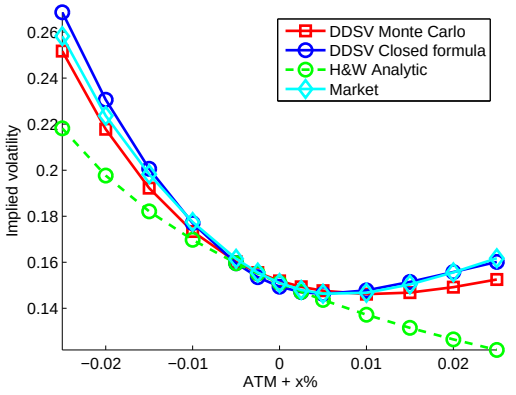

(d) 7Y4Y: Accuracy, ATM 25 bp, max. 84 bp.

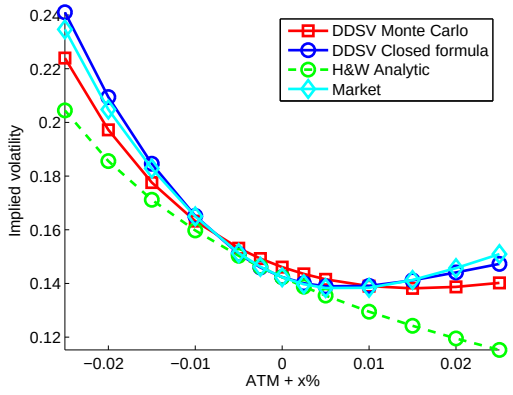

(e) 9Y2Y: Accuracy, ATM 37 bp, max. 70 bp.

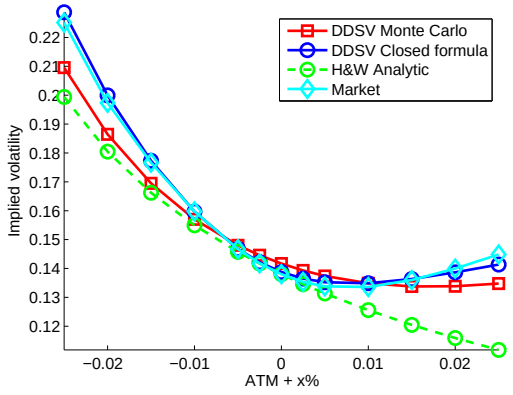

(f) 10Y1Y: Accuracy, ATM 29 bp, max. -78 bp.

Figure C.2: EURO market 19 November 2009: Figures with Cheyette and Hull-White fits to the market skew.

C.3 KRW swaption market 9 August 2010.

Maturity in years	Tenor in years	Strike	Model price	Market price	Relative diff.	Model impl vol.	Market vol.	Diff in bp
1	10	0.0415	945.54	942.85	0.29	20.22	19.47	75
1	10	0.0565	210.64	210.62	0.01	15.10	15.10	0
1	10	0.0715	20.12	22.98	-12.43	16.08	16.59	-51
2	9	0.0409	873.43	868.66	0.55	18.22	17.54	68
2	9	0.0559	239.45	241.99	-1.05	13.62	13.76	-15
2	9	0.0709	45.49	48.89	-6.95	14.65	14.98	-33
3	8	0.0401	795.42	790.37	0.64	17.37	16.81	56
3	8	0.0551	249.34	249.20	0.05	13.22	13.21	1
3	8	0.0701	62.37	67.15	-7.12	13.94	14.31	-37
4	7	0.0393	709.33	703.28	0.86	16.76	16.13	62
4	7	0.0543	242.90	242.54	0.15	12.97	12.95	2
4	7	0.0693	70.23	76.68	-8.41	13.42	13.88	-46
5	6	0.0385	617.96	613.32	0.76	16.27	15.80	48
5	6	0.0535	226.42	225.03	0.62	12.80	12.73	8
5	6	0.0685	72.37	78.01	-7.24	13.06	13.46	-40
6	5	0.0377	524.35	520.63	0.71	16.18	15.78	41
6	5	0.0527	205.55	203.31	1.10	12.94	12.80	14
6	5	0.0677	71.82	78.07	-8.01	12.98	13.46	-47
7	4	0.0367	427.47	423.69	0.89	16.29	15.82	47
7	4	0.0517	177.35	174.69	1.53	13.17	12.97	20
7	4	0.0667	66.52	73.73	-9.78	13.03	13.64	-62
8	3	0.0357	326.85	323.92	0.90	16.52	16.07	45
8	3	0.0507	142.77	139.98	1.99	13.48	13.22	27
8	3	0.0657	57.02	63.83	-10.68	13.16	13.88	-72
9	2	0.0344	221.21	220.33	0.40	16.74	16.55	19
9	2	0.0494	100.04	99.68	0.37	13.71	13.66	5
9	2	0.0644	41.63	48.96	-14.97	13.24	14.34	-110
10	1	0.0317	111.05	109.19	1.71	17.39	16.56	83
10	1	0.0467	51.22	49.99	2.46	14.15	13.80	35
10	1	0.0617	21.79	25.43	-14.33	13.52	14.60	-108

Table C.5: KRW market 9 August 2010: Calibration results.

$\sigma(t)$	0.1476	0.1347	0.1465	0.1507	0.1568	0.1758	0.1868	0.2020	0.2020	0.1924
$\gamma(t)$	0.1769	0.2609	0.2539	0.2616	0.3000	0.3000	0.3000	0.3000	0.3000	0.3000
$\epsilon(t)$	1.5044	1.2467	1.1733	1.1236	1.0805	1.1199	1.0890	1.0890	1.0890	1.0911

Table C.6: KRW market 9 August 2010: $R_0 = 0.05, \beta = 0.20, a = 0.03, V(0) = 1$.

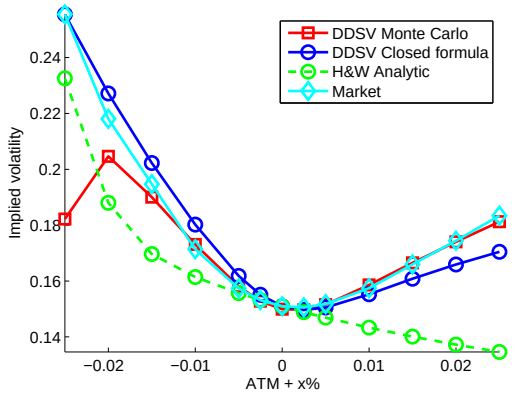

(a) 1Y10Y: Accuracy, ATM -10 bp, max. 120 bp.

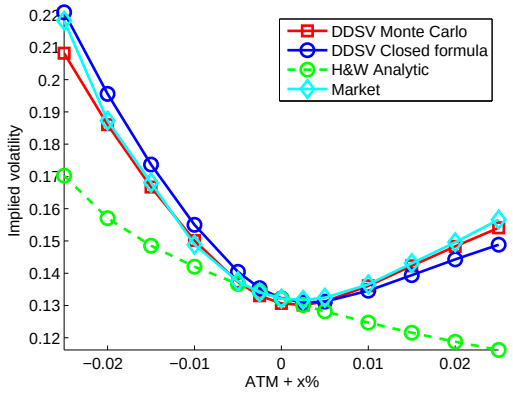

(b) 3Y8Y: Accuracy, ATM -15 bp, max. 70 bp.

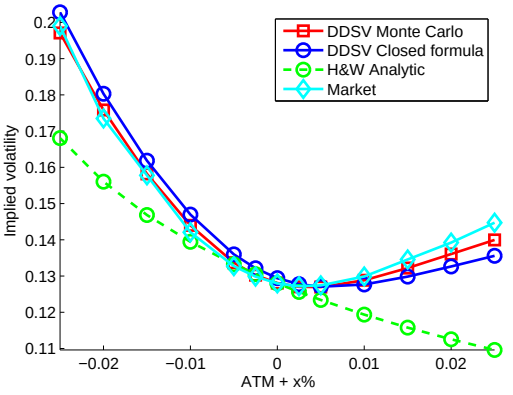

(c) 6Y5Y: Accuracy, ATM -13 bp, max. 36 bp.

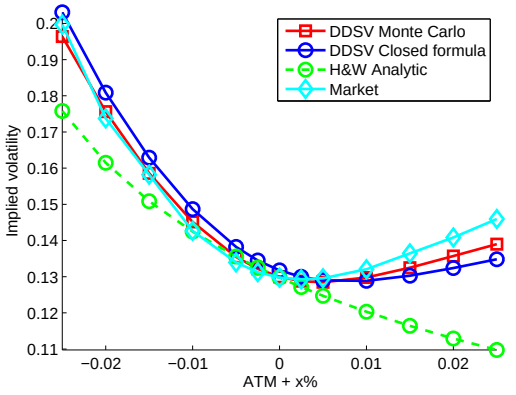

(d) 7Y4Y: Accuracy, ATM -18 bp, max. 43 bp.

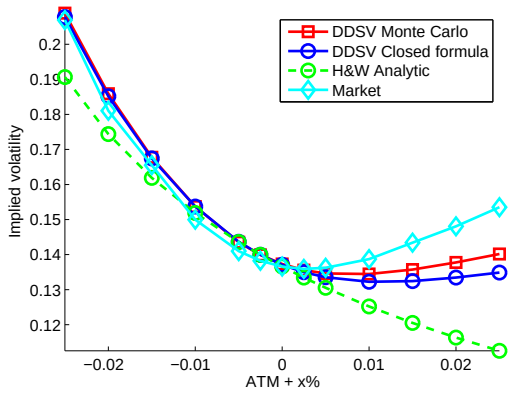

(e) 9Y2Y: Accuracy, ATM 2 bp, max. 33 bp.

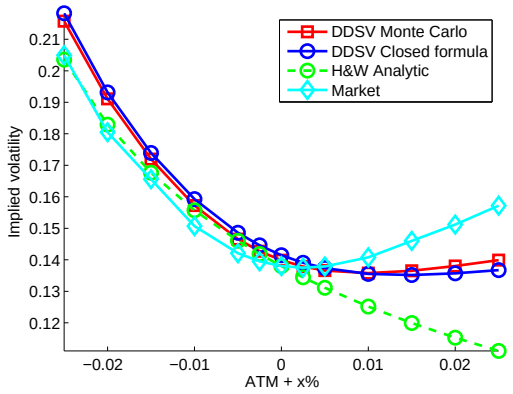

(f) 10Y1Y: Accuracy, ATM -15 bp, max. 20 bp.

Figure C.3: KRW market 9 August 2010: Figures with Cheyette and Hull-White fits to the market skew.

C.4 KRW swaption market 19 November 2009

Maturity in years	Tenor in years	Strike	Model price	Market price	Relative diff.	Model impl vol.	Market vol.	Diff in bp
1	10	0.0452	933.06	929.48	0.39	21.23	20.50	73
1	10	0.0602	239.84	239.63	0.09	16.49	16.48	1
1	10	0.0752	35.57	38.98	-8.76	17.60	18.06	-46
2	9	0.0442	865.79	858.07	0.90	18.81	17.88	93
2	9	0.0592	253.33	257.27	-1.53	13.97	14.18	-22
2	9	0.0742	60.87	60.77	0.17	15.40	15.39	1
3	8	0.0429	787.78	779.41	1.07	17.64	16.80	84
3	8	0.0579	250.61	255.30	-1.84	12.98	13.22	-24
3	8	0.0729	76.70	74.72	2.64	14.51	14.37	14
4	7	0.0419	704.58	694.42	1.46	17.07	16.11	96
4	7	0.0569	242.65	247.30	-1.88	12.68	12.92	-24
4	7	0.0719	85.32	85.16	0.18	14.03	14.02	1
5	6	0.0408	615.00	607.21	1.28	16.68	15.94	74
5	6	0.0558	226.22	230.22	-1.74	12.58	12.80	-22
5	6	0.0708	86.65	86.09	0.64	13.69	13.65	4
6	5	0.0398	523.43	517.56	1.13	16.68	16.08	60
6	5	0.0548	206.61	208.82	-1.06	12.82	12.96	-14
6	5	0.0698	85.10	86.03	-1.08	13.65	13.72	-7
7	4	0.0386	430.14	423.45	1.58	17.20	16.42	78
7	4	0.0536	184.12	184.66	-0.29	13.53	13.58	-4
7	4	0.0686	81.72	85.99	-4.96	14.02	14.37	-35
8	3	0.0375	330.16	326.72	1.05	17.57	17.07	49
8	3	0.0525	149.52	151.06	-1.02	14.02	14.17	-15
8	3	0.0675	69.86	76.41	-8.57	14.26	14.92	-66
9	2	0.0359	224.27	223.24	0.46	18.00	17.79	21
9	2	0.0509	105.87	108.36	-2.29	14.47	14.82	-35
9	2	0.0659	51.35	58.07	-11.58	14.50	15.47	-97
10	1	0.0330	113.98	111.79	1.96	19.04	18.11	92
10	1	0.0480	55.48	56.32	-1.49	15.26	15.50	-24
10	1	0.0630	27.65	33.46	-17.35	15.07	16.72	-165

Table C.7: KRW market 19 November 2009: Calibration results.

$\sigma(t)$	0.2072	0.1624	0.1664	0.2034	0.2193	0.2523	0.2992	0.2992	0.3000	0.3000
$\gamma(t)$	0.2406	0.2136	0.2993	0.2948	0.3000	0.3000	0.3000	0.3000	0.3000	0.3000
$\epsilon(t)$	1.4860	1.5358	0.9768	0.4695	0.4667	0.0100	0.0102	0.0102	0.0102	0.0102

Table C.8: KRW market 19 November 2009: $R_0 = 0.04, \beta = 0.05, a = 0.03, V(0) = 1$.

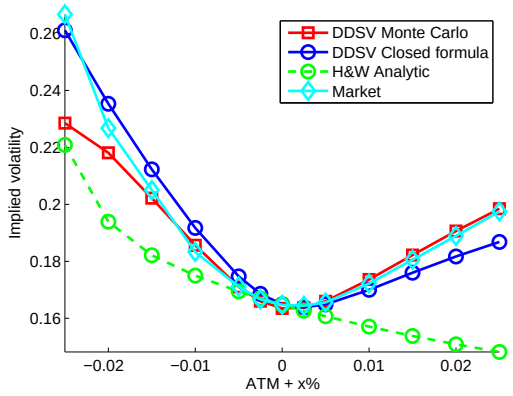

(a) 1Y10Y: Accuracy, ATM -14 bp, max. 101 bp.

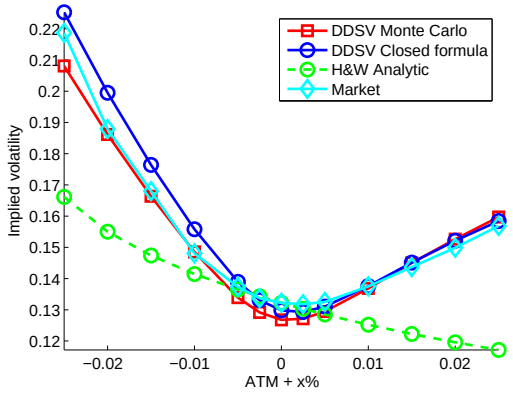

(b) 3Y8Y: Accuracy, ATM -30 bp, max. 100 bp.

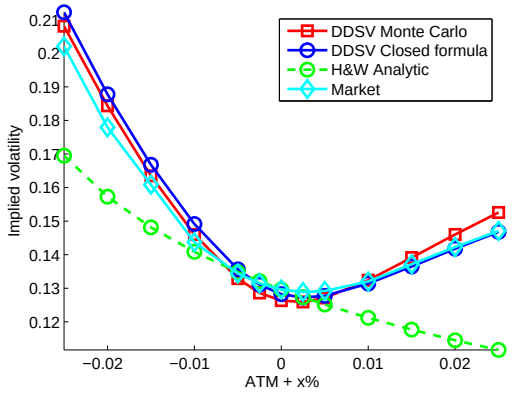

(c) 6Y5Y: Accuracy, ATM -19 bp, max. 32 bp.

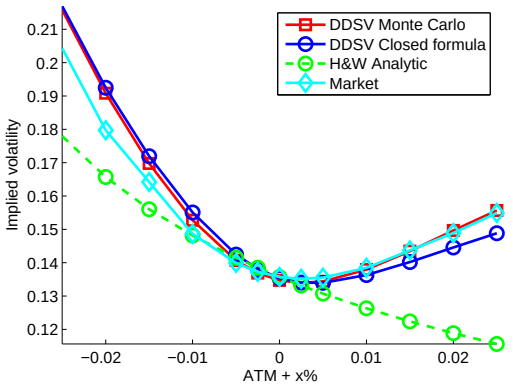

(d) 7Y4Y: Accuracy, ATM -6 bp, max. 32 bp.

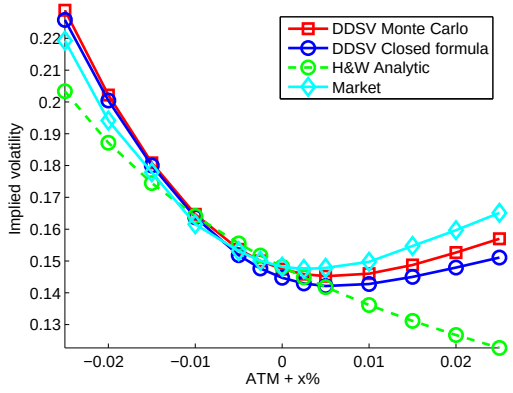

(e) 9Y2Y: Accuracy, ATM 27 bp, max. 37 bp.

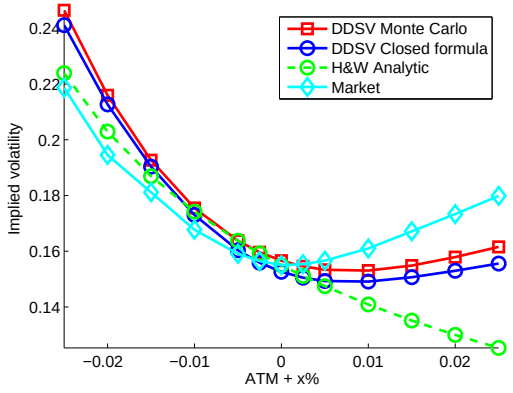

(f) 10Y1Y: Accuracy, ATM 39 bp, max. 42 bp.

Figure C.4: KRW market 19 November 2009: Figures with Cheyette and Hull-White fits to the market skew.

C.5 USD swaption market 9 August 2010.

Maturity in years	Tenor in years	Strike	Model price	Market price	Relative diff.	Model impl vol.	Market vol.	Diff in bp
1	10	0.0171	1335.84	1325.58	0.77	42.40	38.08	432
1	10	0.0321	337.56	337.22	0.10	30.22	30.19	3
1	10	0.0471	35.02	44.12	-20.63	27.54	29.22	-168
2	9	0.0201	1243.78	1229.39	1.17	38.04	35.77	227
2	9	0.0351	428.50	427.70	0.19	28.15	28.09	5
2	9	0.0501	102.67	116.59	-11.94	25.81	27.03	-122
3	8	0.0227	1138.29	1126.89	1.01	34.35	33.08	127
3	8	0.0377	454.37	454.03	0.08	26.00	25.98	2
3	8	0.0527	148.79	160.43	-7.26	24.07	24.85	-78
4	7	0.0249	1016.57	1006.75	0.98	31.60	30.66	94
4	7	0.0399	444.29	445.75	-0.33	24.32	24.40	-8
4	7	0.0549	172.38	181.67	-5.12	22.67	23.23	-56
5	6	0.0265	880.73	869.42	1.30	29.40	28.35	105
5	6	0.0415	408.83	415.02	-1.49	22.94	23.30	-36
5	6	0.0565	174.51	186.32	-6.34	21.42	22.13	-71
6	5	0.0276	744.24	735.49	1.19	28.56	27.71	85
6	5	0.0426	367.38	369.65	-0.62	22.55	22.70	-14
6	5	0.0576	171.23	179.88	-4.81	21.01	21.56	-55
7	4	0.0283	602.07	596.25	0.98	27.99	27.35	64
7	4	0.0433	312.20	311.90	0.09	22.32	22.30	2
7	4	0.0583	155.02	163.77	-5.34	20.71	21.34	-64
8	3	0.0289	454.41	449.91	1.00	27.44	26.82	61
8	3	0.0439	245.06	243.60	0.60	22.07	21.93	14
8	3	0.0589	127.51	135.82	-6.12	20.40	21.15	-75
9	2	0.0294	303.47	299.61	1.29	26.82	26.08	74
9	2	0.0444	168.65	167.19	0.88	21.72	21.53	20
9	2	0.0594	90.75	97.67	-7.09	20.01	20.90	-89
10	1	0.0296	149.61	148.50	0.75	25.93	25.51	41
10	1	0.0446	84.45	84.48	-0.04	21.09	21.10	-1
10	1	0.0596	46.16	50.54	-8.66	19.38	20.47	-108

Table C.9: Calibration results.

$\sigma(t)$	0.2350	0.2414	0.2327	0.2261	0.2032	0.2222	0.2147	0.2047	0.1896	0.1449
$\gamma(t)$	0.3000	0.3000	0.3000	0.3000	0.2936	0.3000	0.3000	0.3000	0.3000	0.2999
$\epsilon(t)$	1.0734	1.5080	2.2441	2.2790	2.2939	2.2078	2.2106	1.9635	1.9623	2.0840

Table C.10: USD swaption 9 August 2010: $R_0 = 0.07, \beta = 0.40, a = 0.03, V(0) = 1$.

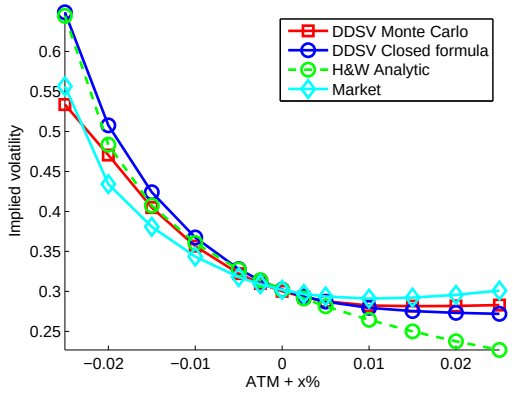

(a) 1Y10Y: Accuracy, ATM -20 bp, max. 192 bp.

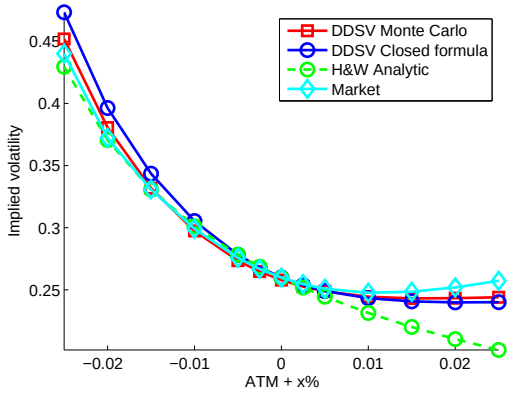

(b) 3Y8Y: Accuracy, ATM -21bp, max. 115 bp.

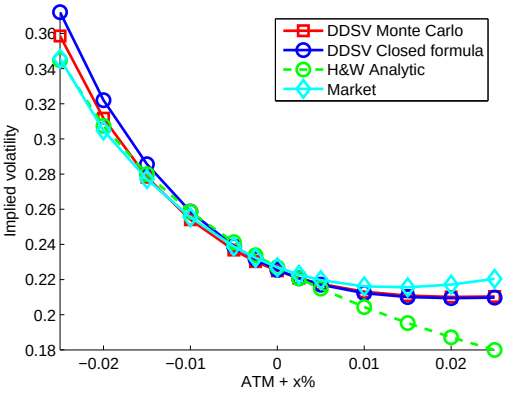

(c) 6Y5Y: Accuracy, ATM -5 bp, max. 74 bp.

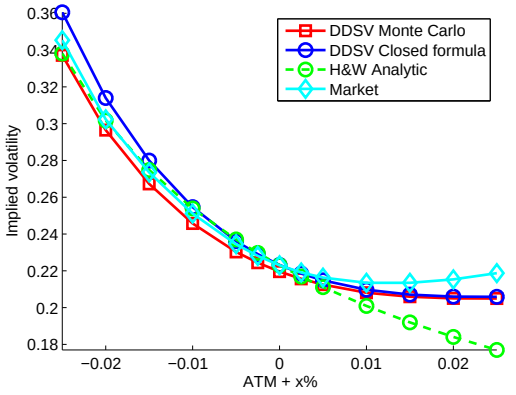

(d) 7Y4Y: Accuracy, ATM -36 bp, max. 126 bp.

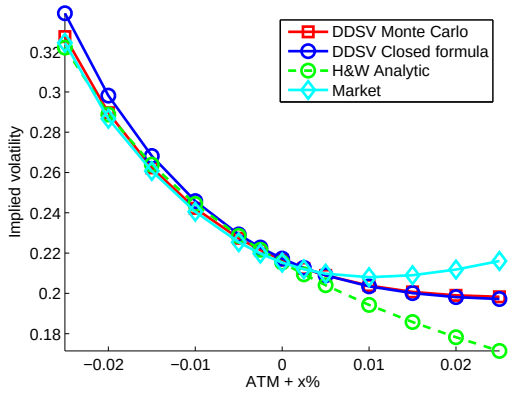

(e) 9Y2Y: Accuracy, ATM -7.2 bp, max. 58 bp.

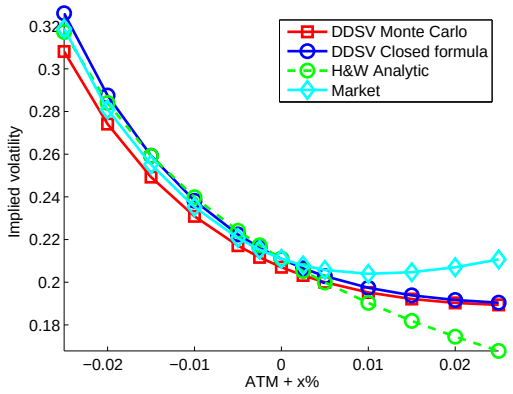

(f) 10Y1Y: Accuracy, ATM -39 bp, max. 100 bp.

Figure C.5: USD swaption 9 August 2010: Figures with Cheyette and Hull-White fits to the market skew.

C.6 USD swaption market 19 November 2009

Maturity in years	Tenor in years	Strike	Model price	Market price	Relative diff.	Model impl vol.	Market vol.	Diff in bp
1	10	0.0239	1326.85	1292.38	2.67	42.49	34.97	752
1	10	0.0389	431.29	429.51	0.42	33.12	32.98	14
1	10	0.0539	82.99	115.98	-28.44	30.15	33.79	-364
2	9	0.027	1269.8	1219.07	4.16	38.81	33.39	542
2	9	0.042	545.65	541.66	0.74	31.33	31.1	23
2	9	0.057	185.51	236.28	-21.49	28.38	31.67	-329
3	8	0.0292	1169.17	1119.79	4.41	35.36	31.18	418
3	8	0.0442	564.16	559.64	0.81	29.03	28.79	24
3	8	0.0592	233.38	283.92	-17.8	26.33	29.09	-276
4	7	0.0306	1047.13	1002.89	4.41	33.08	29.61	347
4	7	0.0456	539.87	538.19	0.31	27.28	27.2	9
4	7	0.0606	250.68	294.79	-14.96	24.89	27.18	-229
5	6	0.0316	912.66	874.76	4.33	31.71	28.71	300
5	6	0.0466	494.79	496.07	-0.26	26.23	26.3	-7
5	6	0.0616	249.3	285.66	-12.73	24.01	25.95	-195
6	5	0.0322	762.58	732.17	4.15	30.18	27.56	262
6	5	0.0472	426.09	427.19	-0.26	25.04	25.1	-7
6	5	0.0622	224.45	254.59	-11.84	22.94	24.71	-177
7	4	0.0326	608.44	583.15	4.34	28.95	26.41	254
7	4	0.0476	348.03	347.11	0.26	24.07	24	7
7	4	0.0626	189.42	214.02	-11.49	22.05	23.74	-169
8	3	0.0331	454.05	435.75	4.2	27.81	25.5	231
8	3	0.0481	264.6	264.1	0.19	23.18	23.13	4
8	3	0.0631	147.6	167.96	-12.12	21.24	23	-177
9	2	0.0336	297.8	287.1	3.73	26.32	24.4	192
9	2	0.0486	175.12	175.76	-0.37	22.01	22.1	-8
9	2	0.0636	98.73	114.07	-13.45	20.17	22.08	-191
10	1	0.0341	147.36	142.04	3.74	25.15	23.33	182
10	1	0.0491	87.55	87.14	0.47	21.1	21	10
10	1	0.0641	49.96	56.61	-11.74	19.34	20.92	-158

Table C.11: USD market 19 November 2009: Calibration results.

$\sigma(t)$	0.2703	0.2620	0.2231	0.2147	0.2155	0.1855	0.1754	0.1632	0.1249	0.1280
$\gamma(t)$	0.3000	0.3000	0.3000	0.3000	0.3000	0.3000	0.3000	0.3000	0.3000	0.3000
$\epsilon(t)$	1.0532	0.4094	1.9795	1.9830	1.9826	2.2898	2.2725	2.2717	2.2737	2.2726

Table C.12: USD market 19 November 2009: $R_0 = 0.08, \beta = 0.40, a = 0.03, V(0) = 1$.

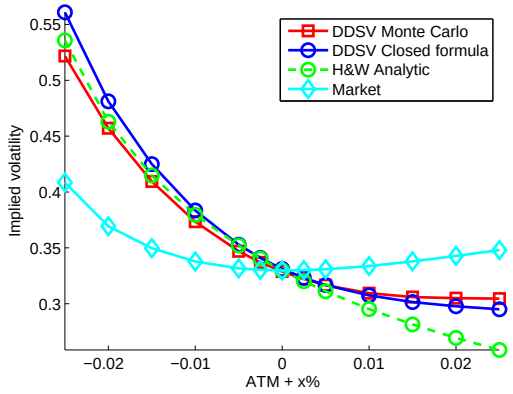

(a) 1Y10Y: Accuracy, ATM -23 bp, max. 150 bp.

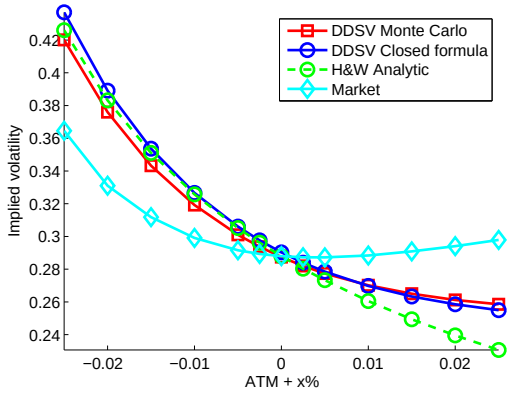

(b) 3Y8Y: Accuracy, ATM -28 bp, max. 103 bp.

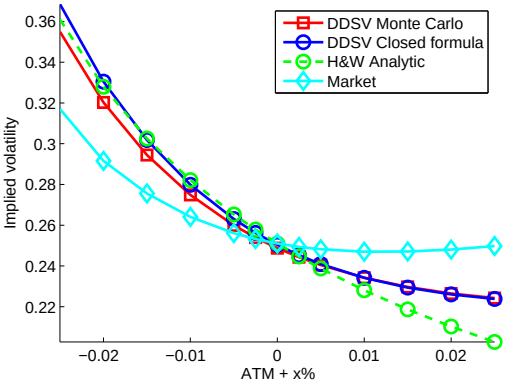

(c) 6Y5Y: Accuracy, ATM -16 bp, max. 73 bp.

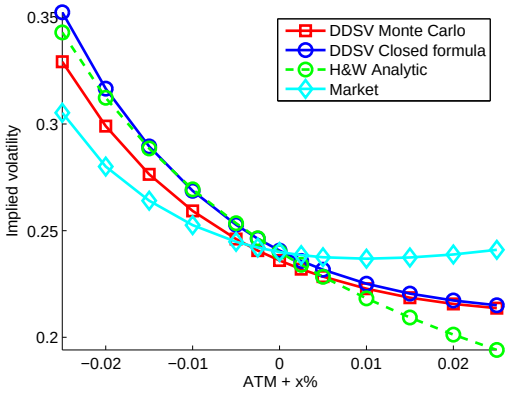

(d) 7Y4Y: Accuracy, ATM -46 bp, max. 93 bp.

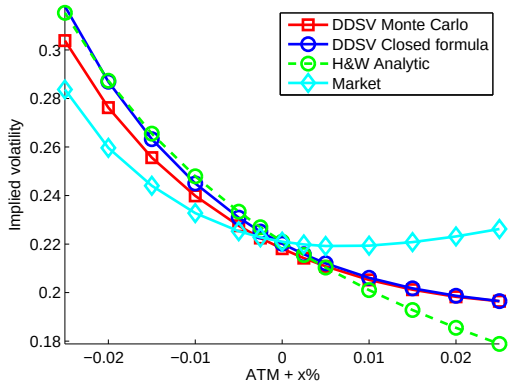

(e) 9Y2Y: Accuracy, ATM -21 bp, max. 75 bp.

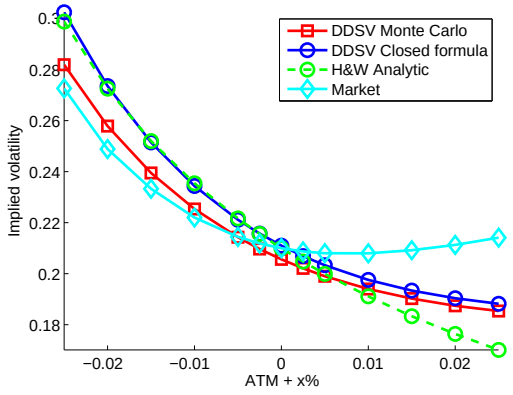

(f) 10Y1Y: Accuracy, ATM -53 bp, max. 119 bp.

Figure C.6: USD market 19 November 2009: Figures with Cheyette and Hull-White fits to the market skew.

Appendix D

Skew and curvature impact

In this appendix we include results from the skew and curvature impact analysis, which we have not listed in the main text. We subdivide this into three parts. In Appendix D.1 we include calibration results, in Appendix D.2 we include tables with pricing results for the digital cap and in Appendix D.3 we include tables with pricing results for the RAC and callable RACS.

D.1 Calibration results

D.1.1 13 April 2011: calibration to 4Y1Y and 10Y1Y swaptions

The DDSV model is calibrated to swaptions with strikes ATM − 150bp, ATM, ATM + 150bp.

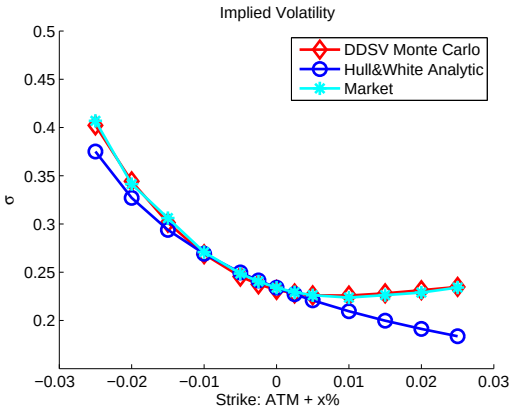

(a) 4Y1Y: Fit to the market skew

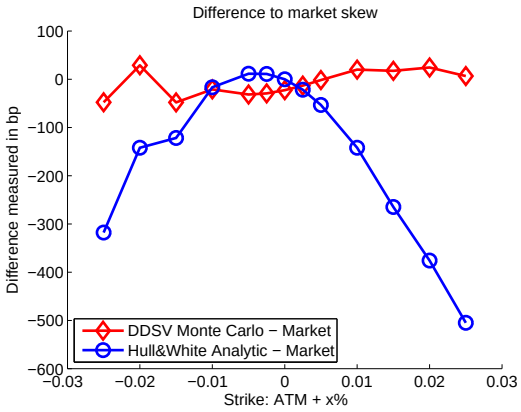

(b) 4Y1Y: Difference in basis points.

Figure D.1: 13 April 2011: Calibration results 4Y1Y swaption skew. ATM = 4.11%.

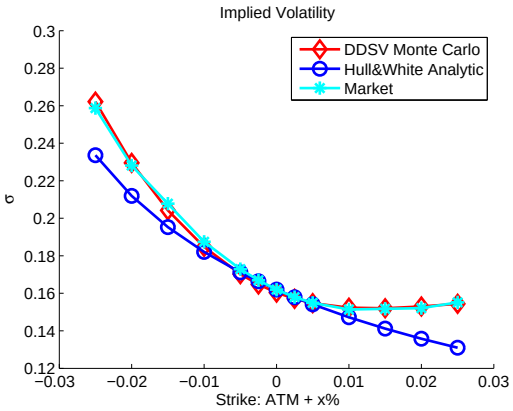

(a) 10Y1Y: Fit to the market skew

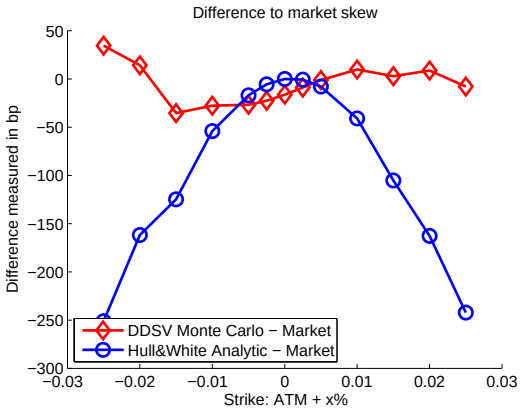

(b) 10Y1Y: Difference in basis points.

Figure D.2: 13 April 2011: Calibration results 10Y1Y swaption skew. ATM = 4.80%.

D.1.2 13 April 2011: calibration to 5Y1Y, 6Y1Y, ... 9Y1Y swaptions

The DDSV model is calibrated to swaptions with strikes ATM − 150bp, ATM, ATM + 150bp.

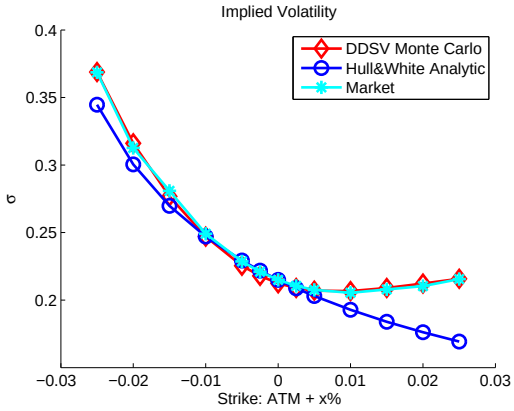

(a) 5Y1Y: DDSV accuracy, ATM -25 bp, max. 40 bp.

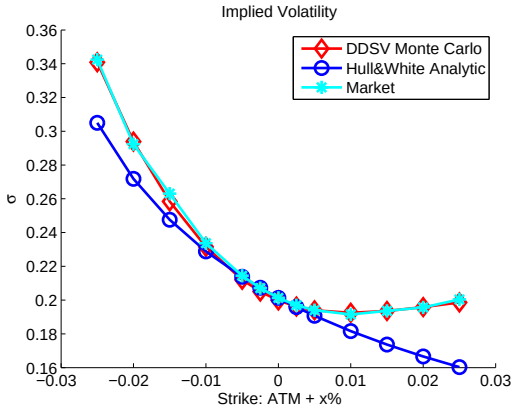

(b) 6Y1Y: DDSV accuracy, ATM -15 bp, max. 45 bp.

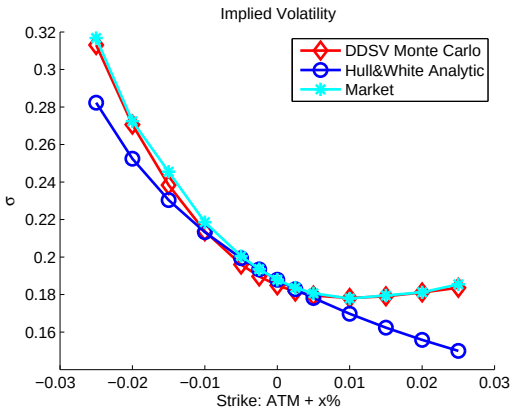

(c) 7Y1Y: DDSV accuracy, ATM -30 bp, max. 70 bp.

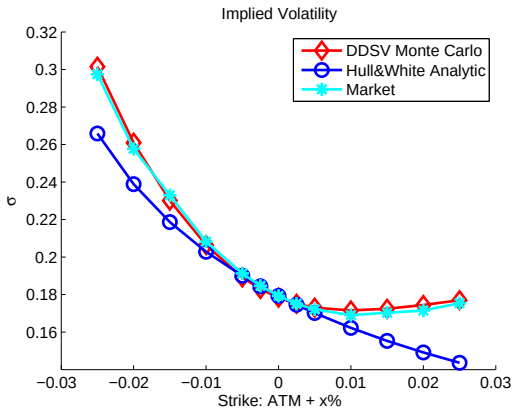

(d) 8Y1Y: DDSV accuracy, ATM -9 bp, max. 93 bp.

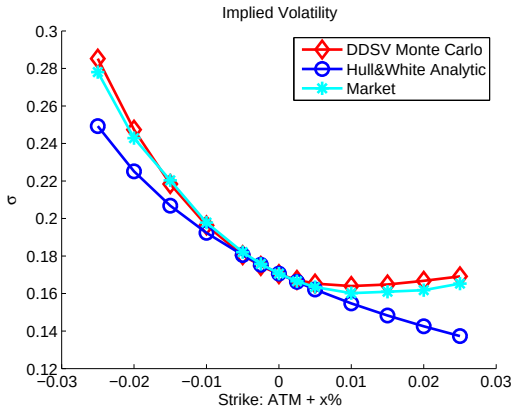

(e) 9Y1Y: DDSV Accuracy, ATM -3 bp, max. 49 bp.

D.1.3 30 June 2010: calibration to 5Y1Y, 6Y1Y, ... 9Y1Y swaptions

The DDSV model is calibrated to swaptions with strikes ATM − 150bp, ATM, ATM + 150bp.

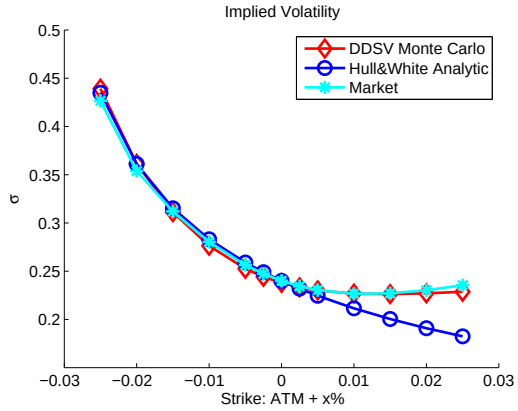

(f) 5Y1Y: DDSV accuracy, ATM -21 bp, max. 76 bp

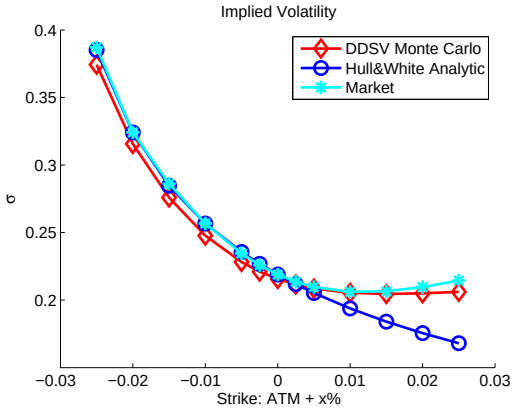

(g) 6Y1Y: DDSV accuracy, ATM -33 bp, max. 102 bp

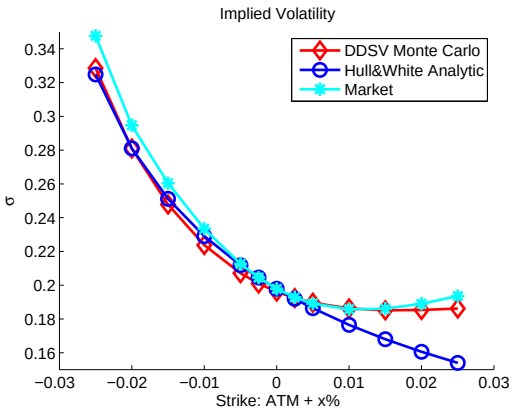

(h) 7Y1Y: DDSV accuracy, ATM -18 bp, max. 137 bp

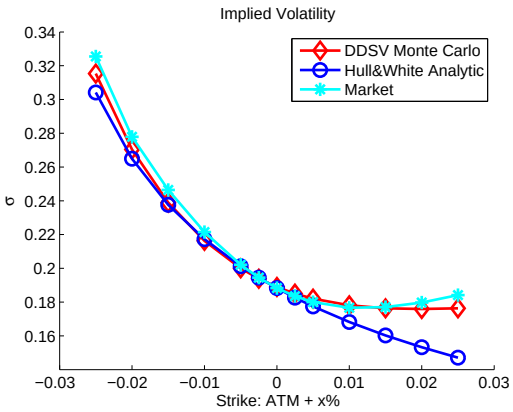

(i) 8Y1Y: DDSV accuracy, ATM 6 bp, max. 75 bp

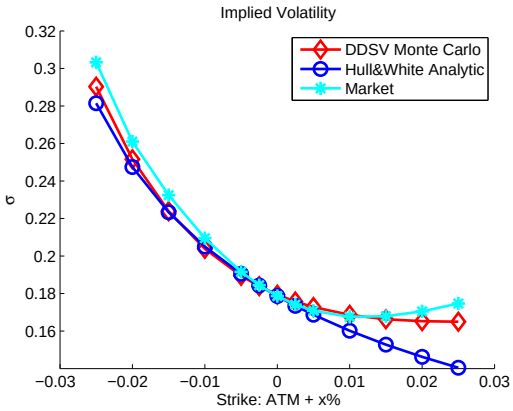

(j) 9Y1Y: DDSV Accuracy, ATM 7 bp, max. 94 bp

D.1.4 13 April 2011: calibration to 1Y10Y, 2Y9Y, ... 10Y1Y swaptions

The DDSV model is calibrated to swaptions with strikes ATM − 150bp, ATM, ATM + 150bp.

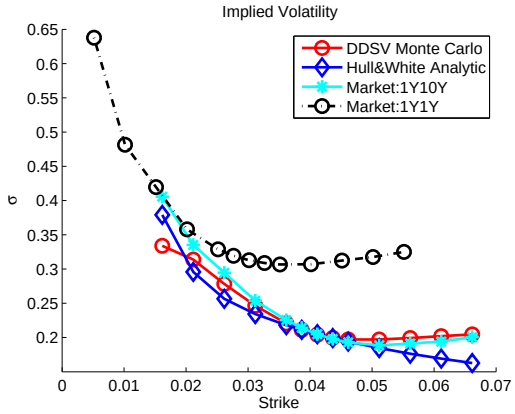

(k) 1Y10Y

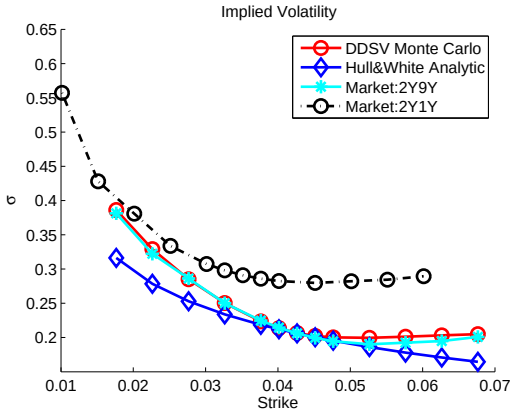

(l) 2Y9Y

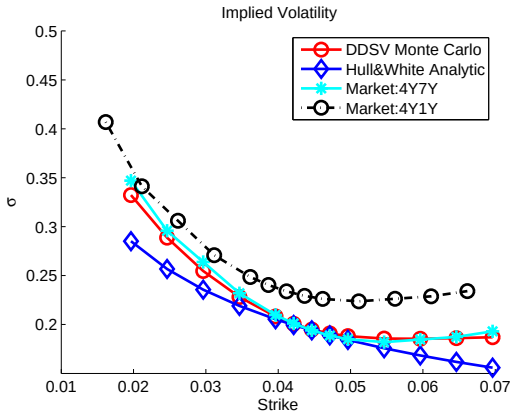

(m) 4Y7Y

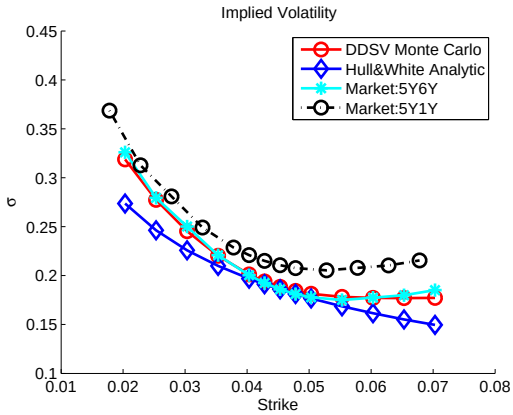

(n) 5Y6Y

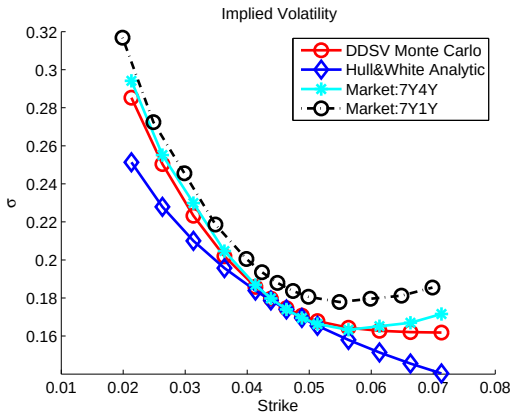

(o) 7Y4Y

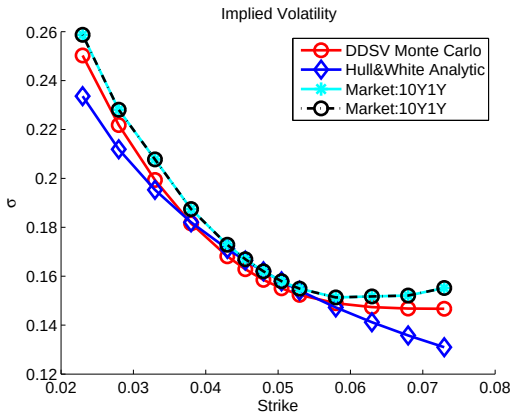

(p) 10Y1Y

D.2 Digital cap

In this section we include the tables with the results for the digital cap. In the main text we included the results for 13 April 2011, in this section we show the results for 16 December 2010 and 30 June 2010.

B - ATM	B	SR	H&W price	H&W - SR	DDSV price	DDSV - SR
-0.02	0.0241	1268.46	1255.14	-13.32	1284.88	16.42
-0.015	0.0291	1156.76	1151.7	-5.06	1178	21.24
-0.01	0.0341	1035.71	1032.89	-2.82	1043.47	7.76
-0.005	0.0391	891.75	903.39	11.63	885.2	-6.55
0	0.0441	720.18	769.24	49.06	717.23	-2.94
0.005	0.0491	555.05	635.9	80.85	561.52	6.46
0.01	0.0541	414.19	510.55	96.36	429.17	14.98
0.015	0.0591	298.86	396.78	97.92	325.38	26.52
0.02	0.0641	212.99	299	86.01	247.85	34.86

Table D.1: Pricing results: 16 December 2010, digital cap starting in 5Y. The ATM level of the 5Y5Y swaption is 4.41%. H&W 99% confidence interval width, < 9.4. DDSV 99% confidence interval width, < 12.1.

B - ATM	B	SR	H&W price	H&W - SR	DDSV price	DDSV - SR
-0.02	0.019	1373.7	1366.74	-6.96	1393.82	20.12
-0.015	0.024	1258.8	1253.33	-5.47	1286.92	28.12
-0.01	0.029	1133.43	1119.24	-14.19	1143.18	9.75
-0.005	0.034	968.71	968.73	0.03	963.11	-5.6
0	0.039	768.2	809.81	41.61	764.14	-4.06
0.005	0.044	572.28	653.6	81.32	579.74	7.47
0.01	0.049	402.4	506.32	103.92	427.72	25.32
0.015	0.054	273.18	377.6	104.42	313.22	40.04
0.02	0.059	184.99	269.54	84.55	231.28	46.29

Table D.2: Pricing results: 30 June 2010, digital cap starting in 5Y. The ATM level of the 5Y5Y swaption is 3.9%. H&W 99% confidence interval width, < 8.8. DDSV 99% confidence interval width, < 12.1.

D.3 RAC and callable RAC results

In this section we include the tables with the results for the RAC and the callable RAC. In the main text we included the results for 13 April 2011, in this section we show the results for 16 December 2010 and 30 June 2010. We use the following abbreviations in the tables with results, K is the fixed rate of the underlying RAC, B is the barrier of the digitals in the payoff function.

D.3.1 16 December 2010: Tables with RAC and callable RAC results

K	B	SR price	H&W price	H&W − SR	DDSV price	DDSV − SR
0.0613	0.0286	-1264.54	-1391.76	-127.22	-1487.40	-222.86
0.0613	0.0386	-317.45	-445.56	-128.12	-449.39	-131.94
0.0613	0.0486	561.07	383.55	-177.52	500.22	-60.85
0.0713	0.0286	-955.52	-1103.52	-148.00	-1214.49	-258.97
0.0713	0.0386	146.11	-2.92	-149.03	-7.09	-153.20
0.0713	0.0486	1167.98	961.49	-206.49	1097.47	-70.51
0.0813	0.0286	-646.51	-815.27	-168.76	-941.57	-295.06
0.0813	0.0386	609.67	439.73	-169.94	435.20	-174.46
0.0813	0.0486	1774.89	1539.42	-235.47	1694.72	-80.17

Table D.3: Pricing results: Hull-White and DDSV prices for the range accrual, compared to the static replication price. H&W 99% confidence interval width, < 57. DDSV 99% confidence interval width, < 59.

K	B	RAC HW	RAC DDSV	C-RAC H&W	C-RAC DDSV	C-RAC DDSV − C-RAC H&W
0.0613	0.0286	-1391.76	-1487.40	492.54	513.19	20.65
0.0613	0.0386	-445.56	-449.39	755.46	800.51	45.05
0.0613	0.0486	383.55	500.22	1054.00	1154.71	100.71
0.0713	0.0286	-1103.52	-1214.49	649.54	659.42	9.88
0.0713	0.0386	-2.92	-7.09	1029.77	1080.97	51.20
0.0713	0.0486	961.49	1097.47	1474.37	1617.09	142.72
0.0813	0.0286	-815.27	-941.57	823.20	817.71	-5.49
0.0813	0.0386	439.73	435.20	1334.78	1389.45	54.67
0.0813	0.0486	1539.42	1694.72	1937.01	2116.65	179.64

Table D.4: Pricing results: The Hull-White and DDSV callable range accrual prices.

D.3.2 30 June 2010: Tables with RAC and callable RAC results

K	B	SR price	H&W price	H&W − SR	DDSV price	DDSV − SR
0.0500	0.0226	-1205.54	-1299.29	-93.75	-1406.65	-201.11
0.0500	0.0326	-418.72	-461.34	-42.62	-530.12	-111.41
0.0500	0.0426	376.72	262.57	-114.16	355.98	-20.74
0.0600	0.0226	-894.40	-1006.92	-112.52	-1135.66	-241.26
0.0600	0.0326	49.85	-1.31	-51.16	-83.75	-133.60
0.0600	0.0426	1004.45	867.44	-137.01	979.66	-24.79
0.0700	0.0226	-583.27	-714.55	-131.28	-864.67	-281.40
0.0700	0.0326	518.42	458.72	-59.70	362.63	-155.79
0.0700	0.0426	1632.18	1472.32	-159.86	1603.33	-28.85

Table D.5: Pricing results: Hull-White and DDSV prices for the range accrual, compared to the static replication price. H&W 99% confidence interval width, < 49. DDSV 99% confidence interval width, < 52.

K	B	RAC HW	RAC DDSV	C-RAC H&W	C-RAC DDSV	C-RAC DDSV − C-RAC H&W
0.0500	0.0226	-1299.29	-1406.65	367.63	388.39	20.75
0.0500	0.0326	-461.34	-530.12	585.54	614.75	29.21
0.0500	0.0426	262.57	355.98	842.57	959.17	116.61
0.0600	0.0226	-1006.92	-1135.66	510.66	511.04	0.38
0.0600	0.0326	-1.31	-83.75	849.64	869.64	19.99
0.0600	0.0426	867.44	979.66	1266.48	1430.17	163.69
0.0700	0.0226	-714.55	-864.67	672.52	646.81	-25.72
0.0700	0.0326	458.72	362.63	1152.39	1159.14	6.75
0.0700	0.0426	1472.32	1603.33	1748.58	1948.22	199.64

Table D.6: Pricing results: The Hull-White and DDSV callable range accrual prices.